The Pennsylvania State University
The Graduate School
Department of Energy and Mineral Engineering

PREDICTION OF FLOWING FRICTIONAL PRESSURE DROP IN DEVIATED GAS CONDENSATE WELLS THROUGH UTILIZATION OF ARTIFICIAL NEURAL NETWORKS

A Thesis in
Petroleum and Mineral Engineering
by
Doruk Seren

Submitted in Partial Fulfillment
of the Requirements
for the Degree of
Master of Science

May 2008

The thesis of Doruk Seren was reviewed and approved*
by the following:

Turgay Ertekin

Professor of Petroleum and Natural Gas Engineering

Graduate Program Chair

Thesis Adviser

Zuleima T. Karpyn

Assistant Professor of Petroleum and Natural Gas Engineering

David W. Krout

Research Associate

*Signatures are on file in the Graduate School.

Abstract

This thesis presents an inverse solution to the prediction of pressure drop observed in flowing deviated gas condensate wells through the use of an Artificial Neural Network (ANN) which is trained entirely with data from a deepwater, high-pressure rich gas field in the Gulf of Mexico. The field data is obtained from downhole pressure gauges (DHPGs) which are installed at a significant distance above perforations. The ANN is trained first to predict pressure drop between the DHPG and wellhead, and then adapted to predict true flowing sandface pressure (P_{SF}). In order to validate the ANN predictions of true P_{SF}, history matching studies are conducted on the field.

The ANN designed in this study is a feedforward-backpropagation network, and requires supervised learning. During training, wellhead pressures (P_{WH}), fluid rates, static well parameters, and node-to-node lengths, and functional links are used as inputs, and output is DHPG reading. To adapt the same network to 'extrapolation'- that is, prediction of pressures outside the training range, with greater well deviation in the section between gauges and perforations, adapted normalization parameters had to be applied to the training data. To validate ANN predictions of P_{SF}, three history matching studies were conducted. First, bottomhole pressure (P_{BH}) behavior is matched to uncorrected DHPG data, then lift-table corrected P_{WH} behavior is matched to P_{WH} history, and lastly, P_{BH} behavior is matched to ANN-corrected 'true' P_{SF} history. The reservoir property distributions that produce satisfactory history matches for each stage are compared against the properties taken from whole cores, and the match to ANN-corrected P_{SF} history proves to be the most reasonable match.

While the ANN proved highly successful in predicting pressure drop between wellhead and DHPG, the 'true' P_{SF} predictions show some

irregularities and are not reliable under all conditions, due to the extrapolation of the prediction outside the range of the original training data. However, use of the ANN predictions along with good engineering judgment in a history matching study demonstrated a more reasonable reservoir property distribution than alternatives. Furthermore, the training process identified strong dependence of pressure drop on the average deviation parameter, as observed from weights. Additionally, the success of the training process demonstrates that the ANN is robust to the nonlinearities that cause difficulty in application of classic semi-empirical lift correlations in highly deviated gas condensate wells such as unsteady liquid holdup, slugging, and transitioning flow regimes.

The contributions of this work are diverse. In addition to the design and validation of an artificial expert system to model flowing frictional pressure drop in wells that are unreliably modeled by other means, weaknesses of the other methods are identified in the process. These include the deviation parameter applied to the ANN training data (absent from existing correlations) and the significance of phase change within the production tubing identified by internal inconsistencies among semi-empirical correlations in liquid holdup and flow regime calculations. The importance of the ANN's predictions are validated by their application to a history matching study, and the ANN proves useful in an extrapolation mode, unlike the more common interpolation mode often used in similar applications.

Table of Contents

List of Figures vi
List of Tables ix
Chapter 1: Introduction 1
Chapter 2: Background 4
Chapter 3: Problem Statement 7
Chapter 4: Solution Methodology and Training Data 9
4.1. Gauge Setting Depth 10
4.2. Fluid Behavior 12
Chapter 5: Artificial Expert System 17
5.1. Stage 1: Initial Experiments 20
5.1.1. System Design Details 20
5.2. Stage 2: More Advanced ANN Designs 22
5.3. Stage 3: Reversal of ANN Prediction 'Direction' 25
5.4. ANN Prediction of 'True' Sandface Pressures 28
Results and Observations 31
Chapter 6: Comparison to other methods 35
6.1. ANN Study Recap 35
6.2. Comparative Analysis of ANN Performance 35
6.2.1. Published Work on Flowing Pressure Loss in Producing Wells 35
6.2.2. Well Test Quality Control as Correlation Testing Approach 37
Chapter 7: Case Study 45
7.1. Part I: History Match to Uncorrected DHPG Data 47
7.2. Part II: History Match to WHP with Lift Tables 53
7.3. Part III: History Match to ANN-Corrected BHP's 55
7.4. History Matching Results Comparison 59
7.5. Reservoir Performance Forecasts 61
Chapter 8: Conclusions 64
References 66
Appendix A: Wellpath Deviation / Angle Parameters used in ANN Design 68
Appendix B: Reservoir Model Details 69
Appendix C: Well Deviation Surveys 74
Appendix D: Tables of ANN Training and Simulation Values 76
Appendix E: Final Network Weights 86
Appendix F: Well Test QC Study on Auger Well A14 92

List of Figures

Figure 1: Deviation Summary, Auger Shallow Gas Sand Producers... 11
Figure 2: Condensate Yield Change over time, Auger Gas Sands..... 14
Figure 3: Representative Reservoir Fluid Phase Envelope..... 15
Figure 4: Permanent Downhole Pressure Gauge recordings, Auger O Sand 16
Figure 5: Conceptual Diagram of Stage 1 ANN 20
Figure 6: Conceptual Diagram of Stage 2 ANN 23
Figure 7: Training errors from Stage 2 ANN 24
Figure 8: Cross-plot of neural network training results in Stage 2 24
Figure 9: Conceptual diagram of Stage 3 ANN..... 26
Figure 10: Crossplot of Stage 3 ANN predictions vs. Field Measurements 27
Figure 11: Crossplot of Extrapolation Network Predictions..... 30
Figure 12: Hinton Plot of Weights from First (Input) Layer, Extrapolation Network..... 31
Figure 13: Hinton Plot for 90-neuron Middle, or 'Hidden', Layer, Extrapolation Network..... 32
Figure 14: Hinton Plot for first-layer weights from alternate 5-layer network 34
Figure 15: Early-Life Flowing Gradient Traverse of A14 Well..... 38
Figure 16: Mid-Life Flowing Gradient Traverse of A14 Well..... 39
Figure 17: Late-Life Flowing Gradient Traverse of A14..... 40
Figure 18: Auger A14 Well Test QC Plot 42
Figure 19: Liquid Hold-Up Plot, Auger A14 Well. 43
Figure 20: Top Structure Map, Auger O Massive 46
Figure 21: Match to Uncorrected Gauge Pressure History..... 47
Figure 22: Permeability (k) distribution used in history match to uncorrected DHPG data. 50
Figure 23: Porosity (Φ) distribution used in history match to uncorrected DHPG data. 51
Figure 24: Relative Permeability relationships (and P_c curve) used in match to 'raw' DHPG data..... 52
Figure 25: Rough Match to Wellhead Pressure with Beggs and Brill Lift Table, Well A14..... 54
Figure 26: Rough Match to Wellhead Pressure with Beggs and Brill Lift Table, Well A16ST 55
Figure 27: Approximate Match to ANN-Predicted 'true' Sandface Pressures 56
Figure 28: Comparison of BHP at the A16ST Well to Gauge History .. 56
Figure 29: Approximate Match to Water Production Rate, Auger O Massive Sand, A14 Well..... 57

Figure 30: Approximate Match to Water Production Rate, Auger O Massive Sand, A16ST Well 57
Figure 31: Permeability Distribution used in Match to ANN-Corrected BHP 58
Figure 32: History Match Results Comparison- Late-Time Pressure Distribution 60
Figure 33: Proposed New Well Location, Superimposed on 4350 day Gas Saturation Map from ANN-Match and 2832 day DHPG Match (inset) 61
Figure 34: Cumulative Gas Recovery for ANN-Matched and DHPG Matched Reservoir Models with Additional Well 63
Figure 35: Late-Time gas saturation distribution with new well 63
Figure 36: Phase Envelopes from commercial PVT code 70
Figure 37: Pre-Production Down-dip Wireline Log with Gas 'Show' ... 71
Figure 38. Gas and Condensate Density vs. Pressure T_{RES}, PR EOS ... 72
Figure 39: Gas Formation Volume Factor and Viscosity used in history matching studies 73
Figure 40: Deviation Survey, A16ST 74
Figure 41: Deviation Survey, A14 75
Figure 42: Well Test QC Plot, A14 Well 93
Figure 43: Well Test QC Plot, A14 Well 94
Figure 44: Well Test QC Plot, A14 Well 94
Figure 45: Well Test QC Plot, A14 Well 95
Figure 46: Well Test QC Plot, A14 Well 95
Figure 47: Well Test QC Plot, A14 Well 96
Figure 48: Well Test QC Plot, A14 Well 96
Figure 49: Well Test QC Plot, A14 Well 97
Figure 50: Well Test QC Plot, A14 Well 97
Figure 51: Well Test QC Plot, A14 Well 98
Figure 52: Well Test QC Plot, A14 Well 98
Figure 53: Well Test QC Plot, A14 Well 99
Figure 54: Well Test QC Plot, A14 Well 99
Figure 55: Well Test QC Plot, A14 Well 100
Figure 56: Well Test QC Plot, A14 Well 100
Figure 57: Well Test QC Plot, A14 Well 101
Figure 58: Well Test QC Plot, A14 Well 101
Figure 59: Well Test QC Plot, A14 Well 102
Figure 60: Well Test QC Plot, A14 Well 102
Figure 61: Well Test QC Plot, A14 Well 103
Figure 62: Well Test QC Plot, A14 Well 103
Figure 63: Well Test QC Plot, A14 Well 104
Figure 64: Well Test QC Plot, A14 Well 104
Figure 65: Well Test QC Plot, A14 Well 105
Figure 66: Well Test QC Plot, A14 Well 105

Figure 67: Well Test QC Plot, A14 Well..... 106
Figure 68: Well Test QC Plot, A14 Well..... 106
Figure 69: Well Test QC Plot, A14 Well..... 107
Figure 70: Well Test QC Plot, A14 Well..... 107
Figure 71: Well Test QC Plot, A14 Well..... 108
Figure 72: Well Test QC Plot, A14 Well..... 108
Figure 73: Well Test QC Plot, A14 Well..... 109
Figure 74: Well Test QC Plot, A14 Well..... 109
Figure 75: Well Test QC Plot, A14 Well..... 110
Figure 76: Well Test QC Plot, A14 Well..... 110
Figure 77: Well Test QC Plot, A14 Well..... 111
Figure 78: Well Test QC Plot, A14 Well..... 111
Figure 79: Well Test QC Plot, A14 Well..... 112
Figure 80: Well Test QC Plot, A14 Well..... 112
Figure 81: Well Test QC Plot, A14 Well..... 113
Figure 82: Well Test QC Plot, A14 Well..... 113
Figure 83: Well Test QC Plot, A14 Well..... 114
Figure 84: Well Test QC Plot, A14 Well..... 114
Figure 85: Well Test QC Plot, A14 Well..... 115
Figure 86: Well Test QC Plot, A14 Well..... 115
Figure 87: Well Test QC Plot, A14 Well..... 116
Figure 88: Well Test QC Plot, A14 Well..... 116
Figure 89: Well Test QC Plot, A14 Well..... 117
Figure 90: Well Test QC Plot, A14 Well..... 117
Figure 91: Well Test QC Plot, A14 Well..... 118
Figure 92: Well Test QC Plot, A14 Well..... 118
Figure 93: Well Test QC Plot, A14 Well..... 119
Figure 94: Well Test QC Plot, A14 Well..... 119
Figure 95: Well Test QC Plot, A14 Well..... 120
Figure 96: Well Test QC Plot, A14 Well..... 120
Figure 97: Well Test QC Plot, A14 Well..... 121
Figure 98: Well Test QC Plot, A14 Well..... 121

List of Tables

Table 1: Well performance data used in previous ANN studies, reproduced from Osman, E.A., et al., 2005. 6
Table 2: RFT-Reported Initial Compositions, 471-1 (N and O Sands) and 426-1BP3 (O Sand) 12
Table 3: Direct Inputs for Phase 1 ANN (Ch. 4.1)..... 76
Table 4: Normalized Inputs / Outputs for training of Tansig/Logsig Networks and Extrapolation Network..... 80
Table 5: Layer 1 Weights, Final 'Extrapolation' Network..... 87
Table 6: Layer 2 Weights, Final 'Extrapolation' Network..... 87
Table 7: Final Layer Weights, Final 'Extrapolation' Network 91

Acknowledgements

The research presented in this thesis was conducted as part of the Petroleum Geosystems Initiative at The Pennsylvania State University, which is sponsored by the Shell Foundation, Shell Exploration and Production Company, and Chevron. Additionally, software and support from Landmark Graphics, Paradigm Geophysical, Petroleum Experts, and Object Reservoir were significant contributions to this research.

I thank my advisors, Turgay Ertekin and Peter Flemings, who ensured that my graduate studies were a learning experience in many ways. Dr. Ertekin's guidance always kept me on the right track, while allowing me to tackle challenges in my own way. The rest of the PNGE faculty and David Krout of the PSU Applied Research Lab were also unendingly supportive and encouraging as I pursued my research.

Heather Nelson, Christie Rosenhoover, Tom Canich, Damien Futrick, and Bob Byers all helped survive all manner of difficulties in getting work done, along with other staff in EGEE. Replacing computers and installing software on short notice made my life a lot easier.

I acknowledge my Geosystems teammates, Charles "Spike" Bohn, Matthew Reilly, and Joe Valenti, for their enthusiastic discussions and professionalism throughout the course of our work. I am also thankful for being the only member of Geosystems Team 4 to survive his graduate studies with all limbs intact. My fellow students in both PNGE and Geoscience also contributed to my graduate experience.

I am thankful for the support and encouragement of my family, both immediate and extended. In our conversations regarding my

progress with my studies, my mother and father never failed to find a ‘when I was in graduate school’ story that inevitably had the ring of a ‘when I was your age’ story. My sister was also always ready to provide some levity.

My fiance, Burcu, has been my companion at a distance through my studies. She made the challenging parts of my work go by smoothly, and always kept my spirits up. Despite the time we’ve had to spend apart, she has been the best thing in my life these past two years and will continue to be through our future together.

Chapter 1: Introduction

Flowing frictional pressure drop in producing oil and gas wells has been an important area of study since the early years of the oil and gas industry. While a multitude of research has increased the accuracy of these predictions over the years, the semi-empirical correlations that might be considered mainstays of the industry are, for the most part, several decades old. With the relatively recent advent of highly deviated or extended reach wells and other directional drilling developments, combined with increased profitability of gas reservoirs, the ranges of operating parameters used in the development of existing lift correlations is no longer able to capture the physics at work in the case of particularly high condensate yield, or 'rich', gasses. Though existing work has always sought to generalize solutions to different fluid types and flowing conditions, it is now recognized that liquid holdup, for example, is often difficult to predict accurately using existing methods, particularly in the case of gas / condensate wells.

Recently, mechanistic approaches have been developed [Gomez et al., 1999, Ansari et al., 1994, and Hasan and Kabir, 1988]. These approaches seek to develop non-empirical models from fundamental equations of fluid flow, but many simplifications are required to successfully develop these models. For this reason, these methods continue to focus on oil / oil-water flow, and even simplify further to steady-state flow. These limitations cause these methods to have difficulty in reliably producing accurate results [Osman, 2005], even when applied to vertical, two-phase flow. As in the case of the empirical correlations, this accuracy can be expected to suffer further when applied to gas/condensate wells.

This work outlines a novel approach to prediction of flowing bottomhole pressures through the use of an ANN-based artificial expert system that is trained with field data from a 'rich', or condensate, gas produced from a turbidite reservoir under the deep waters of the Gulf of

Mexico. By training the ANN exclusively with data measured in the field, this artificial expert system gains the advantage that training data may incorporate various quickly-transitioning flow regimes and holdup conditions. The final product is an Artificial Neural Network that could be trained as a model of a representative well in a given field, and applied as a bottomhole pressure predictor for all future wells in the same reservoir. A field case study is conducted to demonstrate this potential by history matching to ANN-corrected data. However, due to comparatively limited training data, for the field validation study this ANN is used in an extrapolation mode, as compared with the more reliable interpolation mode. While experimentation with normalization parameters allows some useful predictions in extrapolation mode, this is best considered a demonstration for the potential of the methodology. Addition of, for example, drill-stem test data to the training set would populate the outer ranges of pressures needed for interpolation-mode predictions by the ANN, and combined with later-life data for one or two wells in a given field, as is used here, would produce more reliable results.

This process is dependent on the availability of pressure data from multiple depths in a well, but even in wells instrumented in this fashion, offers the advantage of a potentially more accurate prediction of the significant pressure drop that occurs between the sandface and downhole pressure gauges. Furthermore, the problem of directionality and curvature of a well complicates matters further in that the slimming of the hole in highly curved sections also can prevent setting of gauges at the zone of interest. Ultimately, the accurate prediction of flowing bottomhole pressure is necessary, even in the presence of permanently installed downhole pressure instrumentation, because the downhole gauge does not measure the pressure at the true location of interest.

The importance of predicting 'true' flowing bottomhole pressures is a result of the fact that all reservoir behavior calculations (pressure transient analysis, rate transient analysis, numerical simulation, inflow performance relationships, and material balance / analytical solutions) are based on pressures observed at the sandface, i.e., at the perforations themselves. Reliable forecasts or reservoir property estimates to be drawn from application of these methods is dependent on the accuracy of the field measurements on which these studies would be based. Though the extrapolation-mode predictions of the ANN require some engineering judgment to apply correctly, as not all predictions are physically reasonable, they nonetheless supply some additional information for true sandface pressures where none are available otherwise. A history matching study is conducted with a commercial numerical simulation code. The objective of this was to determine the impact of matching to first raw gauge data, matching to wellhead pressures as determined by application of an empirical lift correlation, and using ANN-corrected bottomhole pressures in conjunction with other available data to drive the reservoir modeling study. This serves as a sample application of the artificial expert system described, and validates the practical applicability of the method.

Chapter 2: Background

Artificial Neural Networks are processing systems that are based on a computational analogy to biological neuron networks. First used in the 1950s, research into applications was slow due to limitations of early networks and limitations imposed by computing power. However, with the development of the backpropagation algorithm in the 1980s and ever-faster computers becoming available, new research in practical applications of ANNs has been pursued in the last two decades [Hagan, 1996]. Potential applications exist in many industries. However, due to the unique challenges with direct measurement, data availability and data reliability in the oil and gas industry, ANN's can be a particularly useful tool for petroleum engineers [Mohagegh, 2000].

ANNs have been successfully applied to a range of problems in the oil and gas industry. They have been used for automation of log interpretation [Chawathe, 1994], 'intelligent' seismic inversion [Artun, 2005, and Balch, 1999], characterization of fracture networks with geomechanical stress conditions as inputs [El Ouahed, 2003], and reservoir characterization from production history [Ramgulam, 2007]. ANNs have also been used for automation of some of the data-preparation and data-interpretation required in analysis of relevant-time production data and screening of noise from downhole equipment [Aggrey and Davies, 2007]. In all these cases, the ANN is able to supply an advantage either in accuracy, required computational time, or required human input.

ANNs have also been used to predict pressure drop in production and surface tubing [Osman, 2001, 2005]. In this work, pressure histories, fluid characteristics, and tubing designs from a broad selection of different wells and fields were integrated, but the work focused on volatile oils with low GORs (similar to those fluids used for construction of semi-empirical correlations), and also used relatively shallow, relatively low-pressure, and

vertical wellpaths. This is reflected in the data summary reproduced in Table 1. Because of these relatively ideal conditions, this study only serves as a first step in the area of an ANN solution for prediction of pressure drop in real flowing wells. While study of vertical, low-gas wells serves as a useful starting point, the practical applicability of an ANN developed specifically for prediction of pressure drop in those cases is marginalized by the availability of the data from which the ANN was trained- that is, directly measured bottomhole pressure. However, modern deviated wells offer an important application for such an ANN, because downhole pressure gauges are, by necessity, installed as much as several thousand feet above the perforations to be observed. In this case, a successfully trained ANN tool would be able to predict 'true' flowing bottomhole pressures without having to rely on semi-empirical lift correlations that are sometimes unreliable and inaccurate.

A range of other successful ANN applications are shown in literature. For example, Chawathe (1994) designed a Kohonen self-organizing network to classify lithologic units from well logs at whole-field scale. In this case, the use of the ANN helped avoid the problem of 'localized solutions' common to traditional well log interpretation, wherein spatial variation in rock properties may be exaggerated.

Recent literature also includes research on analysis and prediction of multiphase flow phenomena in pipes, but focuses specifically on horizontal flow as in surface equipment. These applications successfully used ANNs to identify flow regimes, predict slugging and calculate pressure drop in a variety of circumstances. However, deviated flow applications have not been pursued. In this thesis, they are successfully modeled with an ANN and favorable results highlight the importance of curvature.

Table 1: Well performance data used in previous ANN studies, reproduced from Osman, E.A., et al., 2005.

In addition to the fact that data used in this previous study came from vertical wells only, other input data here represents significantly less intense non-linearities: shallower, lower pressure and significantly lower gas rate wells, combined with a simpler phase behavior (volatile oil to black oil range) than the retrograde phase behavior of the gas present in the Auger field. While the authors were successful in modeling flowing pressure drop in these vertical oil wells, the addition of well directionality and phase / flow-regime transition (gas at perforation to mist-froth at wellhead) represent significant nonlinearities in the pressure drop calculation that were not modeled in the work of Osman, et. al.

	Training Data			Validation Data			Testing Data		
Property	Min.	Max.	Avg.	Min.	Max.	Avg.	Min.	Max.	Avg.
BHP, psi	1227	3217	2222	1911	3124	2517.5	1906	2984	2445
Oil Rate, STB/D	280	19618	9949	469	17243	8856	840	16437	8638.5
Gas Rate, mscf/D	33.6	13562.2	6797.9	81.6	12586	6333.8	134.4	8278.1	4206.2
Water Rate, STB/D	0	11000	5500	0	9300	4650	0	10500	5250
Depth, ft	4550	7100	5825	4964	7043	6003.5	4550	6933	5741.5
API gravity	30	37	33.5	30	37	33.5	30	37	33.5
Pwh, psi	80	780	430	95	960	527.5	180	750	465

Chapter 3: Problem Statement

This work outlines the development of an artificial expert system that can be used to predict flowing bottomhole pressures in highly deviated, high-rate condensate gas wells, given commonly measured wellhead data. While the problem of pressure drop in producing tubing has been an important area of study for many years, highly directional wells and phase change of reservoir fluids in production tubing cause significant unreliability in existing correlations, particularly in the case of liquid hold-up from retrograde gases. Consequently, downhole instrumentation has increased in popularity in recent decades, but directional wells often restrict setting of downhole gauges near the perforations. In the case of the data used to train the artificial expert system described in this work, permanent downhole gauges are in fact positioned as much as two thousand feet above perforations. This necessitates computation of flowing bottomhole pressures despite the presence of instrumentation.

Literature shows several examples of the capabilities of ANNs recognize the influences of a diverse mix of inputs to associated dependent outputs [Mohagegh, 2000]. Here, the concept of the inverse solution was used to train the network by supplying wellhead pressures, rates, and static well description parameters as inputs, and allowing the network to 'map' these inputs to associated downhole-gauge pressures recorded at corresponding dates. The resulting network predicts downhole pressures at gauge depth given wellhead-recorded pressure and the associated fluid production rates, in addition to angle and deviation parameters.

In addition, the ANN was able to predict 'true' flowing bottomhole pressures given a remote pressure reading, associated rates, and static parameters describing only the portion of the well between the location of the remote pressure reading and perforations. Because well deviation and hole angle are largest in the portion of the well beneath the pressure gauge,

the values of angle and deviation parameters used in the original training process were normalized to too small a value, and had to be revised to accomplish this. Similarly, 'true' bottomhole pressures are greater than that recorded at any other point in the production tubing. The highest normalized gauge pressure, a value of 1 in the original training process, is still roughly 80% of the greatest 'true' flowing bottomhole pressure. This results in physically unrealistic predictions when extending ANN predictions past the depth of the gauge. The original training data was therefore revised such that predictions of pressures outside of the original training ranges (in terms of input pressures, angle parameters and deviation parameters) would produce meaningful values. Input pressure values proved most effective when normalized to a value 30% larger than the largest available parameter in the training data. In contrast, the average angle parameter was most effective when normalized to 90°, and the average deviation parameter was normalized to the effective deviation of a wellpath at exactly 45° from vertical- the square root of two.

This produced physically meaningful predictions of true flowing bottomhole pressures. However, unlike the initial goal of 'mapping' pressure drop between gauge and wellhead with the ANN, field data to compare the ANN output with is not available- hence the need for the ANN. In order to understand the advantages of the ANN output over both uncorrected downhole gauge data and pressures corrected by more traditional means, three history matching studies are carried out on the same reservoir.

In this process, core data is largely used as a starting point, and pressure and water production rate histories are used to tune the matching process. The final matches show reservoir properties that are highly incompatible with the original core and RFT data from both the match to uncorrected data and to lift-table corrected wellhead pressure response, but show sensible values can be produced by matching to ANN output.

Chapter 4: Solution Methodology and Training Data

In experimenting with different computational approaches to understanding or analyzing any field phenomena, importance of the field data to be used is critical. In the case of some studies, the amount of noise present may be important however, literature suggests that ANNs are generally successful at becoming robust to noise, given effective training data [Mohagegh, 2000]. However, in this case, the input data to be used has some unique qualities as compared against other studies in the literature. Many other studies (both those of ANN's and of mechanistic or semi-empirical models) pool data from various different wells and fields; this study instead seeks to create a highly accurate model of a representative well within a given field.

The data used to train the artificial expert system in this study comes from a deepwater Gulf of Mexico (GoM) field called Auger. The Auger field consists of multiple stacked pays which are turbiditic in nature, and exhibit the unconsolidated sandstone lithology common to GoM turbidite sands. This study focuses on two similar shallow pays, the N and O Sands. These sands both contain a similar retrograde-like 'rich' gas, which makes them ideal for this study. Also, as the wells in both are significantly deviated and the sands are similar in terms of depositional environment, the data from all six instrumented / observed wells in these shallow sands can be pooled into a common training data set for the artificial expert system.

The fluid composition found initially in the shallow sands of the Auger field (the N and O Sands are the focus of this work) has significant implications for the complexity of any engineering analysis to be conducted on this field. Two exploratory-well RFT reports suggest compositional grading in the O Sand; meanwhile, the N sand exhibits a similar overall composition. Another particularly noteworthy characteristic is the relatively high fraction of heavies (C_{10+}) in all three RFT reports.

While these wells have produced since the mid-1990's, due to some of the difficulties posed by this reservoir, there are still some questions regarding reservoir compartmentalization and potentially unswept regions left behind sealing or partially sealing faults. With these questions in mind, the problem of more accurate prediction of bottomhole pressures can be framed as an effort to better understand the reservoir used in the sample field application of this work. To that end, a history matching study is conducted with 3 sets of data: uncorrected pressures as recorded by the downhole gauges, wellhead data corrected by different lift correlations, and finally, with 'true' flowing sandface pressure as predicted by the artificial expert system.

4.1. Gauge Setting Depth

The gauges in the wells producing from the shallow sands at Auger are placed as much as 1600 ft (TVD) or 2500 (MD) above perforations. This is partly by design, as instrumentation in directional deepwater wells is often `flowed` into place- That is, pushed into place by fluid. Because of this, the gauges will be set in such a way that they stand a lower chance of becoming stuck because of the slimming of the casing in highly-deviated wells. While prevention of stuck equipment is certainly important, downhole gauges that are intended to monitor sandface pressures face a built-in limitation when installed in this fashion- in some wells, the slimming of the hole may occur too shallow for the gauge to directly read bottomhole pressures and will instead read a 'proxy' value that can at least be checked against lift correlations in calculation of flowing bottomhole pressures. The Auger wells are a good example of the drawbacks of this approach. The placement of the downhole gauges [**Figure 1**] this far from the perforations means that there is a significant frictional pressure drop in the tubing.

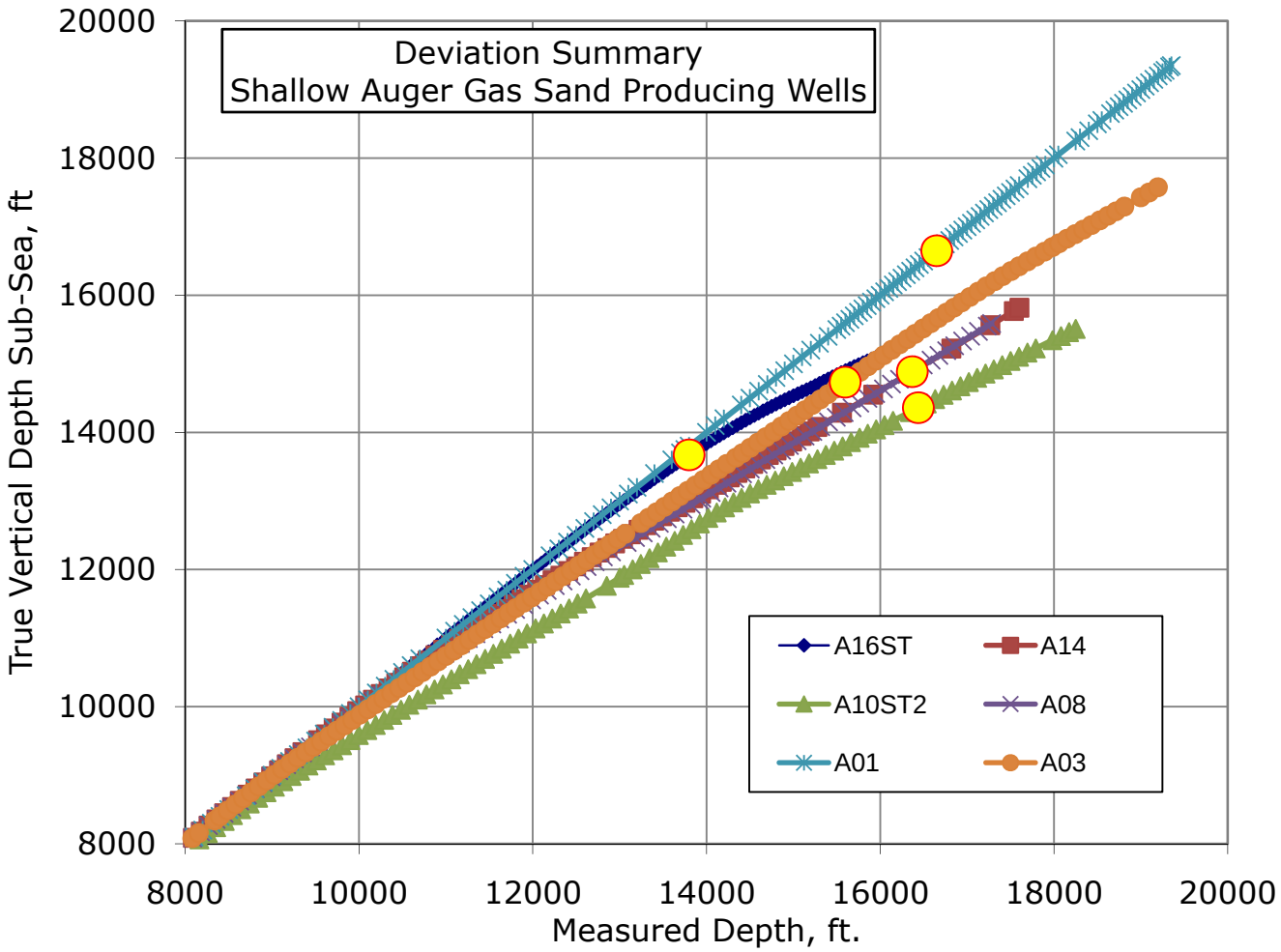

Figure 1: Deviation Summary, Auger Shallow Gas Sand Producers

Filled circles denote gauge placement. In the case of the shallow sands, wells are vertical or nearly-vertical from sea floor to approximately 8000 feet TVD. At this point, wells are 'steered' to precise targets, which results in increasing deviation and consequently, 'slimming' of tubing and associated changing of slugging, mist, and holdup conditions. Gauges installation depth is limited due to well curvature, meaning that downhole-gauge pressures are not measured at the producing formation.

Therefore, despite the advantage of installation of gauges in these wells, the information supplied by these gauges is incomplete. While this pressure drop between gauges and perforations might be considered a measurement error, it is an error that is correctable, given a reliable method for computation of flowing frictional pressure drop. The classical approach to this problem is the calculation of flowing frictional pressure drop through lift

correlations. In this way, the readings of the gauges could be corrected to the formation depth and more closely represent flowing sandface pressures. These corrections to pressure, however, are only as valid as the frictional pressure drop calculations used to produce them.

4.2. Fluid Behavior

The retrograde condensate gasses in the shallow sands of the Auger field were noted early on as an unusual feature in the field: see sample compositions as measured by RFT tools in Table 2.

Table 2: RFT-Reported Initial Compositions, 471-1 (N and O Sands) and 426-1BP3 (O Sand)

Initial compositions are reported by pre-production RFTs. The significant difference in C_1 and C_{10+} fractions suggest compositional grading in the O Sand. Reservoir compartmentalization is another possible interpretation of these compositional differences, but similar producing GOR's and pressure communication between producing wells better supports a conclusion of compositional grading. While additional RFT reports for the N Sand are unavailable, similar behavior such as increasing condensate yield over time in production history suggests that the N Sand is also compositionally graded.

Well Name	471-1	471-1	426-1BP3
Sand	N	O	O
SAMPLE DEPTH (ft, TVDSS)	15386	15954	16177
	Mole Percent	Mole Percent	Mole Percent
Methane	78.26	78.13	73.94
Ethane	5.44	5.54	6.09
Propane	3.03	3.01	3.54
Isobutane	0.68	0.7	0.76
n-Butane	1.47	1.5	1.8
Isopentane	0.66	0.69	0.79
n-Pentane	0.85	0.88	0.96
Hexane	1.55	1.59	1.62
Heptane	1.33	1.23	1.62
Octane	1	1.09	1.43
Nonane	0.82	0.86	1.1
Decane +	4.91	4.78	6.35
(SUM)	100	100	100

Further, though composition information is limited, two early fluid samples in the Blue "O" Sand suggest compositional grading, as demonstrated by significant change in heavy fractions— notice C_{10+} readings at two different depths in the O Massive Sand. Over the life of these high-rate, water-driven gas wells, water sweeps updip from the aquifer, and the produced gas and increasing condensate yields over time reflect a change in gas composition between original well locations and original gas-water contact. The resulting phase behavior of these gasses falls into a range that would ordinarily be described as a retrograde condensate. However, due to significant pressure support (see characterization paper. Bohn et al., 2008, and reservoir model discussion), pressures in the formation do not seem to reach the fluid's dew point. This produces a higher-than-ordinary density, single-phase gas at reservoir conditions, as opposed to the true retrograde condensate fluid that might be expected based on PVT. Modeling of these fluids is something of a quandary, as gas to oil ratios through producing life falls between strict definitions for volatile oils and rich gasses. Additionally, the high GOR of 5000+ SCF / STB falls outside the ranges considered by researchers through the 1970s, when the majority of the commonly-used semi-empirical correlations were developed using approximate laboratory studies based around kerosene-water experiments [Brown, 1977]. Converting to a condensate yield demonstrates another reason this fluid is difficult to classify, as condensate yields range from 200-400 STB / MMscf [**Figure 2**].

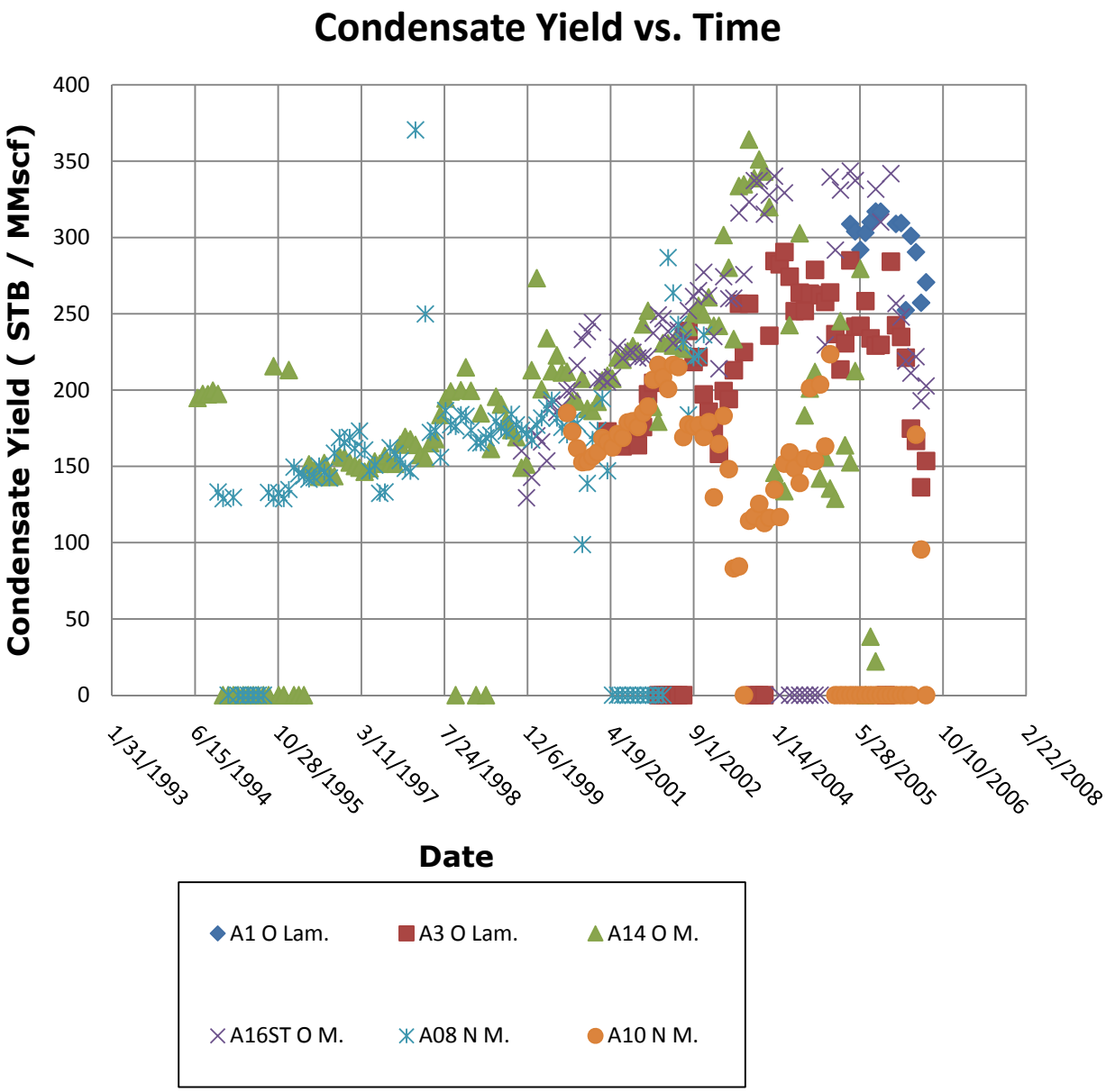

Figure 2: Condensate Yield Change over time, Auger Gas Sands

The condensate yield increases over time and follows a similar trend in three distinct sands, the N Massive, the O Laminate, and the O Massive. Together with this history, the different compositions observed at different depths in exploratory well RFT's suggest compositional grading as opposed to reservoir compartmentalization. An additional implication is similar fluid sourcing / migration pathways.

Also, while reservoir pressures remain high enough that liquid drop-out in the reservoir is limited, the pressure in the production tubing drops far

enough under some conditions to allow liquid drop-out in the well. See composition and phase behavior P-T diagrams, [**Figure 3**].

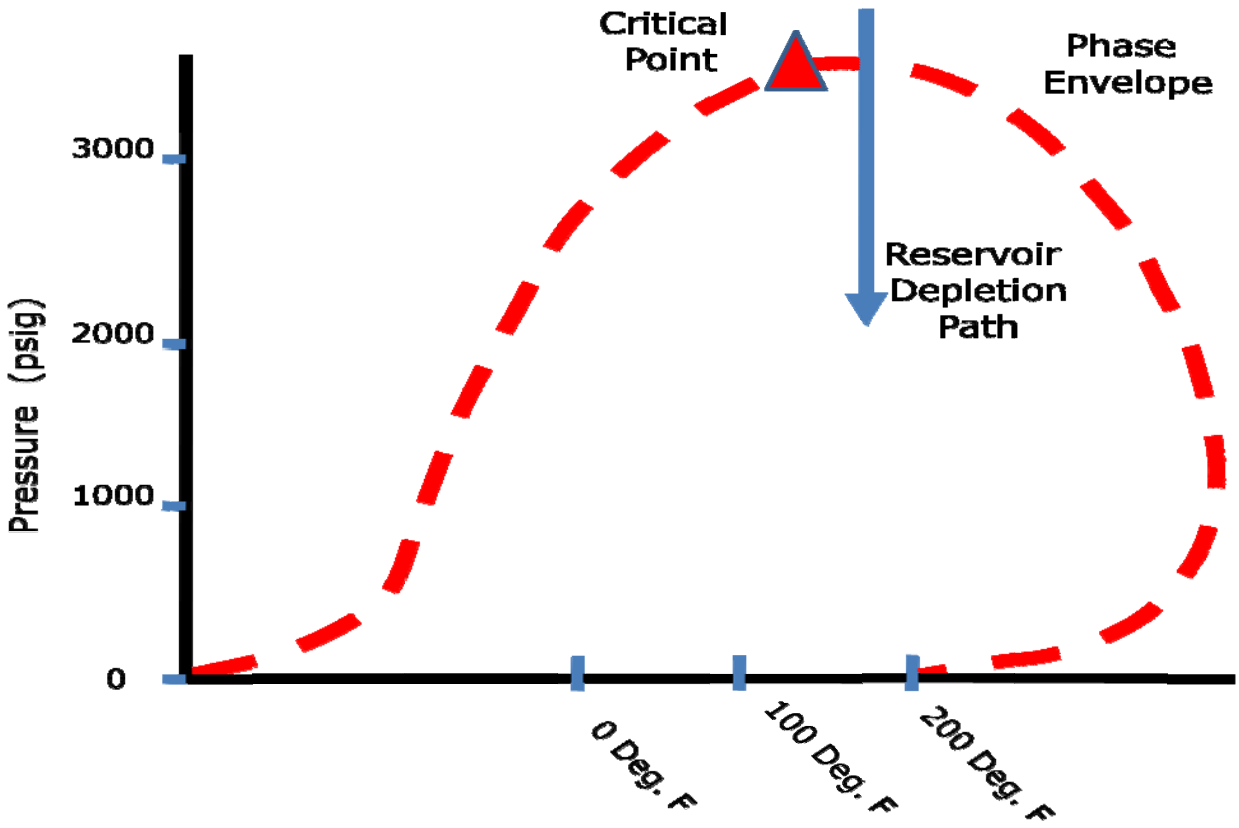

Figure 3: Representative Reservoir Fluid Phase Envelope

Using Peng-Robinson Equation-of-State, fluid phase behavior is computed from RFT samples. Though the RFT samples exhibit some variation, dew point pressure does not vary significantly. This phase envelope serves as a good representation of the 'average' behavior of this field.

For this study, a black-oil model was used, based on the assumption that the reservoir pressure would not decrease to dew point through the producing life of these wells. This assumption is supported by DHPG data that, excluding unreliable points, show gauge pressures remaining significantly above dew points indicated by phase behavior modeling [**Figure 4**].

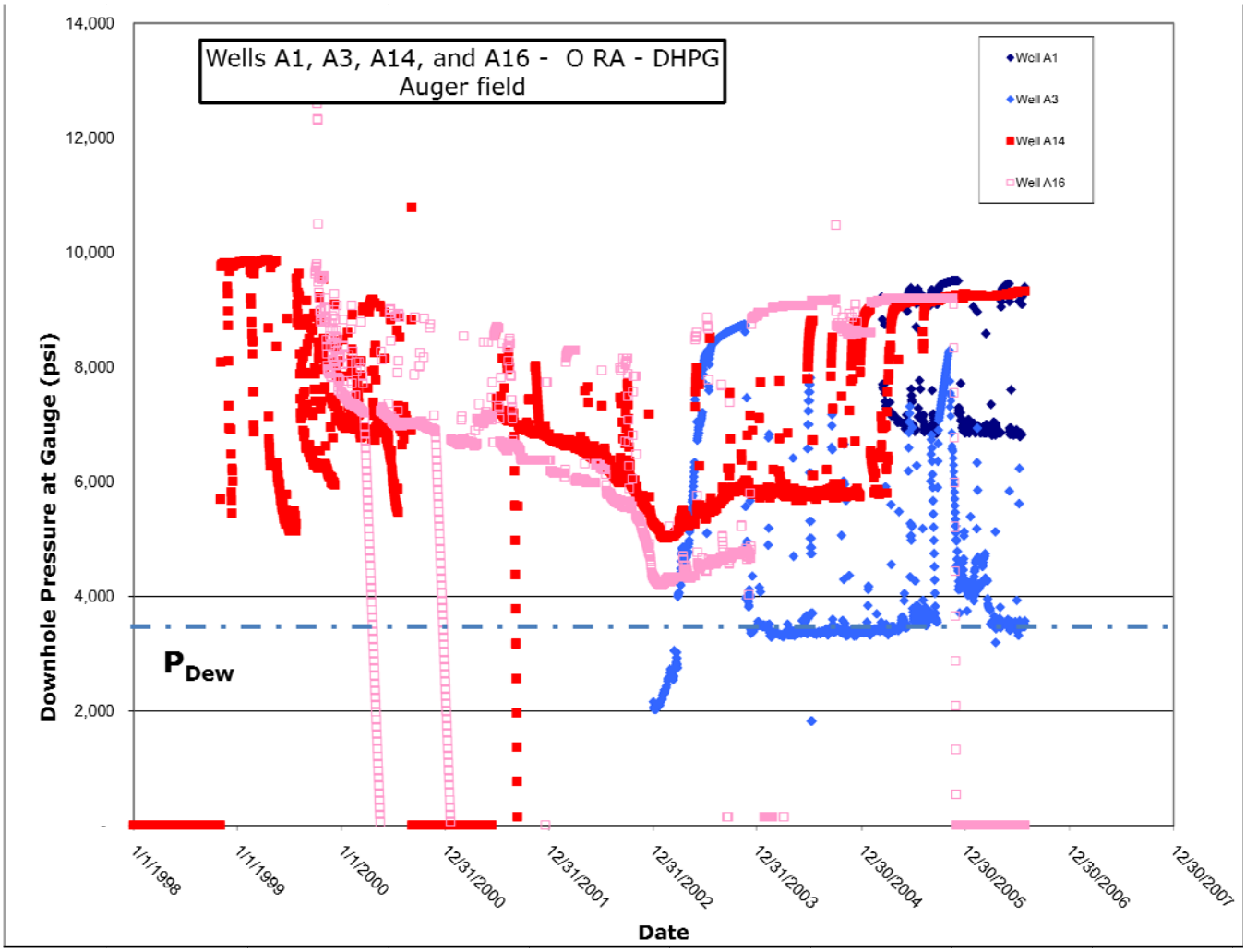

Figure 4: Permanent Downhole Pressure Gauge recordings, Auger O Sand

Plot of pressure histories recorded by downhole pressure gauges in positions marked on **Figure 1**. Additionally, the dew point pressure calculated by phase behavior modeling, shown in **Figure 3**, is plotted in blue. Outside of suspicious and obviously erroneous points, the pressures recorded at gauges are entirely above dew point. Therefore, this fluid is most appropriately classified as a retrograde gas or 'very wet' gas, because phase change does not occur in the reservoir, but instead in the production tubing.

Chapter 5: Artificial Expert System

In terms of strategy, the ANN approach to the Auger gas VLP problem was applied in such a way as to make it flexible and adaptable to two different modes of application: The neural network was designed to model a representative well, which could then be applied to other wells in the same field. To this end, data from all wells was combined into one training set. However, generalizing the model for several wells requires creation of several parameters that represent the degree of the curvature in the well caused by deviated wells.

1. Use as a classic nodal-analysis approach. That is, the neural network could be used as a simple calculation of flowing frictional and gravitational pressure losses from one node to another.
2. In addition, the neural network should be adaptable to a simple wellhead-to-formation pressure loss calculation. This would allow its use as a plug-and-play prediction of P_{bh} from P_{wh} for any new wells in a given field.

The only requirement is a small series of wellhead data combined with corresponding bottomhole data. In theory, a welltest could be used to 'calibrate' an artificial expert system by this approach, then used for all future predictions of bottomhole pressures. The approach could also be extended to prediction of condensate-drop-out and gas evolution in wellbore flow.

The design of the neural network was intended to be flexible, so that it can be 'trained' with information generally available in modern wells- a series of bottom-hole pressure measurements, wellhead-pressure measurements, and production rates combined with some static parameters that describe tubing design and well plan (Appendix C).

In the example outlined here, the artificial expert system is trained with data from multiple wells simultaneously. In this way, a general system that is applicable for any well in this field with the same tubing design is created. While this system is only applicable to the Auger field, the approach could be applied to create an artificial expert system effective for other fields.

Artificial Neural Network experiments were carried out with the MATLAB[1] neural network toolbox. The ANN experiments were carried out in three stages:

1. A computationally and architecturally simple neural network was constructed and trained with only one dynamic parameter. Experiments for this phase used a variety of different architectures, but relied on linear transfer functions and raw data. Because of this, success of this stage was limited. This is largely due to the dominant magnitude of the pressure and depth values (10^4 psi) in comparison to the values of well plan parameters (10^{-1}, dimensionless); with linear transfer functions this lends the pressure and depth values dominance. In addition, the only dynamic input parameter used in this early stage is gauge pressure, leading to a network that is indifferent to watercut and flowing liquid / gas ratios.

2. More complex networks were obviously needed. The main step in designing these networks was the normalization of input and output data. Without normalized data, the use of non-linear transfer functions is ineffective because values greater than 1 as input return a maximum value of 1 from log-sig and tan-sig transfer functions. While this does not return errors in the training process, the resulting weights and biases show the smaller-magnitude inputs being

[1] Matlab Version R2006a, The MathWorks, Inc., Natick, Massachusetts.

'swamped', or reduced to nearly 'noise' levels, by the larger-magnitude inputs. In this case, bottomhole pressures on the order of 10^4 being used alongside watercuts of the order 10^{-1} meant that normalization was absolutely necessary.

3. In making predictions looking downhole from gauges (a nonlinear 'extrapolation'), the network needed to be able to predict flowing frictional pressure for more severe hole angles. This involved changing the normalization parameters such that the average hole angle parameter is maintained at a value between 0 and 1 (log-sig and tan-sig transfer functions are not effective with input values outside the range –1 to +1), for example. Similarly, pressure and deviation normalizations required adjustments as well.

In designing network architecture, care was taken to avoid excess computational expense. For example, the number of hidden layers and neurons were kept as low as possible. Also, though this decision limits availability of training data, only field data was used in the training process. The purpose of this restriction is to ensure that this approach can, if successful, be applied to any field and any reservoir fluid without major changes.

In all experiments, roughly 10% of available data was set aside for validation. The 10% used for validation were randomly re-selected before beginning each new stage in the ANN development; This was done with the intention of maximizing use of data, as two hundred and one input-output sets were available for ANN design.

5.1. Stage 1: Initial Experiments

Notice that the Stage 1 ANN uses only two dynamic parameters, BHP and P_{wh}. This is intended to test the response of the network over the life of the well; If pressures alone produce accurate predictions (i.e., low training error), then this network is ideal as it uses a minimum of input data. However, intuition would suggest that additional information is necessary- particularly in regard to mixture of flowing phases. Additional parameters are included in later evolutions of the ANN.

5.1.1. System Design Details

The first attempt at an effective network used a simple array of input values in a 3 layer network. The input parameters are shown in **Figure 5**.

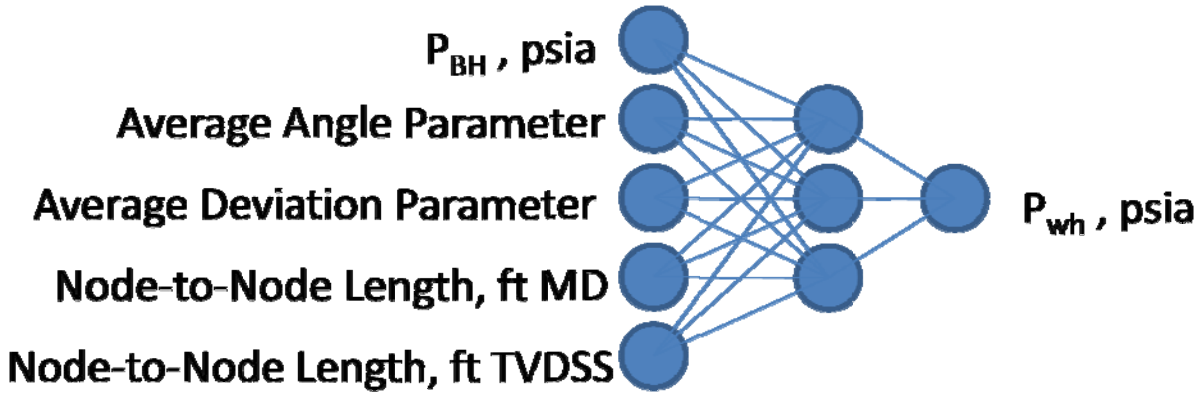

Figure 5: Conceptual Diagram of Stage 1 ANN

Input parameters used in this stage of ANN experiments are shown. An important distinction at this stage is the exclusion of dynamic parameters other than wellhead-pressure.

This first-pass network had difficulty modeling pressure drop as watercut increased. This was an expected result due to the limited range of input parameters included- This was merely a test of the effectiveness of the static input parameters developed to model well deviation, and included no

dynamic parameters other than bottomhole pressure and wellhead pressure. However, it did establish the validity of the static well plan parameters developed. Static input parameters are:

- **Node-to-node length**, in feet of measured depth: This is effectively both a flowing tubing length as well as a functional link to radius of curvature.
- **Node-to-node length**, in feet of true vertical depth. This helps account for pressure loss due to fluid density, or gravity; Also, inclusion of true vertical depth node-to-node length helps tie together measured-depth length and the following parameters representing deviation and inclination.
- **Average Deviation Parameter** (dimensionless), α_{dev}. This is a functional link between node-to-node lengths, and serves as a proxy for curvature. This parameter is calculated as a length-weighted average of the ratio of measured depth to true vertical depth, between the two endpoint nodes in question.
- **Average Angle Parameter** (dimensionless), $\alpha_{\emptyset}$. This is again a length-weighted average of dip angle in the well. However, this parameter was originally normalized to the maximum angle available in the well set. Moving forward, a more flexible definition was adopted; Instead of normalization by maximum average angle parameter in well set, the length-weighted average dip angle is divided by 90 degrees. The reason why normalization is needed is described in following sections.

The artificial expert system consists of a Matlab ANN toolbox-designed three-layer network using tan-sigmoid / log-sigmoid / tan-sigmoid transfer functions and proved successful for 0-watercut parts of the well history. It is

interesting to note that the pressure drop in the well, though clearly heavily affected by watercut for example, is not significantly affected by the lack of tubing information in the input parameter set. This is most likely because these wells share the same general tubing design, and, for a given distance, pressure drop is more heavily influenced by the well trajectory and deviation. This is evidenced by the satisfactory performance of the network considering its simplicity. However, to deal with the more complicated flowing conditions present with increasing watercuts and changing gas composition (and with composition, condensate yield), a more complex network was necessary.

5.2. Stage 2: More Advanced ANN Designs

In order to use log-sigmoid and tangent-sigmoid transfer functions, input and output data had to be normalized. Use of normalized data facilitated the addition of rate information to the list of input parameters: condensate rate, gas rate, water rate, and watercut. This is due to the difference in magnitude of values of, for example, gas rates (10-70 MMscf/d) and bottomhole pressures (thousands of *psia*). In addition to these wellhead rate data, the four static parameters used in Stage 1 were used in this phase as well. This results in a new input vector composed of the original four static parameters from Stage 1, bottomhole pressure, and oil rate (STB / D), gas rate (mmscf/D), water rate (STB / D), and water cut ($STB/B_{oil,\ eqv}$), represented in the new conceptual arrangement shown in **Figure 6**.

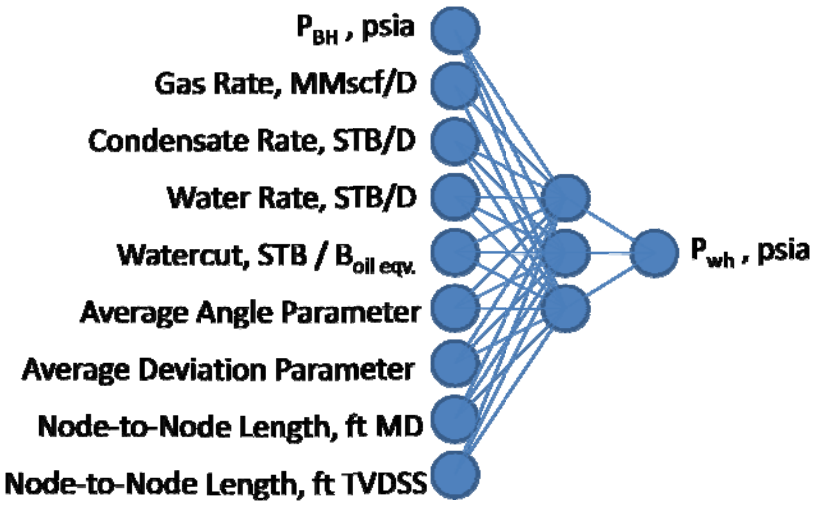

Figure 6: Conceptual Diagram of Stage 2 ANN

Sketch of the Stage 2 ANN. This network used log-sigmoid transfer functions in conjunction with a new input vector. This new input vector carries additional dynamic information as compared with the Stage 1 ANN, which did not include fluid rates or watercut- only P_{wf} and static parameters.

As discussed above, the Stage 1 ANN showed a nearly-constant pressure drop from gauge to wellhead for a given well. Due to the simplicity of the input vector used in Stage 1, the lack of system response to shut-ins, slugging, or increases in watercut is intuitively unavoidable, as the ANN was not provided any data by which to identify such phenomena. By comparison, the low training error values of the Stage 2 network suggest that this architecture is successful at capturing dynamic effects [**Figure 7**].

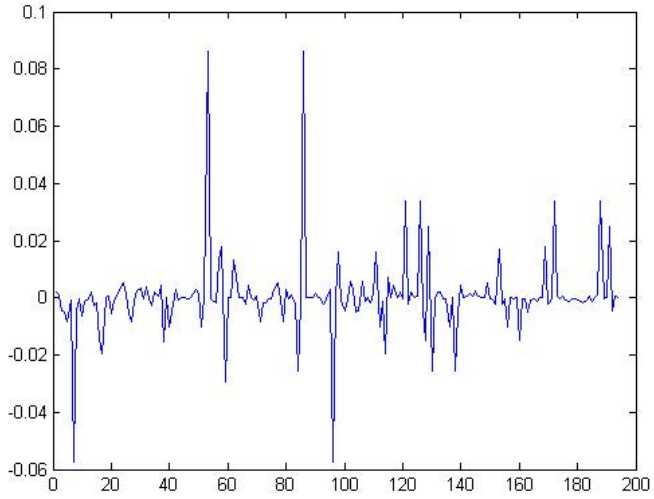

Figure 7: Training errors from Stage 2 ANN

Training error results of Phase 2 network. Training error is particularly low, with average error less than 3%.

This is a direct result of the inclusion of rate data for each phase and a functional link between gas rate and water rate. The crossplot of the resulting ANN output compared to field observations [**Figure 8**] shows a strong correlation between the two, indicating a successful training process.

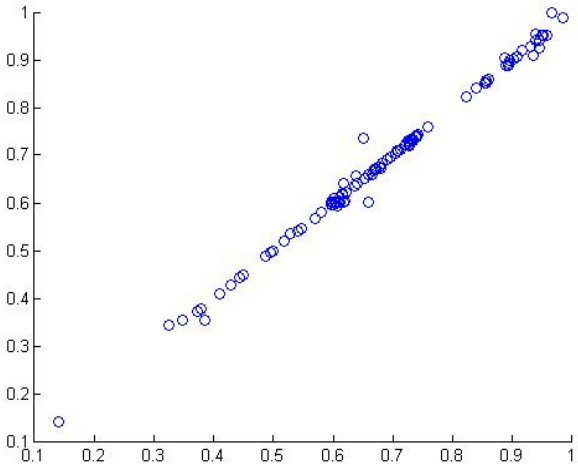

Figure 8: Cross-plot of neural network training results in Stage 2

This traditional crossplot shows results of simulating validation data and comparing trained ANN output to recorded result. Outside of two points, the phase 2 ANN output displays a strong correlation to field measurements.

An important point to note here is that while traditional lift correlations rely on PVT calculations of fluid properties at each node along the wellpath, the ANN is able to achieve success without additional information outside of the directly measured wellhead fluid rates. This, in effect, removes any uncertainty associated with the characterization of fluid behavior, and instead capitalizes on the relatively high confidence with which wellhead rate measurements can be made. The success of the Stage 2 network is largely due to the change from absolute data to normalized data and the change in transfer functions that normalization allows. This means that all of the values in a given input/output parameter's training set are divided by the largest value in the set, resulting in outputs of percentages; in Stage 2, the largest errors are still less than $\pm$10%. This compares favorably to the success of published correlations, for which the standard deviation for predicted pressures at gauge depth is >300 psia across 65 well tests, and the largest errors are as much as 2000 psia (see Chapter 6.2. Comparative Analysis of ANN Performance, and Appendix F: Well Test QC Study on Auger Well).

5.3. Stage 3: Reversal of ANN Prediction 'Direction'

With the effectiveness of the approach proven in a general sense, the final phase of the neural network experiments consisted of reversing the direction of the pressure correction. While stages 1 and 2 predicted flowing wellhead pressure, given bottomhole pressure and associated parameters, the final phase uses the same network trained in the Stage 2 study, but re-trains it to use the same set of input parameters in the opposite direction. That is, the Stage 3 network starts from the Stage 2 network— using the same list of input parameters with the same normalization scheme— except that the input parameter representing the 'known' pressure is actually the pressure read at the wellhead, whereas the output parameter is now the

corresponding pressure at gauge depth. With that done, the trained network was ready for testing of its performance in its intended role- that of a 'true' sandface pressure predictor [**Figure 9**].

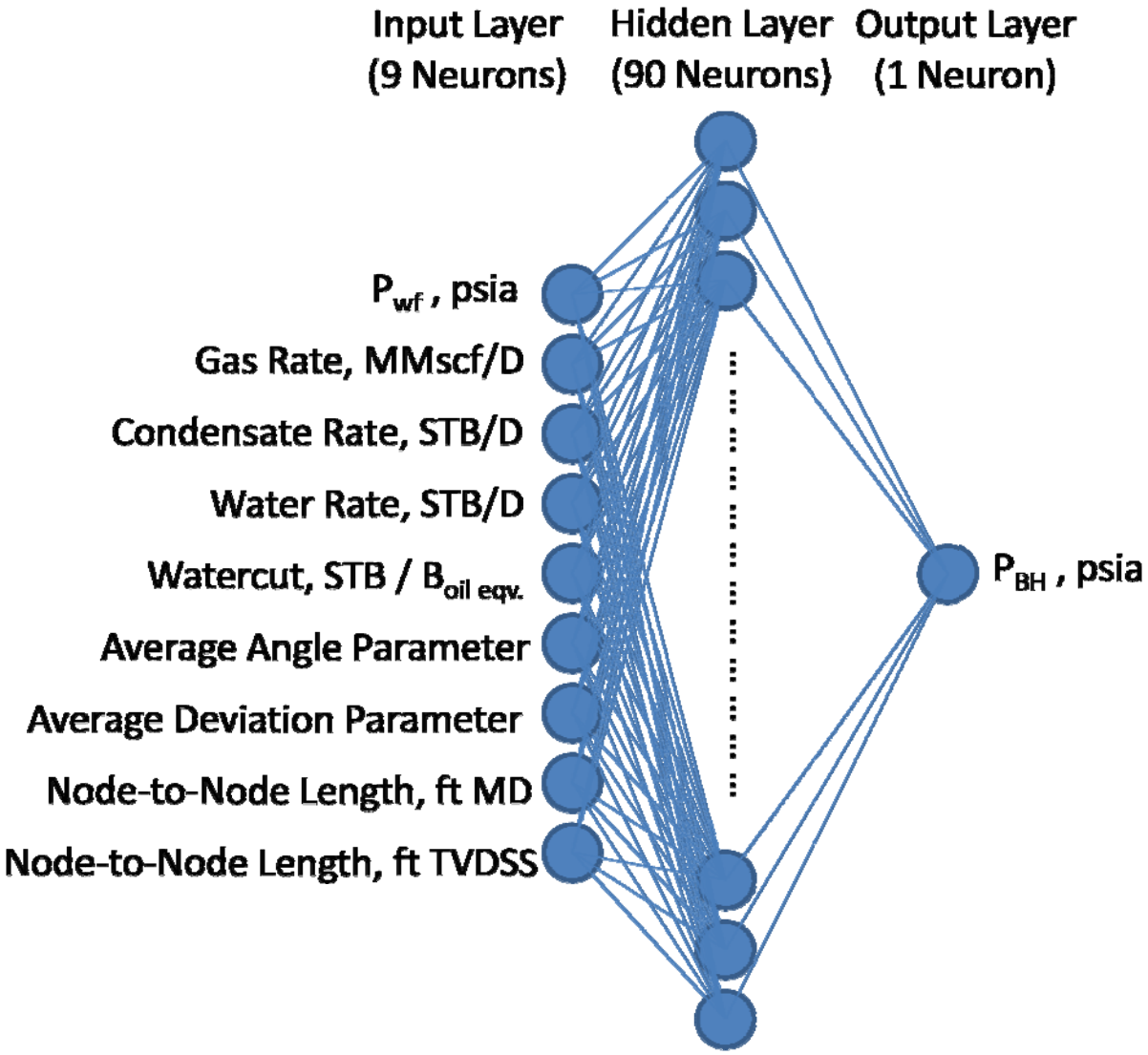

Figure 9: Conceptual diagram of Stage 3 ANN

The ANN architecture used at this stage is nearly identical to the Stage 2 ANN, but reverses the prediction direction.

The change applied in the final stage of ANN experiments is the use of wellhead pressure as an input parameter rather than output. This allows the ANN to become downhole-looking as opposed to the upward-looking design

used in earlier sections. However, experimentation at this phase showed slight improvement in correlation with the addition of hidden layers and increase in number of neurons per layer. Many different ANN designs were considered, but none showed a significant advantage, as all had satisfactory correlation between predictions and targets [**Figure 10**].

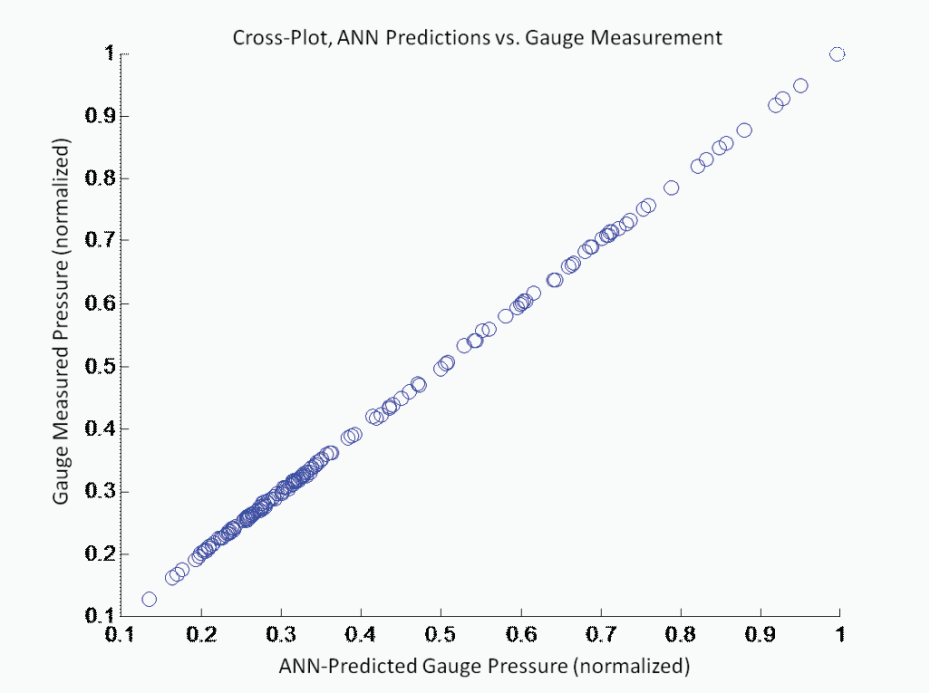

Figure 10: Crossplot of Stage 3 ANN predictions vs. Field Measurements

Crossplot of predicted results vs. field measurements displays a strong correlation of predictions to targets, and indicates a successfully trained ANN, regardless of the reversal of prediction direction.

This in itself suggests that the input parameters 'map' effectively to the output parameter, which is a promising result. Cases considered included as many as seven layers (or 5 hidden layers), as many as ninety neurons per layer, and combinations of transfer functions, none of these showed significant improvement in average training / validation error. Therefore the simplest effective network is selected for the basis of the final experiments. A 3-layer design with log-sigmoid transfer functions proved most effective.

5.4. ANN Prediction of 'True' Sandface Pressures

Though the artificial expert system has now proven effective in mapping pressure drop inside the limits of the data to input parameters, the question of accuracy of predictions looking from gauge-to-perforation remains largely unanswered. While training results show that the ANN is now able to predict pressure drop between the gauge location and the wellhead, the portion of the well between the gauge location and the perforations is more severely deviated than the portion between wellhead and gauge (see **Figure 1** and Appendix C). While obtaining highly-accurate predictions of 'true' sandface pressures is the ultimate goal of this study, the difficulty of measuring true sandface pressures in the case of these wells makes an exact determination of accuracy impossible. Therefore, in order to test true sandface pressure predictions, a new set of corrected history data was created with the trained ANN. The corrected sandface pressure history was then used in a history matching study to compare the quality of the reservoir models constructed using the three different sets of matching data, as described in Chapter 7.

In order to use the ANN in extrapolation mode, normalization parameters required significant adjustment. While rate data remained unchanged, all pressure, angle, and deviation parameters required a new normalization value because the section of well between gauge and perforation is more severely angled / deviated than the section between wellhead and gauge, and the pressure recorded at the gauge is lower than that that would be expected at the perforations.

Normalization parameter for average angle was selected as 90°, but deviation was set at the deviation that would result from a 45° wellpath. While these parameters are not consistent with one another, the ANN requires only that normalization for each given parameter is independently consistent. However, pressure normalization required greater adjustment.

The training data consisted of a set of input vectors containing one pressure each, and an output pressure associated with each input vector. Previously, these pressure sets were normalized separately- that is, the input pressures were all normalized to the maximum pressure in the set of input pressures, and the output pressures were normalized to the maximum output pressure in the set. However, in this case, the training data consisted of a series of wellhead pressures as inputs, whereas the extrapolation inputs were to consist of a series of gauge pressures. This would result in a different normalization scale between training inputs and extrapolation inputs, and render the results meaningless. To correct this, all pressure values, both input and output, were normalized to a pressure 20% greater than the largest pressure value being used in the input set. In this way, the extrapolation becomes possible, though validation of the predictions by traditional means used in ANN studies is impossible (due, once again, to the lack of any direct measurements of pressure at the perforations).

This change in normalization parameters decreased the effectiveness of the training data to some degree in that the resulting crossplot shows more scatter [**Figure 11**].

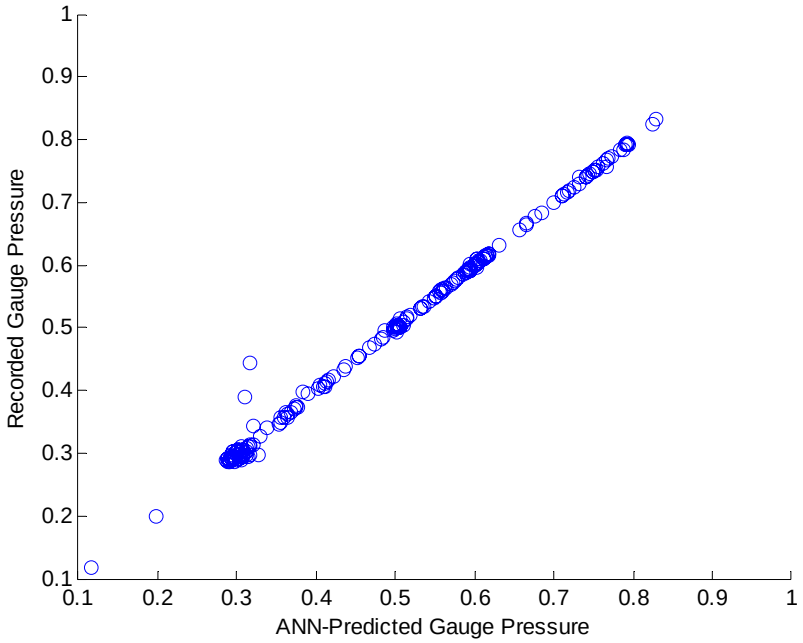

Figure 11: Crossplot of Extrapolation Network Predictions

Crossplot representing the near 1-to-1 correspondence of ANN predictions to recorded data. However, it may also indicate some problematic areas in the training or noise in the training data. The problematic points coincide with the middle-to-low pressure gauge recordings.

Though the 3-layer network architecture was maintained because additional layers tended to cause memorization, the number of neurons in the hidden layer was increased to 90. However, average error remains at an acceptable level, 1.5654e-005 (normalized), or roughly 0.18 psia. This demonstrates that the reliability of the network in predicting gauge pressures has not been negatively affected by the change in normalization parameters. Therefore, the network maintains the flexibility of being used both in a node-to-node fashion and as a 'true' bottomhole pressure predictor in extrapolation mode. It is also noteworthy that this final error value is an improvement of four orders of magnitude over the errors in empirical correlations.

Results and Observations

This section has described various experiments used to develop the artificial expert system. The training successes alone indicate that the problems of wellbore deviation and phase change can be recognized by the ANN, and given sufficient data, this ANN could successfully predict gauge pressures in an interpolation application. This could be used to check gauge data or duplicate gauge data in the case of malfunctioning downhole equipment.

Additionally, some important conclusions can be drawn from the weights of the trained network [**Figure 12, Figure 13**].

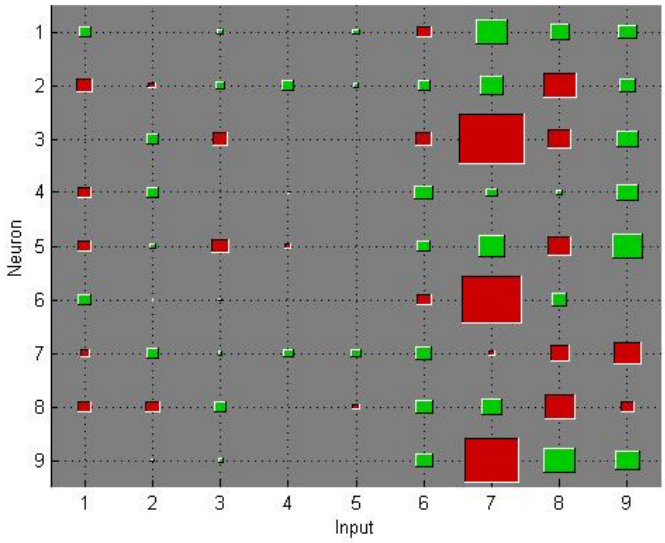

Figure 12: Hinton Plot of Weights from First (Input) Layer, Extrapolation Network

Weight magnitudes are plotted with size of square representing magnitude, and color representing sign- green is positive, red is negative. These weights indicate strong sensitivity to both input 1, input pressure, and input 7, Deviation Parameter. From a sensitivity perspective, this is an important result, as it explains the difficulties in adapting pressure drop correlations developed for vertical flow to a deviated flow model (see Chapter 6). Inputs 8 and 9 also show significance, which is in accord with most published work on the subject- generally, 90% of pressure drop in a flowing well is assumed to be static head, and friction would therefore account for only 10%. However, the larger weights of the deviation parameter indicate that this is more significant than either MD or TVD node-to-node length, which is a significant disagreement with accepted knowledge on the subject.

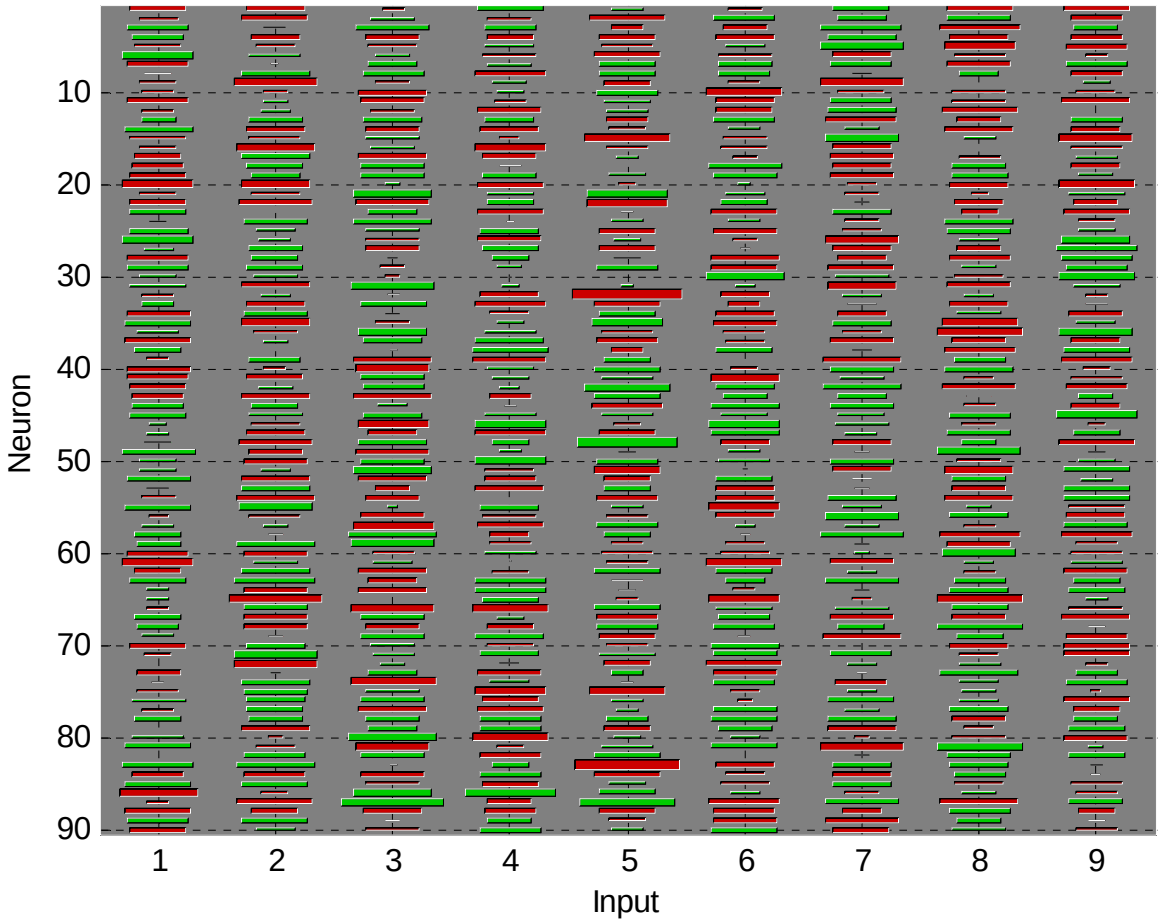

Figure 13: Hinton Plot for 90-neuron Middle, or 'Hidden', Layer, Extrapolation Network

Hidden-layer Hinton Plot from final, 'extrapolation' network design plots the larger weights which have been applied to other parameters as well as the deviation parameter (Input 7) as shown from the Layer 1 weights after training.

Particularly, the impacts of the deviation parameter (Input 7) and, to a lesser extent, average angle parameter (Input 6), both demonstrate a marked break from accepted knowledge on the subject. Generally, the pressure drop in production tubing is assumed to be the sum of static head and frictional loss (no acceleration is usually assumed), with a weighting of roughly 90% and 10% respectively. The deviation parameter, however, likely alludes to the fact that liquid loading / holdup can occur in the sections of tubing with the most curvature, and this in turn has the most significant

impact on pressure drop for a given length of tubing. Though the final network arrangement selected was a 3-layer backpropagation network, several other architectures were tested, and led to similar conclusions in terms of relative significance of inputs [**Figure 14**].

The other weights involved have a comparatively smaller impact on the overall pressure drop involved, but unlike the impact of the deviation parameter, this is in agreement with common knowledge. That is, if static head accounts for roughly 90% of pressure drop at a 'low' production rate, but a 'high' production rate increases friction head such that the ratio becomes 89/11 static-to-frictional, then the rates would be statistically less significant than the node-to-node length.

The network successfully modeled the pressure drop between wellhead and gauge, but absent the deviation parameter, would not have been able to produce reliable results. This problem could be avoided by training an ANN for a single well with extremely high-frequency data, but the problem of changing composition or increasing watercut later in life would prevent construction of an effective training data set for predictions of the same well's performance.

Testing of the network in extrapolation mode requires a different approach. As no directly-measured data exists for true flowing sandface pressures in this case, ANN-predicted sandface pressures are used as history to be matched in Chapter 7.

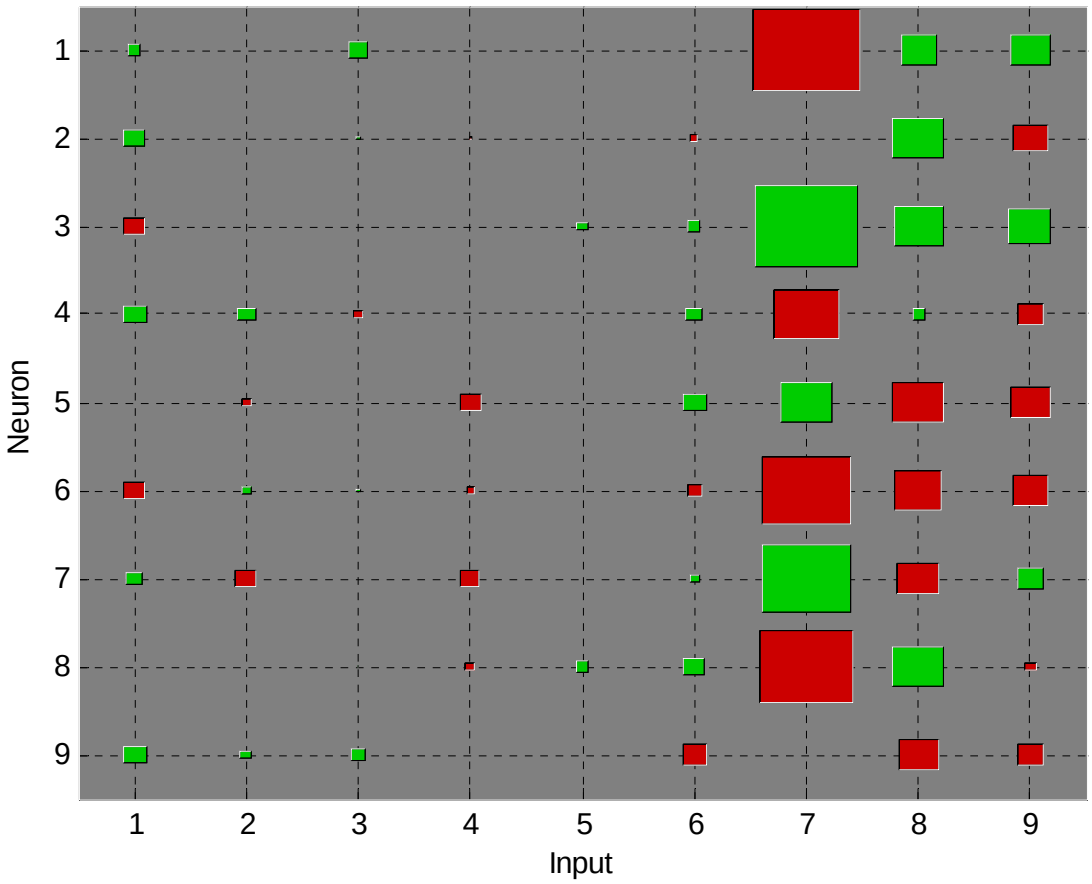

Figure 14: Hinton Plot for first-layer weights from alternate 5-layer network

Weights derived in training of a 5-layer network are consistent with the results of training 3-layer networks. That is, while node-to-node length shows significance in accord with the general knowledge on the subject, the deviation parameter requires larger weights. Despite the consistency with the 3-layer network, training took slightly more computation time than the 3-layer network, while errors were not significantly reduced. Further, the training process required careful supervision to avoid overtraining, or 'memorization', leading to the selection of the 3-layer networks as preferable.

Chapter 6: Comparison to other methods

6.1. ANN Study Recap

In Chapter 4, the details of the neural network design research undertaken to solve the lift problem are described. In short, these involved a progressive increase of network complexity and training data, resulting in progressively improved training results. The end product of this work is an artificial expert system that can effectively reproduce field data for bottomhole pressures, given wellhead pressures, rate information, and some simple static well parameters. To quantitatively compare this with the success of published correlations, a commercial production engineering code, Petroleum Experts Prosper[1], was used to construct lift curves for behavior of the Auger wells under a variety of conditions where original field data was available.

6.2. Comparative Analysis of ANN Performance

6.2.1. Published Work on Flowing Pressure Loss in Producing Wells

The traditional approach to calculation of flowing frictional pressure drop in tubing or surface pipeline has, naturally, been researched heavily since the earliest years of oil and natural gas engineering. Much of this work, however, has focused on problems from which the adaptation to retrograde condensates or 'rich' gasses is not a simple transition. For example, some of the more commonly used published lift correlations (Fancher Brown, Beggs and Brill, Hagedorn and Brown) used only two fluids for their experiments-

[1] IPM 6.0 Prosper v.10.0, Build #109, Petroleum Experts Ltd
Petex House,
10 Logie Mill
Edinburgh, EH7 4HG
Scotland, UK

water and air, kerosene and air, or water and kerosene (Brown, 1977). The equations for oil, water, and gas were then adapted from the relationships established with these experiments. While semi-empirical work is often used with caution, the concerns for accuracy should grow as the conditions of the system to be modeled (actual wells) deviate further from the experiments used to develop the equations.

By the same token, the correlations that use crude oils or true multiphase tubing flow (e.g., Hagedorn and Brown, Orkiszewski), are less applicable in that the ratios of free gas considered are low by comparison to a rich or retrograde condensate gas, as studied in this work. An example is the GORs considered in the examples published by the above authors. Both the examples published by Hagedorn and Brown and Orkiszewski used a GOR of 500 SCF/STB, as compared to the average GOR of the shallow Auger sands (around 5000 SCF/STB when converted from condensate yield). However, these classic correlations are nonetheless used in lift problems throughout industry. While the fact that these correlations are still in use might suggest that they are in fact valid for a larger range of problems, the discussion below will demonstrate the significant error present when these correlations are applied to high-GOR or high-yield condensate as in the Auger field.

In recent years, researchers have sought to improve on the mostly semi-empirical approach taken by earlier studies with mechanistic models (Osman, 2005). However, the vast majority of this work has been shown to produce only limited accuracy, often due to unpredictable interactions between phases and dynamic effects such as hold-up, slugging, and rapid changes in flow regime.

6.2.2. Well Test Quality Control as Correlation Testing Approach

Analysis can be done to ascertain which lift correlations best meet the production conditions in a given field. This process is often called a Well Test Quality Check. The process of 'quality checking' well test data consists of plotting wellhead and gauge pressures, then producing a gradient traverse with lift correlations. The gradient traverse that best meets the recorded pressures (particularly in cases where multiple downhole pressure readings are taken, as in tests of multilayer reservoirs or multizone completions) is assumed to be the most appropriate correlation for the field. Later in life, this process serves to evaluate the reliability of well test results. That is, the process is repeated, but this time with only the 'trusted' correlation plotted as a gradient traverse. Discrepancies at this stage are assumed to identify such things as leaking tubing, completion problems, solids buildup, or malfunctioning downhole equipment. The key assumption in this process is that lift correlations are accurate, but recorded pressure values are of questionable validity.

The large errors found in the process of 'Quality Checking' Auger well tests demonstrate the difficulties in predicting flowing bottomhole pressures for the fluid conditions found in the shallow Auger sands. While the Auger wells produced at a considerably higher rate than many fields, the fluid properties themselves are not outside the normal behavior of retrograde condensates. In a traditional approach to selecting the lift correlation to be used for a given well or field, several short well tests would be analyzed in a 'quality check' process to identify which published correlation best matches the pressure drops observed in the wells. The best match would then ordinarily be 'tuned' to meet the recorded history by small adjustments (up to plus or minus 10%) to either the final density term or the final friction

term in the pressure drop correlations. In the case of Auger data, however, the difficulty of modeling retrograde condensate gasses with correlations originally designed for oil and water or low GORs is evident, as shown in selected well test plots below [**Figure 15, Figure 16, Figure 17**]. In all these QC plots, DHPG 'test points' are plotted along with the extrapolation network's 'true' sandface pressure prediction. While the test points are sometimes within the extremes predicted by empirical correlations, particularly after watercuts increase, some ANN predictions appear unreliable.

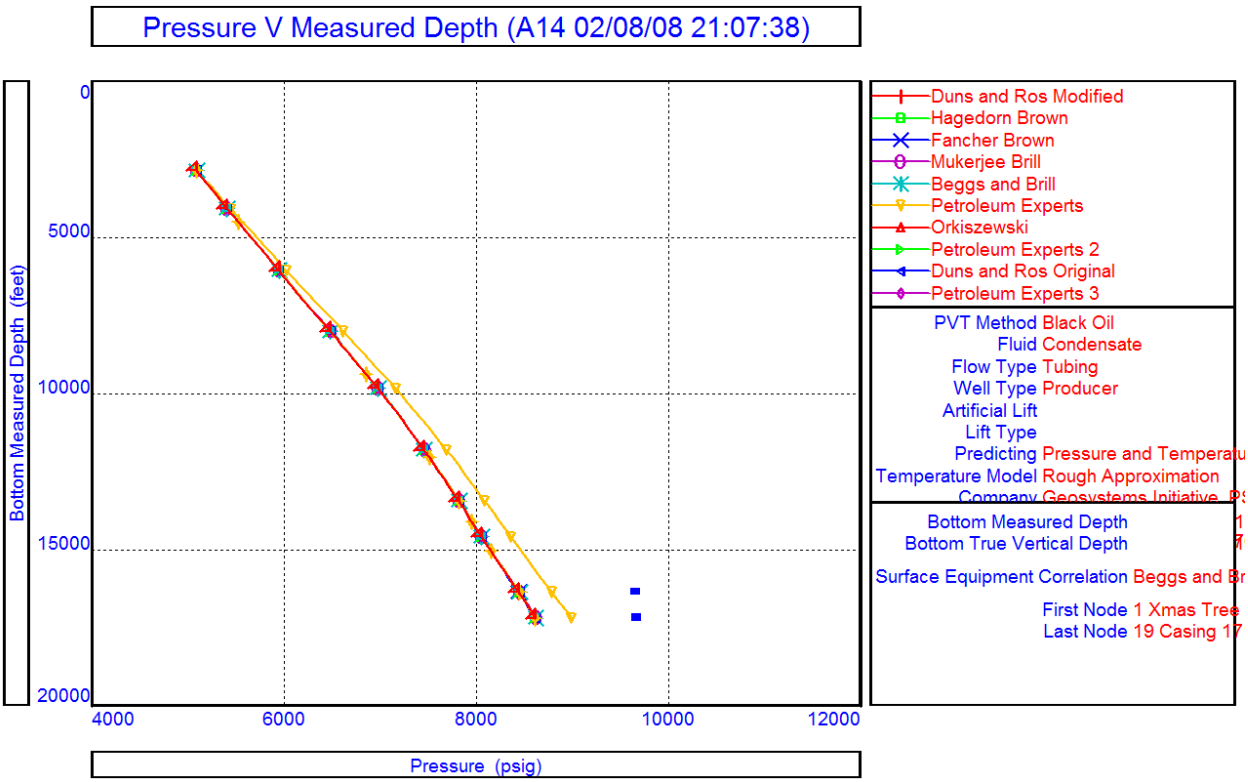

Figure 15: Early-Life Flowing Gradient Traverse of A14 Well

Here, though the many published correlations agree on pressure drop for these conditions, they all underpredict pressure drop by approximately 1500 psi. In this case, the 'bookend' cases of Fancher and Brown and Duns and Ros Modified agree with one another, the PE(1) correlation predicts larger pressure drop. Even the PE(1) prediction however does not match the existing flowing conditions.

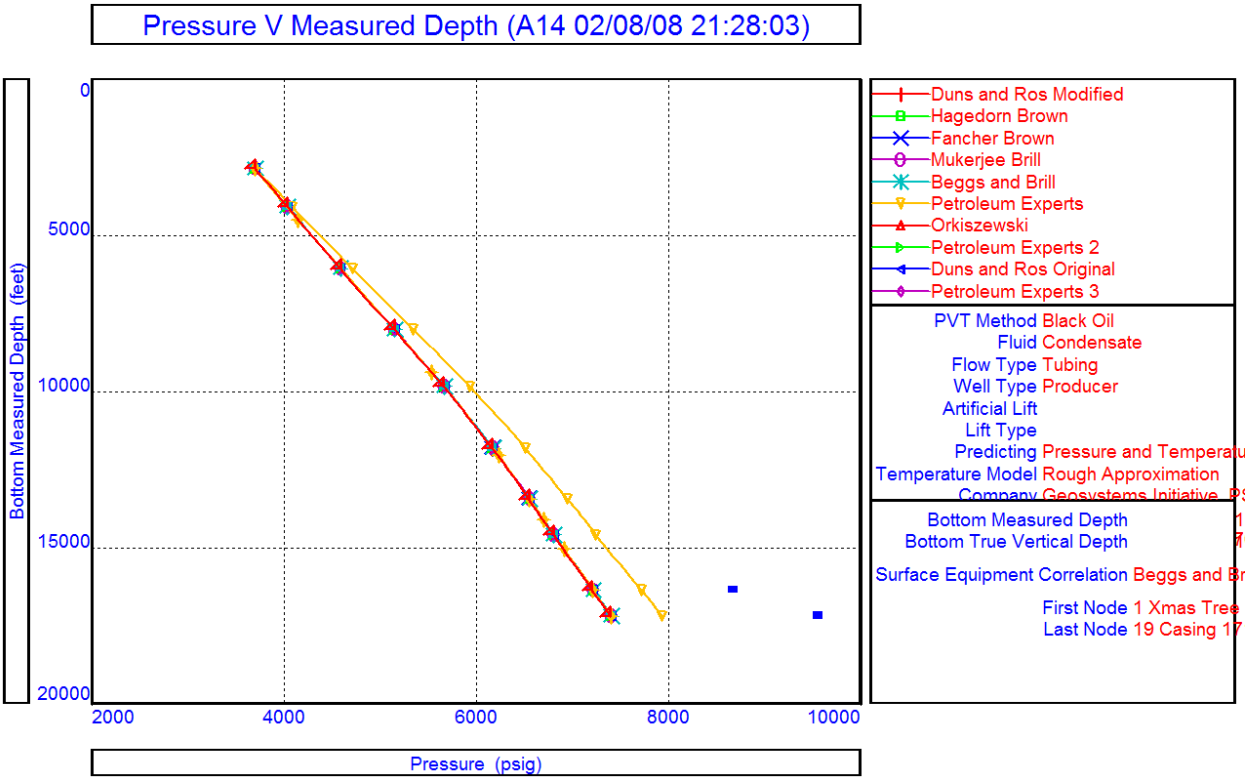

Figure 16: Mid-Life Flowing Gradient Traverse of A14 Well

Later in life, condensate yield has begun to rise but watercut remains low. At this stage, neither the test point nor the ANN prediction are well matched by the empirical correlations.

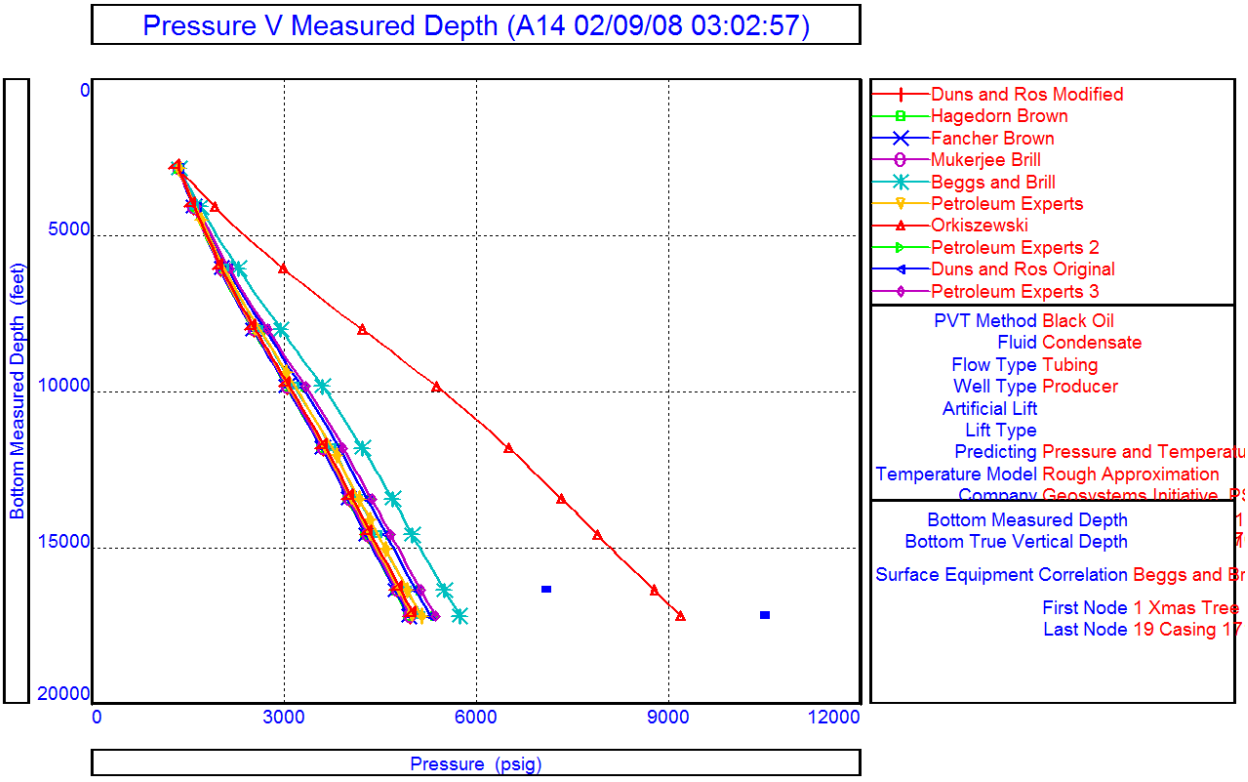

Figure 17: Late-Life Flowing Gradient Traverse of A14

Later in producing life, water production has begun to increase flowing frictional pressure drop. Here, the test point DHPG recording (which was easily matched by the ANN in 'interpolation' mode) is not matched by empirical correlations. Engineering judgment suggests that the ANN prediction at this point is erroneous, because it is too near to initial reservoir pressure. However, an unexpected result was that the error between the ANN predicted 'true' sandface pressure and the Orkiszewski correlation is small, and in fact is even smaller in some other well tests [Appendix F].

Overall, for a given well, tuning the correlations to best meet over 60 'valid' test points shows a standard deviation of $\pm$ 320 psi for most, and 500 for the Orkiszewski model; Worse still is that the best-match correlation changes from one well test to the next. The simplest part of the quality check, in fact, is the level of agreement or disagreement with the cases represented by the Fancher and Brown and the Duns and Ros Modified methods. These are considered useful 'bookend' approximations because:

1. The Fancher and Brown correlation is based on a no-slip holdup approximation. This results in a low-end prediction (or

underprediction) of pressure gradient under flowing conditions. As such, the test points should always show higher pressure than this correlation if well and well test data are valid.

2. The Duns and Ros Modified method is known to overpredict slug density. Therefore, in a slugging or liquid-loaded flow regime, this method should be the 'high-end' or overprediction to which well test data should be compared. In the case of the Auger wells, flow regime as calculated with traditional correlations is more often in the mist or transition range; Therefore the validity of the book-end assumption is somewhat questionable here. However, as it is a standard practice, it serves to help identify inaccurate correlations in the case of the Auger rich gas.

In the case of the Auger wells, the process leads to severe underprediction of flowing frictional pressure drop. Though the Orkiszewski correlation can sometimes serve as the 'high-end' limit according to the Auger data, the observed pressure drop from gauge to wellhead is only approximated in about one third of the recorded well tests for a given well. However, even in cases where observed pressure drop falls within the 'range' predicted by the different empirical lift correlations, the correlation that best matches observed data varies from one well test to another.

The main concern in the use of the semi-empirical correlations is their disagreements in terms of liquid hold-up. When tubing pressure drops below dew point [**Figure 18**], the condensate produces a transitional, mist, or even froth flow regime depending on conditions.

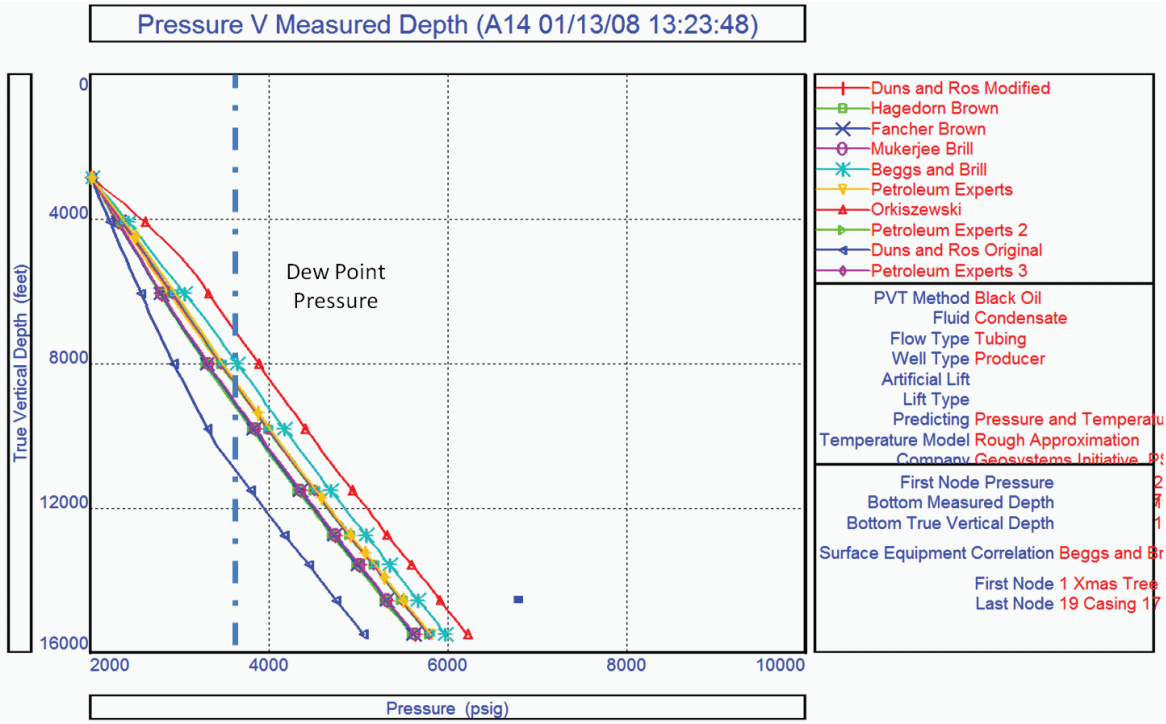

Figure 18: Auger A14 Well Test QC Plot

This plot marks dew point pressure of the Auger gas against flowing gradient traverses from an assortment of semi-empirical correlations. The placement of the dew point line is important, as liquid hold-up is a significant factor in modeling tubing pressure drop. The flowing gradient below the dew-point pressure is predicted identically by these correlations for this case, but because none of them can match the liquid holdup that occurs in the uppermost portion of the wellbore, none of these correlations match the recorded data (represented by the blue point here- this is gauge data plotted at the appropriate depth).

Tubing curvature compounds this problem, and predictions of pressure drop become unreliable in these flow regimes. The calculated liquid-holdup values [**Figure 19**] impact resulting pressures strongly, and are largely responsible for the difficulty in matching gauge data with these well tests.

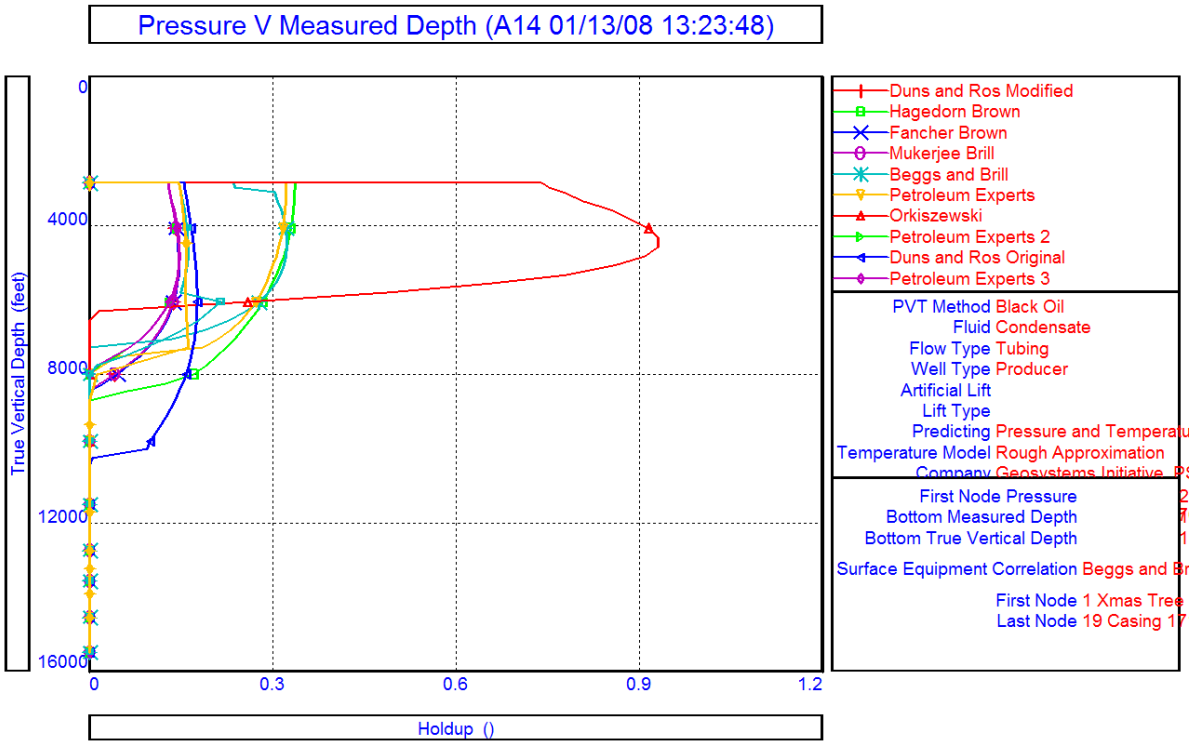

Figure 19: Liquid Hold-Up Plot, Auger A14 Well.

Liquid holdup for welltest in **Figure 18**, displaying strong disagreements among common lift correlations. Liquid hold-up in the transitional, mist, and froth flow regimes is difficult to quantify and model, causing the bulk of disagreement among commonly used lift correlations. The holdup curves all show values of zero while pressure is above dew point, but disagree significantly after liquid condenses.

These disagreements result from several conditions. In part, disagreements between semi-empirical correlations' calculation of holdup parameter has a significant impact on resulting pressure drop, as this parameter controls mixture density. Without additional information, further verification of flow regime and holdup behavior is impossible, but the training success of the ANN alone suggests that the nonlinearities of slugging or extreme holdup conditions are 'captured' in the training data, and are recognized by the ANN.

Additionally, the variation in fluid properties over time and flowing conditions that occur in the Auger wells make some earlier techniques inapplicable here. These changing conditions may be observed in other

retrograde condensate reservoirs with significant aquifer drive. In cases like the Auger wells, where compositional grading is evident, the heavier components present at the original gas-water contact are driven towards the updip-located wells. Consequently, the fluid properties of the produced fluid vary significantly over the life of the wells. Combined with the limited consideration of heavy or ‘rich’ gasses in the development of the original lift correlations, the changing properties of the produced fluid represent a major challenge to the efficacy of existing methods.

Chapter 7: Case Study

As the rate and pressure behavior observed at a well are fundamental data used in a history matching study, it is important that these data are reliable and, furthermore, applied correctly. The data recorded by the permanent downhole pressure gauges in the wells of the shallow Auger sands are a good example of field data that must be used with caution. Unlike vertical wells, the downhole pressure gauges in a directional well are often set a significant distance from the perforations— a potentially significant pressure drop exists between the point of measurement and the point of interest. An approximate calculation of the static pressure gradient at near-reservoir pressures suggests that even under shut-in conditions, the downhole pressure gauges will indicate an artificially low pressure with an error easily in the hundreds of *psi*. This chapter seeks to demonstrate the larger degree of inaccuracy possible under dynamic conditions, through an example history matching process.

The history matching study is conducted with data from the same reservoir that provided the training data for the ANN design process, and is detailed in [see insert]. This history matching study is carried out on a well-by-well basis, because there are only two wells in each of three isolated sands available for this study.

Here, the O Massive Sand [**Figure 20**] is considered due to the longer period of production from this sand (i.e., more history is available for matching, [**Figure 4**]).

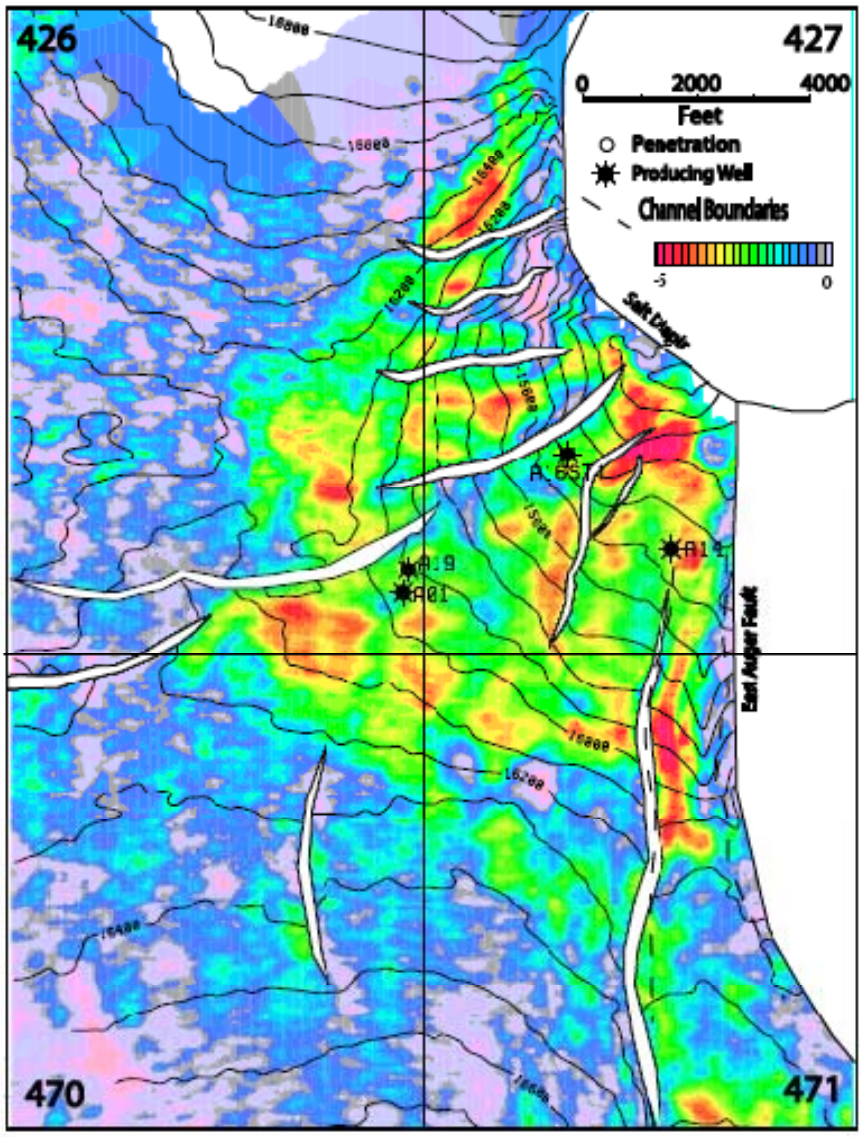

Figure 20: Top Structure Map, Auger O Massive

Reproduced from Bohn, et al., 2008, this top structure map is produced from well-tied depth converted seismic. While fault geometry is clearly outlined here, seismic resolution at this depth (15000-17000 ft TVD) is roughly 80 ft. Therefore, sub-seismic faulting that can still create flow baffling is possible. In addition, changes in litho-facies may create barriers to aquifer communication that become extremely significant as aquifer water sweeps towards producing wells. The A14 and A16ST are the only wells that produced from the O Massive Sand, but the A19ST was perforated there and immediately produced significant water and, most likely, sanded out due to collapse of the highly unconsolidated reservoir rock after pore pressure depletion.

The study is conducted with gas-rate specification at the two wells, and resulting bottomhole pressure and water rates are used simultaneously as matching criteria.

7.1. Part I: History Match to Uncorrected DHPG Data

An initial match was conducted with uncorrected down hole pressure gauge data [**Figure 21**].

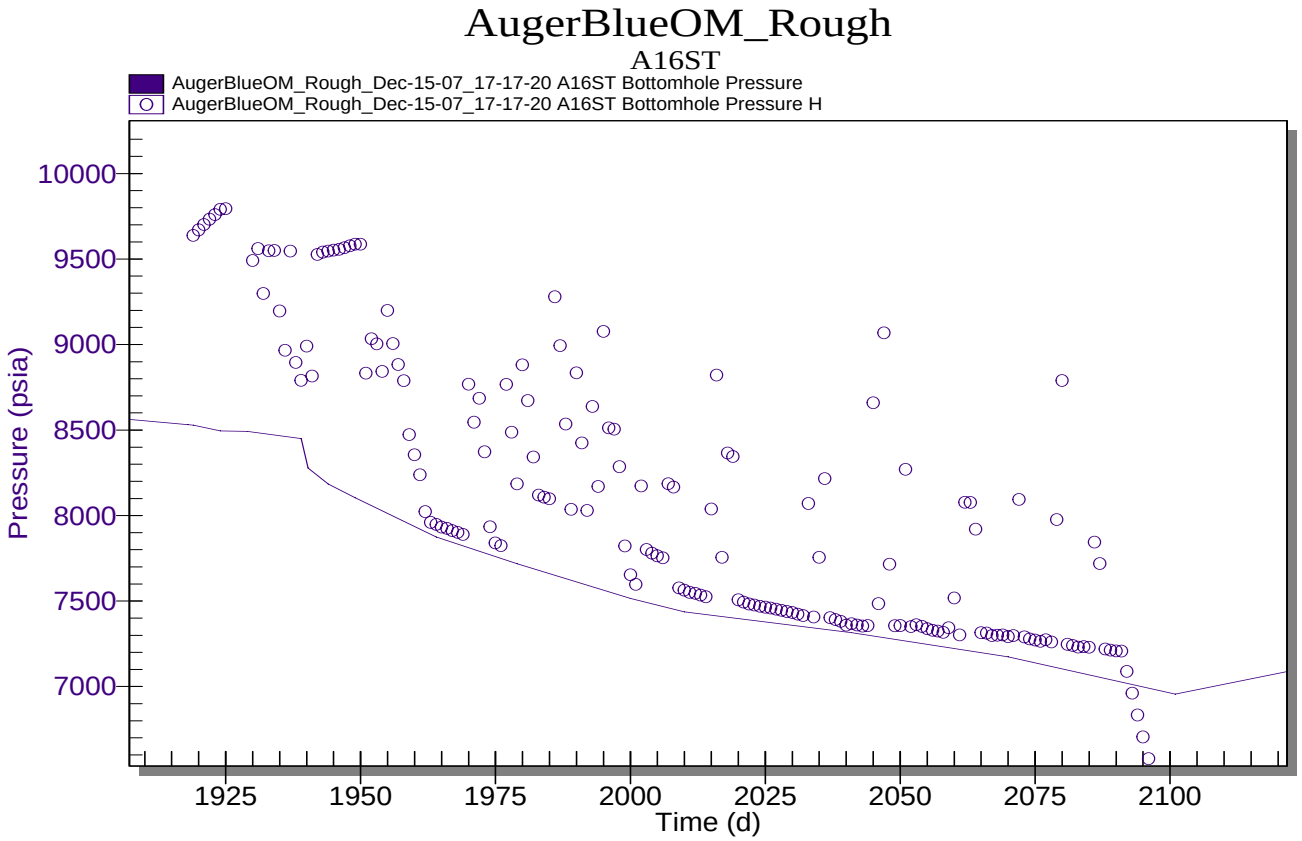

Figure 21: Match to Uncorrected Gauge Pressure History

This plot shows a rough history match which honors structural data and seismic data, but disregards core data. As there is only one exploratory core available for this study, this was considered a reasonable assumption for a real-field scenario. The match succeeds in modeling data in the first year of production from the second well in the O Massive Sand, but fails later in time. This is due in large part to the artificially low pore volume compressibility and small aquifer size needed to match the DHPG data directly.

Though 'raw' data is often used with caution, in the case of fields with less deviated wells the flowing frictional pressure drop between sandface and

gauges might be small. Therefore, uncorrected pressure history might be used as a 'guide' in initial history matching studies. A history matching study was conducted using the uncorrected pressures recorded at the downhole pressure gauges of the Auger wells in this manner.

The aim of this initial history matching study is to identify possible misinterpretations of reservoir parameters with analysis of raw data. To this end, well log measurements of thickness and porosity, and estimations of reservoir extent based on depth-converted seismic were considered, but core data was ignored. RFT data was used as a starting point for fluid properties, and relative permeability and capillary pressure relationships as well as residual saturations taken from cores were used as starting points, but permeability values and pore volume compressibility were disregarded. In this way, the 'initial' history match would use some of the more common data as opposed to the expensive whole core data which often supplies the greatest wealth of information to reservoir studies.

The exercise proved informative. In the process, only some of the earliest 'raw' data was considered. That is, wellhead pressure computations were also eschewed in favor of matching only raw downhole pressure history. The single whole core taken from the exploratory well 471-1 is disregarded in this study, except as a starting point and for comparison purposes. With geologic architecture fairly well-constrained from well log data and seismic data, the properties left to be varied in the matching process were permeability (and permeability distribution), saturations, relative permeability relationships, and pore volume compressibility. While the amalgamated channel sand deposits of such turbiditic reservoirs often result in multiple different facies present in one reservoir body, the repeating nature of this type of depositional sequence suggests that the different facies will often exhibit similarities in terms of properties such as sorting, grain size distribution and mineralogy. Therefore, though core-measured

properties would almost certainly require adjustment to be appropriate at the field scale, the properties of the core should nonetheless be approximately representative.

The properties required to match producing pressure history with DHPG data represent a good demonstration of the dangers of using un-corrected data. A conceptual 'halo' model is used as a guide for permeability distribution in the absence of distributed core data, wherein permeability downgrades from a maximum at the highest points in the reservoir to a minimum somewhere downdip, and is generally considered a reasonable model in the case of turbidite reservoirs such as this. However, core data is only used as a starting point for permeability and porosity distribution. During the matching process, permeability and pore volume compressibility had to be reduced to physically unrealistic values in order to reproduce well pressure history: the 'halo' model was used, but maximum permeability had to be reduced from core values of 800-1800 md to a final maximum of 175 md, and aquifer porosity was reduced to 1 md [**Figure 22**].

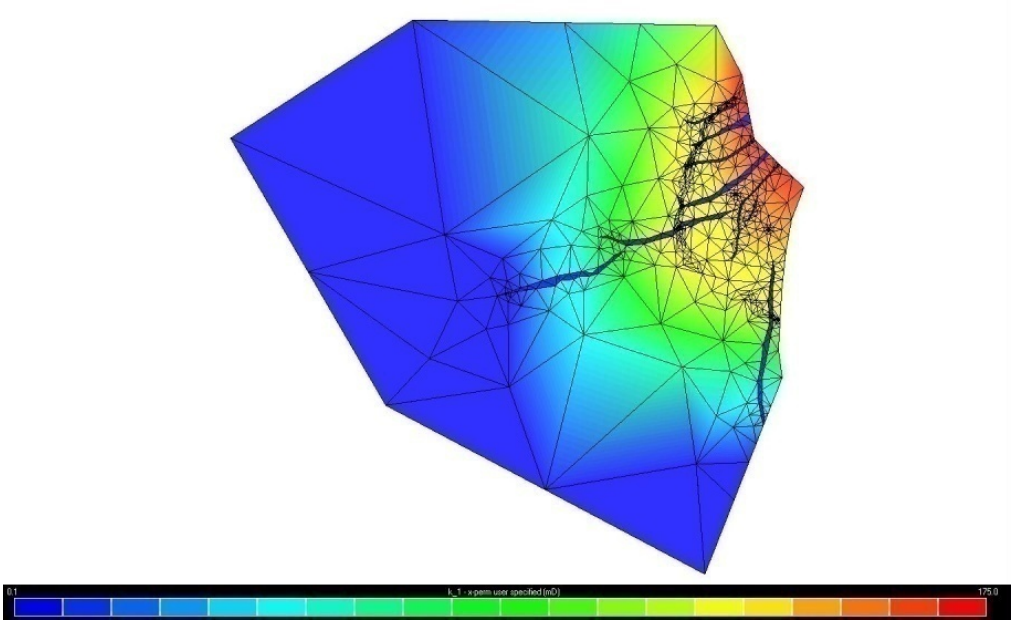

Figure 22: Permeability (*k*) distribution used in history match to uncorrected DHPG data.

The best match to raw DHPG data resulted in a permeability distribution that does not honor the local geologic conditions common in deepwater turbiditic systems. Using core data as a starting point and a 'halo' model to produce a reasonable, degrading-downdip permeability distribution (core data is only available from one well), the history matching study was conducted by reducing permeability at all points until flowing bottomhole pressures dropped sufficiently. In conjunction with an unrealistic pore volume compressibility, the permeability distribution shown was eventually realized. Maximum permeability is 175 millidarcy, as compared with an estimate from exploratory well cores suggesting 800-1800 md permeability. Aquifer permeability is 1 millidarcy, and aquifer size is at the minimum required to support observed production.

Porosity distribution required a similar reduction from maximum core values of roughly 30-34% to final aquifer porosity of about 5% [**Figure 23**].

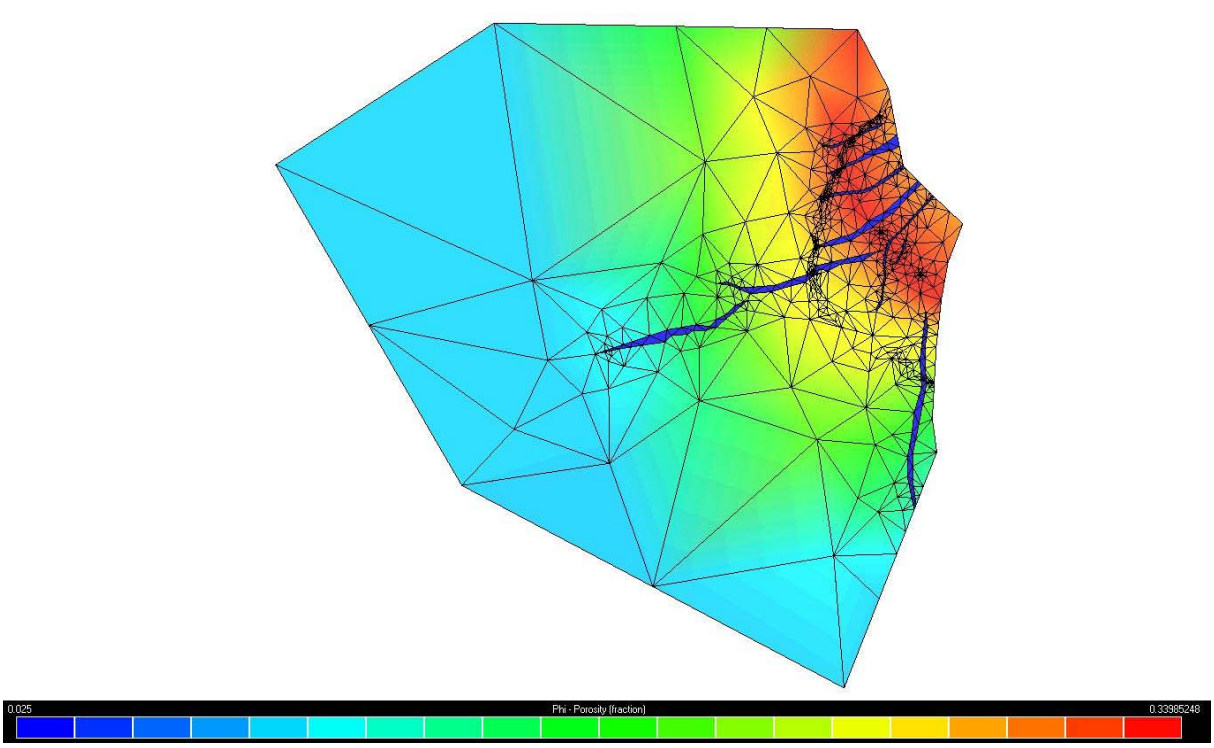

Figure 23: Porosity (Φ) distribution used in history match to uncorrected DHPG data.

History matching of the porosity distribution was conducted by comparing predicted water production rates to water production history in gas-rate specified cases. Once again, the simple 'halo' model was applied, which uses a degrading-downdip porosity distribution, as often observed in turbidite deposits. However, to support early production, the porosity near the salt dome which serves as the North-Northeast boundary of the reservoir was kept at the original maximum as observed from core data, about 34%. Then, using water production rates as a basis for matching, the aquifer porosity was adjusted until water rate predictions were comparable to history. However, as in the case of the permeability distribution, the history match suggests unreasonably-low porosity, particularly in the aquifer (around 2.5%).

The relative permeability characteristics [**Figure 24**] used in this stage of history matching were also questionable. To support observed production rates, extremely low residual gas saturation was used. Without this change, convergence became a significant issue simply due to the lack of mobile gas remaining after only a short period of production from the A14 and A16ST wells.

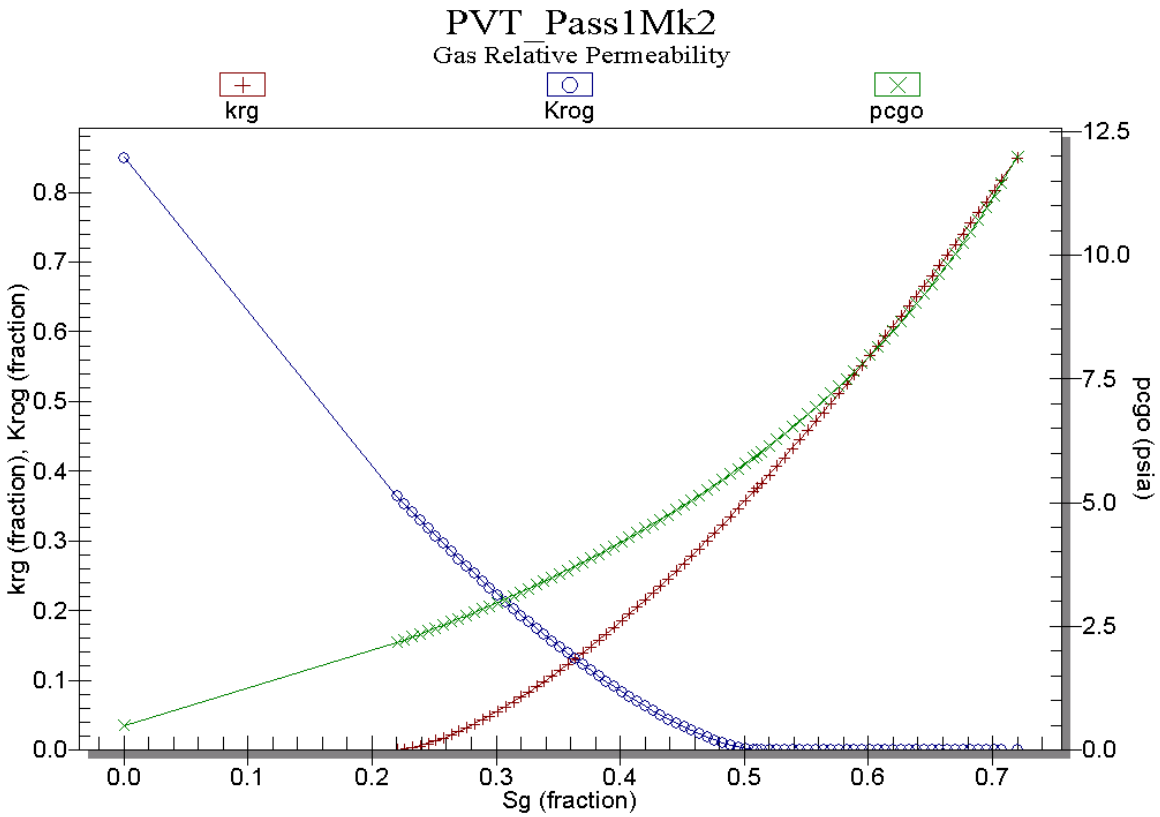

Figure 24: Relative Permeability relationships (and P_c curve) used in match to 'raw' DHPG data.

These relative permeability curves were used in the Corey model for three-phase permeability, and are another source of concern with uncorrected DHPG data- To match pressure response of the A14 and A16ST wells, a significant reduction in porosity and permeability from expected values was needed. With these changes in place, the observed extremely high rate history caused significant convergence problems; In order for simulation models to complete timesteps, residual gas saturation had to be reduced to 0.5%. This increase in mobile gas near the wells improved convergence, but confidence would automatically be low in a prediction of such a small residual saturation value.

7.2. Part II: History Match to WHP with Lift Tables

Uncorrected DHPG data is rarely used as a reference for history matching, and only in wells with gauges set closer to perforations. Though they may be used as a rough reference, the pressure drop between gauge and perforation is known to be significant. The production tubing lift correlations discussed in the previous chapter, though also used to analyze tubing designs, are also used to generate lift tables. These tables are used in reservoir modeling studies both for history matching and forecasting- in history matching, they are important in the prediction of precise wellhead pressures to match to wellhead pressure history, whereas in forecasting phases, this information is used in the design of surface gathering networks and facilities. However, as demonstrated in Chapter 6, these empirical correlations have difficulty in the case of these highly-deviated wells, and particularly so if phase change occurs in production tubing.

The wellhead history is difficult to match. In early life, the Beggs and Brill correlation, like most of the empirical solutions applied in the earlier Well Test quality check study, underpredicts pressure drop in the well [**Figure 25**, **Figure 26**]. This, combined with severe fluctuations in well conditions, makes matching this behavior directly difficult. While pressures had to be kept lower than the expected real ranges for the earlier history matching study in 7.1., this model started from the property distribution used in that match and it was found that initial reservoir pressure had to be reduced to 7000 psia from the RFT-reported 10,600 psia. This resulted in unsolveable timesteps after roughly five years, six months of production, due to the volume of gas produced early in the well life.

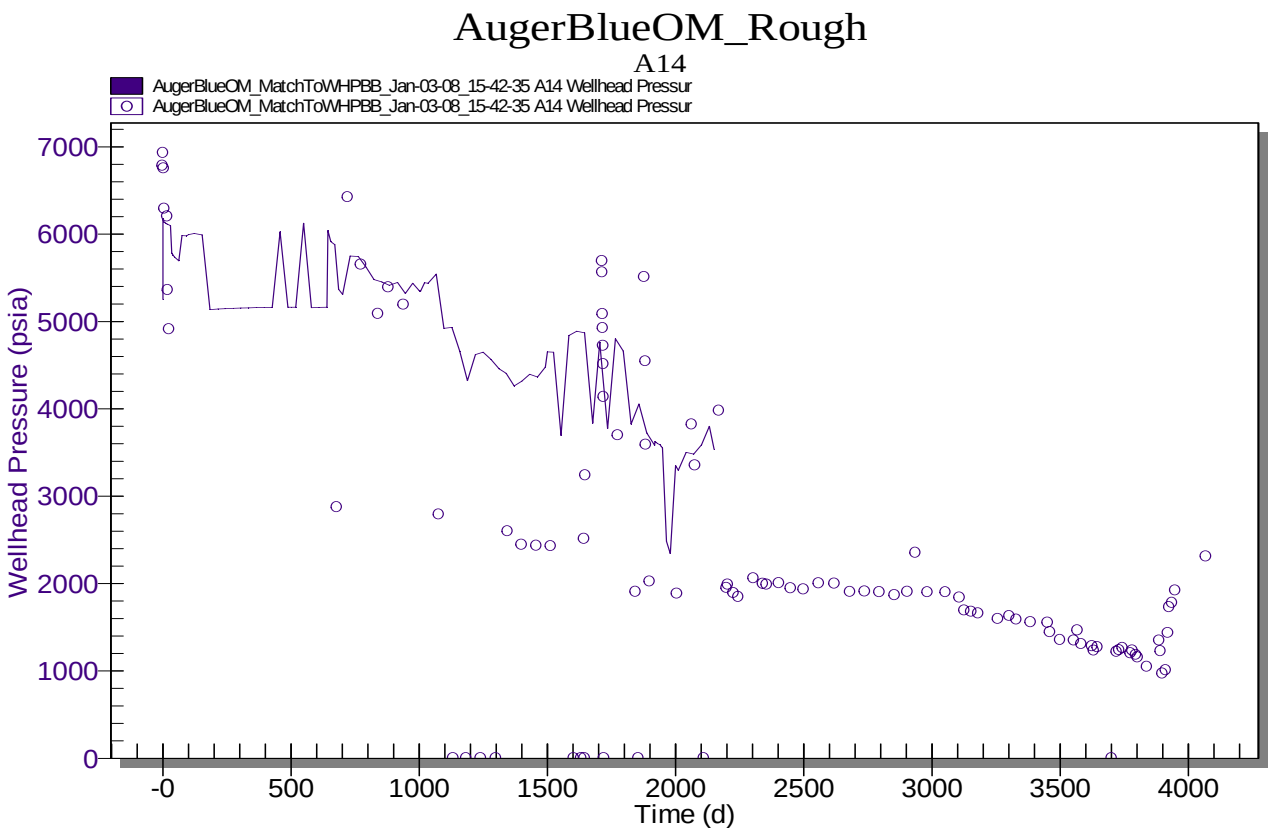

Figure 25: Rough Match to Wellhead Pressure with Beggs and Brill Lift Table, Well A14

The Beggs and Brill correlation shows highly erratic behavior when used with the Auger reservoir model. Matching the wellhead pressure history requires a reduction of pore volume compressibility, overall field permeability, and initial reservoir pressure to unrealistic levels.

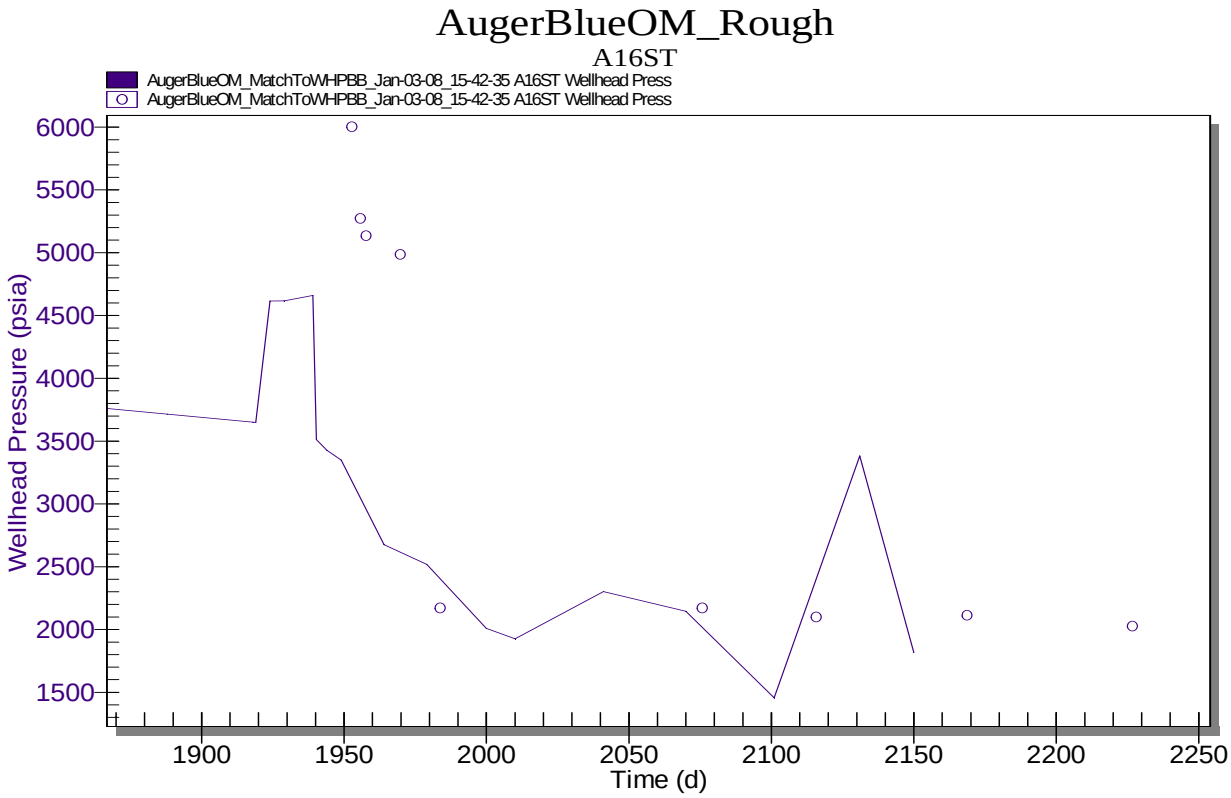

Figure 26: Rough Match to Wellhead Pressure with Beggs and Brill Lift Table, Well A16ST

The Beggs and Brill correlation, as with the A14 well, shows erratic behavior when trying to match BHP history.

7.3. Part III: History Match to ANN-Corrected BHP's

The history matching study was repeated with the new information supplied by the neural network used as pressure constraints. However, as the output of the neural network was in the form of bottom-hole pressure data, it was used as history to be matched. The model was run with an incremental gas production specification, as this data was available without adjustment. ANN-corrected flowing sandface pressures were 'matched' but unreliable points were ignored [**Figure 27, Figure 28**], and water production rate matching was conducted simultaneously [**Figure 29, Figure 30**].

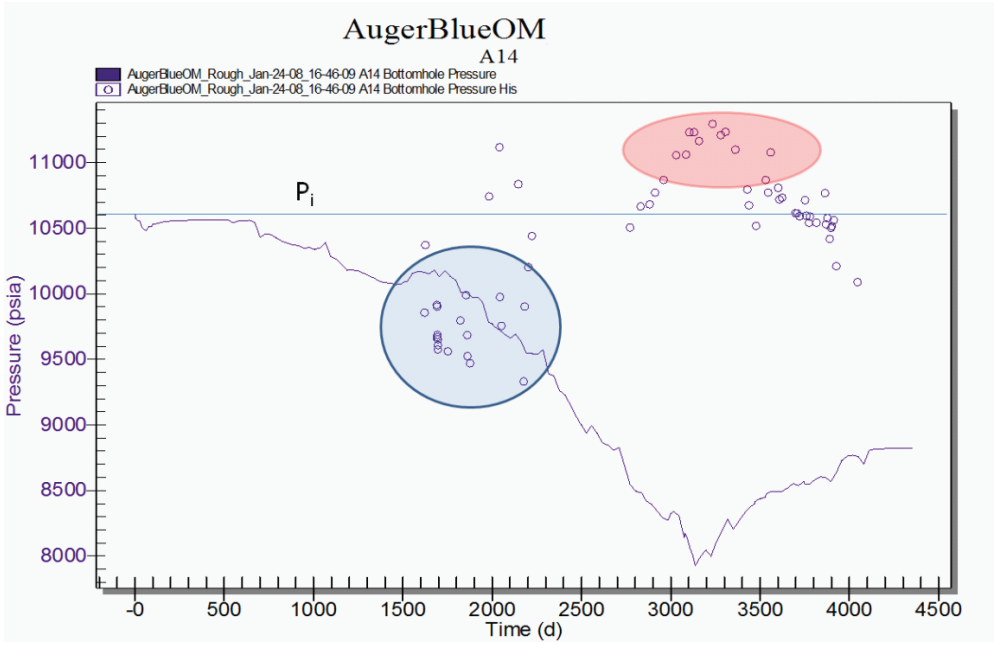

Figure 27: Approximate Match to ANN-Predicted 'true' Sandface Pressures

The matching process and engineering judgment eliminate certain ANN output. In this case, all points above, or too near to, original reservoir pressure are immediately disregarded. However, the grouping of points outlined in blue, though erratic, is useable as a rough guide. The overpredicted BHP's are a result of a sudden increase in water production, which causes an overprediction of pressure drop by the ANN— and thus extremely high pressures shown.

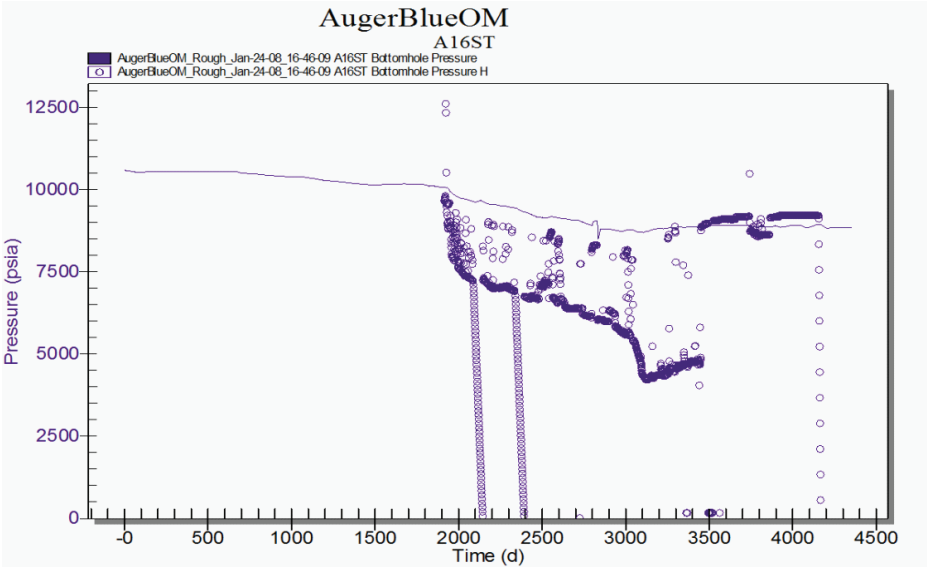

Figure 28: Comparison of BHP at the A16ST Well to Gauge History

As the ANN predictions of 'true' sandface pressure fail in the case of the A16ST well, the sandface pressure results from the simulator are compared to the gauge pressure. While this again requires some engineering judgment, the general trends in the two behaviors should roughly correspond.

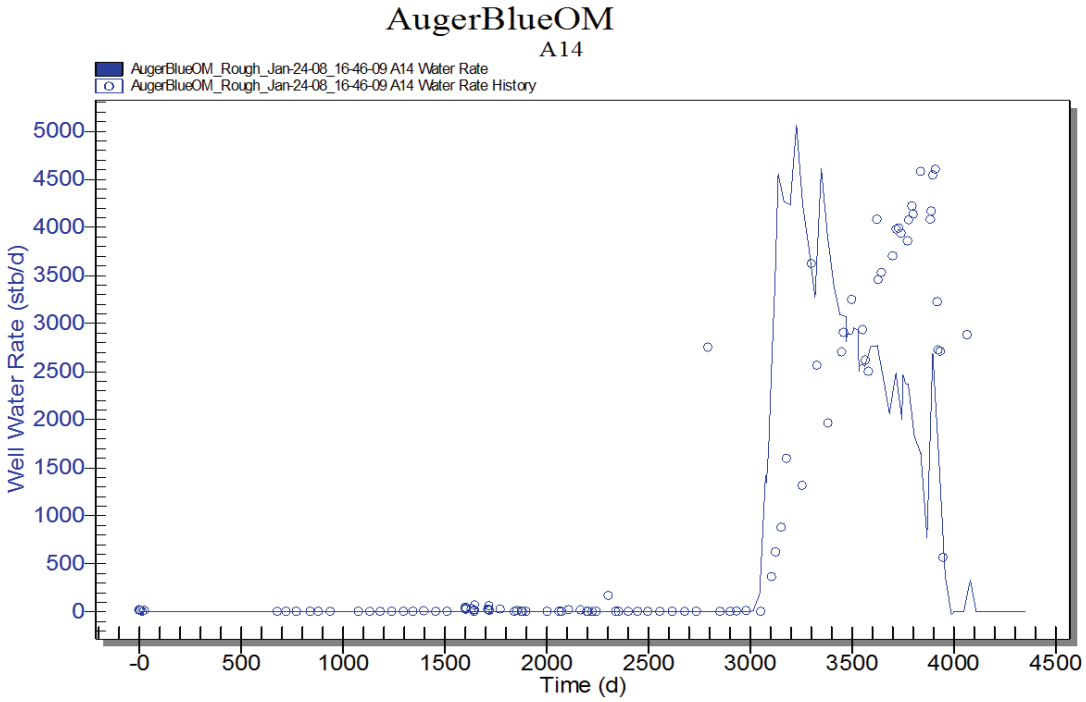

Figure 29: Approximate Match to Water Production Rate, Auger O Massive Sand, A14 Well

Water Production Rates are matched in conjunction with bottom-hole pressure history. The two different matching histories used in conjunction allow tuning of the reservoir model and help to constrain the parameters that can be used to match the ANN-predicted BHP History.

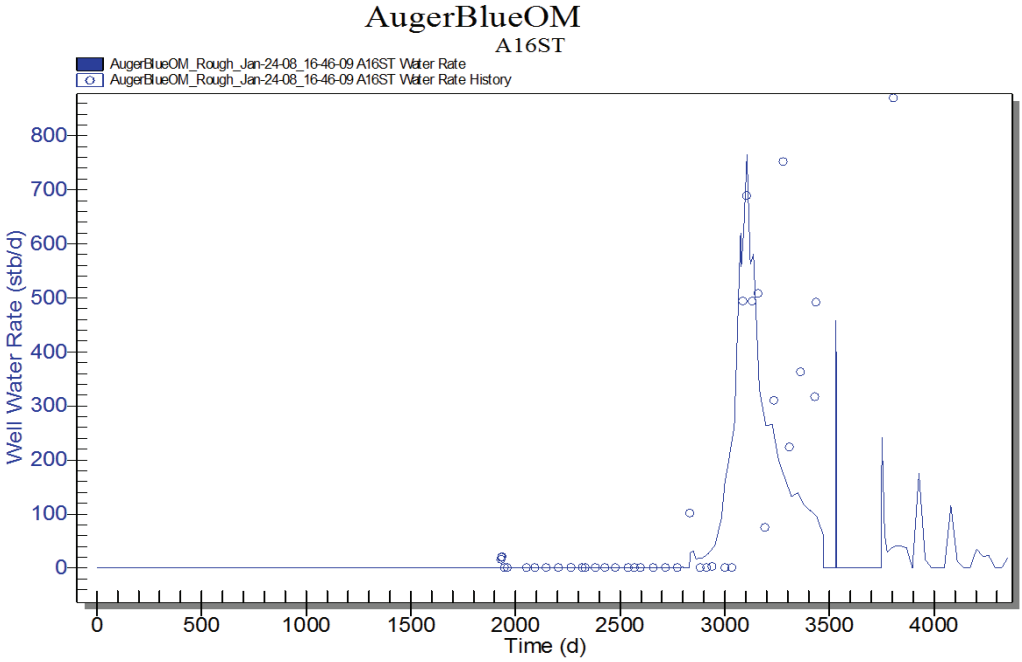

Figure 30: Approximate Match to Water Production Rate, Auger O Massive Sand, A16ST Well

Again, water production rate match helps constrain reservoir properties used in the matching process while duplicating ANN-predicted BHPs.

The history match to ANN-corrected values resulted in a reasonable property distribution. Permeability values and pore volume compressibility approached core values, and the size of the 'aquifer' zones was increased significantly [**Figure 31**].

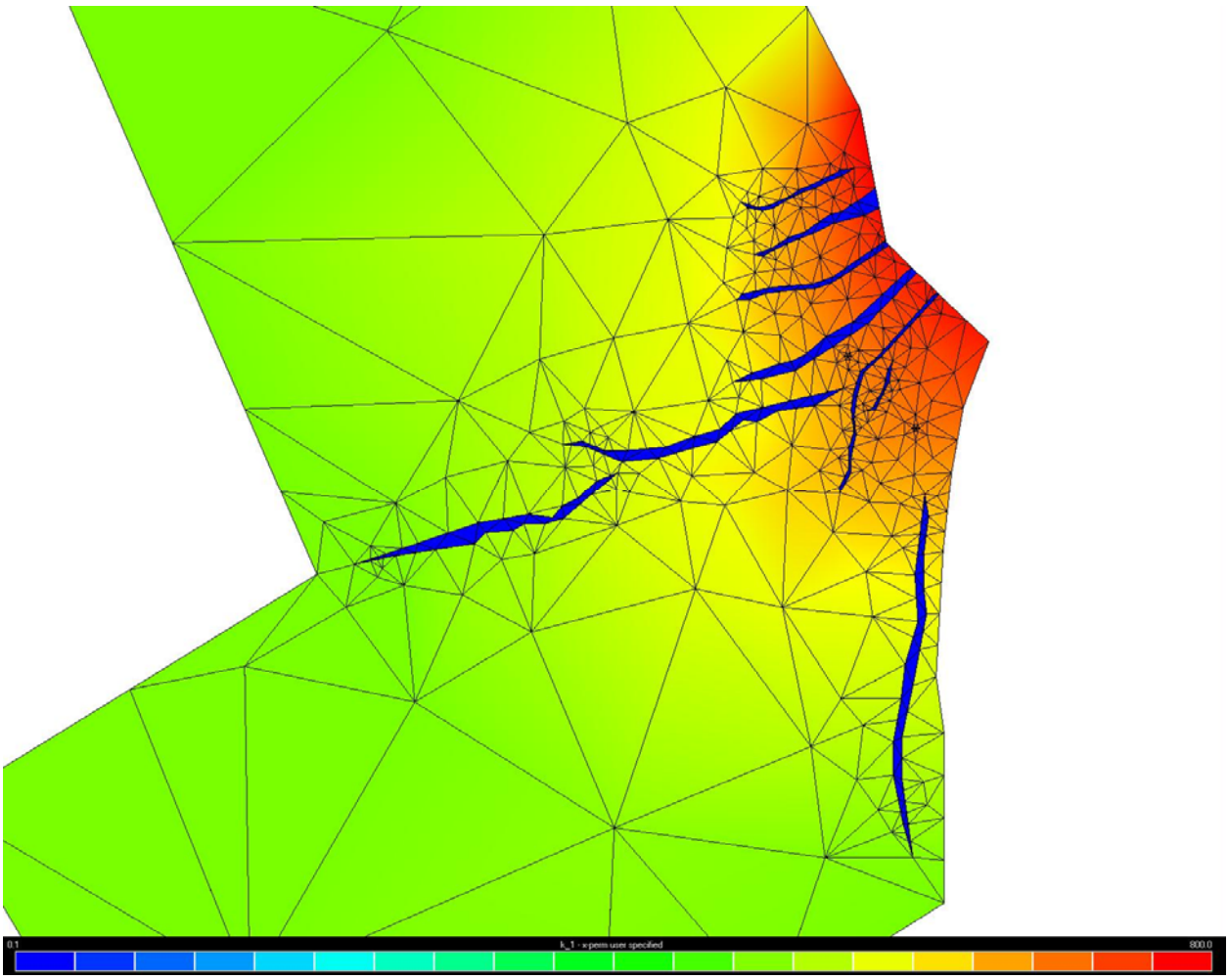

Figure 31: Permeability Distribution used in Match to ANN-Corrected BHP

The permeability distribution resulted in a maximum permeability of 950 md, showed leaky faults, and used a pore volume compressibility of 5.0e-5. A significant change from the earlier history matching models is the size of the aquifer required to support true reservoir pressures and later, water production rates when aquifer water reaches producers.

7.4. History Matching Results Comparison

Results of the history matching study are informative. While the properties of the reservoir are, to some extent, supplied by the exploratory cores, the degree of amalgamation from different depositional events does suggest significant variability in reservoir properties. In the case that a history match might be used to prepare forecasts of future performance, these variations in reservoir properties would become crucial. This would be particularly true in the case of forecasting future performance of new wells, because the properties at the exact location of the new well would be difficult to constrain geologically.

In the case of the Auger O Massive Sand, use of DHPG pressure histories would have caused significant underprediction of recoverable reserves. In 7.1 and 7.2, the history matches with early data (up to 3-5 years of production) result in model instability later in history, as the production rates observed became unsupportable as aquifer water arrived at the producing wells [**Figure 32**].

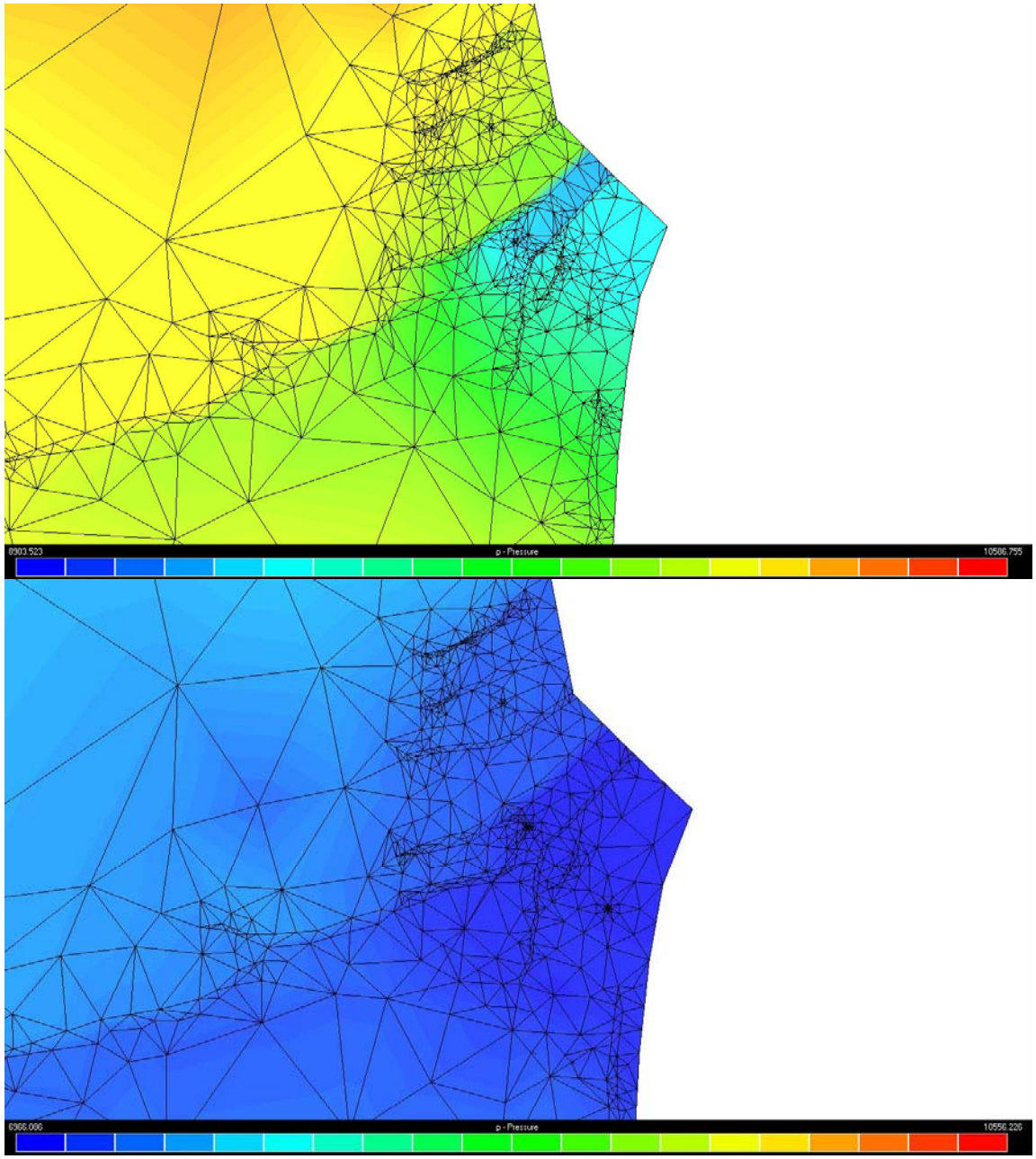

Figure 32: History Match Results Comparison- Late-Time Pressure Distribution

Pressure distributions from match to ANN-corrected BHP history at 4350 days (top) and match to uncorrected DHPG data at 4350 days (bottom). While the match to ANN-corrected data shows local depletion near the original producers, A14 and A16ST, pressure has not decreased significantly elsewhere in the reservoir. By contrast, the match to uncorrected DHPG recordings indicates significant pressure depletion throughout the reservoir.

7.5. Reservoir Performance Forecasts

In order to quantify the impact of the different approaches to history matching, the models were run in forecasting mode with an additional well added in the northern fault block. Both models showed unswept gas in this region [**Figure 33**].

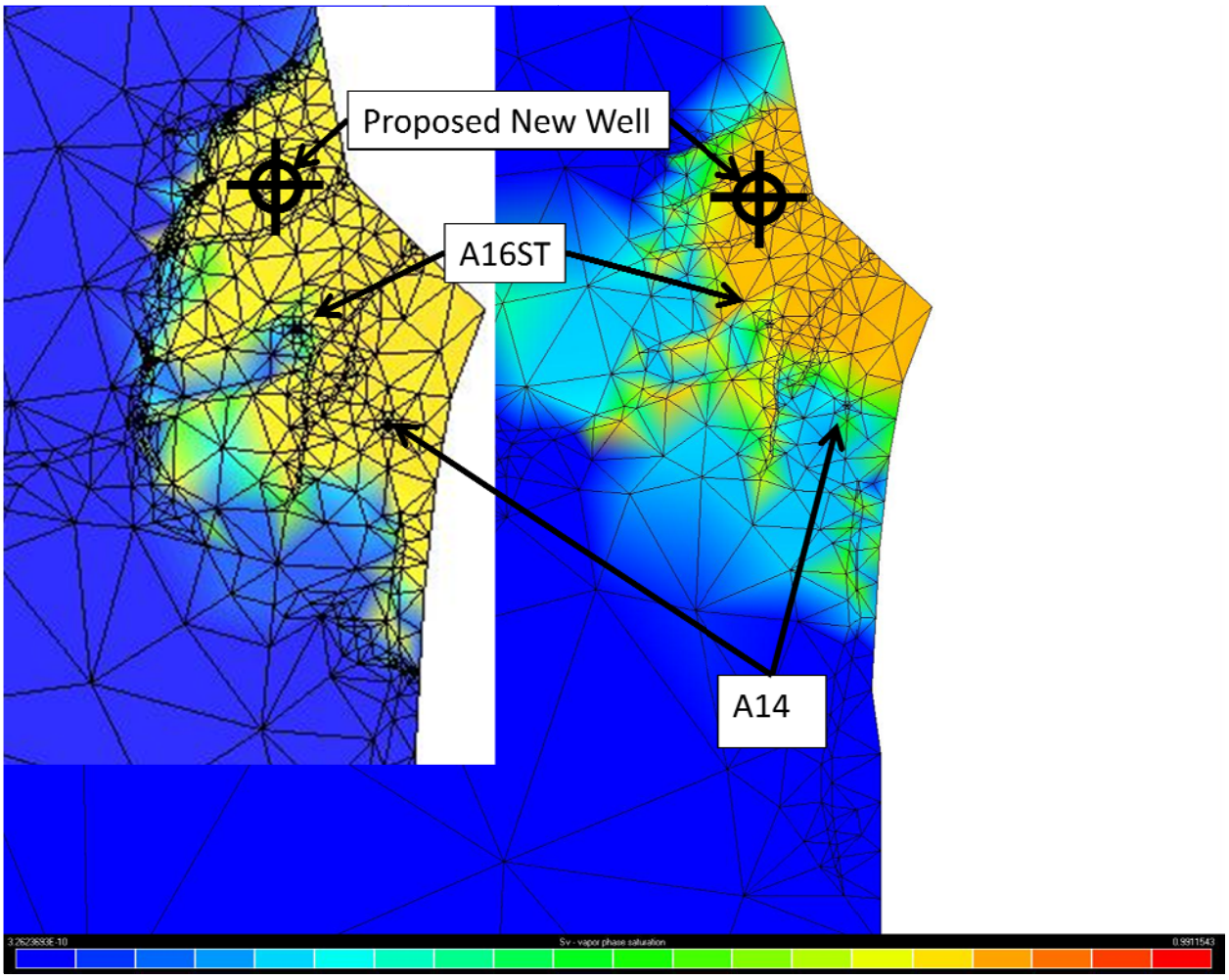

Figure 33: Proposed New Well Location, Superimposed on 4350 day Gas Saturation Map from ANN-Match and 2832 day DHPG Match (inset)

The proposed new well was located behind several faults, where aquifer water had not yet swept gas towards the other two wells completed in this sand. Though each model shows significantly different behavior later in time, both show some remaining unswept gas in this region.

Completing a well in a zone with unswept gas is a reasonable test of the production difference between the two matching approaches. However, the low pressure readings at the DHPGs caused model crashes if rate-specified production was used past the first year of production from the second well, A16ST. Therefore, the forecasting approach was use of specified-pressure production from the original producers after the first year of A16ST production, and a similar pressure profile was used at the new well.

The ANN-matched reservoir model, while able to support the specified rates for history matching, used the same bottomhole pressure specified production schedule at the new producer. This created as direct a comparison as possible between the two different reservoir models. The new well in the ANN-matched reservoir produced a gas rate profile very similar to the original producers, and produced at high rates for two years before water arrival began reducing gas production. Results show a dramatic difference in recovery [**Figure 34**], with a whole-field improvement of 82 bscf, and a recovery difference of 30 bscf from the additional well alone.

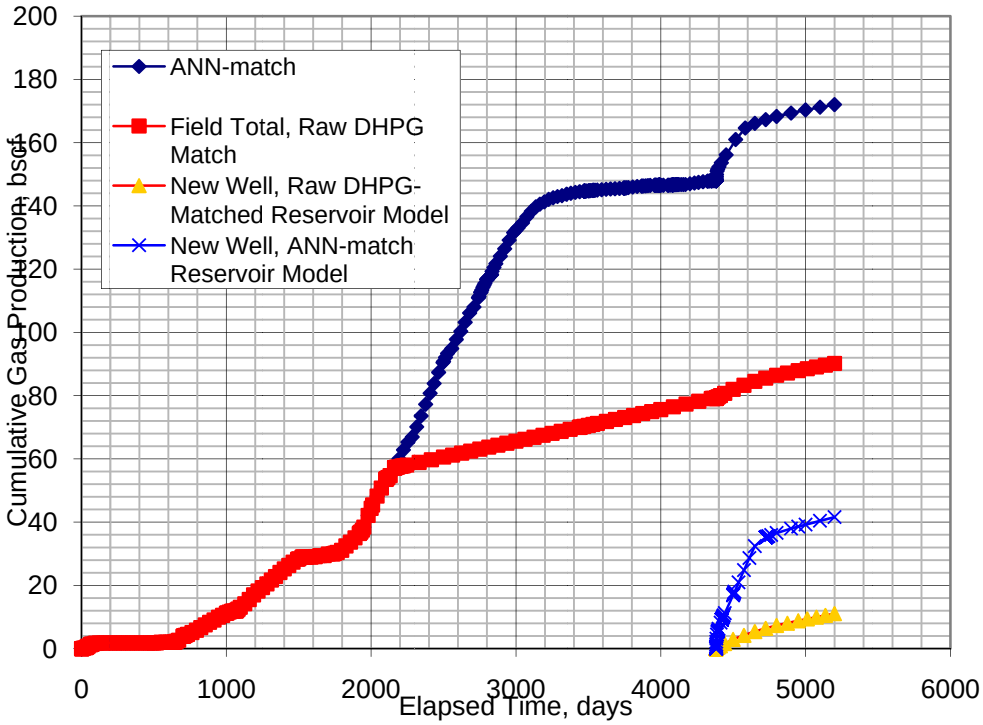

Figure 34: Cumulative Gas Recovery for ANN-Matched and DHPG Matched Reservoir Models with Additional Well

Field and new well recoveries are plotted versus time. Whole field cumulative gas production shows a difference of 82 bscf, with the DHOG-matched model producing 90 bscf and the ANN-matched model produces 172 bscf. The results for the new well alone are particularly dramatic, with the new well in the DHPG-matched model producing 11 bscf and the ANN-matched model producing 41 bscf.

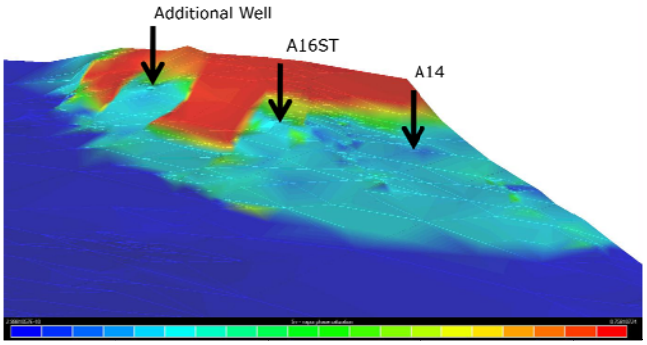

Figure 35: Late-Time gas saturation distribution with new well

The ANN-matched results show the new well produces a similar 'sweep' to those observed in the A14 and A16ST well.

Chapter 8: Conclusions

This work has advanced the methods of prediction of downhole pressures in deviated wells using an artificial expert system based on a feedforward-backpropagation ANN. The ANN proved successful in learning to recognize the impact of input variables (including static well description parameters, rate data, and one directly measured pressure reading) on the output variable, a remote pressure reading. During the process of developing the ANN, weaknesses in empirical correlations were identified and the weights developed for the network during training demonstrated that the deviation parameter is the most significant in this problem. This deviation parameter was originally intended as a functional link, but its importance suggests that it serves as a proxy for liquid hold-up and slugging. As this direct measurement is often not practical, this conclusion is significant because any future work on this subject will require a more rigorous treatment of holdup and slugging than is currently available for gas / condensate reservoirs.

Use of the network in extrapolation mode proved possible, but presented certain challenges. The network tended to overpredict pressure drop when watercuts increased significantly; this is largely due to careful water production management in the operation of the field. The training data therefore includes a sudden change from 0.3 stb/MMscf to 1200+ stb/MMscf in the space of just a few months for all wells in the shallow gas sands at Auger. Additionally, the deviation of the most severely deviated well in this dataset, the A16ST, between gauge and perforations proved to be too far outside the range of training data to produce useable results. However, using the results of the ANN prediction as BHP history in the A14 well proved successful in producing a more reasonable well-level history-matched model than the other available history data.

This work can be extended in the future to be more successful as a 'true' bottomhole-pressure predictor. Additional parameters representing curvature, such as radii of curvature or coefficients describing wellpath as a polynomial, might be useful in cases of extreme directionality, extended-reach wells or fully horizontal wells. Additional dynamic parameters such as fluid compositions, wax deposition quantities or sand production rates could produce reliable extensions of this model. Downhole flow-metering data might supply gas fraction / flow regime data that could be used to extend this work. The existing network could be made more effective through the use of sandface-BHP data from a well test, it might be sufficient to 'teach' the network the proper weights required for the most deviated portion of the well.

References

Ansari, A.M., Sylvester, N.D., Sarica, C., Shoham, O., Brill, J.P. *A Comprehensive Mechanistic Model for Upward Two-Phase Flow in Wellbores.* Society of Petroleum Engineers' Journal of Production and Facilities, May 1994.

Artun, E., Mohagegh, S.D., Toro, J., and Wilson, T. *Reservoir Characterization Using Intelligent Seismic Inversion.* 2005, Society of Petroleum Engineers, Paper No. 98012.

Balch, R. S., Stubbs, B.S., Weiss, W. W., and Wo, S. *Using Artificial Intelligence to Correlate Multiple Seismic Attributes to Reservoir Properties.* Society of Petroleum Engineers, Paper No. 56733, 1999.

Brown, K. *Technology of Artificial Lift Methods, v.1.* Petroleum Publishing Company, Tulsa, OK.

Bohn, C., Reilly, M., Seren, D., Valenti, J., Flemings, P.B. , Ertekin, T., *Characterization of the N and O Sands in Auger Field, Gulf of Mexico, USA.* AAPG Publication in progress.

Chawathe, A. *The Application of Kohonen Type Self Organization Algorithm to Formation Evaluation.* Society of Petroleum Engineers, Paper No. 29179, 1994.

El Ouahed, A.K., Tiab, D., Mazouzi, A., Jokhio, S.A. *Application of Artificial Intelligence to Characterize Naturally Fractured Reservoirs.*Society of Petroleum Engineers, Paper No. 84870, 2003.

Gomez, L.E., Shoham, O. and Schmidt, Z. *A Unified Mechanistic Model for Steady-State Two-Phase Flow in Wellbores and Pipelines.* Society of Petroleum Engineers, Paper No. 56520, 1999.

Hagan, M.T., Demuth, H.B., Beale, M. *Neural Network Desgn.* PWS Publising Company, 1996.

Hasan, A. R., Kabir, C.S. *Predicting Multiphase Flow Behavior in a Deviated Well.* SPE Production Engineering, November, 1988.

Hasan, A.R., Kabir, C. S. *A Study of Multiphase Flow Behavior in Vertical Oil Wells, Part II- Field Application.* Society of Petroleum Engineers, Paper No. 15139, 1999.

Mohagegh, S. *Virtual-Intelligence Applications in Petroleum Engineering, Parts 1-3.* Society of Petroleum Engineers, Paper Nos. 58046, 61926 & 62415, 2000.

Osman, E.A., Ayoub, M.A., Aggour, M.A. *Artificial Neural Network Model for Predicting Bottomhole Flowing Pressure in Vertical Multiphase Flow.*Society of Petroleum Engineers, Paper No. 93632, 2005

Osman, E.A. *Artificial Neural Network Model for Identifying Flow Regimes and Predicting Liquid Holdup in Horizontal Multiphase Flow.* Society of Petroleum Engineers, Paper No. 68219, 2001.

Ramgulam, A., Ertekin, T., Flemings, P.B. *Utilization of Artificial Neural Networks in the Optimization of History Matching.*Society of Petroleum Engineers, Paper No. 107468, 2007.

Appendix A: Wellpath Deviation / Angle Parameters used in ANN Design

1. Node-to-Node Length, TVD

2. Node-to-Node Length, MD

3. Average Deviation Parameter, α_{dev}

   This parameter is effectively a functional link between measured-depth length and true vertical depth length. The well path is discretized into a series of 'sub-nodes', as defined by the directional survey. The deviation parameter, αdev, for the wellpath between the nodes at which pressures are measured is calculated as shown below:

$$\alpha_{dev} = \frac{\sum_1^n \frac{\Delta MD_n}{\Delta TVD_n}}{n} \qquad \text{(I)}$$

   In the case of the data used here, these sub-nodes were generally separated by increments of 100 feet of Measured Depth.

4. Average Angle Parameter, $\alpha_{\emptyset}$

$$\alpha_{\emptyset} = \frac{\sum_1^n [\emptyset_n * \Delta MD_n]}{\sum_1^n \Delta MD_n} \qquad \text{(II)}$$

   Like the average deviation parameter described in (I), this is a length-weighted average of hole inclination parameter.

Appendix B: Reservoir Model Details

The reservoir modeling in this study uses a commercial simulator based on a multiphase black-oil Finite Element formulation, called Resolve[1]. This appendix contains description and discussion of some basic reservoir properties and well logs used to construct the model for the history matching study Chapter 7.

The shallow sands at Auger field contain a 'rich' gas which might be ordinarily considered a retrograde condensate. However, due to the pressure support in the system, reservoir pressures do not reach the dew point of the gas. This allows the use of a black-oil model, using tabulated PVT data created with the Peng-Robinson equation of state. This eliminates the need to simplify composition for a compositional simulator, 'lump' heavies into a pseudo-component or otherwise manipulate the PVT data.

However, the compositional grading inferred from exploratory RFT's adds an element of complexity to the problem of modeling these fluids. Different commercial and PVT codes show different results for density and phase envelope calculations, most importantly in terms of the location of the critical point; PETEX's PVTp[2] was eventually chosen in order for better consistency with lift calculations in Chapter 6. Further, the deeper of the two O Massive Sand RFT's (Table 2) exhibits a volatile-oil characteristic (judging purely by location of critical point) as opposed to the obviously retrograde character of the shallower sample [**Figure 36**].

[1] Resolve 3.5, Object Reservoir
500 Capital of Texas Hwy N
Building 6, Suite 225
Austin, Texas, 78746

[2] PVTp v.8.0, IPM 6.0 Build #109, Petroleum Experts Ltd
Petex House,
10 Logie Mill
Edinburgh, EH7 4HG
Scotland, UK

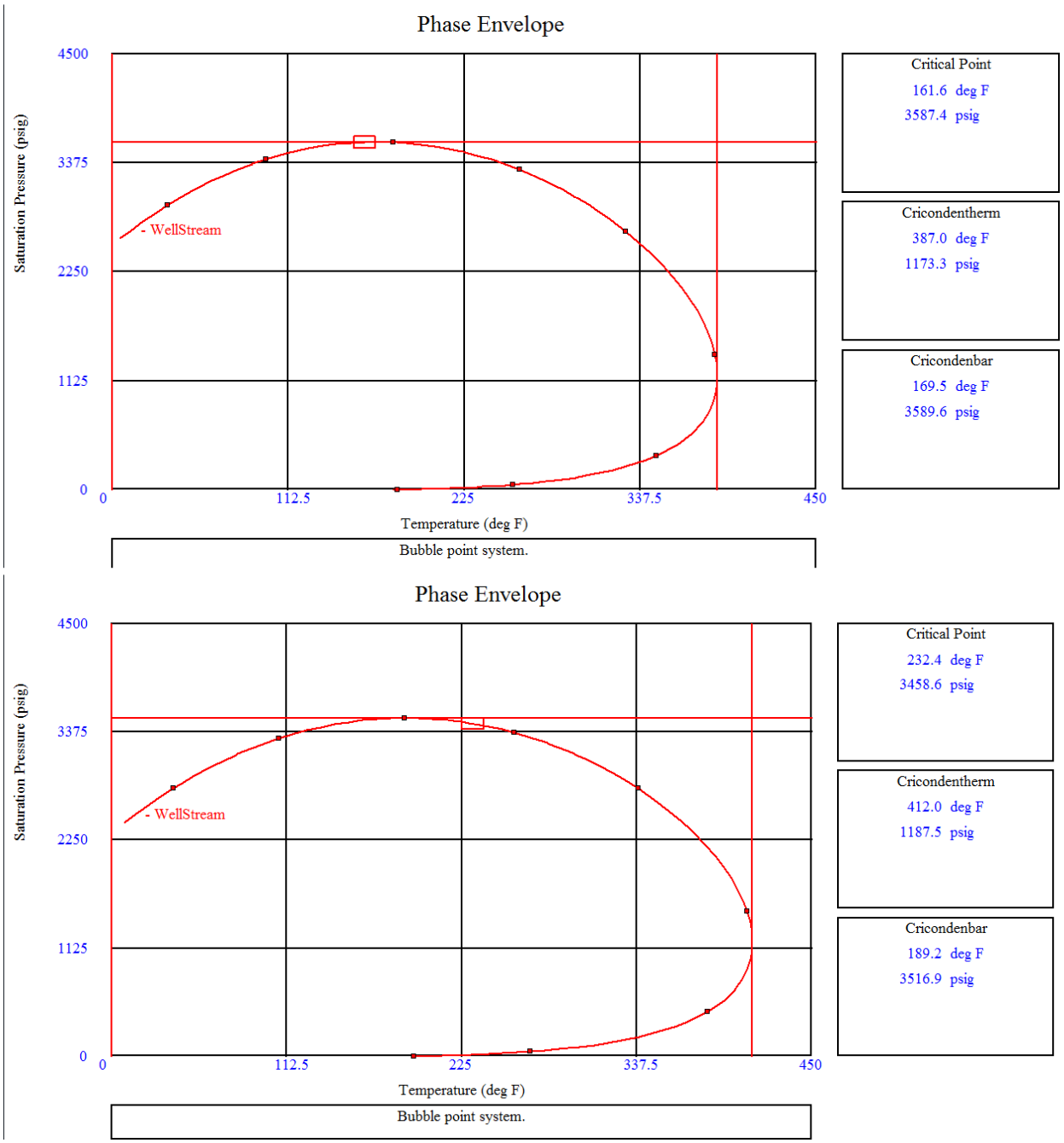

Figure 36: Phase Envelopes from commercial PVT code

Phase envelopes computed with PR EOS from two different RFT-reported compositions, 426-1BP3 and 471-1. The shallower sample in 471-1 indicates a retrograde gas, though P_{dew} is significantly below initial reservoir pressure (10,600 *psia*). The critical point passes to the right (higher temperature) of the reservoir depletion path (marked by the black arrow) for the sample taken nearest to the OGWC (bottom).

However, the near-OGWC gas nonetheless exhibits a gas-like neutron density crossover in terms of well log character [**Figure 37**].

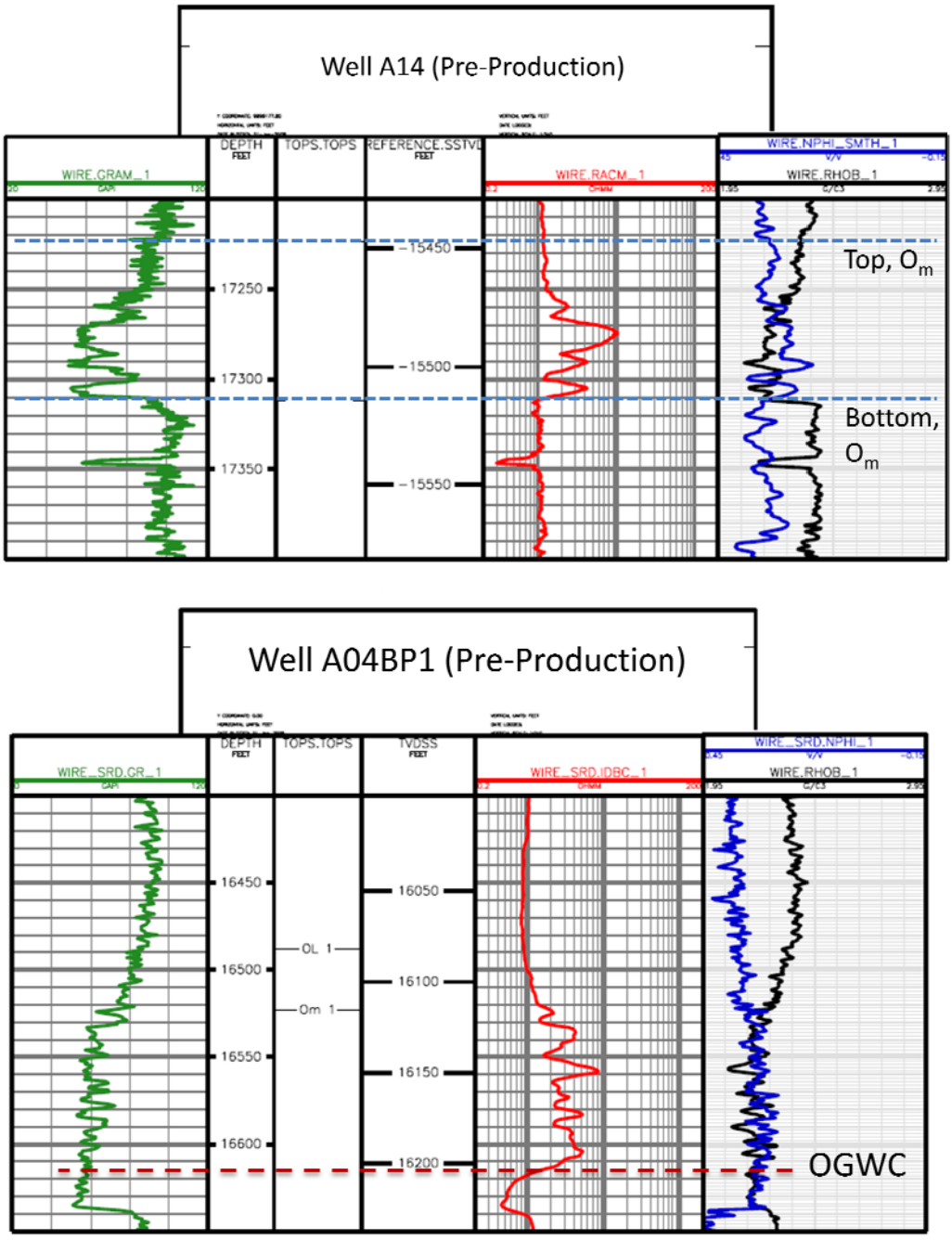

Figure 37: Pre-Production Down-dip Wireline Log with Gas 'Show'

Though phase-behavior modeling shows a much more 'oil-like' fluid at the bottom of the hydrocarbon column [**Figure 36**], the density of the reservoir fluid is such that it is indistinguishable from gas in several ways. The overall fluid density is nearly identical, the bubble point of the oil-like fluid is nearly identical to the dew point of the gas, and a neutron density crossover (bottom), even at a different pre-production well, indicates a gas show.

The gas model is the more reasonable approach to black-oil modeling because the heighth of hydrocarbon column between 426-1BP3 (16177 ft TVDSS) and 471-1 (15954 ft TVDSS) is much smaller than that between 471-1 and the highest point on mappable on structure (roughly 15000 ft TVDSS, see Figure 20). In addition, the OGWC at roughly 16,205 ft TVDSS means that any oil behavior would occur at or near the contact.

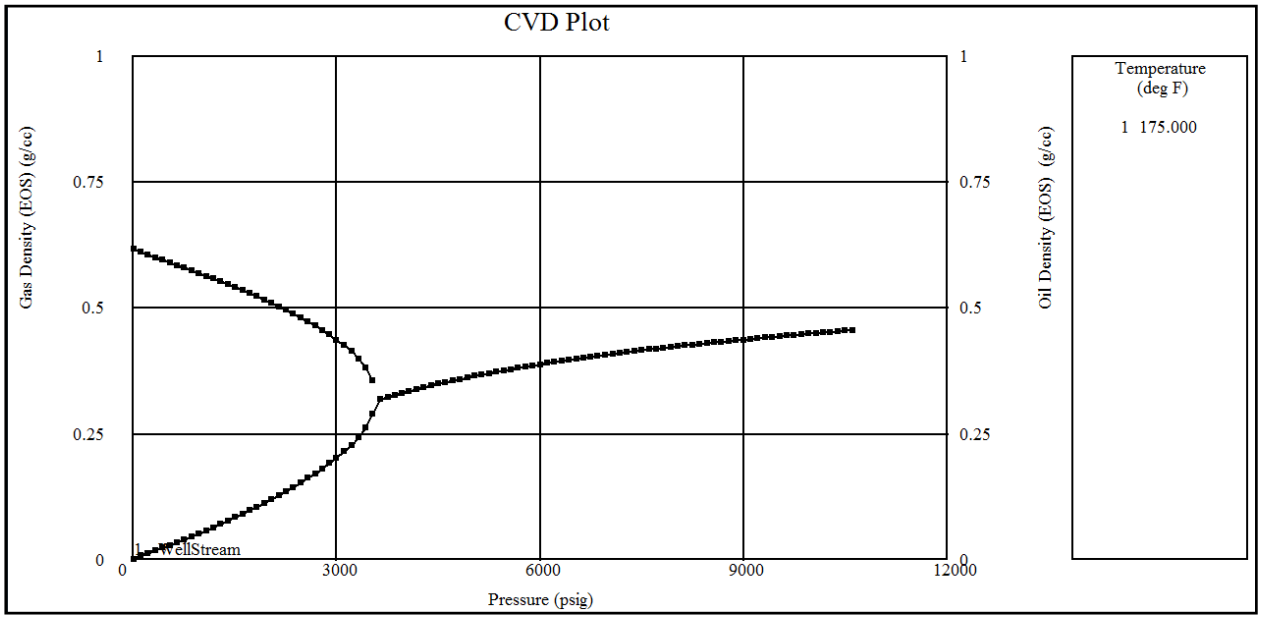

Figure 38. Gas and Condensate Density vs. Pressure T_{RES}, PR EOS

The two density curves split as the Reservoir Depletion Isotherm (theoretical) crosses into the two-phase region [Figure 36]. In the case of the heavier hydrocarbon composition in well 426-1BP3, the density curves are identical in pressure ranges above the phase envelope, but according to fundamental definitions, the gas phase is evolved from the liquid phase in that case.

Using the selected gas model, black-oil tables of viscosity and B_g were constructed for use in the reservoir model [**Figure 39**]. Above dew-point pressure, the single-phase assumption holds, and therefore the black-oil model is sufficient to capture the physics at work for this study. Though a compositional model might have yielded additional insights into reservoir fluid behavior, wellhead compositional data over time is not available;

lacking this data, the compositional model would not be sufficiently constrained.

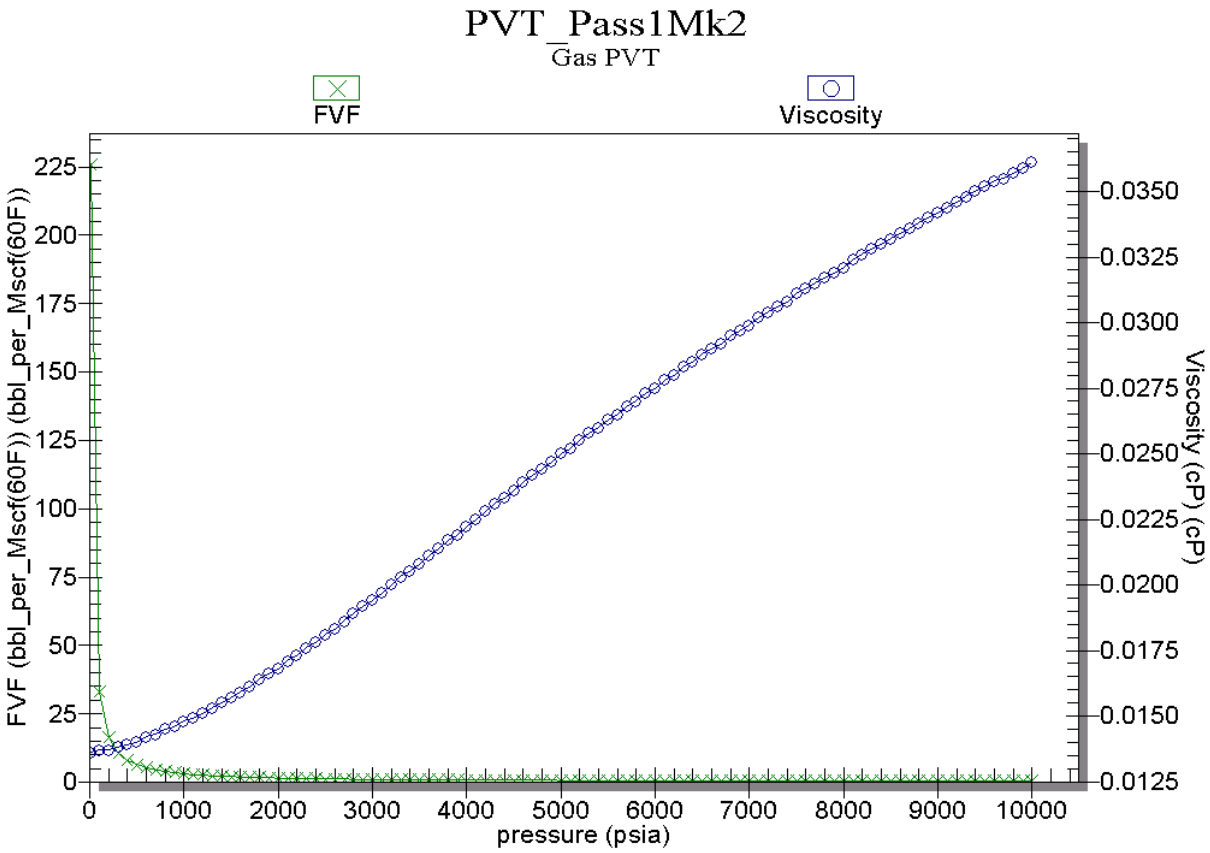

Figure 39: Gas Formation Volume Factor and Viscosity used in history matching studies

Gas formation volume factor (B_g) and viscosity, μ, used in history matching. These are computed with the PR EOS and the Lee, et al., correlation, respectively.

Appendix C: Well Deviation Surveys

The wells of the Auger field are drilled from a seafloor pad and use a DVA, wet-tree strategy. Because these are all drilled from a common pad on the sea floor, steering becomes a necessity. Though **Figure 1** summarizes the MD vs. TVDSS relationships of the wells used in this study, the A14 and A16ST are particularly deviated. Cumulative displacement plots [**Figure 40, Figure 41**] are a useful representation of the curvature of the wells, and as seen in Chapter 5, this curvature has an important impact on flowing frictional pressure drop in wells steered to these extremes.

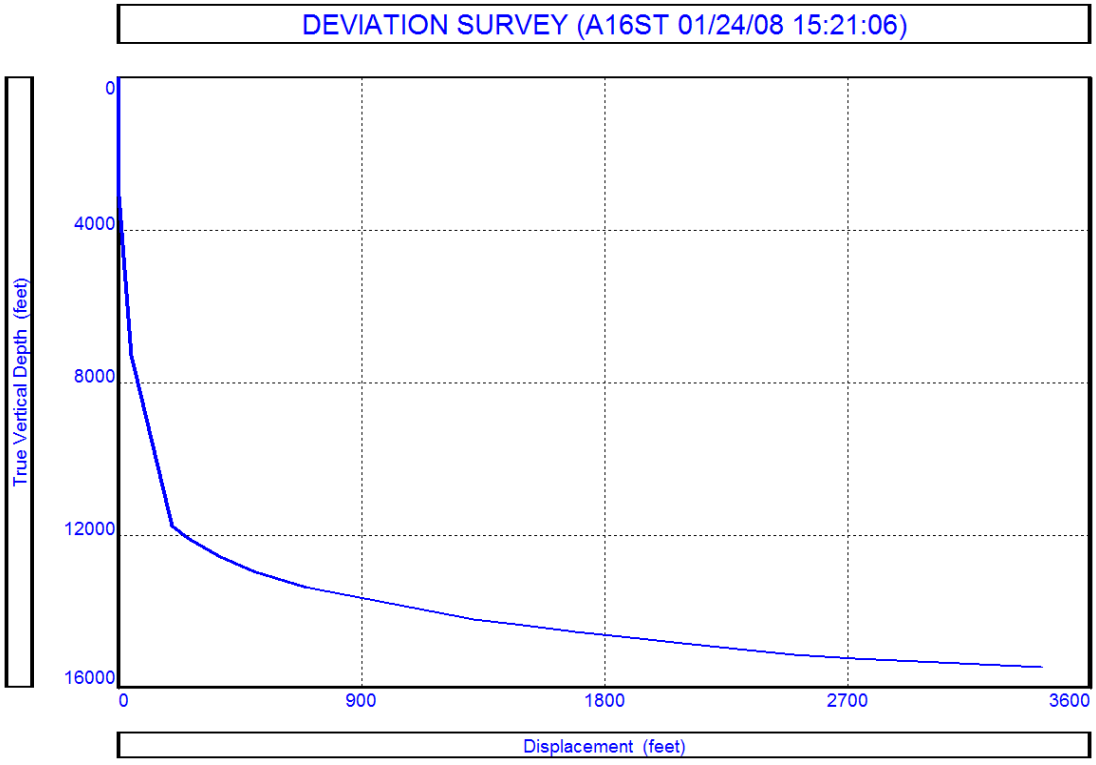

Figure 40: Deviation Survey, A16ST

A16ST is the most deviated well used in this dataset, and becomes nearly horizontal (~75 degrees from vertical) at the penetration of the O Massive Sand used in this study.

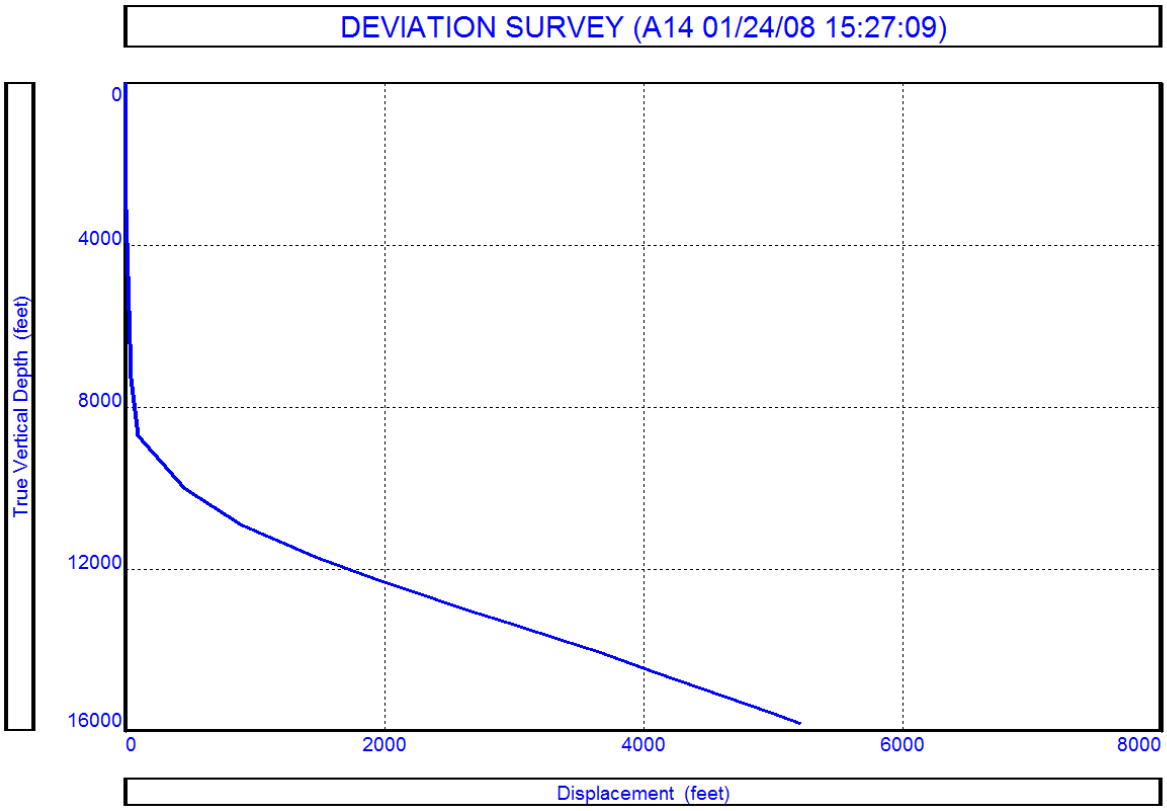

Figure 41: Deviation Survey, A14

The A14 well was the first producer in the O_m^1 Sand. While the wells at Auger are drilled from a common seafloor pad, the A16ST required greater steering to reach the partly-sealed fault block West of the A14's penetration of the O_m^1.

Appendix D: Tables of ANN Training and Simulation Values

ANN training data was taken from the Auger shallow gas sands, operated by SEPCO, and is represented here in Table 3 and Table 4. Adjustments needed to convert raw field data into ANN training data are also represented by the normalization parameters along the top row of each table.

Table 3: Direct Inputs for Phase 1 ANN (Ch. 4.1)

		DIRECT INPUTS									
		Pwh	GAS	OIL	WTR	WTRCUT	Avg.Angle	Avg. Dev.	MD	TVD	BHP
	Norm. Param.	**5997**	**13412**	**81528**	**4600**	**0.374**	**90**	**1.414**	**17820**	**17204.99524**	**11591**
A14	12/10/98	2510	7,839	43,254	14	5.24E-05	21.91249	1.023483	15917.999	15099.72222	6485.4263
	12/15/98	3238	5,578	29,250	66	0	21.91249	1.023483	15917.999	15099.72222	6181.0098
	2/18/99	5690	5,731	31,469	23	6.15E-05	21.91249	1.023483	15917.999	15099.72222	9202.8672
	2/19/99	5560	6,044	32,985	18	6.1E-05	21.91249	1.023483	15917.999	15099.72222	9098.8418
	2/20/99	5082	7,345	40,740	15	0.000364	21.91249	1.023483	15917.999	15099.72222	9658.8066
	2/21/99	4922	7,786	43,110	16	0.000118	21.91249	1.023483	15917.999	15099.72222	8778.3838
	2/22/99	4718	8,146	45,276	20	8.83E-05	21.91249	1.023483	15917.999	15099.72222	8575.2988
	2/23/99	4510	8,439	47,292	59	5.96E-05	21.91249	1.023483	15917.999	15099.72222	8457.3281
	2/24/99	4135	9,149	50,996	18	6E-05	21.91249	1.023483	15917.999	15099.72222	8225.5811
	4/20/99	3695	9,737	53,220	24	7.15E-05	21.91249	1.023483	15917.999	15099.72222	8677.9951
	6/29/99	1902	8,436	47,586	0	0.000202	21.91249	1.023483	15917.999	15099.72222	5230.0098
	8/1/99	5507	6,170	32,724	0	5.71E-05	21.91249	1.023483	15917.999	15099.72222	8934.1963
	8/7/99	4542	8,316	45,360	0	2.82E-05	21.91249	1.023483	15917.999	15099.72222	8718.6104
	8/8/99	3585	10,025	55,494	0	3.12E-05	21.91249	1.023483	15917.999	15099.72222	8233.9766
	8/23/99	2022	11,206	62,830	0	7.29E-05	21.91249	1.023483	15917.999	15099.72222	6794.9038
	12/7/99	1882	11,461	47,028	0	0	21.91249	1.023483	15917.999	15099.72222	9089.124
	2/3/00	3820	7,728	28,448	0	2.94E-05	21.91249	1.023483	15917.999	15099.72222	7141.395
	2/6/00	3820	5,791	31,904	0	0	21.91249	1.023483	15917.999	15099.72222	8309.6318
	2/15/00	3350	7,632	43,170	0	0	21.91249	1.023483	15917.999	15099.72222	7022.1724
	5/19/00	3975	6,702	28,422	14	0.000118	21.91249	1.023483	15917.999	15099.72222	7169.8042
	6/18/00	1947	8,241	55,374		0	21.91249	1.023483	15917.999	15099.72222	6479.228
	6/23/00	1985	10,296	52,842		0	21.91249	1.023483	15917.999	15099.72222	6377.0195
	7/14/00	1890	7,954	38,172		0	21.91249	1.023483	15917.999	15099.72222	8641.8701
	8/3/00	1844	4,112	21,810		0	21.91249	1.023483	15917.999	15099.72222	7083.0352
	2/4/02	1898	10,877	48,930	2,747	0.009023	21.91249	1.023483	15917.999	15099.72222	6711.7378
	4/4/02	1865	10,817	47,502	0	0	21.91249	1.023483	15917.999	15099.72222	6586.3081

	5/24/02	1902	10,405	45,776	0	0	21.91249	1.023483	15917.999	15099.72222		6462.1616
	6/24/02	2350	9,396	40,700	5	1.97E-05	21.91249	1.023483	15917.999	15099.72222		6524.4551
	8/10/02	1897	9,576	40,712	8	3.15E-05	21.91249	1.023483	15917.999	15099.72222		6140.3848
	10/20/02	1897	9,312	37,186	0	0	21.91249	1.023483	15917.999	15099.72222		5911.9155
	12/13/02	1837	7,819	31,385	360	0.001836	21.91249	1.023483	15917.999	15099.72222		5486.9897
	1/1/03	1690	8,216	29,542	618	0.003332	21.91249	1.023483	15917.999	15099.72222		5271.0254
	1/28/03	1675	6,414	22,347	875	0.006228	21.91249	1.023483	15917.999	15099.72222		5068.7969
	2/24/03	1655	5,043	18,230	1,592	0.013913	21.91249	1.023483	15917.999	15099.72222		5028.2769
	5/12/03	1592	3,934	10,122	1,311	0.020273	21.91249	1.023483	15917.999	15099.72222		5269.0488
	6/26/03	1625	3,617	10,287	3,617	0.055357	21.91249	1.023483	15917.999	15099.72222		5426.4541
	7/23/03	1585	3,535	9,400	2,560	0.042713	21.91249	1.023483	15917.999	15099.72222		5614.8809
	9/16/03	1555	1,925	5,537	1,960	0.055766	21.91249	1.023483	15917.999	15099.72222		5756.7808
	11/22/03	1550	748	3,732	2,700	0.116681	21.91249	1.023483	15917.999	15099.72222		6000.54
	12/1/03	1440	605	4,891	2,902	0.096892	21.91249	1.023483	15917.999	15099.72222		5816.1465
	1/10/04	1353	519	4,424	3,244	0.119868	21.91249	1.023483	15917.999	15099.72222		7106.7119
	3/4/04	1345	977	4,018	2,930	0.116803	21.91249	1.023483	15917.999	15099.72222		5817.8613
	3/17/04	1462	653	3,130	2,614	0.134513	21.91249	1.023483	15917.999	15099.72222		6195.8613
	4/1/04	1305	1,665	4,200	2,497	0.092946	21.91249	1.023483	15917.999	15099.72222		5782.915
	5/13/04	1280	1,020	4,256	4,079	0.1536	21.91249	1.023483	15917.999	15099.72222		5806.877
	5/20/04	1230	657	4,027	3,451	0.139047	21.91249	1.023483	15917.999	15099.72222		5724.3408
	6/4/04	1270	788	4,584	3,524	0.124558	21.91249	1.023483	15917.999	15099.72222		5820.1377
	8/17/04	1217	491	3,644	3,976	0.177857	21.91249	1.023483	15917.999	15099.72222		5816.752
	8/27/04	1235	493	3,696	3,987	0.175879	21.91249	1.023483	15917.999	15099.72222		5803.6528
	9/9/04	1260	437	3,594	3,932	0.178719	21.91249	1.023483	15917.999	15099.72222		5838.2461
	10/10/04	1200	707	3,921	3,854	0.159039	21.91249	1.023483	15917.999	15099.72222		5756.8511
	10/17/04	1232	503	3,784	4,071	0.175421	21.91249	1.023483	15917.999	15099.72222		5964.6235
	11/1/04	1180	367	3,593	4,216	0.192292	21.91249	1.023483	15917.999	15099.72222		5814.0034
	11/7/04	1152	459	3,686	4,133	0.183079	21.91249	1.023483	15917.999	15099.72222		5796.9102
	12/13/04	1045	453	3,630	4,576	0.20582	21.91249	1.023483	15917.999	15099.72222		5878.5737
	1/30/05	1345	1,019	3,334	4,077	0.19393	21.91249	1.023483	15917.999	15099.72222		6543.3452
	2/4/05	1225	463	2,848	4,164	0.237251	21.91249	1.023483	15917.999	15099.72222		6335.6055
	2/12/05	967	504	3,304	4,538	0.223239	21.91249	1.023483	15917.999	15099.72222		5795.3242
	2/25/05	1005	192	3,158	4,600	0.240334	21.91249	1.023483	15917.999	15099.72222		5827.4565
	3/5/05	1432	280	2,213	3,221	0.237572	21.91249	1.023483	15917.999	15099.72222		6491.1865
	3/10/05	1727	302	1,960	2,718	0.225336	21.91249	1.023483	15917.999	15099.72222		6973.0918
	3/21/05	1777	369	2,160	2,706	0.203016	21.91249	1.023483	15917.999	15099.72222		6967.7065
	4/3/05	1917	62	240	561	0.373502	21.91249	1.023483	15917.999	15099.72222		8119.8652
	7/31/05	2307	29	1,370	2,877	0.34877	21.91249	1.023483	15917.999	15099.72222		8396.3486
A16ST	10/15/99	5997	5,000	30,080	15	8.09E-05	20.45488	1.001009	16200	15201.03333		9547.9209
	10/18/99	5267	9,524	48,378	19	6.34E-05	20.45488	1.001009	16200	15201.03333		8966.1133
	10/20/99	5130	10,158	51,696	20	6.24E-05	20.45488	1.001009	16200	15201.03333		8895.0859
	11/1/99	4980	8,243	53,203	0	0	20.45488	1.001009	16200	15201.03333		8832.1221
	11/15/99	2165	12,358	81,528	0	0	20.45488	1.001009	16200	15201.03333		7932.2212
	2/15/00	2165	11,766	73,128	0	0	20.45488	1.001009	16200	15201.03333		7323.6992
	3/26/00	2093	11,673	68,220	0	0	20.45488	1.001009	16200	15201.03333		6449.7866
	5/18/00	2107	11,915	65,994	0	0	20.45488	1.001009	16200	15201.03333		8263.6182
	7/15/00	2020	11,569	58,446	0	0	20.45488	1.001009	16200	15201.03333		6980.7295
	9/14/00	2070	11,556	51,678	0	0	20.45488	1.001009	16200	15201.03333		7002.7734

11/7/00	2065	13,411	57,594	0	0	20.45488	1.001009	16200	15201.03333	8754.6748
11/21/00	1895	13,412	57,594	0	0	20.45488	1.001009	16200	15201.03333	7162.7036
1/8/01	2032	10,991	58,890	0	0	20.45488	1.001009	16200	15201.03333	1351.3359
2/23/01	2028	11,232	58,446	0	0	20.45488	1.001009	16200	15201.03333	6676.769
4/14/01	2035	10,626	51,900	0	0	20.45488	1.001009	16200	15201.03333	6629.168
6/14/01	3190	8,705	41,112	0	0	20.45488	1.001009	16200	15201.03333	7121.1113
7/14/01	1987	10,971	51,198	0	0	20.45488	1.001009	16200	15201.03333	6670.6147
8/12/01	2050	10,735	49,110	0	0	20.45488	1.001009	16200	15201.03333	8344.0195
10/12/01	1940	9,789	48,035	0	0	20.45488	1.001009	16200	15201.03333	6373.4067
12/10/01	1962	10,558	45,894	0	0	20.45488	1.001009	16200	15201.03333	6373.4067
2/4/02	1905	10,144	44,178	0	0	20.45488	1.001009	16200	15201.03333	6142.252
4/4/02	1857	10,010	43,800	101	0.00037	20.45488	1.001009	16200	15201.03333	6013.9004
5/25/02	1908	10,158	43,300	0	0	20.45488	1.001009	16200	15201.03333	5975.1831
6/25/02	3625	8,197	34,300	0	0	20.45488	1.001009	16200	15201.03333	6294.8325
7/20/02	1945	9,240	37,823	2	8.47E-06	20.45488	1.001009	16200	15201.03333	5836.7373
9/19/02	1878	9,283	33,800	0	0	20.45488	1.001009	16200	15201.03333	5595.7314
10/23/02	1877	8,461	33,651	0	0	20.45488	1.001009	16200	15201.03333	7847.2207
12/13/02	1825	5,670	24,195	493	0.003268	20.45488	1.001009	16200	15201.03333	4825.5684
1/1/03	1652	4,225	16,926	688	0.006504	20.45488	1.001009	16200	15201.03333	4329.1665
1/20/03	1643	2,741	11,928	914	0.0123	20.45488	1.001009	16200	15201.03333	4212.1826
1/28/03	1660	2,591	9,938	493	0.007924	20.45488	1.001009	16200	15201.03333	4220.1968
2/25/03	1640	2,160	8,593	507	0.009438	20.45488	1.001009	16200	15201.03333	4286.0122
3/29/03	1642	2,403	7,792	74	0.001505	20.45488	1.001009	16200	15201.03333	4342.5078
5/11/03	1577	1,898	5,991	309	0.008165	20.45488	1.001009	16200	15201.03333	4340.4478
6/24/03	1657	1,126	3,768	751	0.031642	20.45488	1.001009	16200	15201.03333	4668.397
7/24/03	1535	1,490	3,981	223	0.008788	20.45488	1.001009	16200	15201.03333	4571.0371
9/16/03	1547	1,031	3,229	362	0.017741	20.45488	1.001009	16200	15201.03333	4705.0488
11/23/03	1532	940	2,719	316	0.018315	20.45488	1.001009	16200	15201.03333	4778.6421
11/29/03	1542	730	2,529	491	0.030873	20.45488	1.001009	16200	15201.03333	4792.1758
10/2/04	3610	385	2,587	2,367	0.148802	20.45488	1.001009	16200	15201.03333	8719.2646
10/22/04	4090	940	3,126	1,409	0.071537	20.45488	1.001009	16200	15201.03333	8698.959
11/5/04	4222	1,256	3,967	1,160	0.046293	20.45488	1.001009	16200	15201.03333	8659.9707
11/11/04	4135	1,439	4,951	1,439	0.046203	20.45488	1.001009	16200	15201.03333	8581.1777
12/3/04	4257	1,063	3,316	869	0.041462	20.45488	1.001009	16200	15201.03333	8592.124
12/18/04	4280	1,333	5,178	1,387	0.042807	20.45488	1.001009	16200	15201.03333	8610.5479
8/7/05	3950	1,618	4,443	2,427	0.085833	20.45488	1.001009	16200	15201.03333	9195.2324
8/18/05	4250	1,865	6,719	1,792	0.042486	20.45488	1.001009	16200	15201.03333	9195.2324
8/26/05	4362	1,707	5,286	1,046	0.031296	20.45488	1.001009	16200	15201.03333	9195.2324
9/11/05	4312	1,716	6,473	1,716	0.042314	20.45488	1.001009	16200	15201.03333	9195.2324
3/13/05	4280	1,505	4,943	47	0.001508	0.478191	1.000019	15642	15640.90476	7698.3149
3/19/05	4400	1,402	5,119	7	0.000218	0.478191	1.000019	15642	15640.90476	7616.9014
3/23/05	3987	1,437	5,172	234	0.007207	0.478191	1.000019	15642	15640.90476	7720.8237
4/13/05	3617	1,196	4,192	299	0.011348	0.478191	1.000019	15642	15640.90476	7146.3872
4/21/05	3612	1,130	4,069	377	0.014759	0.478191	1.000019	15642	15640.90476	7137.5327
4/30/05	3557	973	3,885	524	0.021579	0.478191	1.000019	15642	15640.90476	7102.2759
5/10/05	3485	1,084	3,764	381	0.016098	0.478191	1.000019	15642	15640.90476	7048.8755
7/2/05	3247	1,031	3,530	362	0.016298	0.478191	1.000019	15642	15640.90476	6899.9951
7/27/05	3337	1,055	3,530	371	0.016685	0.478191	1.000019	15642	15640.90476	7071.2949

	8/10/05	2147	882	2,869	326	0.018015	0.478191	1.000019	15642	15640.90476		6942.0542
	8/25/05	3023	728	2,443	392	0.025478	0.478191	1.000019	15642	15640.90476		6953.5859
	9/9/05	2977	733	2,419	412	0.027022	0.478191	1.000019	15642	15640.90476		7071.0332
	12/16/05	3040	701	2,107	468	0.035075	0.478191	1.000019	15642	15640.90476		7058.7925
	1/13/06	2820	588	1,868	252	0.021363	0.478191	1.000019	15642	15640.90476		6856.2798
	1/17/06	2825	489	1,913	489	0.040862	0.478191	1.000019	15642	15640.90476		6879.7837
	2/5/06	2761	437	1,710	357	0.033374	0.478191	1.000019	15642	15640.90476		6859.1226
	3/4/06	2692	375	1,137	250	0.034737	0.478191	1.000019	15642	15640.90476		6958.6699
	3/24/06	2610	410	1,250	273	0.034513	0.478191	1.000019	15642	15640.90476		6851.6406
	4/8/06	2628	350	1,130	286	0.040112	0.478191	1.000019	15642	15640.90476		6911.4043
	4/20/06	2540	359	1,239	294	0.037726	0.478191	1.000019	15642	15640.90476		6864.6191
	5/4/06	2500	416	1,331	416	0.049512	0.478191	1.000019	15642	15640.90476		6853.5693
	6/10/06	2332	328	1,147	303	0.042025	0.478191	1.000019	15642	15640.90476		6826.7671
	6/25/06	2325	280	949	342	0.057248	0.478191	1.000019	15642	15640.90476		6838.2437
	7/4/06	2332	277	1,067	339	0.050756	0.478191	1.000019	15642	15640.90476		6813.0811
A01	2/6/03	770	1,125	5,912	29	0.000792	21.18991	1.01836	14950	14131.85356		2315.4912
	3/31/03	1620	893	3,538	0	0	21.18991	1.01836	14950	14131.85356		3995.2676
	5/12/03	1565	861	3,369	2	9.49E-05	21.18991	1.01836	14950	14131.85356		5160.957
	11/24/03	2600	1,758	8,262	2	3.9E-05	21.18991	1.01836	14950	14131.85356		4891.9961
	11/25/03	1950	1,856	7,958	4	8.06E-05	21.18991	1.01836	14950	14131.85356		3958.4094
	12/7/03	1910	1,251	5,000	6	0.000192	21.18991	1.01836	14950	14131.85356		4034.5427
	12/12/03	1540	1,279	5,265	5	0.000152	21.18991	1.01836	14950	14131.85356		3355.0823
	1/7/04	1545	1,159	4,708	1	3.4E-05	21.18991	1.01836	14950	14131.85356		3514.5371
	2/15/04	1555	1,312	5,037	7	0.000222	21.18991	1.01836	14950	14131.85356		3413.7751
	3/3/04	1535	1,093	4,566	2	7.02E-05	21.18991	1.01836	14950	14131.85356		3374.8425
	3/20/04	1530	1,219	5,031	5	0.000159	21.18991	1.01836	14950	14131.85356		3331.4294
	5/5/04	1535	1,027	4,289	4	0.000149	21.18991	1.01836	14950	14131.85356		3324.512
	5/14/04	1560	1,047	4,453	4	0.000144	21.18991	1.01836	14950	14131.85356		3334.8408
	6/3/04	1560	989	4,211	4	0.000152	21.18991	1.01836	14950	14131.85356		3371.5959
	6/18/04	1550	976	4,176	13	0.000499	21.18991	1.01836	14950	14131.85356		3370.4651
	7/17/04	1552	1,033	4,465	5	0.00018	21.18991	1.01836	14950	14131.85356		3357.2349
	8/18/04	1557	946	3,971	5	0.000202	21.18991	1.01836	14950	14131.85356		3378.3892
	8/27/04	1545	943	4,020	3	0.00012	21.18991	1.01836	14950	14131.85356		3429.3813
	9/5/04	1552	915	3,947	7	0.000285	21.18991	1.01836	14950	14131.85356		3399.6963
	9/24/04	1565	963	4,162	3	0.000116	21.18991	1.01836	14950	14131.85356		3367.7585
	10/10/04	1565	894	3,947	3	0.000122	21.18991	1.01836	14950	14131.85356		3411.3042
	10/23/04	1542	904	3,654	3	0.000131	21.18991	1.01836	14950	14131.85356		3356.5264
	11/6/04	1562	903	4,030	4	0.000159	21.18991	1.01836	14950	14131.85356		3309.7852
	11/9/04	1572	890	3,924	3	0.000123	21.18991	1.01836	14950	14131.85356		3323.6106
	11/22/04	3588	855	3,733	3	0.000129	21.18991	1.01836	14950	14131.85356		3358.9978
	12/10/04	1572	772	3,498	5	0.00023	21.18991	1.01836	14950	14131.85356		3369.8357
	12/20/04	1575	873	3,581	11	0.000492	21.18991	1.01836	14950	14131.85356		3396.6838
	12/27/04	1560	782	3,474	5	0.000231	21.18991	1.01836	14950	14131.85356		3368.6274
	1/10/05	1550	642	3,350	75	0.003616	21.18991	1.01836	14950	14131.85356		3360.4075
	1/29/05	1564	713	3,274	11	0.00054	21.18991	1.01836	14950	14131.85356		3412.3799
	2/10/05	1552	713	3,180	101	0.005103	21.18991	1.01836	14950	14131.85356		3416.7546
	2/21/05	1545	763	3,289	16	0.000781	21.18991	1.01836	14950	14131.85356		3419.2097
	3/5/05	1530	694	2,292	21	0.001454	21.18991	1.01836	14950	14131.85356		3432.7874

3/15/05	1552	688	2,783	14	0.000805	21.18991	1.01836	14950	14131.85356		3458.0271
3/25/05	1552	844	3,270	17	0.000831	21.18991	1.01836	14950	14131.85356		3510.1538
4/4/05	1535	693	3,114	14	0.000723	21.18991	1.01836	14950	14131.85356		3405.2603
4/19/05	1582	713	3,185	15	0.000757	21.18991	1.01836	14950	14131.85356		3444.146
4/30/05	1545	714	3,186	16	0.000807	21.18991	1.01836	14950	14131.85356		3428.9517
5/13/05	1547	675	3,011	17	0.000907	21.18991	1.01836	14950	14131.85356		3446.1279
5/21/05	1550	621	2,686	13	0.000777	21.18991	1.01836	14950	14131.85356		3633.4224
5/24/05	1547	655	2,669	13	0.00078	21.18991	1.01836	14950	14131.85356		3608.543
7/3/05	1565	709	3,240	30	0.001489	21.18991	1.01836	14950	14131.85356		3587.7104
7/26/05	1580	673	3,009	24	0.001282	21.18991	1.01836	14950	14131.85356		3609.2969
8/14/05	1602	637	2,962	30	0.00163	21.18991	1.01836	14950	14131.85356		3646.8723
9/10/05	1562	641	2,910	41	0.002265	21.18991	1.01836	14950	14131.85356		4513.8369
12/10/05	1790	699	2,635	53	0.00321	21.18991	1.01836	14950	14131.85356		4125.8848
1/3/06	1705	547	2,328	9	0.00062	21.18991	1.01836	14950	14131.85356		4141.7632
1/15/06	1690	530	2,489	40	0.002587	21.18991	1.01836	14950	14131.85356		4019.9893
2/7/06	1774	410	1,768	8	0.000726	21.18991	1.01836	14950	14131.85356		4610.9443
2/14/06	1745	564	2,517	12	0.000766	21.18991	1.01836	14950	14131.85356		4130.5303
2/26/06	1735	477	1,977	15	0.001216	21.18991	1.01836	14950	14131.85356		4247.2021
3/6/06	1841	284	1,331	8	0.000967	21.18991	1.01836	14950	14131.85356		4695.395
3/10/06	1782	476	3,107	53	0.002772	21.18991	1.01836	14950	14131.85356		4741.8027
3/24/06	1540	393	1,658	62	0.005996	21.18991	1.01836	14950	14131.85356		3784.3269
4/1/06	1440	403	2,527	60	0.003855	21.18991	1.01836	14950	14131.85356		3525.8523
4/10/06	1415	416	2,082	57	0.004416	21.18991	1.01836	14950	14131.85356		3539.897
4/18/06	1407	404	2,291	55	0.003887	21.18991	1.01836	14950	14131.85356		3530.175
4/26/06	1400	397	2,280	49	0.003481	21.18991	1.01836	14950	14131.85356		3512.7178
5/1/06	1380	395	2,349	49	0.003382	21.18991	1.01836	14950	14131.85356		3513.458
5/21/06	1397	359	2,649	68	0.004184	21.18991	1.01836	14950	14131.85356		3551.6382
6/6/06	1457	413	2,200	46	0.003379	21.18991	1.01836	14950	14131.85356		3562.6731
6/16/06	1397	352	2,159	57	0.004284	21.18991	1.01836	14950	14131.85356		3515.7078
6/30/06	1387	401	2,063	60	0.004695	21.18991	1.01836	14950	14131.85356		3384.4946
7/16/06	1378	383	2,256	62	0.004454	21.18991	1.01836	14950	14131.85356		3484.0024

*Highlighted lines indicates last set of validation values removed from training process

Table 4: Normalized Inputs / Outputs for training of Tansig/Logsig Networks and Extrapolation Network

NORMALIZED									
WHP	GAS	OIL	WTR	WTRCUT	Avg.Angle	Avg. Dev.	MD	TVD	BHP
0.216555	0.584477	0.530542	0.003043	0.00014	0.243472	0.723712	0.893266	0.877636	0.559543
0.279365	0.415896	0.358772	0.014348	0	0.243472	0.723712	0.893266	0.877636	0.533279
0.490916	0.427304	0.38599	0.005	0.000165	0.243472	0.723712	0.893266	0.877636	0.793996
0.4797	0.450641	0.404585	0.003913	0.000163	0.243472	0.723712	0.893266	0.877636	0.785021
0.43846	0.547644	0.499706	0.003261	0.000976	0.243472	0.723712	0.893266	0.877636	0.833333

0.424656	0.580525	0.528775	0.003478	0.000317	0.243472	0.723712	0.893266	0.877636	0.757373
0.407055	0.607367	0.555343	0.004348	0.000236	0.243472	0.723712	0.893266	0.877636	0.739851
0.389109	0.629213	0.580071	0.012826	0.00016	0.243472	0.723712	0.893266	0.877636	0.729673
0.356756	0.68215	0.625503	0.003913	0.000161	0.243472	0.723712	0.893266	0.877636	0.709679
0.318794	0.725992	0.652782	0.005217	0.000191	0.243472	0.723712	0.893266	0.877636	0.748712
0.164099	0.628989	0.583677	0	0.000541	0.243472	0.723712	0.893266	0.877636	0.45123
0.475128	0.460036	0.401384	0	0.000153	0.243472	0.723712	0.893266	0.877636	0.770816
0.39187	0.620042	0.556373	0	7.54E-05	0.243472	0.723712	0.893266	0.877636	0.752216
0.309303	0.747465	0.680674	0	8.36E-05	0.243472	0.723712	0.893266	0.877636	0.710403
0.174452	0.83552	0.770655	0	0.000195	0.243472	0.723712	0.893266	0.877636	0.586244
0.162373	0.854533	0.576832	0	0	0.243472	0.723712	0.893266	0.877636	0.784183
0.329578	0.5762	0.348935	0	7.87E-05	0.243472	0.723712	0.893266	0.877636	0.616138
0.329578	0.431778	0.391326	0	0	0.243472	0.723712	0.893266	0.877636	0.716931
0.289028	0.569043	0.529511	0	0	0.243472	0.723712	0.893266	0.877636	0.605852
0.342951	0.499702	0.348616	0.003043	0.000315	0.243472	0.723712	0.893266	0.877636	0.61859
0.167981	0.61445	0.679202	0	0	0.243472	0.723712	0.893266	0.877636	0.559009
0.17126	0.767671	0.648145	0	0	0.243472	0.723712	0.893266	0.877636	0.55019
0.163064	0.593051	0.468207	0	0	0.243472	0.723712	0.893266	0.877636	0.745595
0.159095	0.306591	0.267515	0	0	0.243472	0.723712	0.893266	0.877636	0.611103
0.163754	0.81099	0.600162	0.597174	0.024157	0.243472	0.723712	0.893266	0.877636	0.579069
0.160907	0.806517	0.582646	0	0	0.243472	0.723712	0.893266	0.877636	0.568247
0.164099	0.775798	0.561476	0	0	0.243472	0.723712	0.893266	0.877636	0.557536
0.202751	0.700567	0.499215	0.001087	5.28E-05	0.243472	0.723712	0.893266	0.877636	0.562911
0.163668	0.713987	0.499362	0.001739	8.44E-05	0.243472	0.723712	0.893266	0.877636	0.529774
0.163668	0.694304	0.456113	0	0	0.243472	0.723712	0.893266	0.877636	0.510063
0.158491	0.582985	0.38496	0.078261	0.004914	0.243472	0.723712	0.893266	0.877636	0.473401
0.145808	0.612586	0.362354	0.134348	0.008921	0.243472	0.723712	0.893266	0.877636	0.454769
0.144514	0.478228	0.274102	0.190217	0.016674	0.243472	0.723712	0.893266	0.877636	0.437321
0.142789	0.376007	0.223604	0.346087	0.037251	0.243472	0.723712	0.893266	0.877636	0.433825
0.137353	0.293319	0.124154	0.285	0.054279	0.243472	0.723712	0.893266	0.877636	0.454598
0.1402	0.269684	0.126178	0.786304	0.148212	0.243472	0.723712	0.893266	0.877636	0.468178
0.136749	0.26357	0.115298	0.556522	0.114358	0.243472	0.723712	0.893266	0.877636	0.484435
0.134161	0.143528	0.067915	0.426087	0.149305	0.243472	0.723712	0.893266	0.877636	0.496678
0.133729	0.055771	0.045776	0.586957	0.312397	0.243472	0.723712	0.893266	0.877636	0.517709
0.124239	0.045109	0.059992	0.63087	0.259414	0.243472	0.723712	0.893266	0.877636	0.5018
0.116733	0.038697	0.054264	0.705217	0.320931	0.243472	0.723712	0.893266	0.877636	0.613146
0.116043	0.072845	0.049284	0.636957	0.312724	0.243472	0.723712	0.893266	0.877636	0.501948
0.126137	0.048688	0.038392	0.568261	0.360141	0.243472	0.723712	0.893266	0.877636	0.534561
0.112592	0.124143	0.051516	0.542826	0.248851	0.243472	0.723712	0.893266	0.877636	0.498933
0.110435	0.076051	0.052203	0.886739	0.411243	0.243472	0.723712	0.893266	0.877636	0.501
0.106121	0.048986	0.049394	0.750217	0.372278	0.243472	0.723712	0.893266	0.877636	0.493879
0.109572	0.058753	0.056226	0.766087	0.333487	0.243472	0.723712	0.893266	0.877636	0.502144
0.104999	0.036609	0.044696	0.864348	0.476188	0.243472	0.723712	0.893266	0.877636	0.501852
0.106552	0.036758	0.045334	0.866739	0.470892	0.243472	0.723712	0.893266	0.877636	0.500722
0.108709	0.032583	0.044083	0.854783	0.478496	0.243472	0.723712	0.893266	0.877636	0.503707
0.103532	0.052714	0.048094	0.837826	0.425806	0.243472	0.723712	0.893266	0.877636	0.496684
0.106293	0.037504	0.046414	0.885	0.469666	0.243472	0.723712	0.893266	0.877636	0.51461
0.101807	0.027364	0.044071	0.916522	0.514835	0.243472	0.723712	0.893266	0.877636	0.501615

0.099391	0.034223	0.045211	0.898478	0.490168	0.243472	0.723712	0.893266	0.877636	0.50014
0.09016	0.033776	0.044525	0.994783	0.551055	0.243472	0.723712	0.893266	0.877636	0.507186
0.116043	0.075977	0.040894	0.886304	0.519222	0.243472	0.723712	0.893266	0.877636	0.564541
0.105689	0.034521	0.034933	0.905217	0.635208	0.243472	0.723712	0.893266	0.877636	0.546617
0.08343	0.037578	0.040526	0.986522	0.597691	0.243472	0.723712	0.893266	0.877636	0.500003
0.086708	0.014316	0.038735	1	0.643462	0.243472	0.723712	0.893266	0.877636	0.502776
0.123549	0.020877	0.027144	0.700217	0.636066	0.243472	0.723712	0.893266	0.877636	0.56004
0.149	0.022517	0.024041	0.59087	0.603305	0.243472	0.723712	0.893266	0.877636	0.601618
0.153314	0.027513	0.026494	0.588261	0.543547	0.243472	0.723712	0.893266	0.877636	0.601153
0.165393	0.004623	0.002944	0.121957	1	0.243472	0.723712	0.893266	0.877636	0.700558
0.199041	0.002162	0.016804	0.625435	0.933782	0.243472	0.723712	0.893266	0.877636	0.724412
0.517403	0.3728	0.368953	0.003261	0.000217	0.227276	0.70782	0.909091	0.883524	0.823766
0.454421	0.71011	0.593391	0.00413	0.00017	0.227276	0.70782	0.909091	0.883524	0.77357
0.442601	0.757381	0.634089	0.004348	0.000167	0.227276	0.70782	0.909091	0.883524	0.767442
0.42966	0.614599	0.652573	0	0	0.227276	0.70782	0.909091	0.883524	0.762009
0.18679	0.921414	1	0	0	0.227276	0.70782	0.909091	0.883524	0.684369
0.18679	0.877274	0.896968	0	0	0.227276	0.70782	0.909091	0.883524	0.631867
0.180578	0.87034	0.836768	0	0	0.227276	0.70782	0.909091	0.883524	0.556469
0.181786	0.888384	0.809464	0	0	0.227276	0.70782	0.909091	0.883524	0.712961
0.17428	0.862586	0.716883	0	0	0.227276	0.70782	0.909091	0.883524	0.602277
0.178593	0.861616	0.633868	0	0	0.227276	0.70782	0.909091	0.883524	0.604179
0.178162	0.999925	0.706432	0	0	0.227276	0.70782	0.909091	0.883524	0.755328
0.163495	1	0.706432	0	0	0.227276	0.70782	0.909091	0.883524	0.617977
0.175315	0.81949	0.722329	0	0	0.227276	0.70782	0.909091	0.883524	0.116589
0.17497	0.837459	0.716883	0	0	0.227276	0.70782	0.909091	0.883524	0.576052
0.175574	0.792276	0.636591	0	0	0.227276	0.70782	0.909091	0.883524	0.571945
0.275224	0.649046	0.504268	0	0	0.227276	0.70782	0.909091	0.883524	0.614388
0.171432	0.817999	0.627981	0	0	0.227276	0.70782	0.909091	0.883524	0.575521
0.176868	0.800403	0.60237	0	0	0.227276	0.70782	0.909091	0.883524	0.719897
0.167377	0.729869	0.589184	0	0	0.227276	0.70782	0.909091	0.883524	0.549879
0.169276	0.787205	0.562923	0	0	0.227276	0.70782	0.909091	0.883524	0.549879
0.164358	0.756338	0.541875	0	0	0.227276	0.70782	0.909091	0.883524	0.529935
0.160216	0.746347	0.537239	0.021957	0.000991	0.227276	0.70782	0.909091	0.883524	0.518862
0.164617	0.757381	0.531106	0	0	0.227276	0.70782	0.909091	0.883524	0.515521
0.312754	0.611169	0.420714	0	0	0.227276	0.70782	0.909091	0.883524	0.5431
0.167809	0.688935	0.463927	0.000435	2.27E-05	0.227276	0.70782	0.909091	0.883524	0.503576
0.162028	0.692141	0.414581	0	0	0.227276	0.70782	0.909091	0.883524	0.482783
0.161942	0.630853	0.412754	0	0	0.227276	0.70782	0.909091	0.883524	0.677035
0.157456	0.422756	0.296769	0.107174	0.008751	0.227276	0.70782	0.909091	0.883524	0.416336
0.14253	0.315016	0.20761	0.149565	0.017414	0.227276	0.70782	0.909091	0.883524	0.373508
0.141753	0.204369	0.146306	0.198696	0.032932	0.227276	0.70782	0.909091	0.883524	0.363415
0.14322	0.193185	0.121897	0.107174	0.021214	0.227276	0.70782	0.909091	0.883524	0.364106
0.141494	0.16105	0.105399	0.110217	0.025269	0.227276	0.70782	0.909091	0.883524	0.369784
0.141667	0.179168	0.095575	0.016087	0.004031	0.227276	0.70782	0.909091	0.883524	0.374659
0.136059	0.141515	0.073484	0.067174	0.021861	0.227276	0.70782	0.909091	0.883524	0.374481
0.142961	0.083955	0.046217	0.163261	0.084718	0.227276	0.70782	0.909091	0.883524	0.402776
0.132435	0.111095	0.04883	0.048478	0.023528	0.227276	0.70782	0.909091	0.883524	0.394376
0.133471	0.076871	0.039606	0.078696	0.047498	0.227276	0.70782	0.909091	0.883524	0.405938

0.132176	0.070086	0.033351	0.068696	0.049035	0.227276	0.70782	0.909091	0.883524	0.412287
0.133039	0.054429	0.03102	0.106739	0.082657	0.227276	0.70782	0.909091	0.883524	0.413455
0.31146	0.028706	0.031731	0.514565	0.398398	0.227276	0.70782	0.909091	0.883524	0.752272
0.352873	0.070086	0.038343	0.306304	0.191531	0.227276	0.70782	0.909091	0.883524	0.750521
0.364262	0.093647	0.048658	0.252174	0.123942	0.227276	0.70782	0.909091	0.883524	0.747157
0.356756	0.107292	0.060728	0.312826	0.123703	0.227276	0.70782	0.909091	0.883524	0.740359
0.367281	0.079257	0.040673	0.188913	0.111009	0.227276	0.70782	0.909091	0.883524	0.741303
0.369266	0.099389	0.063512	0.301522	0.114611	0.227276	0.70782	0.909091	0.883524	0.742893
0.340794	0.120638	0.054497	0.527609	0.229805	0.227276	0.70782	0.909091	0.883524	0.793338
0.366677	0.139055	0.082413	0.389565	0.113749	0.227276	0.70782	0.909091	0.883524	0.793338
0.37634	0.127274	0.064837	0.227391	0.08379	0.227276	0.70782	0.909091	0.883524	0.793338
0.372027	0.127945	0.079396	0.373043	0.11329	0.227276	0.70782	0.909091	0.883524	0.793338
0.369266	0.112213	0.060629	0.010217	0.004038	0.005313	0.70712	0.877778	0.909091	0.664188
0.379619	0.104533	0.062788	0.001522	0.000584	0.005313	0.70712	0.877778	0.909091	0.657164
0.343987	0.107143	0.063438	0.05087	0.019295	0.005313	0.70712	0.877778	0.909091	0.66613
0.312064	0.089174	0.051418	0.065	0.030383	0.005313	0.70712	0.877778	0.909091	0.616569
0.311633	0.084253	0.049909	0.081957	0.039515	0.005313	0.70712	0.877778	0.909091	0.615805
0.306887	0.072547	0.047652	0.113913	0.057774	0.005313	0.70712	0.877778	0.909091	0.612763
0.300676	0.080823	0.046168	0.082826	0.043099	0.005313	0.70712	0.877778	0.909091	0.608156
0.280142	0.076871	0.043298	0.078696	0.043636	0.005313	0.70712	0.877778	0.909091	0.595311
0.287907	0.078661	0.043298	0.080652	0.044673	0.005313	0.70712	0.877778	0.909091	0.61009
0.185237	0.065762	0.03519	0.07087	0.048233	0.005313	0.70712	0.877778	0.909091	0.59894
0.260816	0.05428	0.029965	0.085217	0.068213	0.005313	0.70712	0.877778	0.909091	0.599935
0.256847	0.054653	0.029671	0.089565	0.072347	0.005313	0.70712	0.877778	0.909091	0.610068
0.262282	0.052267	0.025844	0.101739	0.093907	0.005313	0.70712	0.877778	0.909091	0.609012
0.243301	0.043841	0.022912	0.054783	0.057197	0.005313	0.70712	0.877778	0.909091	0.59154
0.243733	0.03646	0.023464	0.106304	0.109403	0.005313	0.70712	0.877778	0.909091	0.593567
0.238211	0.032583	0.020974	0.077609	0.089354	0.005313	0.70712	0.877778	0.909091	0.591785
0.232258	0.02796	0.013946	0.054348	0.093003	0.005313	0.70712	0.877778	0.909091	0.600374
0.225183	0.03057	0.015332	0.059348	0.092405	0.005313	0.70712	0.877778	0.909091	0.591139
0.226736	0.026096	0.01386	0.062174	0.107395	0.005313	0.70712	0.877778	0.909091	0.596296
0.219144	0.026767	0.015197	0.063913	0.101007	0.005313	0.70712	0.877778	0.909091	0.592259
0.215693	0.031017	0.016326	0.090435	0.132562	0.005313	0.70712	0.877778	0.909091	0.591306
0.201198	0.024456	0.014069	0.06587	0.112516	0.005313	0.70712	0.877778	0.909091	0.588993
0.200594	0.020877	0.01164	0.074348	0.153274	0.005313	0.70712	0.877778	0.909091	0.589983
0.201198	0.020653	0.013088	0.073696	0.135892	0.005313	0.70712	0.877778	0.909091	0.587813
0.066433	0.08388	0.072515	0.006304	0.002122	0.235443	0.720089	0.838945	0.821381	0.199774
0.139769	0.066582	0.043396	0	0	0.235443	0.720089	0.838945	0.821381	0.3447
0.135024	0.064196	0.041323	0.000435	0.000254	0.235443	0.720089	0.838945	0.821381	0.445272
0.22432	0.131077	0.101339	0.000435	0.000104	0.235443	0.720089	0.838945	0.821381	0.422067
0.16824	0.138384	0.097611	0.00087	0.000216	0.235443	0.720089	0.838945	0.821381	0.34152
0.164789	0.093275	0.061329	0.001304	0.000514	0.235443	0.720089	0.838945	0.821381	0.348088
0.132867	0.095362	0.064579	0.001087	0.000407	0.235443	0.720089	0.838945	0.821381	0.289467
0.133298	0.086415	0.057747	0.000217	9.1E-05	0.235443	0.720089	0.838945	0.821381	0.303224
0.134161	0.097823	0.061782	0.001522	0.000594	0.235443	0.720089	0.838945	0.821381	0.29453
0.132435	0.081494	0.056005	0.000435	0.000188	0.235443	0.720089	0.838945	0.821381	0.291171
0.132004	0.090889	0.061709	0.001087	0.000426	0.235443	0.720089	0.838945	0.821381	0.287426
0.132435	0.076573	0.052608	0.00087	0.0004	0.235443	0.720089	0.838945	0.821381	0.286829

0.134592	0.078064	0.054619	0.00087	0.000386	0.235443	0.720089	0.838945	0.821381	0.28772
0.134592	0.07374	0.051651	0.00087	0.000408	0.235443	0.720089	0.838945	0.821381	0.290891
0.133729	0.072771	0.051222	0.002826	0.001337	0.235443	0.720089	0.838945	0.821381	0.290794
0.133902	0.077021	0.054766	0.001087	0.000481	0.235443	0.720089	0.838945	0.821381	0.289652
0.134333	0.070534	0.048707	0.001087	0.00054	0.235443	0.720089	0.838945	0.821381	0.291477
0.133298	0.07031	0.049308	0.000652	0.00032	0.235443	0.720089	0.838945	0.821381	0.295877
0.133902	0.068222	0.048413	0.001522	0.000762	0.235443	0.720089	0.838945	0.821381	0.293316
0.135024	0.071801	0.05105	0.000652	0.00031	0.235443	0.720089	0.838945	0.821381	0.29056
0.135024	0.066657	0.048413	0.000652	0.000327	0.235443	0.720089	0.838945	0.821381	0.294317
0.133039	0.067402	0.044819	0.000652	0.000352	0.235443	0.720089	0.838945	0.821381	0.289591
0.134765	0.067328	0.049431	0.00087	0.000427	0.235443	0.720089	0.838945	0.821381	0.285558
0.135628	0.066358	0.048131	0.000652	0.000329	0.235443	0.720089	0.838945	0.821381	0.286751
0.309562	0.063749	0.045788	0.000652	0.000345	0.235443	0.720089	0.838945	0.821381	0.289804
0.135628	0.05756	0.042906	0.001087	0.000615	0.235443	0.720089	0.838945	0.821381	0.290739
0.135886	0.065091	0.043924	0.002391	0.001317	0.235443	0.720089	0.838945	0.821381	0.293056
0.134592	0.058306	0.042611	0.001087	0.000619	0.235443	0.720089	0.838945	0.821381	0.290635
0.133729	0.047868	0.04109	0.016304	0.009681	0.235443	0.720089	0.838945	0.821381	0.289926
0.134937	0.053161	0.040158	0.002391	0.001447	0.235443	0.720089	0.838945	0.821381	0.29441
0.133902	0.053161	0.039005	0.021957	0.013662	0.235443	0.720089	0.838945	0.821381	0.294788
0.133298	0.056889	0.040342	0.003478	0.00209	0.235443	0.720089	0.838945	0.821381	0.294999
0.132004	0.051745	0.028113	0.004565	0.003892	0.235443	0.720089	0.838945	0.821381	0.296171
0.133902	0.051297	0.034136	0.003043	0.002156	0.235443	0.720089	0.838945	0.821381	0.298348
0.133902	0.062929	0.040109	0.003696	0.002224	0.235443	0.720089	0.838945	0.821381	0.302846
0.132435	0.05167	0.038195	0.003043	0.001934	0.235443	0.720089	0.838945	0.821381	0.293796
0.13649	0.053161	0.039066	0.003261	0.002026	0.235443	0.720089	0.838945	0.821381	0.297151
0.133298	0.053236	0.039079	0.003478	0.00216	0.235443	0.720089	0.838945	0.821381	0.29584
0.133471	0.050328	0.036932	0.003696	0.002429	0.235443	0.720089	0.838945	0.821381	0.297322
0.133729	0.046302	0.032946	0.002826	0.00208	0.235443	0.720089	0.838945	0.821381	0.313481
0.133471	0.048837	0.032737	0.002826	0.002088	0.235443	0.720089	0.838945	0.821381	0.311334
0.135024	0.052863	0.039741	0.006522	0.003986	0.235443	0.720089	0.838945	0.821381	0.309537
0.136318	0.050179	0.036908	0.005217	0.003431	0.235443	0.720089	0.838945	0.821381	0.311399
0.138216	0.047495	0.036331	0.006522	0.004363	0.235443	0.720089	0.838945	0.821381	0.314641
0.134765	0.047793	0.035693	0.008913	0.006064	0.235443	0.720089	0.838945	0.821381	0.389441
0.154436	0.052118	0.03232	0.011522	0.008595	0.235443	0.720089	0.838945	0.821381	0.355969
0.147102	0.040784	0.028555	0.001957	0.00166	0.235443	0.720089	0.838945	0.821381	0.357339
0.145808	0.039517	0.030529	0.008696	0.006925	0.235443	0.720089	0.838945	0.821381	0.346833
0.153055	0.03057	0.021686	0.001739	0.001944	0.235443	0.720089	0.838945	0.821381	0.397819
0.150553	0.042052	0.030873	0.002609	0.002051	0.235443	0.720089	0.838945	0.821381	0.35637
0.149691	0.035565	0.024249	0.003261	0.003255	0.235443	0.720089	0.838945	0.821381	0.366436
0.158836	0.021175	0.016326	0.001739	0.00259	0.235443	0.720089	0.838945	0.821381	0.405105
0.153746	0.035491	0.03811	0.011522	0.007422	0.235443	0.720089	0.838945	0.821381	0.409109
0.132867	0.029302	0.020337	0.013478	0.016052	0.235443	0.720089	0.838945	0.821381	0.326501
0.124239	0.030048	0.030995	0.013043	0.010321	0.235443	0.720089	0.838945	0.821381	0.3042
0.122082	0.031017	0.025537	0.012391	0.011823	0.235443	0.720089	0.838945	0.821381	0.305412
0.121392	0.030122	0.028101	0.011957	0.010407	0.235443	0.720089	0.838945	0.821381	0.304573
0.120788	0.0296	0.027966	0.010652	0.00932	0.235443	0.720089	0.838945	0.821381	0.303067
0.119062	0.029451	0.028812	0.010652	0.009055	0.235443	0.720089	0.838945	0.821381	0.303131
0.120529	0.026767	0.032492	0.014783	0.011202	0.235443	0.720089	0.838945	0.821381	0.306425

0.125706	0.030793	0.026985	0.01	0.009047	0.235443	0.720089	0.838945	0.821381		0.307377
0.120529	0.026245	0.026482	0.012391	0.011469	0.235443	0.720089	0.838945	0.821381		0.303325
0.119666	0.029899	0.025304	0.013043	0.012571	0.235443	0.720089	0.838945	0.821381		0.292004
0.11889	0.028557	0.027671	0.013478	0.011926	0.235443	0.720089	0.838945	0.821381		0.300589

Appendix E: Final Network Weights

The results of the ANN design process in Chapter 5 are a set of weights that could be applied to any future 3-layer network to produce reliable results for wellhead-to-gauge predictions, and, used with caution, for prediction of true flowing bottomhole pressures (see Chapter 7). These are shown in **Table 5,Table 6,** and**Table 7**. The tables are arranged such that the inputs are represented in columns. Inputs 1 through 5 are dynamic inputs: Wellhead Pressue, gas rate, condensate rate, water rate, watercut (STB/MMscf), respectively. Inputs 6 through 9 are static well description parameters: average angle parameter, average deviation parameter, node-to-node length in measured depth, and node-to-node length in true vertical depth, respectively. In Table 5, inputs are sent directly to the neurons, so input numbers correspond to the real inputs. However, in **Tables 6** and **7**, the 'input' to layers 2 and 3 are the outputs of the neurons in the previous layer, so weights do not correlate with real inputs. However, the input layer weights do help to identify sensitivities associated with each input parameter, because these do correspond with inputs.

Table 5: Layer 1 Weights, Final 'Extrapolation' Network

Neurons									
1	8.1978	0.146	4.2482	-1.7111	3.9677	-11.0813	45.1105	18.5386	16.9513
2	-12.226	-4.3296	5.0547	7.8296	3.2756	7.9058	29.1123	-51.6471	14.689
3	-1.6458	8.3281	-12.4328	-0.011	-0.9456	-13.1418	-202.551	-25.8478	21.7743
4	-9.0924	8.3927	0.4728	-2.1248	-1.0048	17.22	7.1707	3.6498	23.4163
5	-8.7669	3.1936	-16.2566	-3.4171	0.2618	9.6033	33.4027	-25.2608	45.0597
6	8.7311	-2.0652	2.5982	-1.1935	1.8912	-11.7025	-177.282	12.1444	0.9548
7	-5.3299	7.9305	2.6539	6.9871	5.5313	13.5196	-3.3263	-19.0032	-36.6335
8	-10.5761	-11.5979	7.697	-0.9977	-4.2457	15.7218	19.1972	-44.5176	-11.1058
9	1.1203	2.5446	2.8958	-0.2295	-1.1582	15.0273	-147.618	47.428	29.4032
Inputs	1	2	3	4	5	6	7	8	9

Table 6: Layer 2 Weights, Final 'Extrapolation' Network

Inputs	(layer 1, neuron 1)	(layer 1, neuron 2)	(layer 1, neuron 3)	(layer 1, neuron 4)	(layer 1, neuron 5)	(layer 1, neuron 6)	(layer 1, neuron 7)	(layer 1, neuron 8)	(layer 1, neuron 9)
1	-3.3024	-3.4843	-0.5928	4.1903	1.0635	-1.2452	3.1613	-4.3494	-4.063
2	-1.5777	-4.2321	1.8669	-1.916	-5.3465	3.6699	2.2158	3.857	-2.7045
3	3.8439	0.5957	4.9731	2.7012	-1.2188	-1.8802	6.3623	-6.2654	1.9464
4	2.7474	-2.553	-2.9109	-2.1208	-2.9786	-3.2866	4.49	-3.4356	-2.513
5	-2.1666	-1.4805	-2.5123	2.458	-2.8743	1.6257	6.497	-5.0038	-3.8298
6	4.7771	2.5605	1.3432	-2.9662	-4.2843	-2.8422	-3.3379	-2.7054	-0.5969
7	-3.5162	-0.1812	2.4155	1.8847	3.0793	2.9917	3.6757	-4.1372	3.6948
8	-0.7624	4.4622	3.7037	-4.9652	3.0558	2.627	0.4141	1.6706	-2.5697
9	-1.4903	-6.5656	-1.3566	1.1833	-2.3318	-1.1273	-6.5581	0.0003	0.7161
10	-1.0986	-0.7286	-4.3729	0.7647	3.8377	-5.6884	-2.1615	-2.9235	-1.5675
11	-3.5181	0.6275	-4.122	-1.0457	2.0759	-3.3251	3.6751	-2.9376	-4.5235
12	-1.0411	0.9648	-1.8631	-3.8961	1.6943	-3.0187	4.5779	-5.5544	0.0828
13	1.2313	2.7377	3.2262	2.3046	-1.6254	3.6903	-4.9238	-1.8522	2.712

14	4.5886	-3.544	-2.8414	-3.3853	-1.574	1.0474	1.3475	-4.7157	-2.3983
15	-2.9632	-2.6063	3.0173	-0.5145	-7.0253	-1.9915	5.1652	1.1187	-5.2236
16	-1.5134	-5.8666	1.8758	-4.9827	-1.6023	-2.2292	-3.2231	0.0222	-2.7527
17	-2.3504	4.6932	-4.6048	-2.8688	0.6711	-0.6609	-4.2324	-1.7733	1.9133
18	-2.7302	3.1946	4.2442	-0.5754	0.0948	5.3522	-3.555	3.0031	-2.3967
19	-3.1285	2.5218	3.9411	2.8093	1.4544	4.0811	-3.866	3.1841	1.2611
20	-4.8764	-4.7172	0.3222	-4.4414	-0.481	0.2792	-0.8965	-3.3281	-5.3857
21	-1.4944	-2.4691	5.9912	2.1127	6.4045	1.5945	-1.197	-0.4193	3.0647
22	-2.9882	-5.3056	-5.2449	2.2891	-6.6442	2.0785	0.2797	-2.4049	-1.9265
23	3.328	-0.0052	2.3335	-4.2106	-0.3193	-4.3106	3.5475	-1.435	-4.2055
24	0.3538	4.1362	6.1767	-0.1664	1.2256	1.0146	-1.2198	4.7836	-1.4796
25	3.4643	1.5744	2.8782	3.4887	-3.1049	-4.0803	-1.6899	3.8131	1.4729
26	4.8745	1.0822	-2.9831	-3.99	0.8783	-0.6619	-5.3328	1.6471	4.6527
27	0.966	2.9097	-2.6844	3.1221	-3.3252	-0.2227	-3.5099	-1.9377	6.1894
28	-3.7248	2.2295	0.2052	1.3511	0.724	-4.6765	-2.5448	-3.6862	4.7014
29	3.7746	3.1914	-0.614	0.6738	3.9263	-4.1285	-4.2483	1.2934	3.575
30	1.3308	2.085	-0.3865	0.1323	0.0514	6.1107	2.8449	-2.4992	5.4318
31	3.0848	-4.4607	6.9692	0.425	0.2906	0.4538	-4.8017	-3.8612	2.2415
32	-1.1092	0.9229	-0.2593	-3.3823	-11.977	-2.4055	1.631	0.9752	-0.5381
33	1.1172	-3.4508	4.3029	-4.9448	-4.4515	-1.1072	-0.9033	-3.2516	-0.607
34	-4.0125	4.1277	0.3517	-1.5399	3.2263	-3.3285	-2.3902	1.8997	-2.9344
35	4.2465	-4.6651	-1.2846	0.8494	4.8573	-4.0011	3.2322	-5.5047	1.5694
36	1.8909	-1.9486	4.715	2.5164	-2.4835	-1.7732	-1.6447	-7.127	5.2787
37	-4.2615	0.7643	3.4118	4.6422	-3.6688	-1.632	-4.1267	-2.8051	-2.422
38	2.2338	0.0195	-0.1684	5.5386	-1.222	3.1831	0.4247	-5.0078	4.2725
39	-0.598	2.6871	-5.8711	-5.1675	2.0592	0.0534	-6.2073	2.6093	-5.1018
40	-4.0281	-0.5762	-5.0355	2.1098	4.5469	-0.809	3.8267	4.4711	-0.8055
41	-3.6456	-3.2139	3.8948	1.4415	2.6169	-4.6603	2.0971	-1.018	-2.706
42	-2.9689	1.2094	3.6992	0.5162	6.9569	3.4061	6.1765	-5.2501	-3.6498
43	-2.5563	-4.5348	-5.9586	-1.7214	4.1868	1.9338	2.4943	-0.6545	1.2435
44	2.769	2.1804	0.8278	-0.2668	-5.2125	4.5577	4.1011	-1.1096	-2.3938
45	3.2245	2.7462	3.221	2.7399	2.4566	2.075	2.1854	3.7573	6.1964
46	0.3709	-2.2852	-4.9467	4.9944	-0.9415	4.9601	2.886	-1.1829	-0.3832
47	0.662	-3.532	-2.2133	-4.9892	-2.9769	4.6796	1.0941	3.8127	2.3004
48	0.8565	-5.4136	4.7265	1.3912	9.8841	-2.329	-3.5525	1.2125	-5.5788
49	5.1812	-2.7736	-4.9936	0.5645	0.4319	1.1125	-0.3774	6.6658	0.352
50	1.5124	-4.1116	3.8405	5.0914	3.7403	2.5827	4.0463	-1.8431	1.4367
51	1.5028	0.8687	5.6887	-2.3832	-4.577	0.1498	-3.452	-4.7047	4.4089

52	3.9283	-4.7749	-4.3156	-2.716	-2.2845	3.2361	-0.4349	3.0296	0.9978
53	0.634	4.6359	-1.1603	-4.5762	2.0143	-3.3619	-0.3715	-2.7332	4.2047
54	-1.2591	-6.1767	-2.8038	0.0599	-3.617	-3.4808	4.4628	-4.7926	4.4626
55	4.479	5.0878	0.2515	3.451	1.0221	-4.9349	1.4368	0.6194	-2.9437
56	-0.474	-2.6975	-3.989	-2.9169	-1.7287	-3.4095	5.2099	3.3361	-3.3485
57	1.0836	0.7132	-6.364	-4.3396	3.6732	0.5112	1.2434	-1.07	3.9395
58	2.0272	-0.3294	7.739	-1.528	2.0727	-0.2026	6.7377	-6.2429	-4.6958
59	1.9731	6.191	6.388	-1.8157	-1.1484	-1.5091	0.3629	-4.1323	-1.6676
60	-3.5285	-3.9218	-1.7791	2.6018	-2.8001	-2.4279	0.3235	5.2093	-2.8232
61	-4.6744	1.8885	1.6639	-0.1222	-1.907	-5.7105	-3.7386	1.0294	2.4589
62	-2.1029	4.3842	-4.5698	-1.4904	4.1028	3.0539	1.0088	-1.0642	-3.994
63	3.1303	6.2178	-2.3664	4.7989	-0.9642	1.5377	5.1852	2.5965	2.042
64	0.5659	-3.9397	-4.6449	5.0913	-0.3937	-0.5618	0.3437	3.2962	3.2866
65	0.5438	-8.6307	-0.0403	3.2194	-0.683	-4.882	-0.5396	-7.0763	0.5345
66	-0.5257	3.8906	-6.5311	-5.4726	4.5335	3.0877	3.0913	3.1419	-2.8437
67	2.1152	-3.9872	3.9232	0.7984	-3.5165	2.5762	-3.8024	-3.0109	-4.5886
68	1.7225	-3.7824	-2.743	-2.1614	3.5688	3.6139	2.1879	7.1414	-0.4265
69	1.1579	-0.3391	4.1756	4.469	-3.2711	-0.2388	-5.7333	2.2508	-3.7234
70	-3.2966	3.415	2.1054	-2.0853	-1.6362	4.5381	0.1134	-3.2888	-4.3869
71	-0.7361	6.5167	1.789	3.3024	2.9903	3.8613	3.6867	-1.4946	-4.0514
72	0.0317	-6.5459	0.6847	0.4494	-2.0001	-5.5924	0.9007	1.7849	-0.5355
73	-1.9236	0.2078	2.3009	-3.9746	1.205	-3.8683	-0.184	6.128	1.641
74	-0.2368	4.7579	-7.1428	1.6611	-0.2785	3.753	-2.6438	1.4979	3.6234
75	-1.6797	4.0976	2.9742	-5.0213	-5.3455	-0.9706	0.9082	1.1974	-0.2163
76	2.8742	3.3136	4.1349	-3.1665	1.22	-0.3062	4.2979	1.6592	-4.2145
77	-1.0413	3.0776	-4.5344	-4.2582	0.5674	4.0336	1.3644	3.5398	-2.0736
78	2.0535	2.8661	2.7676	3.7989	1.795	4.2671	4.3505	-2.9491	1.9541
79	0.0416	-4.6434	2.5153	3.7567	-2.1193	2.8979	-4.5478	-1.007	3.2221
80	2.6631	-0.3068	7.3089	-5.7922	0.7843	0.9211	-0.3101	-2.8443	-3.985
81	4.1979	-1.6926	-5.3624	-0.7649	2.5317	4.1909	-6.5485	7.1966	0.3209
82	-0.0337	3.718	4.0267	-3.8466	4.0757	-0.0619	0.3081	4.0298	3.127
83	5.0742	6.1738	-0.1747	1.3784	-10.37	-3.5081	3.2767	3.2287	0.3057
84	-2.6353	-3.6175	-3.9027	3.6485	-4.3875	-1.6107	-3.4379	2.5665	-0.2076
85	4.3381	4.2233	-2.8551	-3.1266	1.4396	-2.4918	3.2737	-2.3853	-2.4887
86	-6.0019	-0.7914	5.8938	7.7869	3.2542	0.9569	-1.1842	1.2014	-1.7563
87	-0.6641	-5.6404	10.4893	-1.9499	8.5925	-4.9399	5.526	-5.7589	2.8291
88	-4.3398	-2.1893	-3.3031	-2.6319	-3.122	-3.8329	-1.6318	3.7287	-1.3988

89	3.5792	4.3554	-0.2924	1.9983	-1.5485	-3.8625	-5.1814	2.0454	-0.3744
90	-3.1325	1.638	-2.8088	3.8322	1.1923	4.3979	-3.1405	2.9681	-1.9063

Table 7: Final Layer Weights, Final 'Extrapolation' Network

Input (from Layer 2)	Final Neuron Weight
1	1.1704
2	-1.5029
3	-4.0689
4	-0.251
5	-2.3001
6	0.1716
7	-1.209
8	-0.1887
9	1.2928
10	0.1494
11	0.7028
12	0.0289
13	0.655
14	0.6791
15	-3.5157
16	-2.1899
17	-0.8974
18	-1.9361
19	1.2488
20	4.0487
21	-3.9754
22	4.1144
23	0.4696
24	0.8503
25	-2.0455
26	1.3163
27	0.7942
28	-1.1984
29	-1.4156
30	0.9373
31	3.6589
32	5.1549
33	-2.2895
34	-0.5973
35	4.0444
36	-4.7906
37	2.5342
38	-0.9717
39	-5.1079
40	-2.9954
41	-0.2424
42	4.6182
43	-2.039
44	0.3189
45	0.8803
46	1.9988
47	-2.1292
48	5.1676
49	3.4622
50	1.3169
51	-4.5526
52	-1.3842
53	-1.0366
54	-4.1592
55	2.1078
56	-1.6346
57	-2.2503
58	-5.3993
59	2.591
60	0.8075
61	0.7206
62	-1.5713
63	3.8033
64	-0.7816
65	5.4939
66	-4.9633
67	1.696
68	4.3458
69	-2.5019
70	-0.1572
71	-2.444
72	0.3569
73	1.1568
74	3.6472
75	-0.3516
76	-0.0008
77	0.948
78	-0.8574
79	-1.0258
80	3.1967
81	-5.4847
82	0.9125
83	5.5741
84	1.0447
85	-0.0002
86	-5.2584
87	6.207
88	1.7711
89	-0.1047
90	0.4784

Appendix F: Well Test QC Study on Auger Well A14

In current practice, Well Test QC is an approach used to check whether well-test data recorded is 'valid', in that a disagreement between welltest data and the accepted lift correlation for that field would suggest 'bad' data or some unassociated problem like leaking tubing. However, in the case of the Auger wells, several problems exist with applying this approach.

First, gas composition changes over the life of a well: RFT reports show that in the case of the O Sand, the composition can vary just enough to reach a volatile-oil condition just above the OGWC. This is manifested in the increasing condensate yields of the field over time. Changing watercuts and potential skin effects further complicate the problem. Though accepted methodology relies on choice of a 'best fit' empirical correlation and one of tracking well behavior over significant periods of time with significant variations in flowing conditions. A well test, instead, serves as a 'snapshot' of well behavior at an, effectively, bracketed point in time- in this case, the majority of tests were 4-hour 'step tests'.

Despite this difficulty, a well-test QC approach might be employed nonetheless. Worse than all the other difficulties discussed above is the fact that many published correlations do not result in a good match to Auger well tests. This is due to the incompatibility of these published correlations still in use: these were developed empirically, and the experiments used to develop them were conducted with two phases- kerosene and water, or for the cases developed from field data, black-oil (generally low gas) and brine. Extreme disagreements in liquid holdup and flow regime among the different correlations contribute to significant inaccuracy in trying to match DHPG data with classical correlations.

Figures 42-98 show well test QC plots for the A14 well. Many of these plots show rough matches, but no one correlation matches test points

particularly well throughout the production period. Bounds of Orkiszewski (overprediction) and the other correlations used (Beggs and Brill, Hagedorn Brown, Duns and Ros, etc.; underprediction) sometimes form 'bookends' for the test points and ANN predictions. The late-time plots represented by Figures 82-98 are especially noteworthy in that these ANN-predicted sandface pressures are very similar to the predictions of the Orkiszewski correlation. Future work may pursue use of the ANN approach to tune an Orkiszewski-based correlation to correct for the dynamic effects the ANN has more effectively captured.

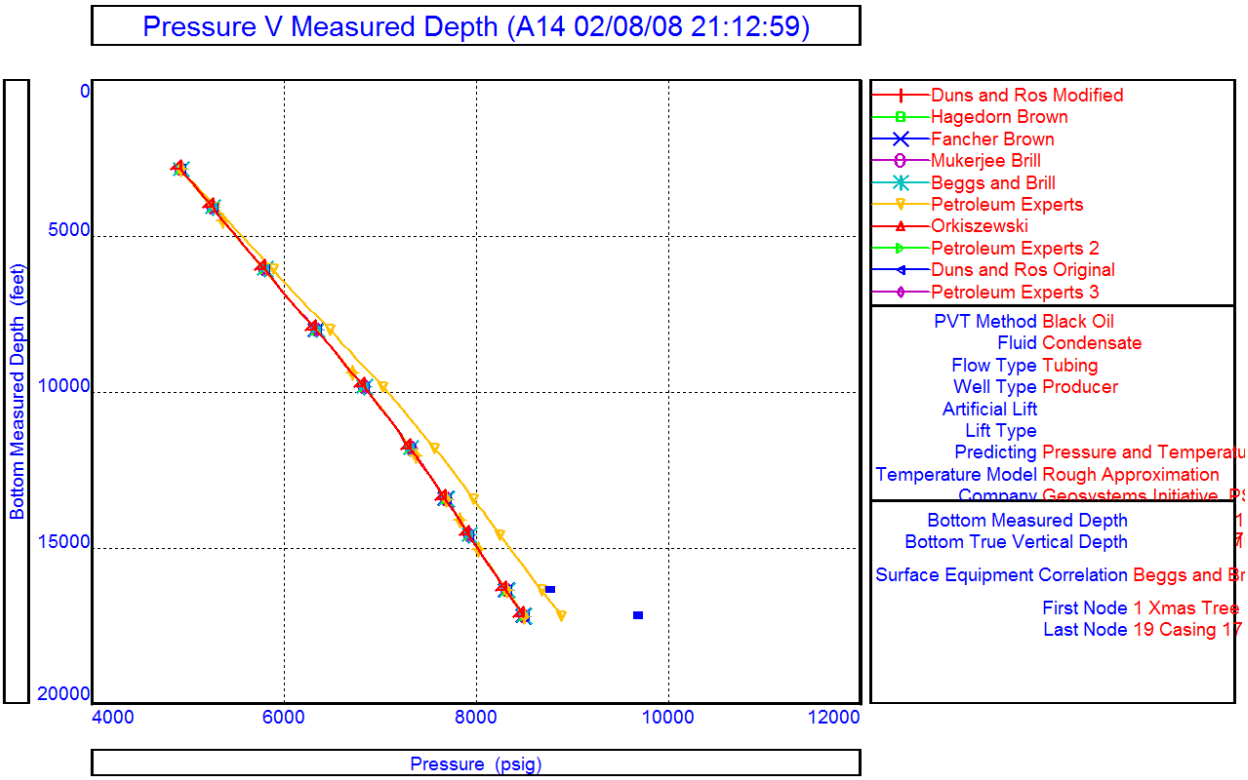

Figure 42: Well Test QC Plot, A14 Well

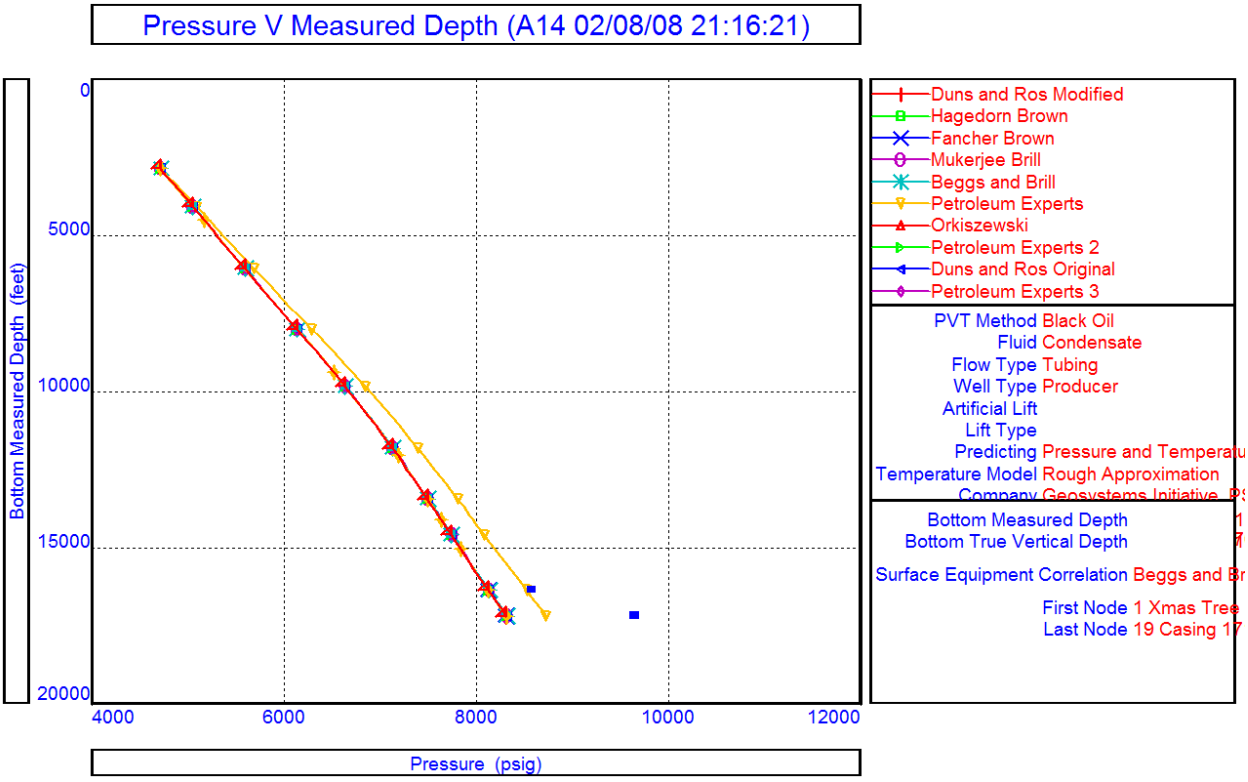

Figure 43: Well Test QC Plot, A14 Well

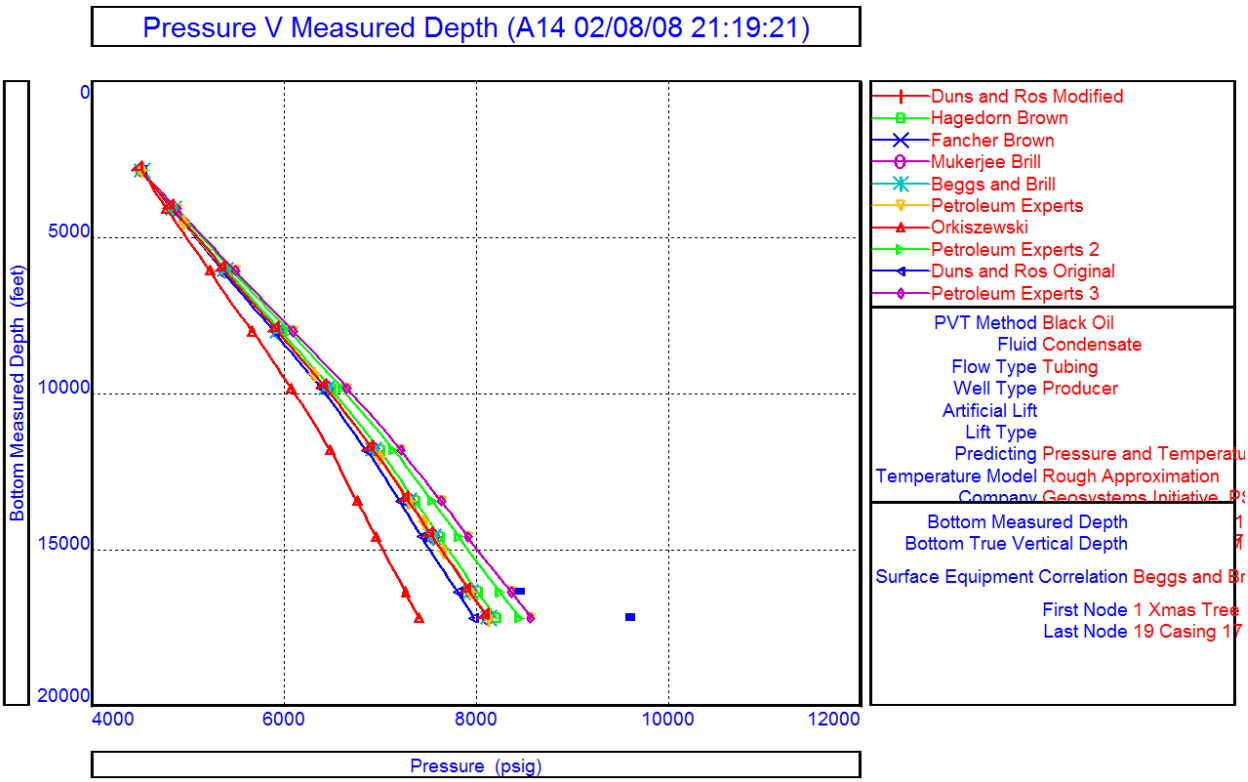

Figure 44: Well Test QC Plot, A14 Well

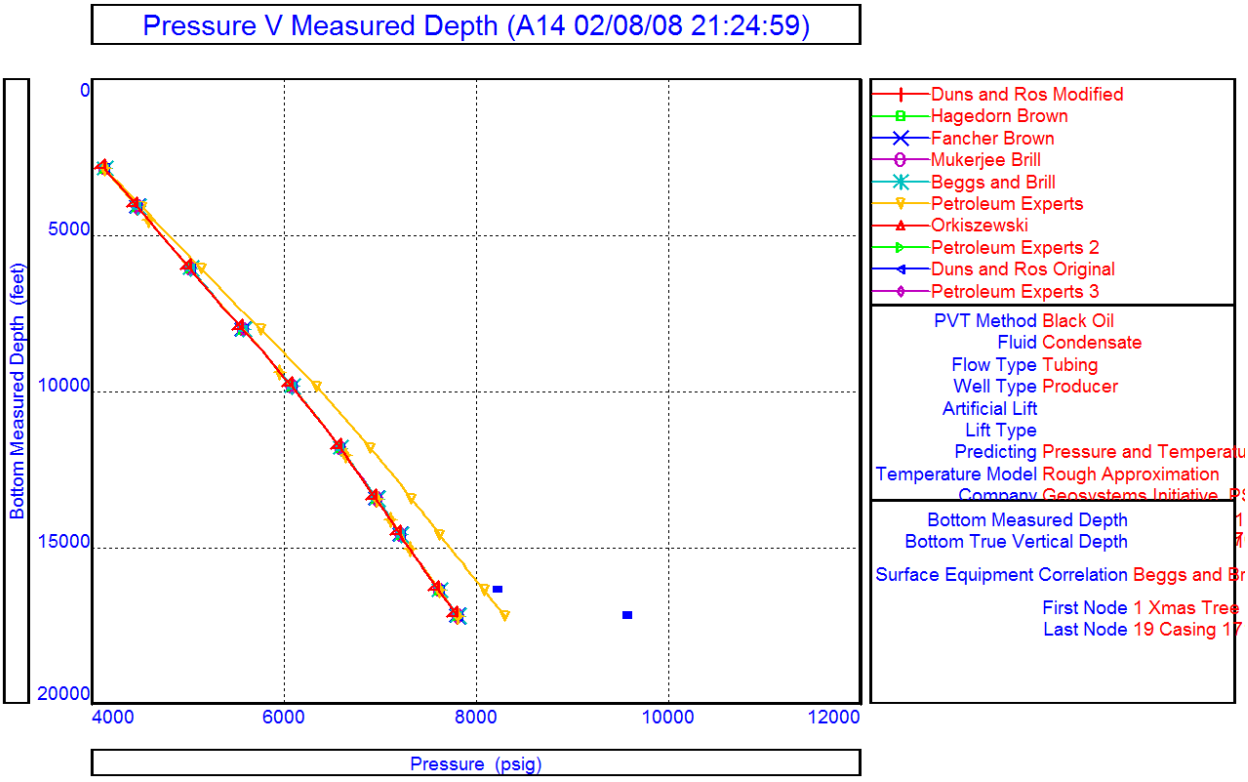

Figure 45: Well Test QC Plot, A14 Well

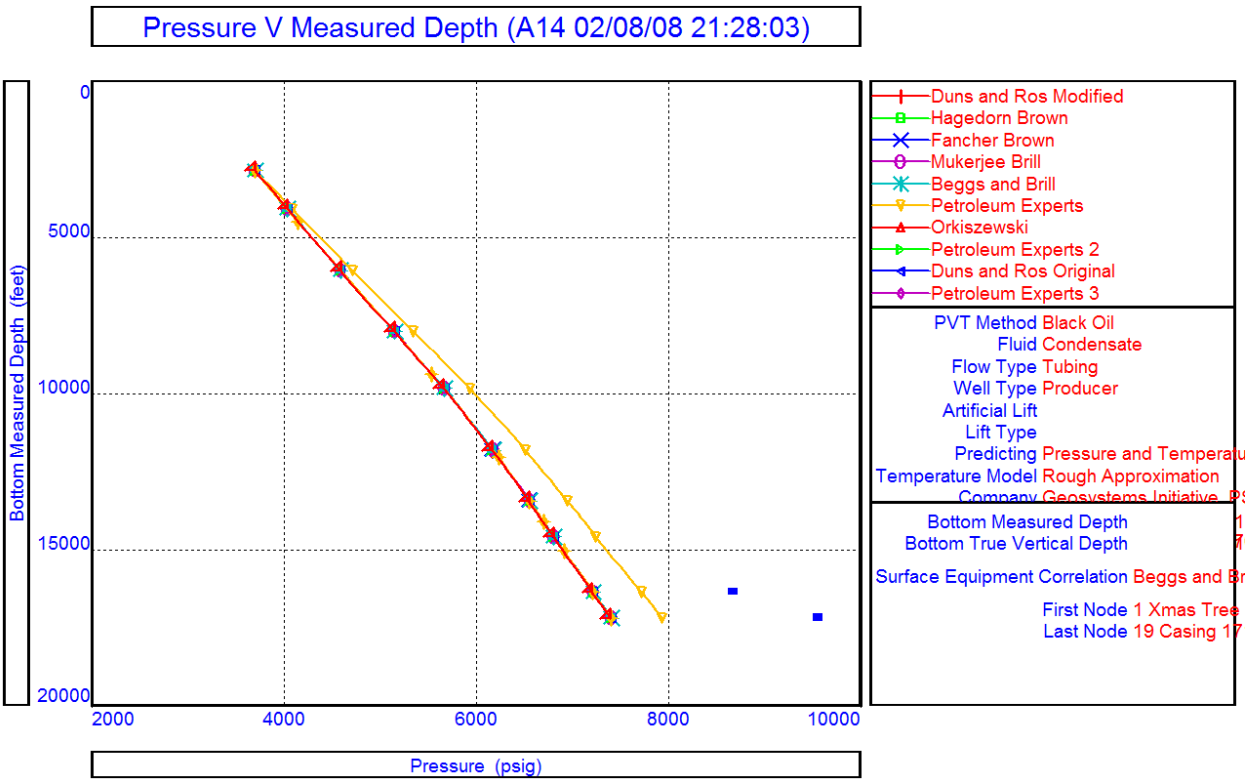

Figure 46: Well Test QC Plot, A14 Well

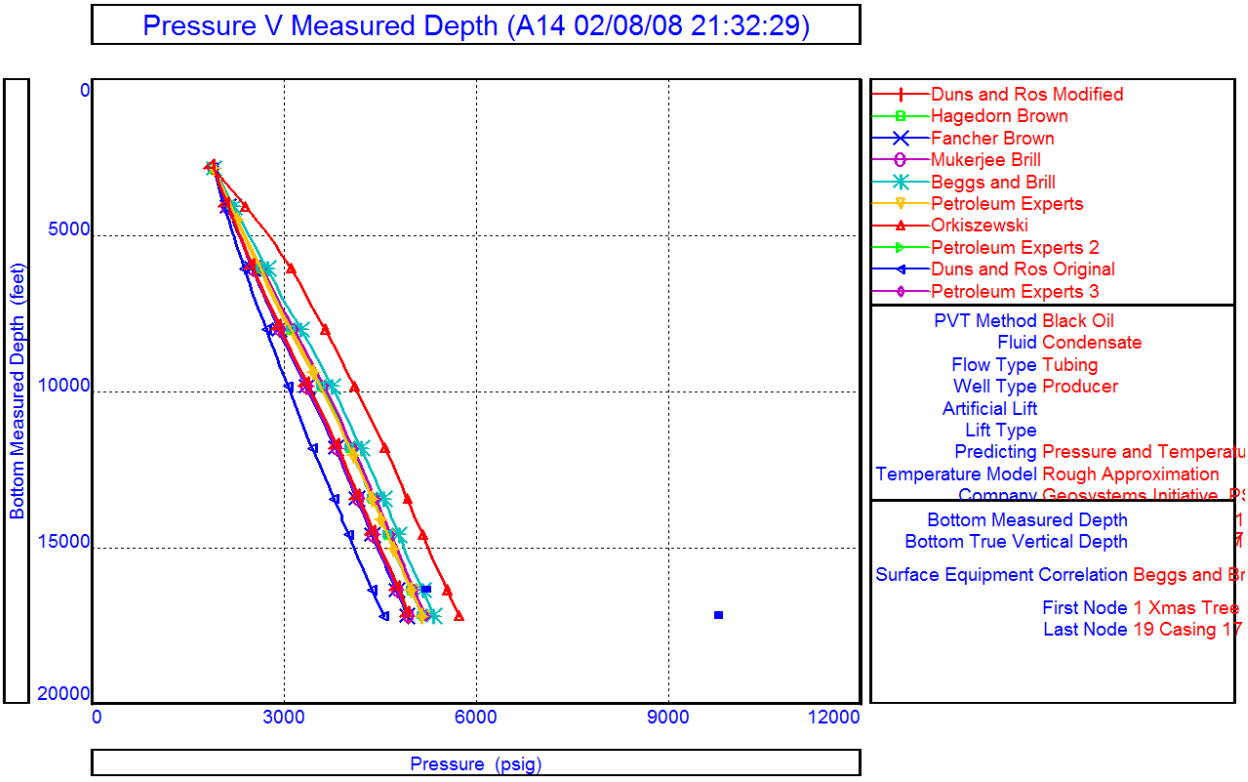

Figure 47: Well Test QC Plot, A14 Well

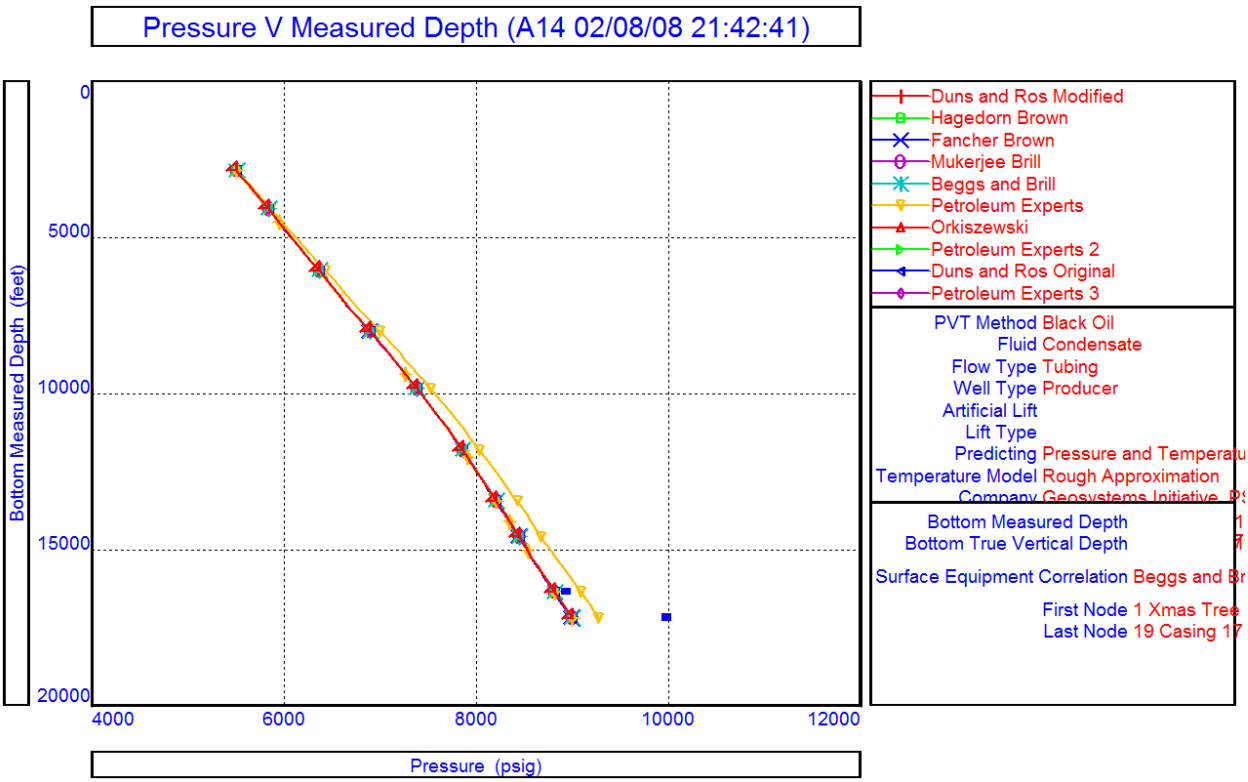

Figure 48: Well Test QC Plot, A14 Well

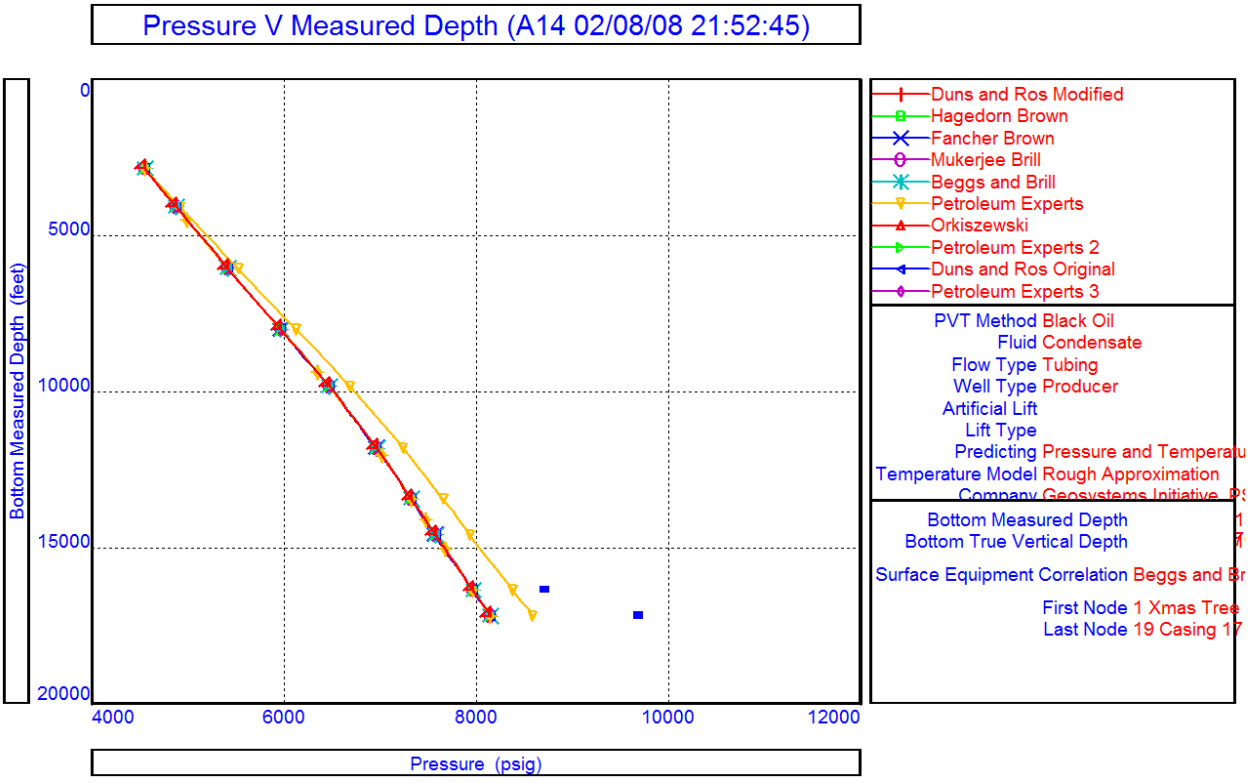

Figure 49: Well Test QC Plot, A14 Well

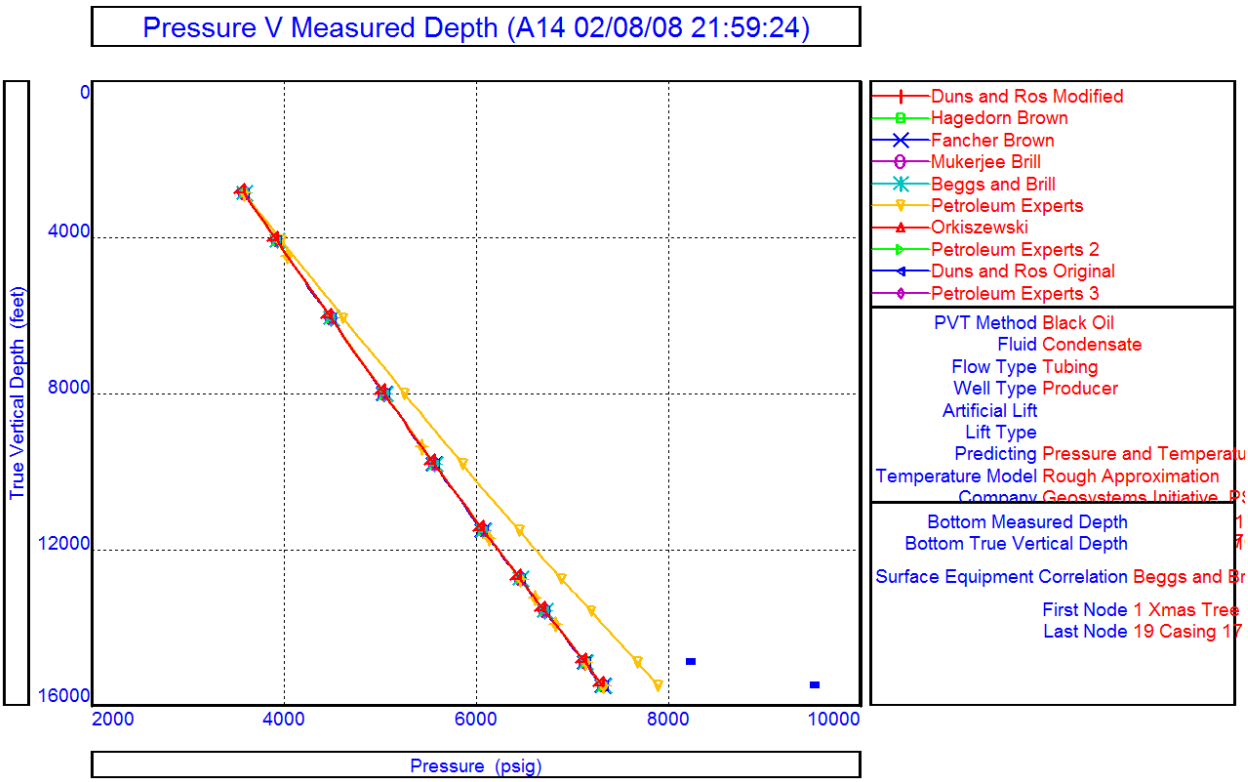

Figure 50: Well Test QC Plot, A14 Well

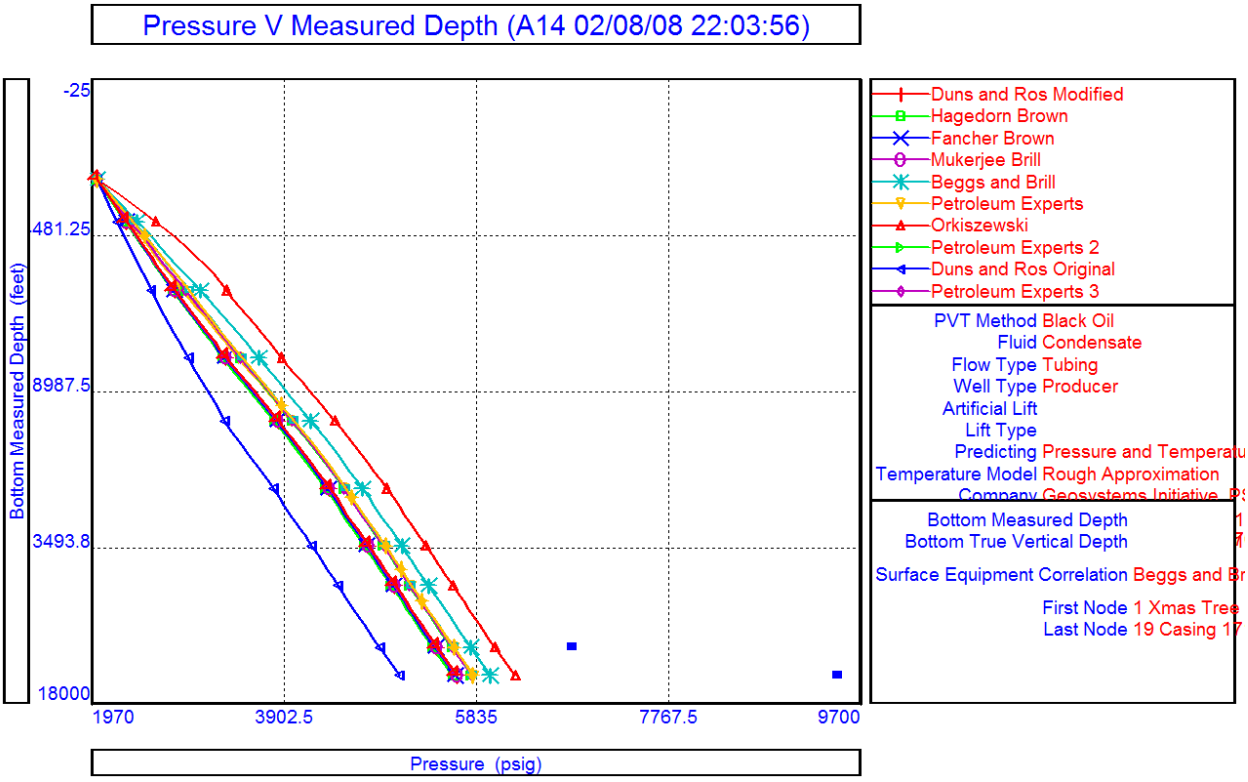

Figure 51: Well Test QC Plot, A14 Well

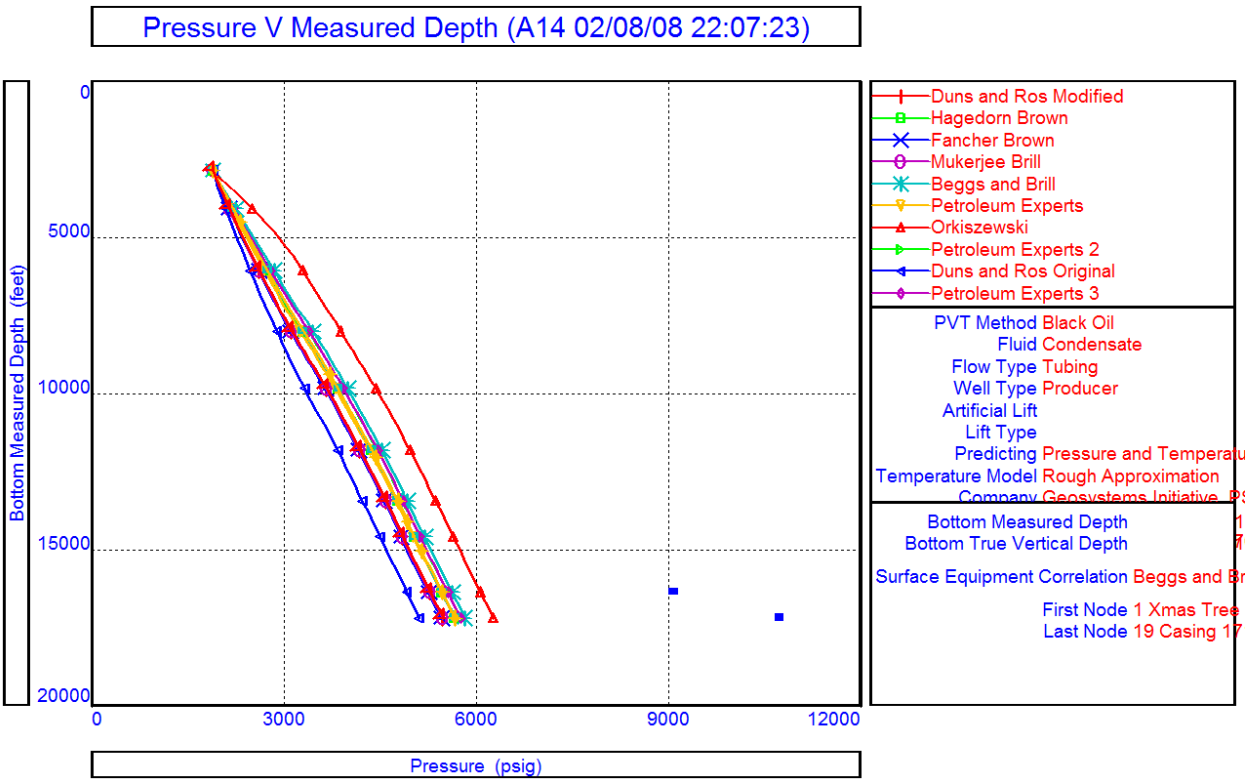

Figure 52: Well Test QC Plot, A14 Well

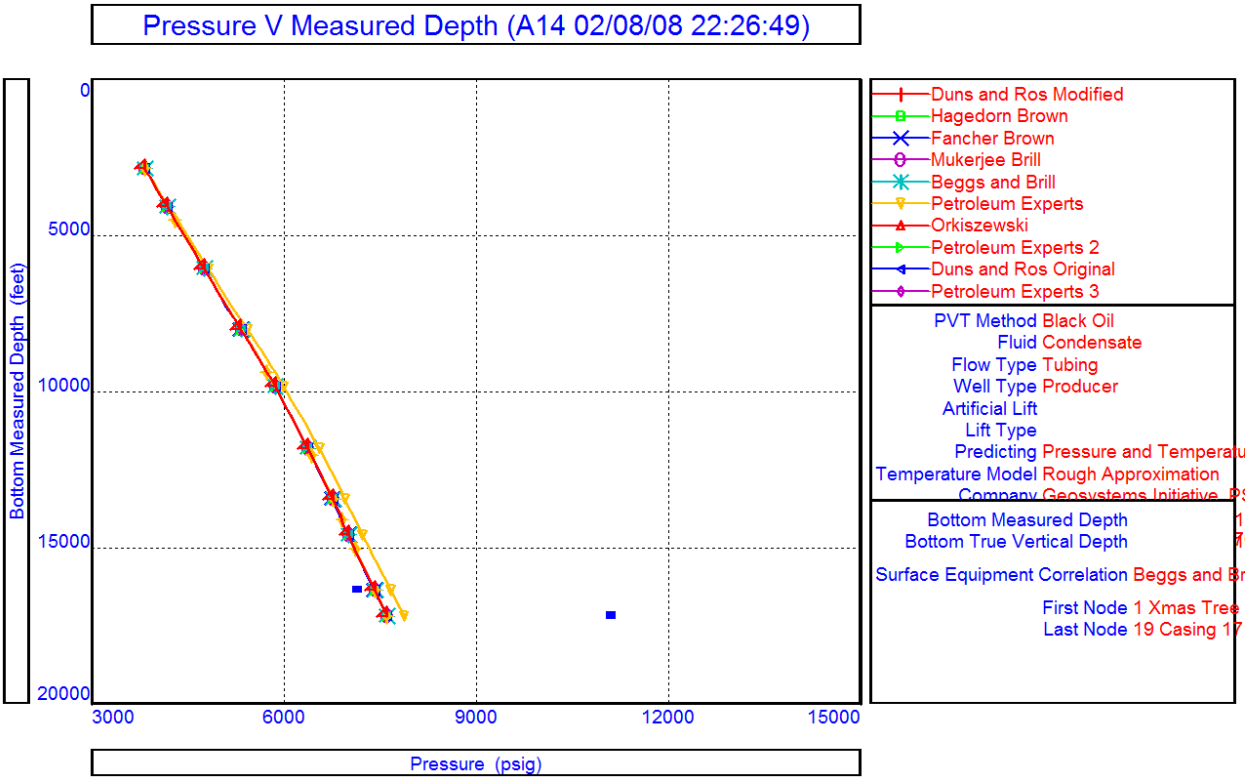

Figure 53: Well Test QC Plot, A14 Well

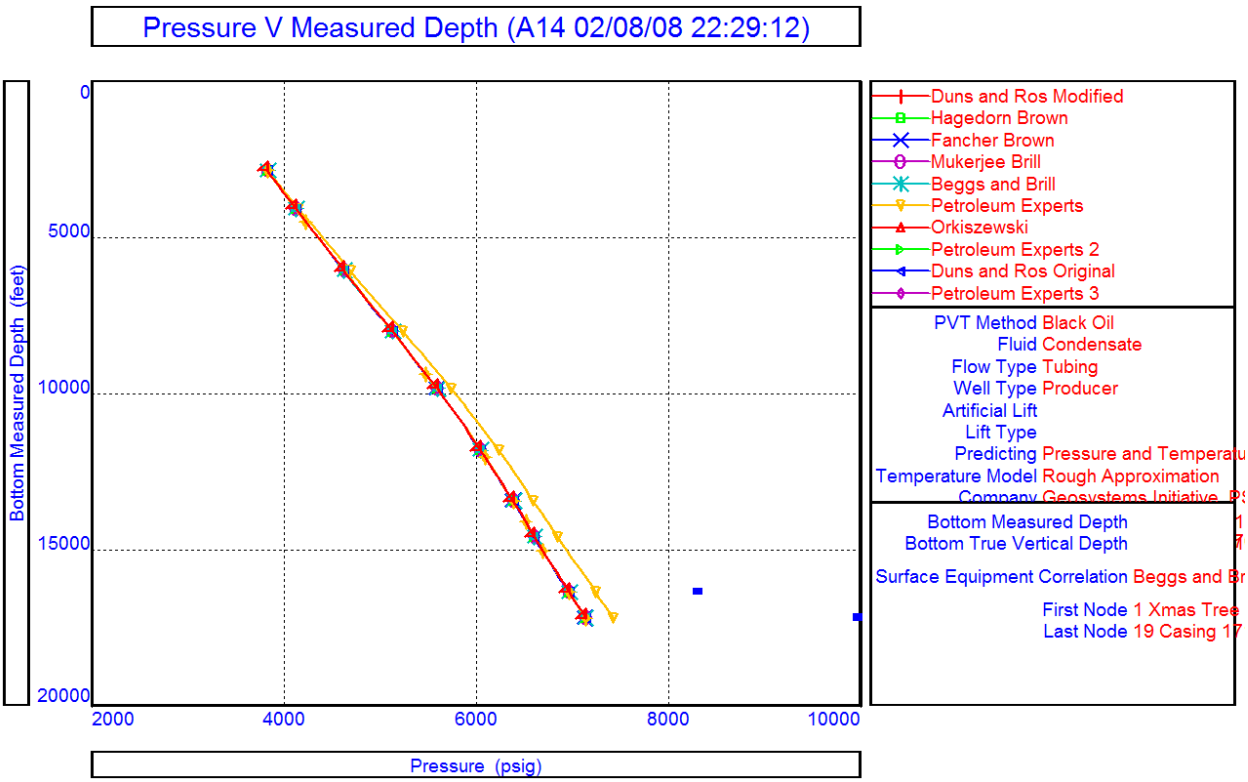

Figure 54: Well Test QC Plot, A14 Well

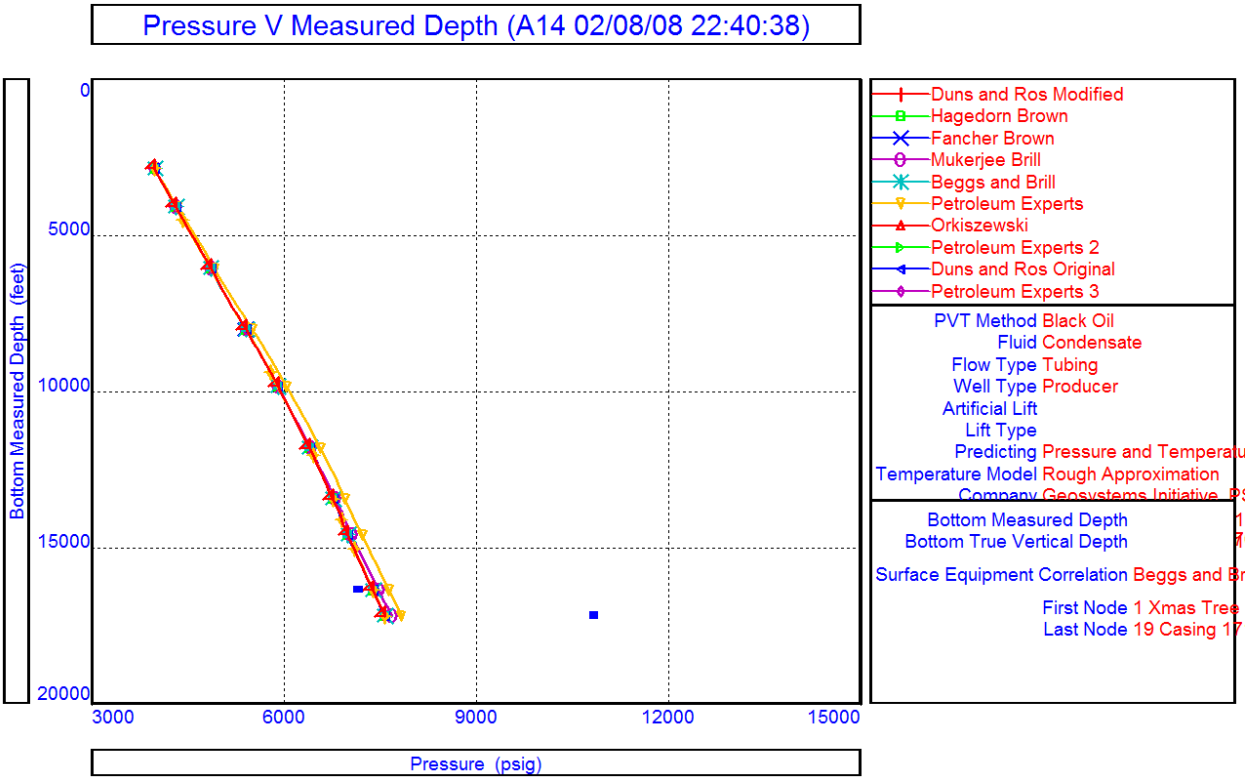

Figure 55: Well Test QC Plot, A14 Well

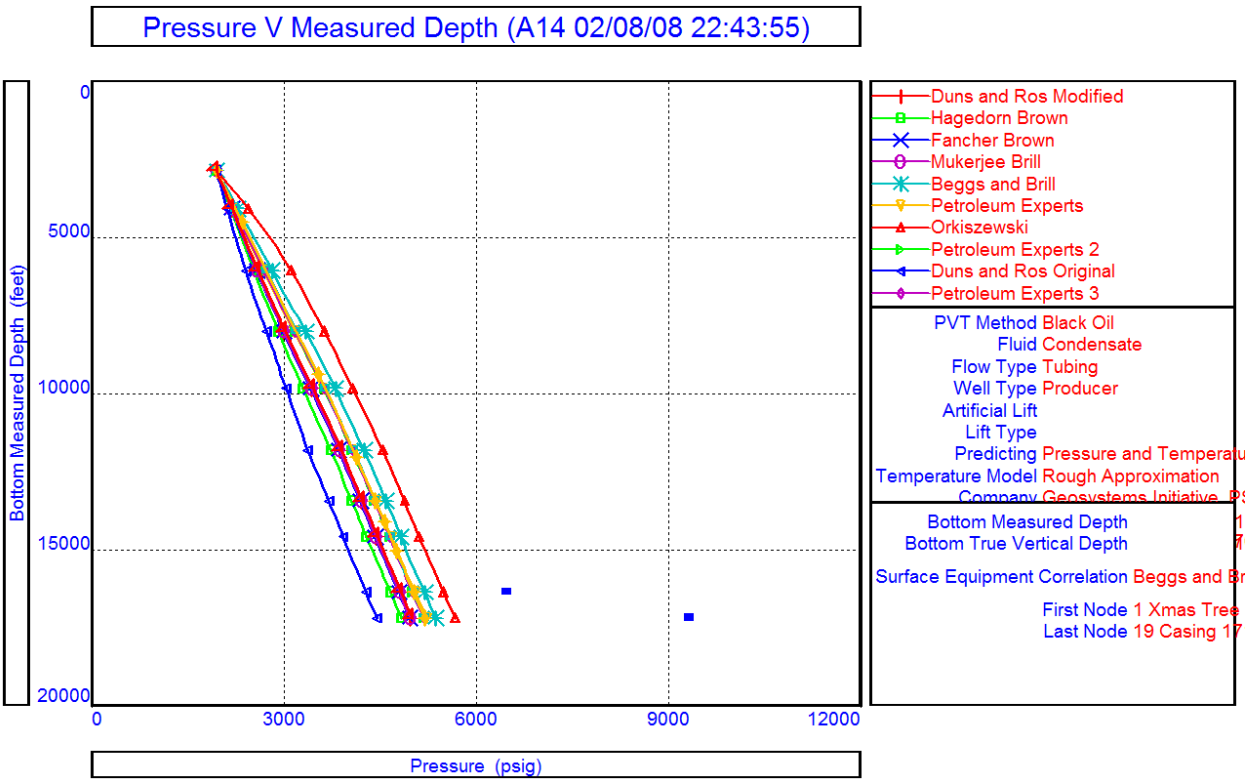

Figure 56: Well Test QC Plot, A14 Well

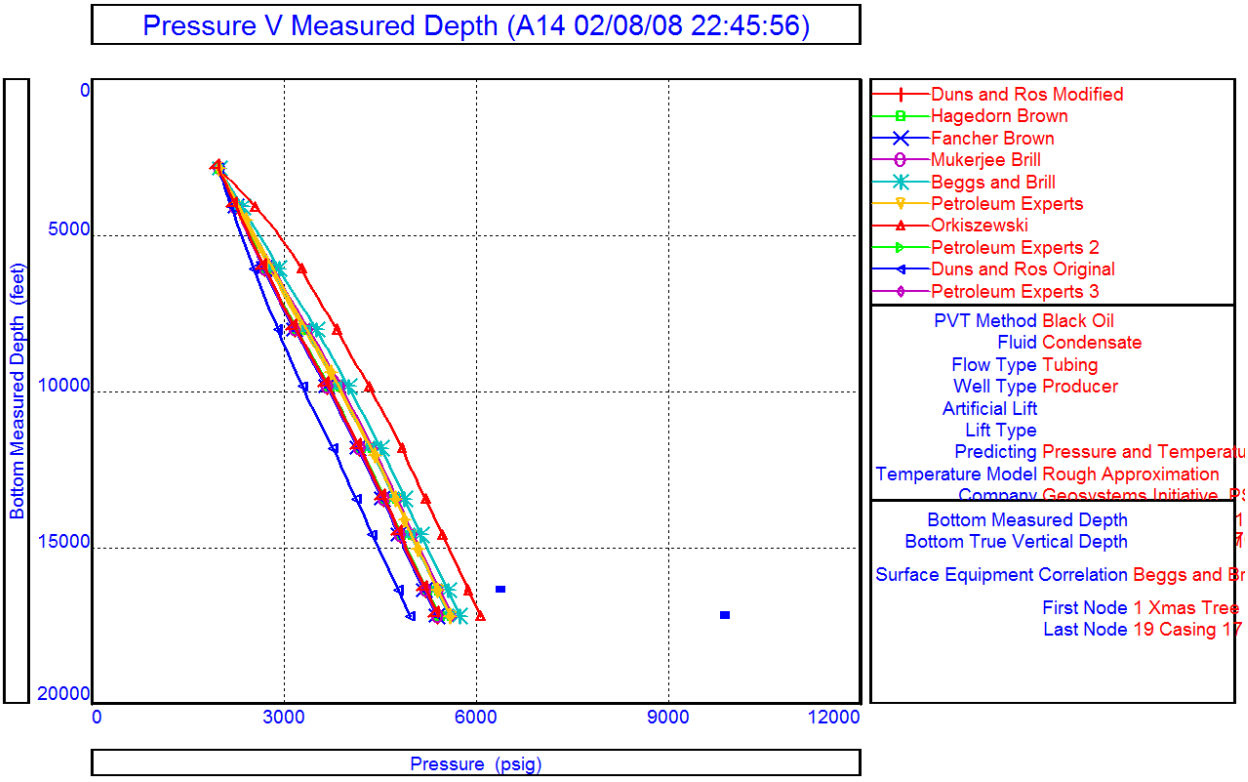

Figure 57: Well Test QC Plot, A14 Well

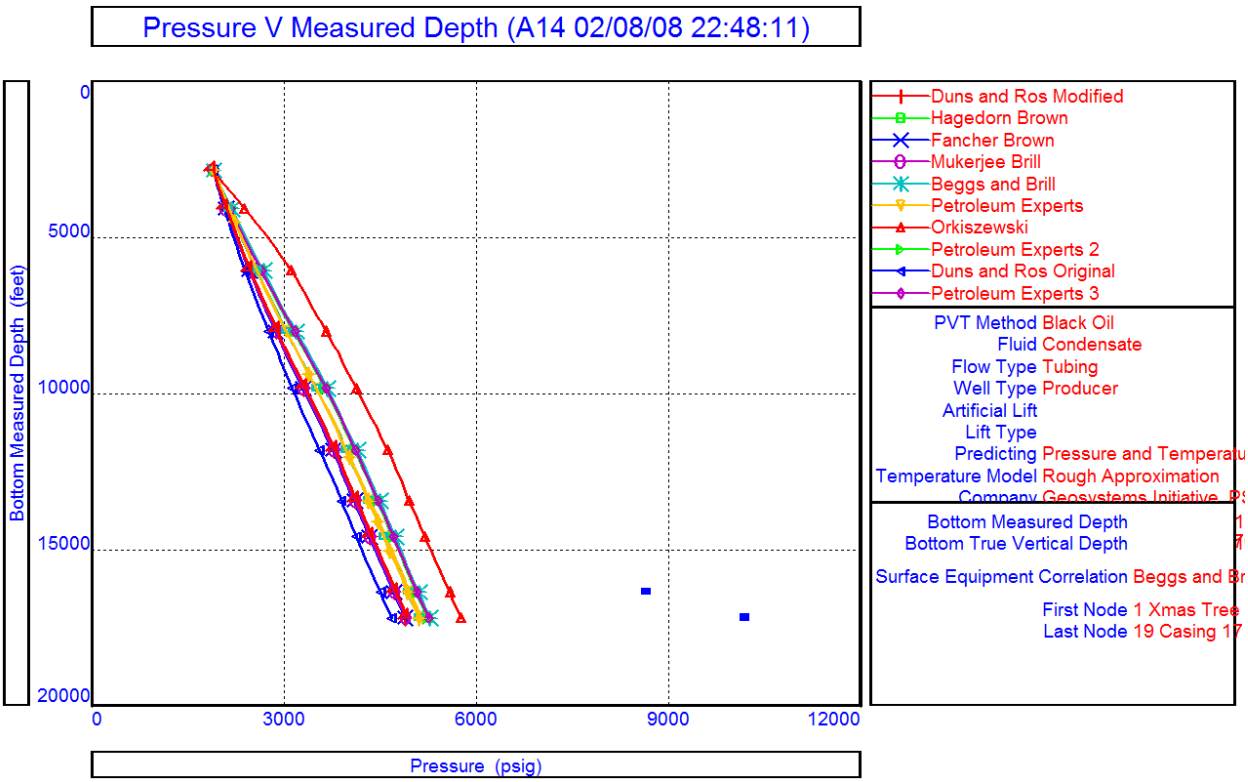

Figure 58: Well Test QC Plot, A14 Well

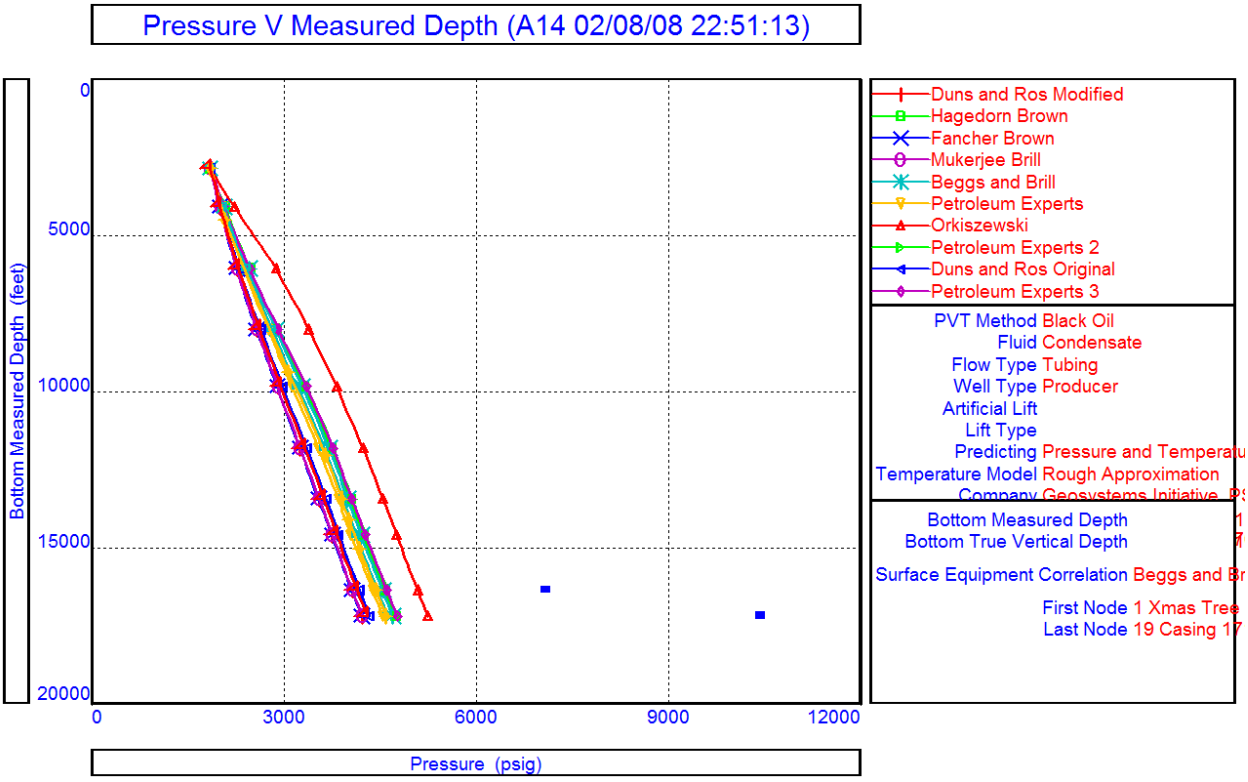

Figure 59: Well Test QC Plot, A14 Well

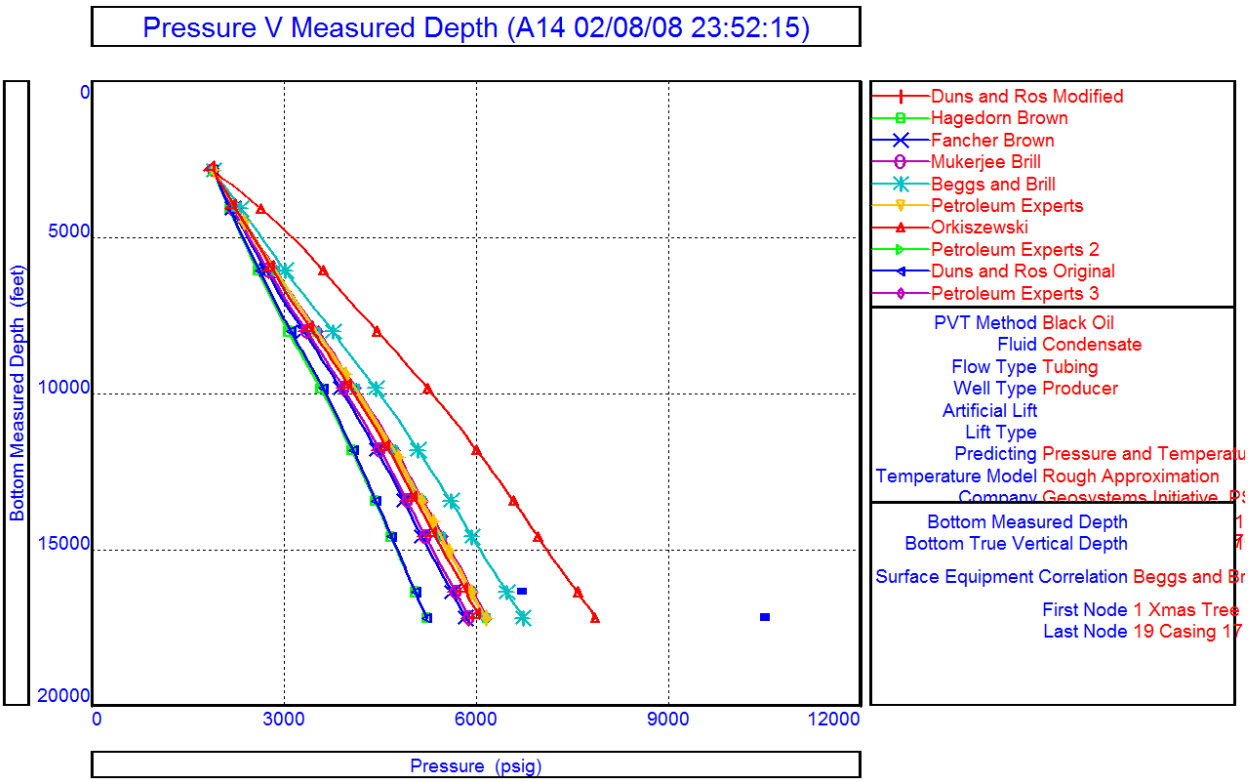

Figure 60: Well Test QC Plot, A14 Well

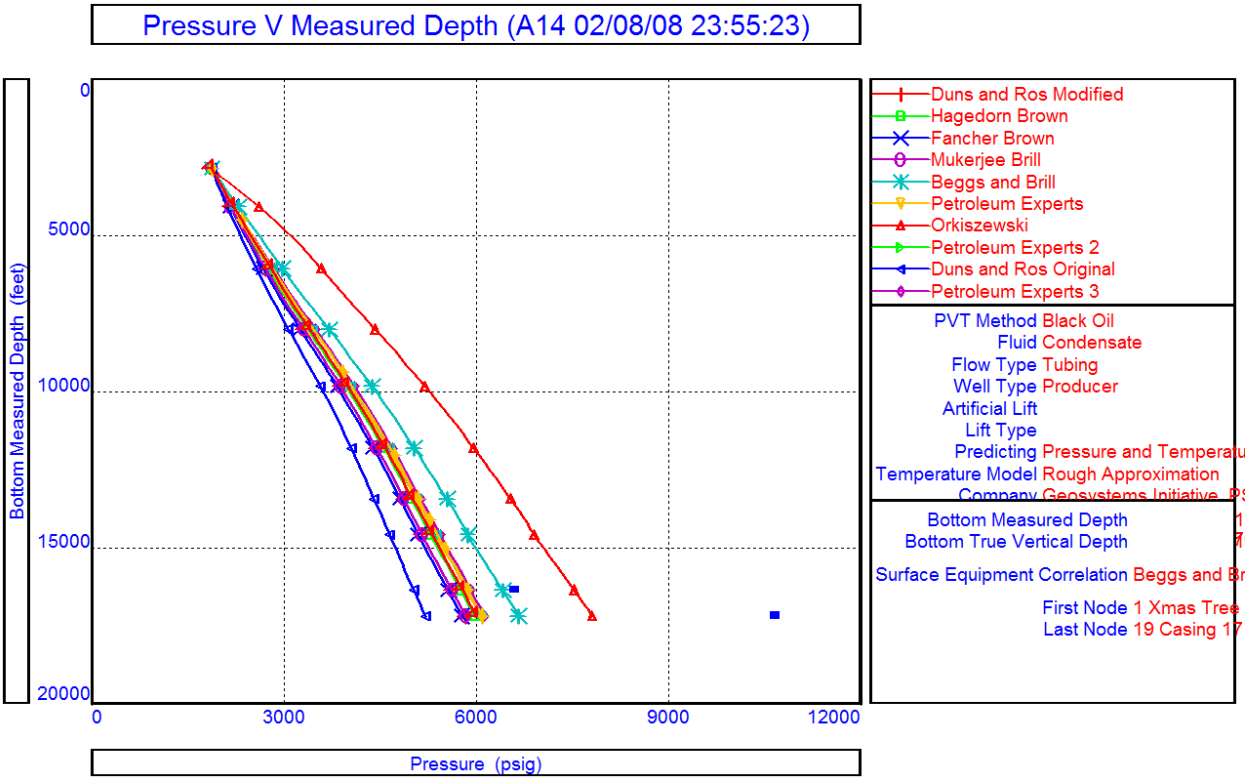

Figure 61: Well Test QC Plot, A14 Well

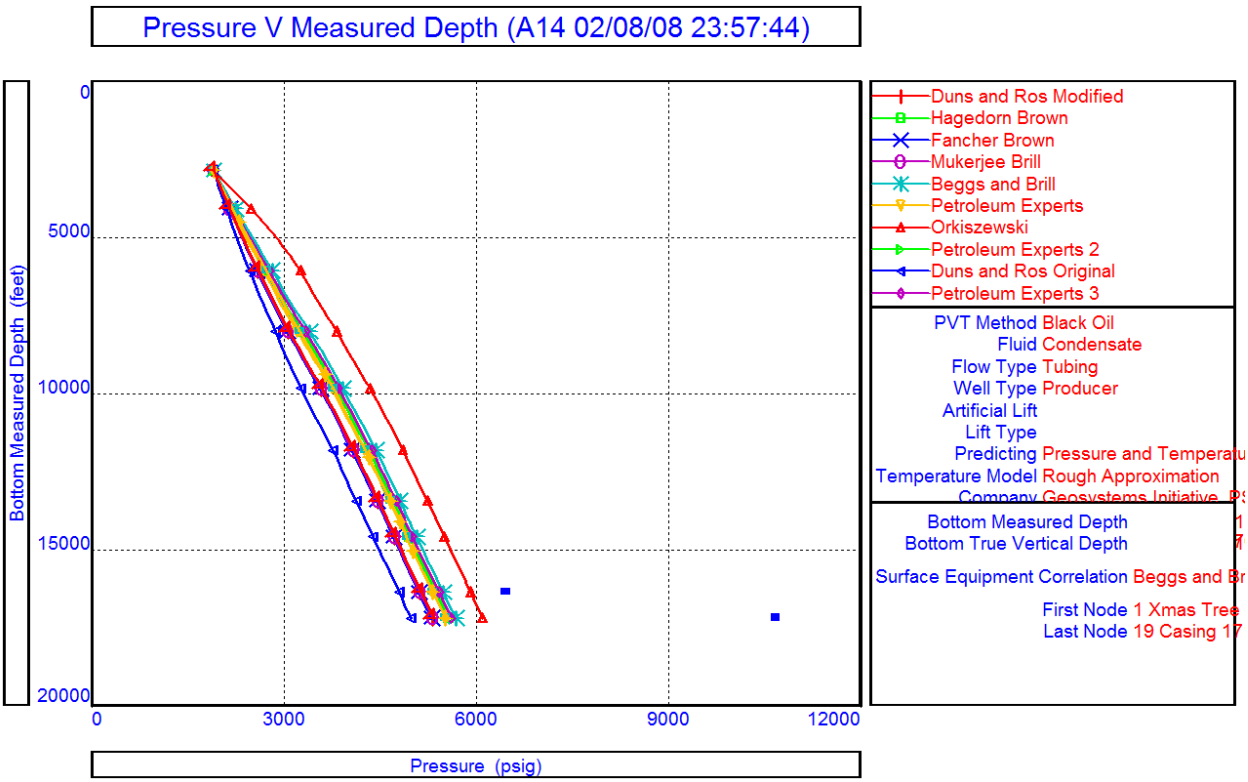

Figure 62: Well Test QC Plot, A14 Well

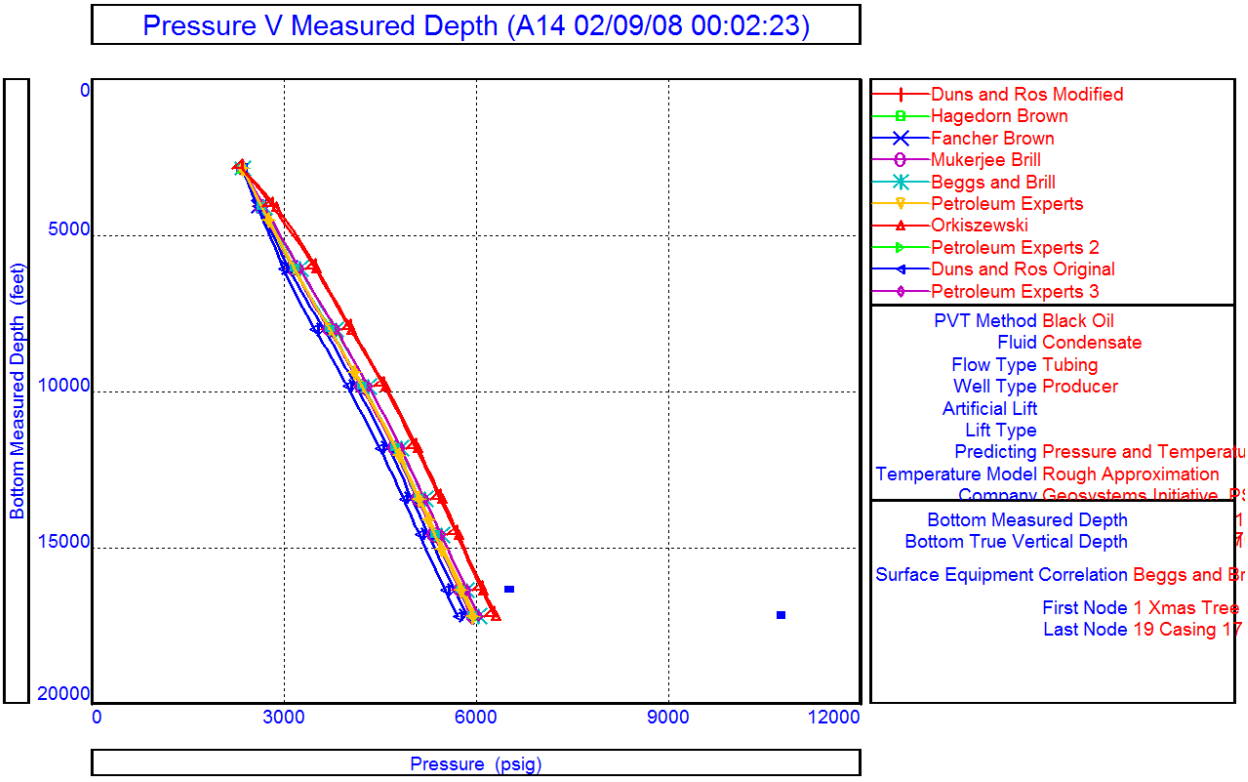

Figure 63: Well Test QC Plot, A14 Well

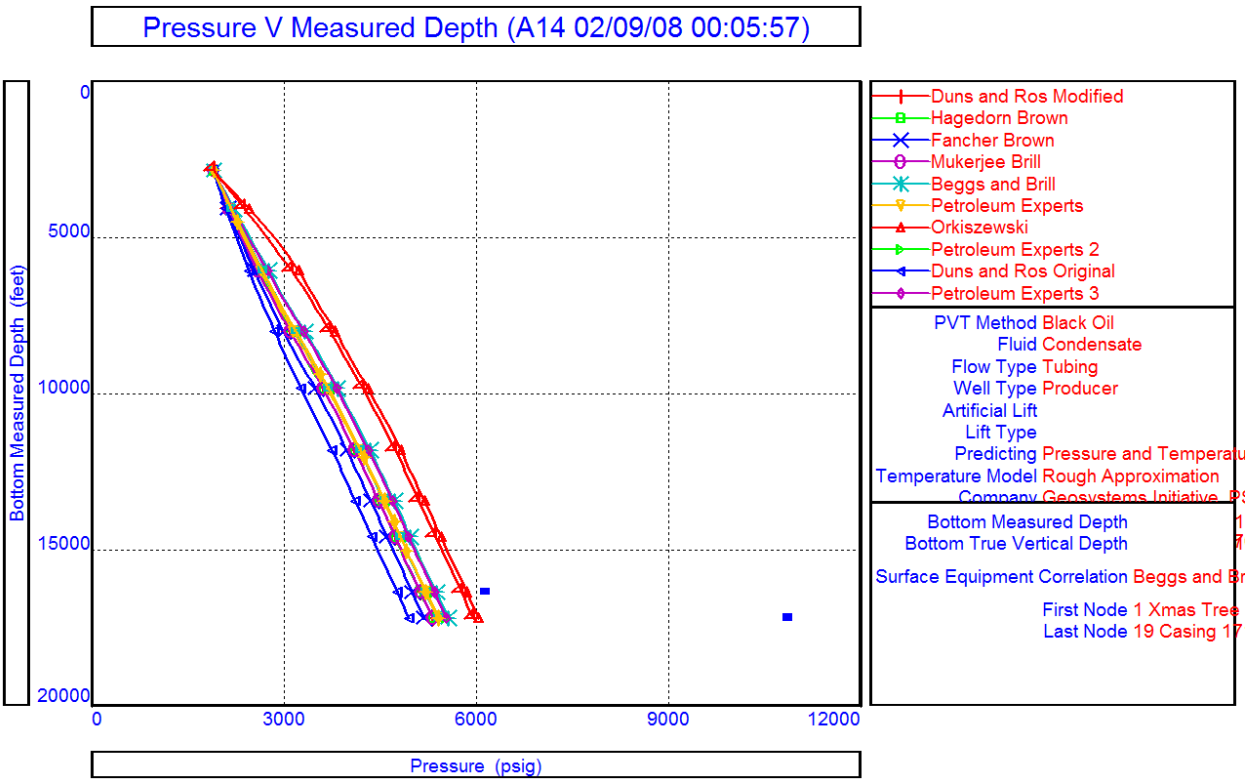

Figure 64: Well Test QC Plot, A14 Well

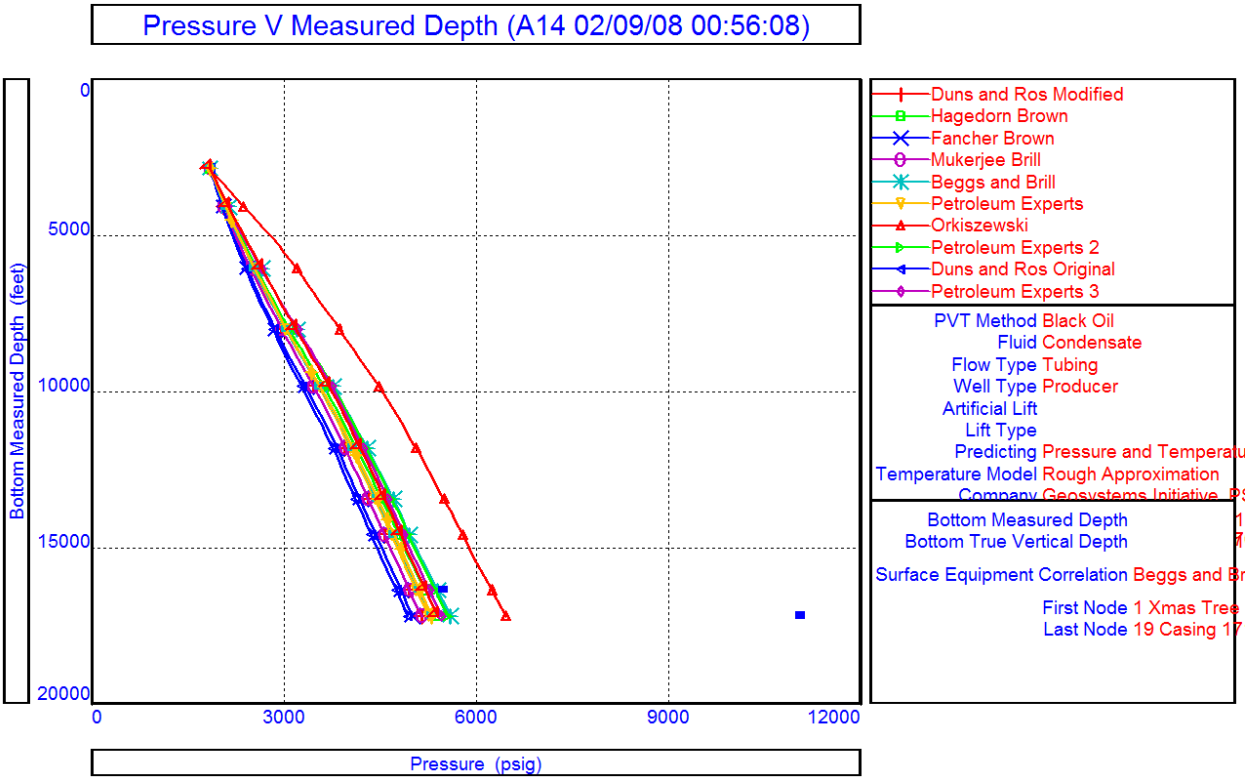

Figure 65: Well Test QC Plot, A14 Well

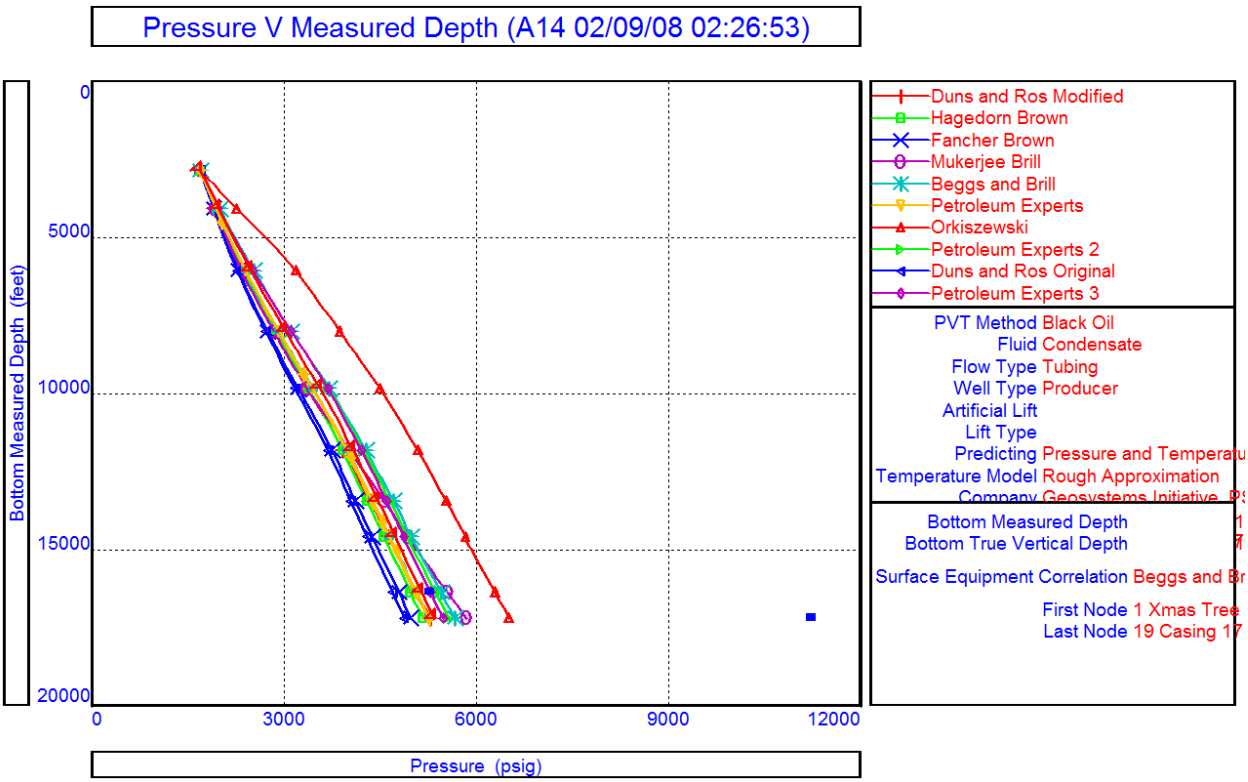

Figure 66: Well Test QC Plot, A14 Well

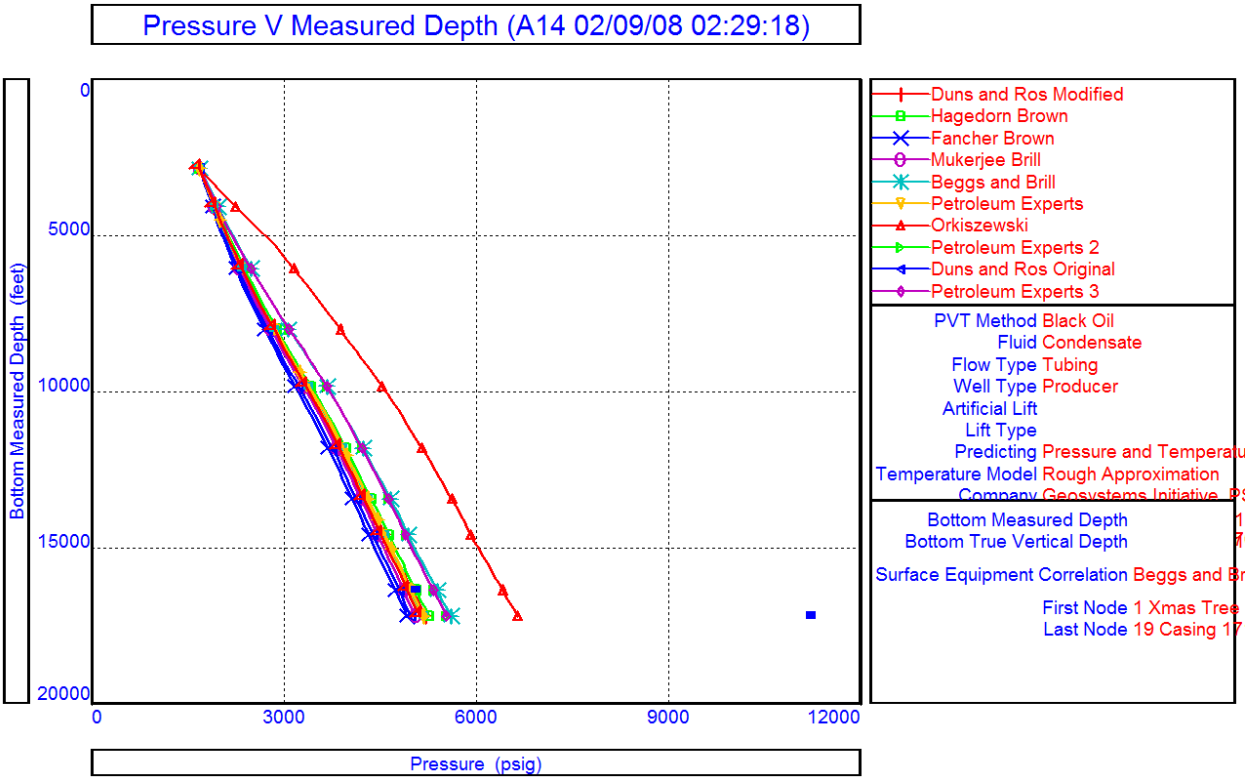

Figure 67: Well Test QC Plot, A14 Well

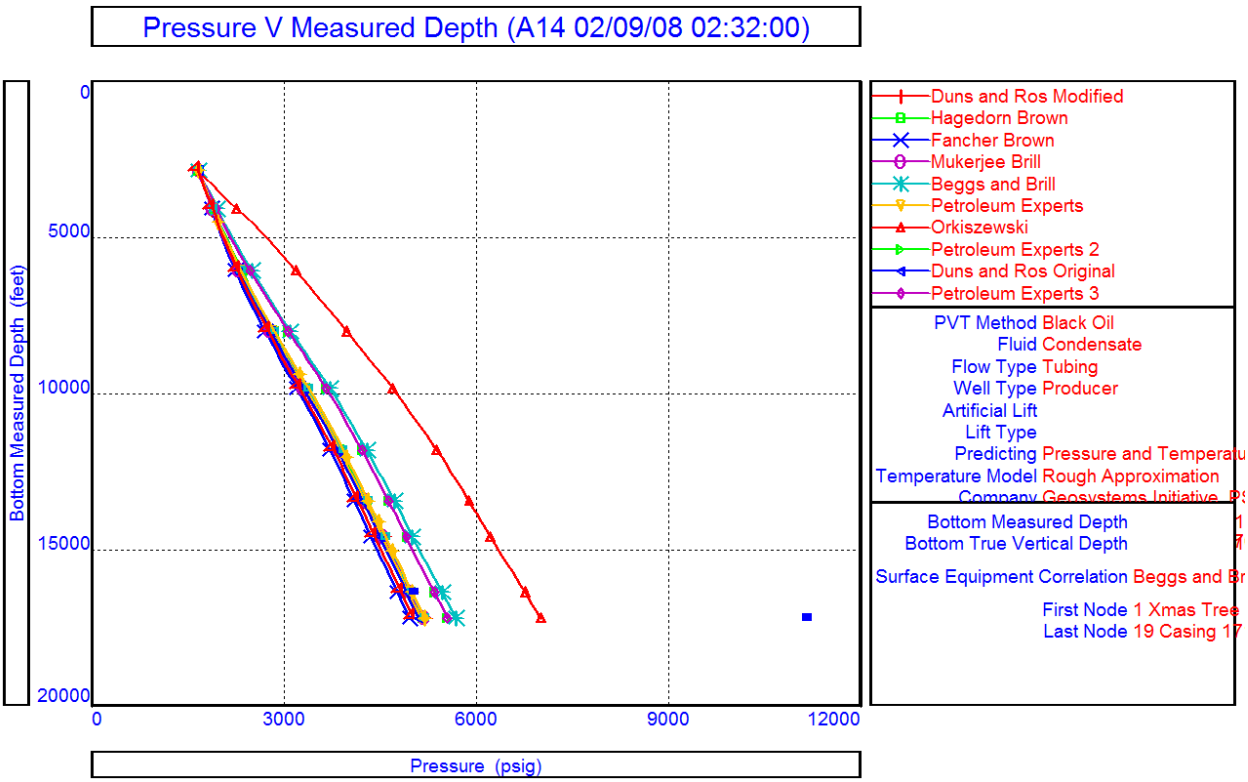

Figure 68: Well Test QC Plot, A14 Well

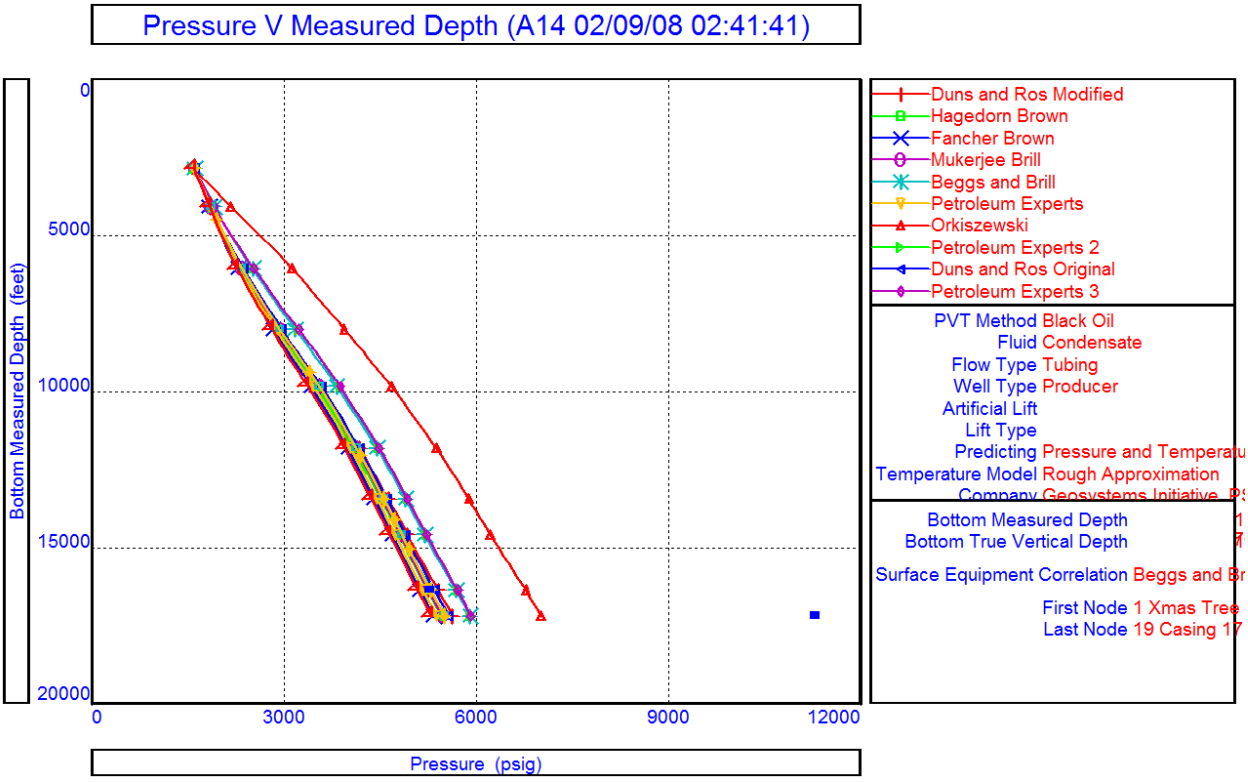

Figure 69: Well Test QC Plot, A14 Well

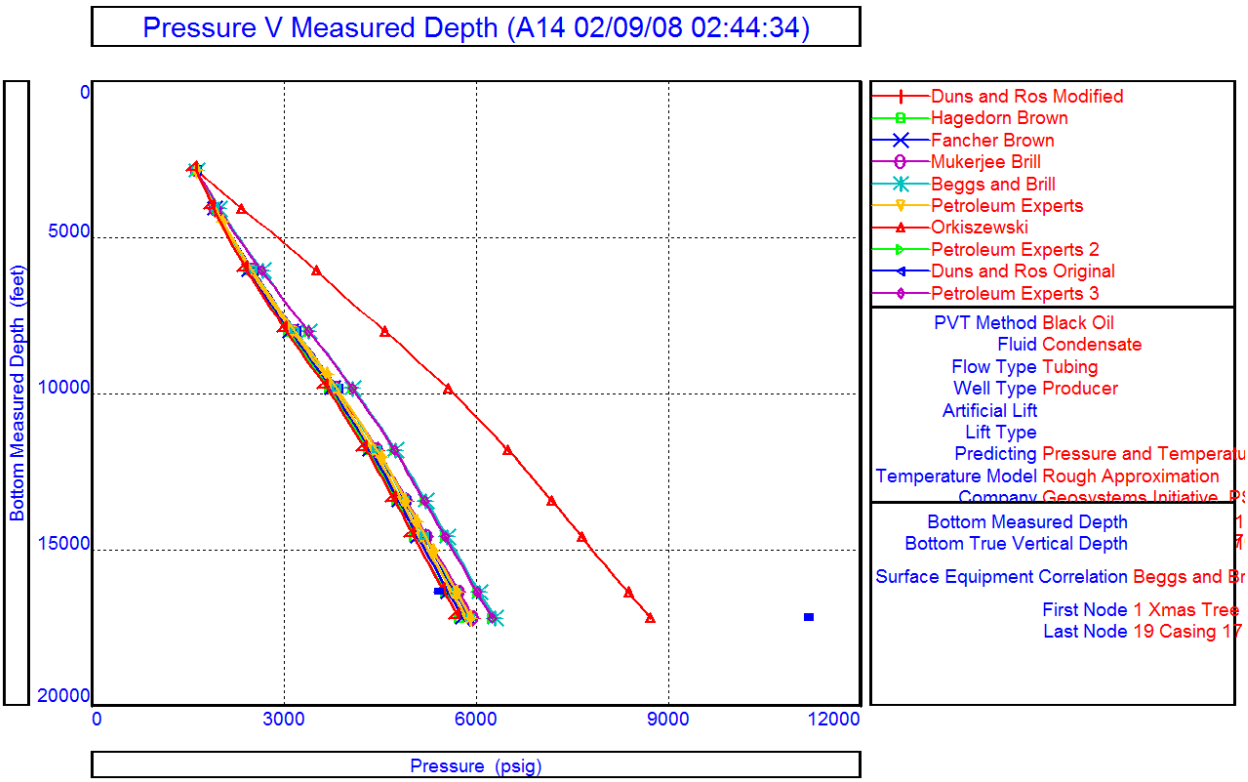

Figure 70: Well Test QC Plot, A14 Well

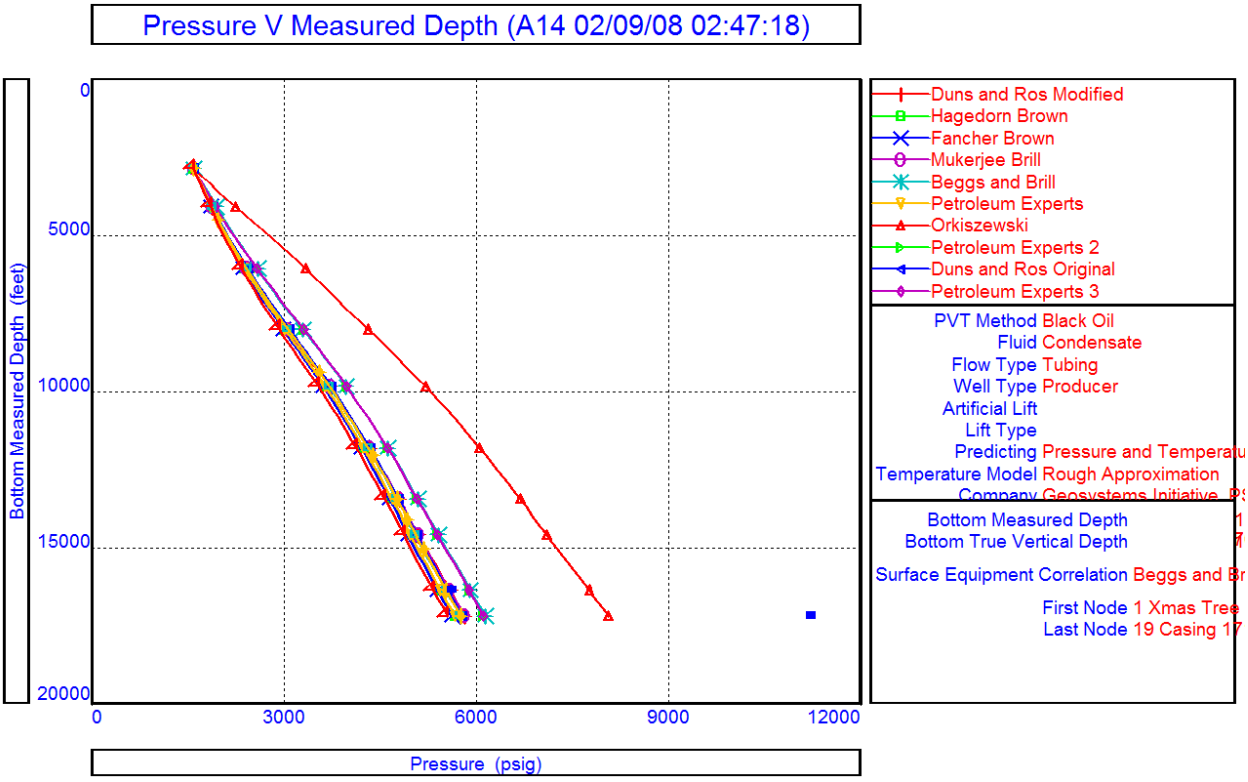

Figure 71: Well Test QC Plot, A14 Well

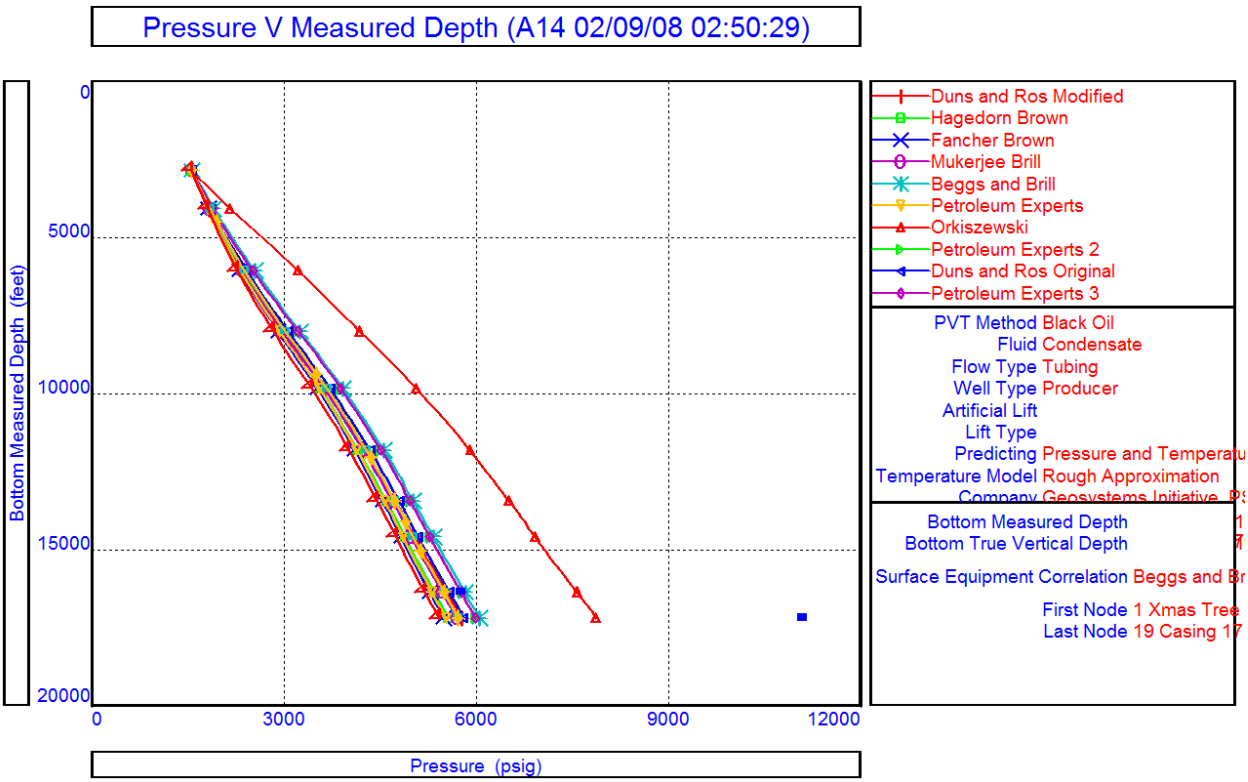

Figure 72: Well Test QC Plot, A14 Well

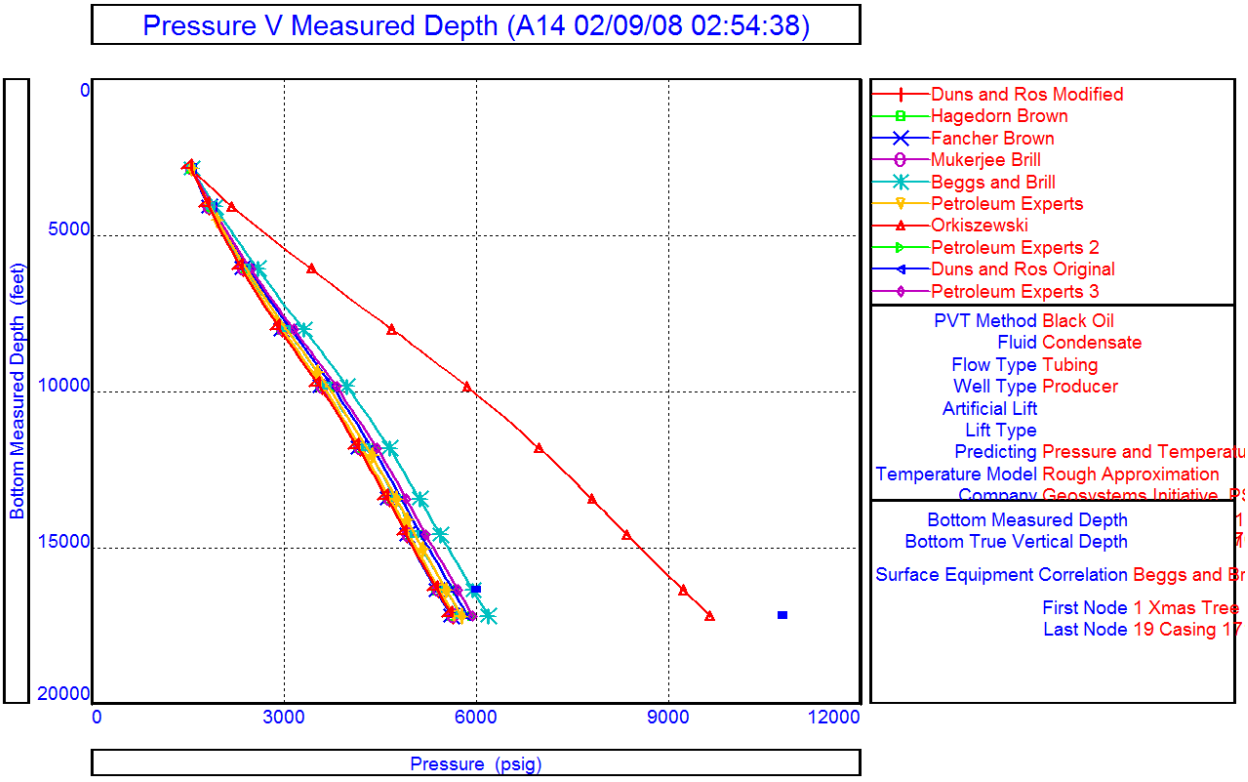

Figure 73: Well Test QC Plot, A14 Well

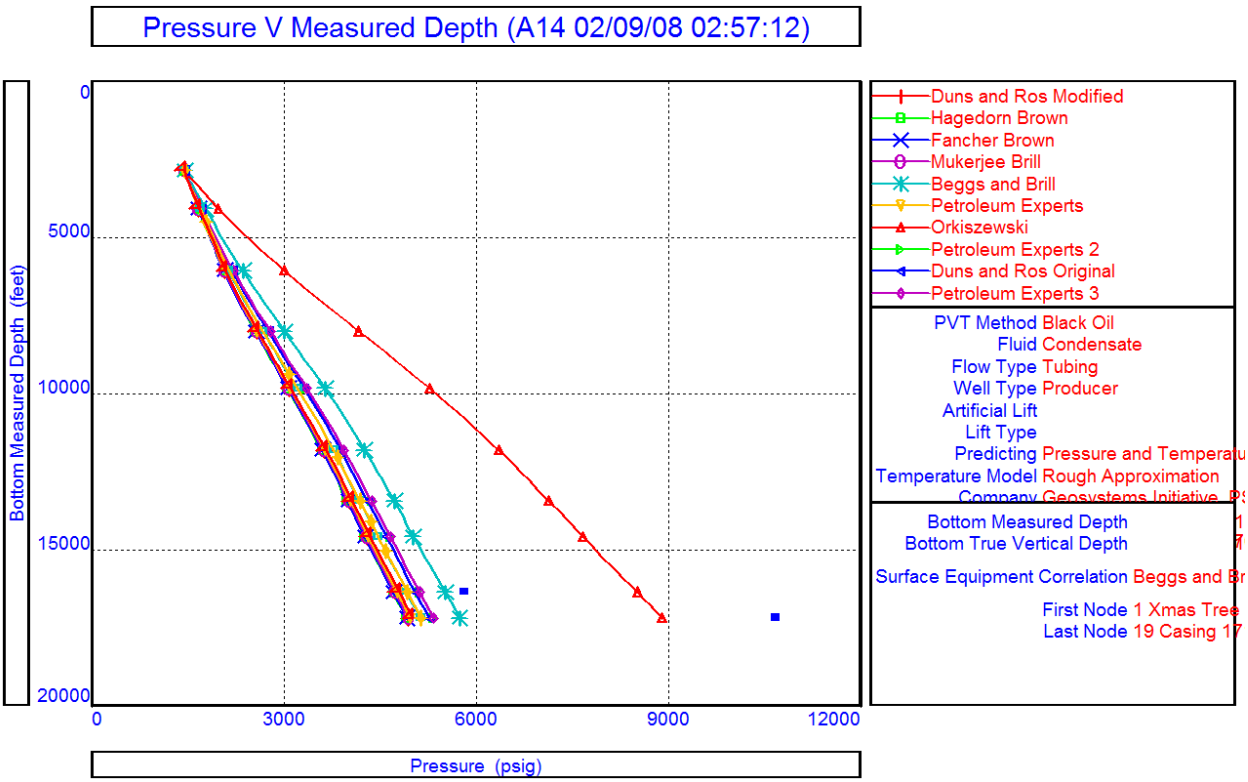

Figure 74: Well Test QC Plot, A14 Well

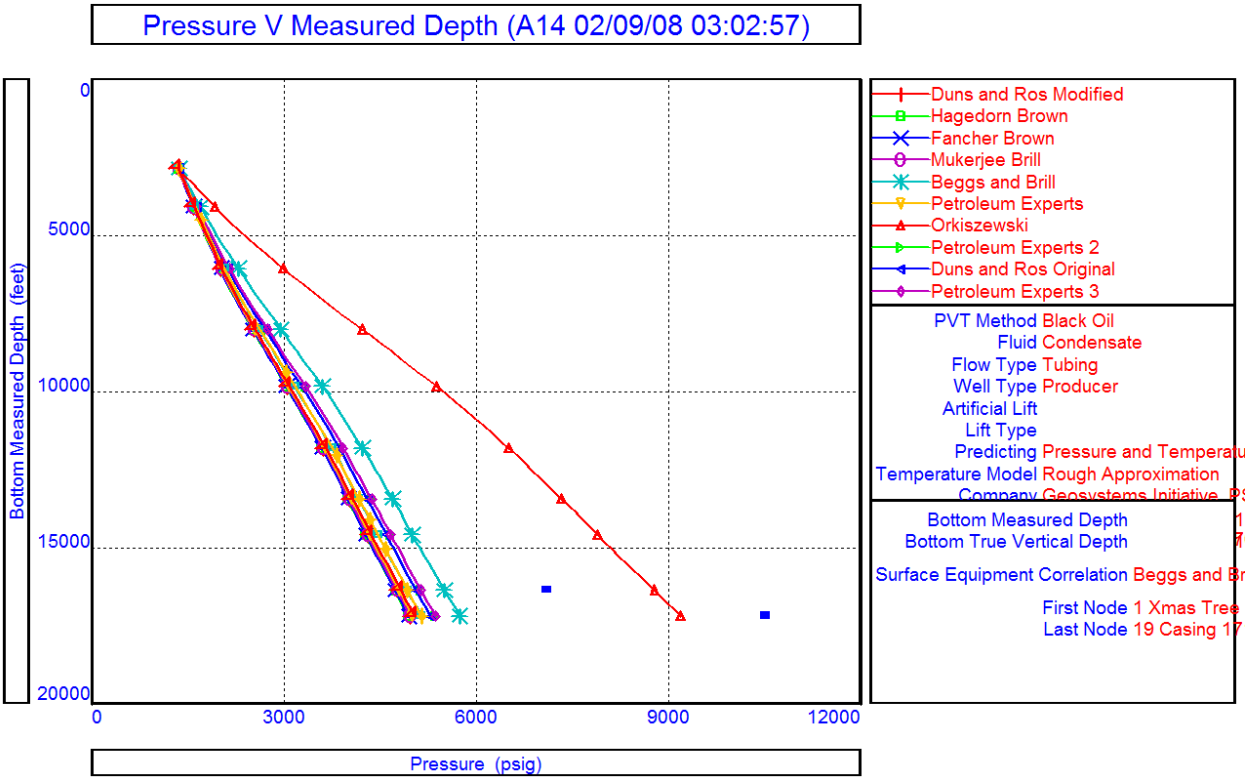

Figure 75: Well Test QC Plot, A14 Well

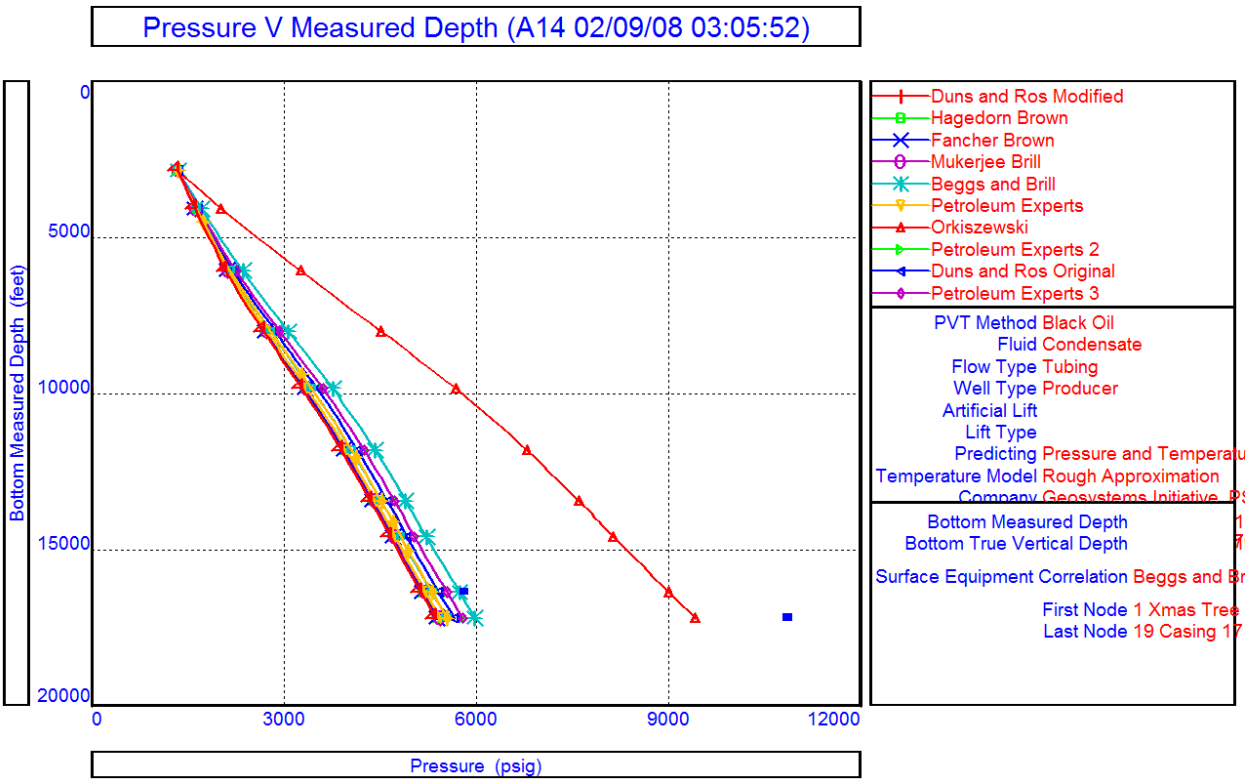

Figure 76: Well Test QC Plot, A14 Well

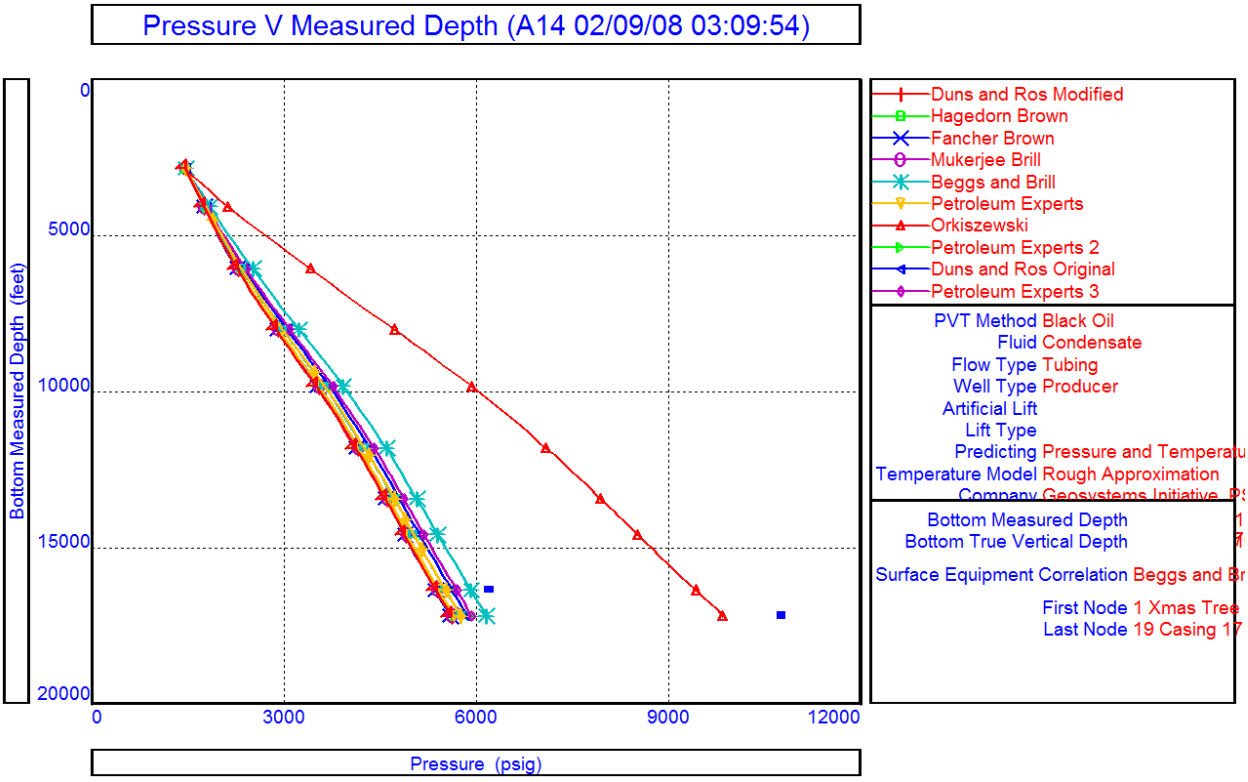

Figure 77: Well Test QC Plot, A14 Well

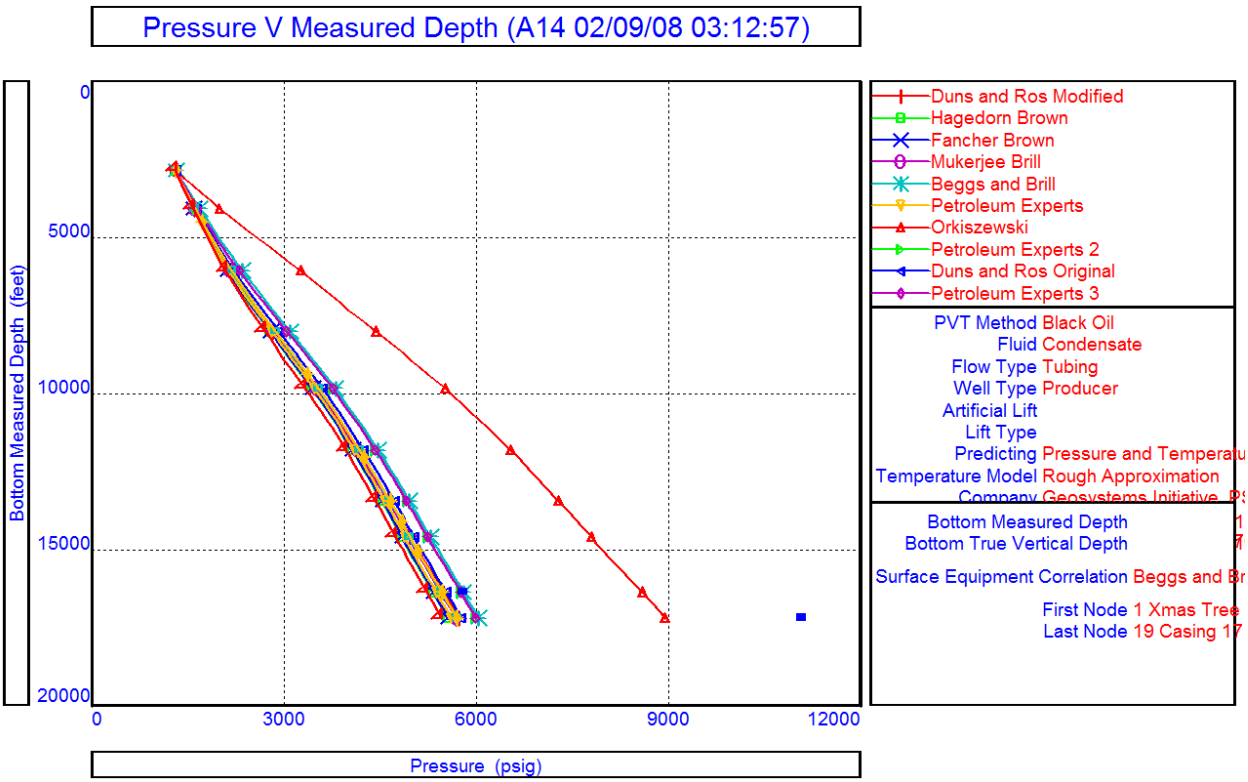

Figure 78: Well Test QC Plot, A14 Well

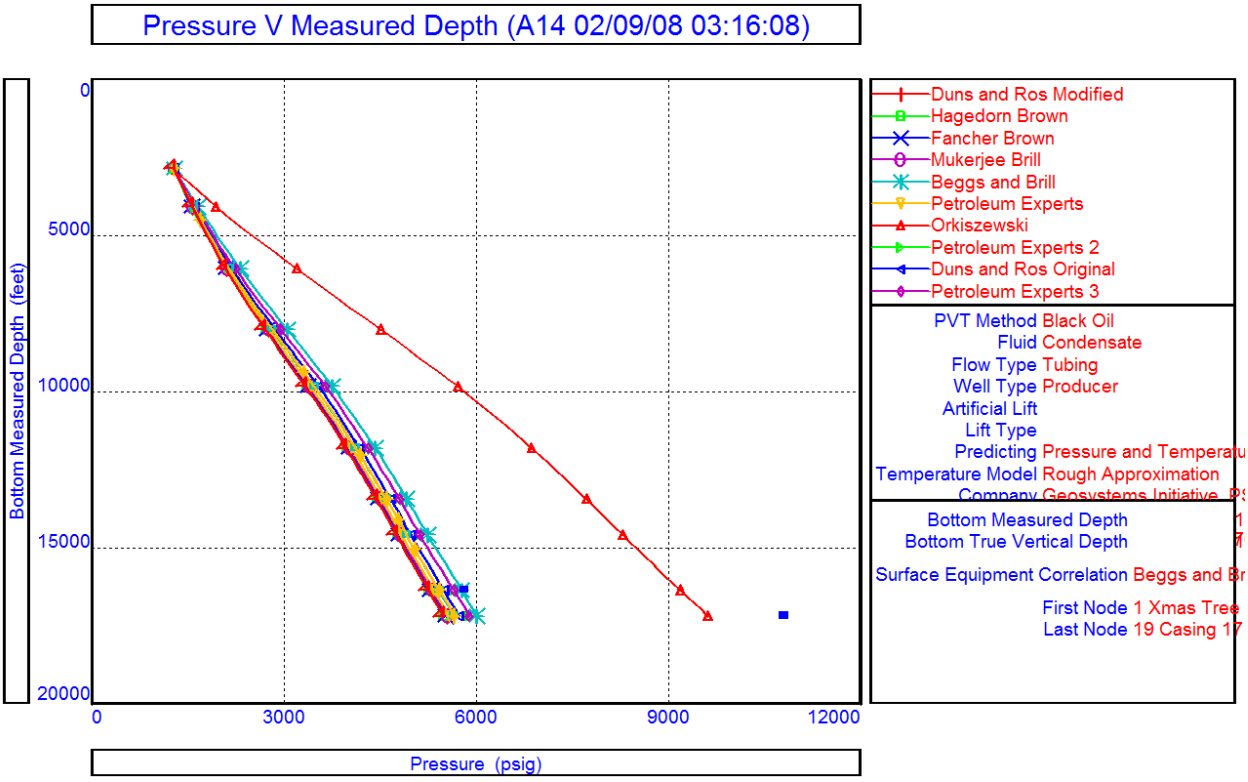

Figure 79: Well Test QC Plot, A14 Well

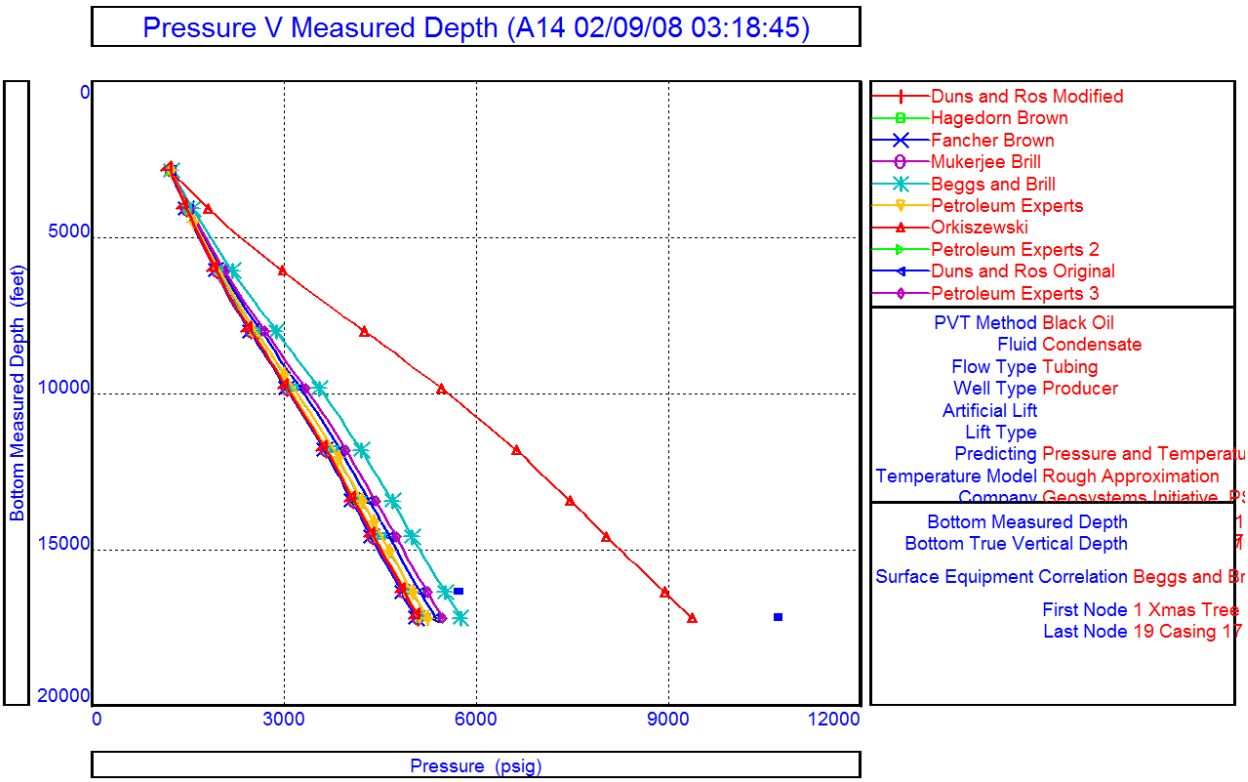

Figure 80: Well Test QC Plot, A14 Well

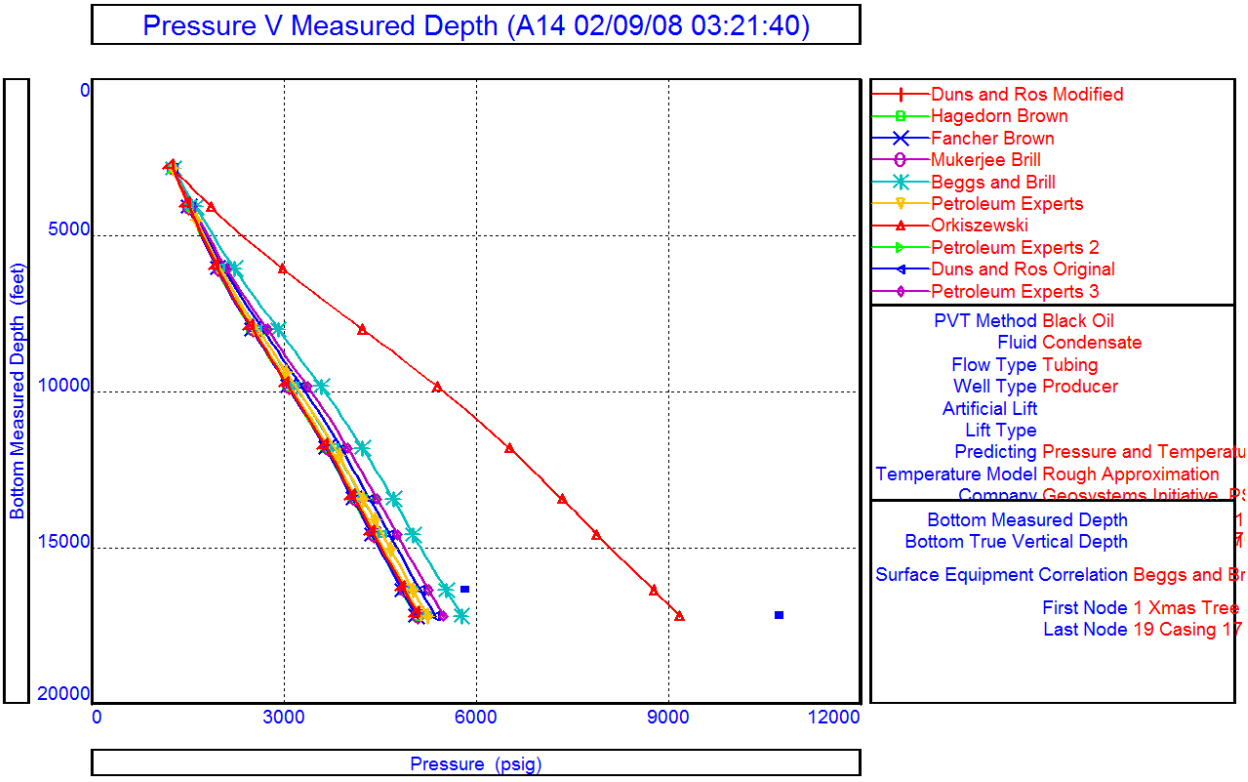

Figure 81: Well Test QC Plot, A14 Well

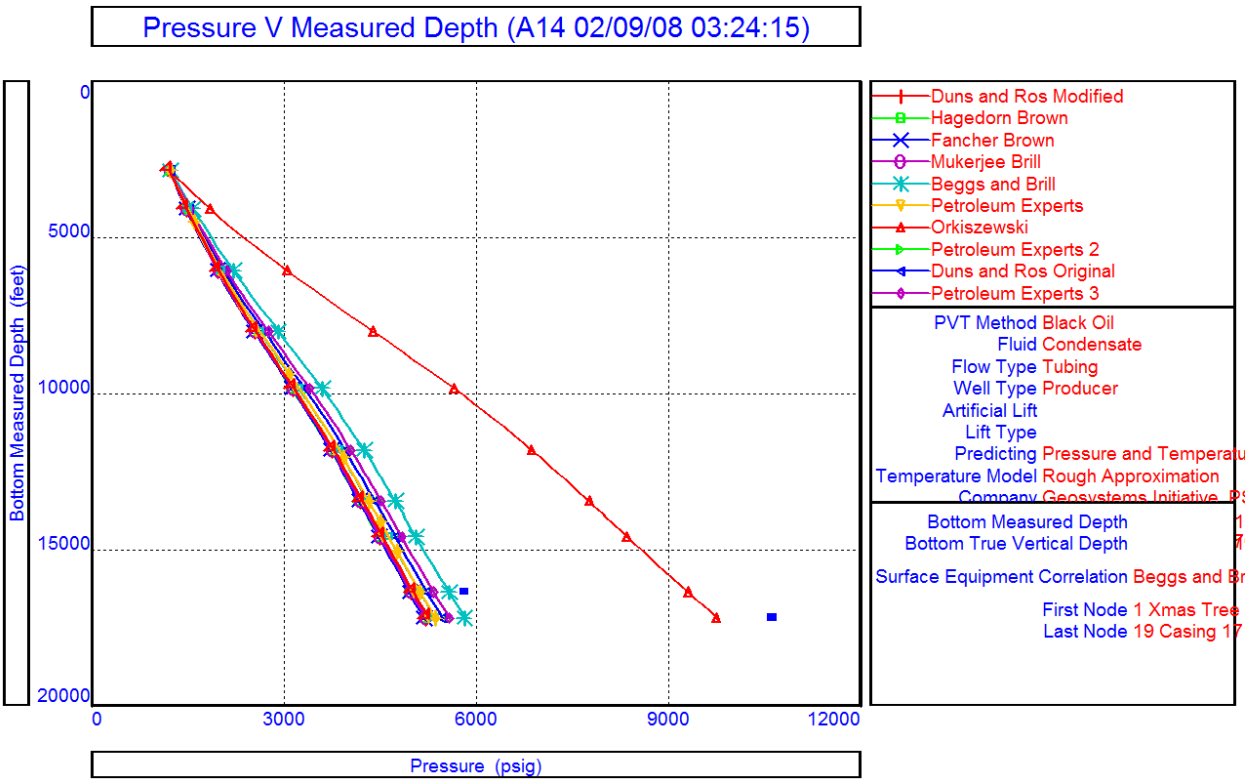

Figure 82: Well Test QC Plot, A14 Well

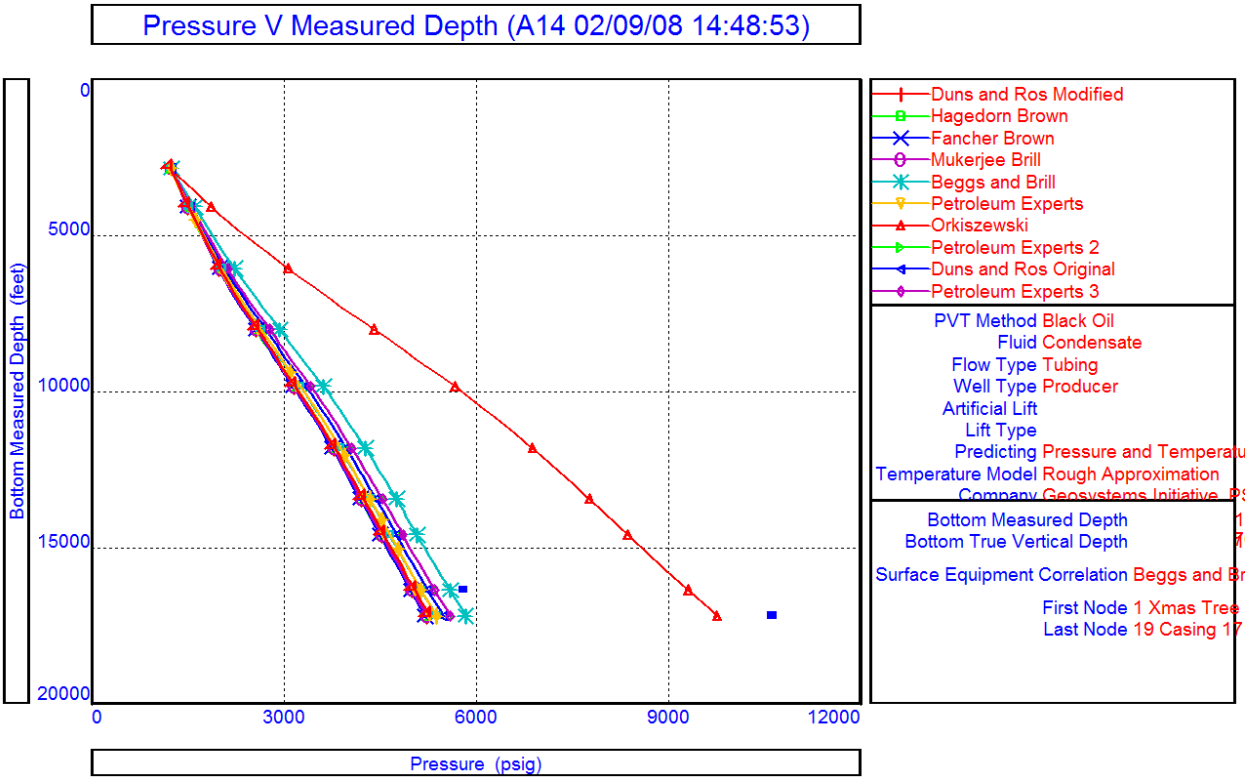

Figure 83: Well Test QC Plot, A14 Well

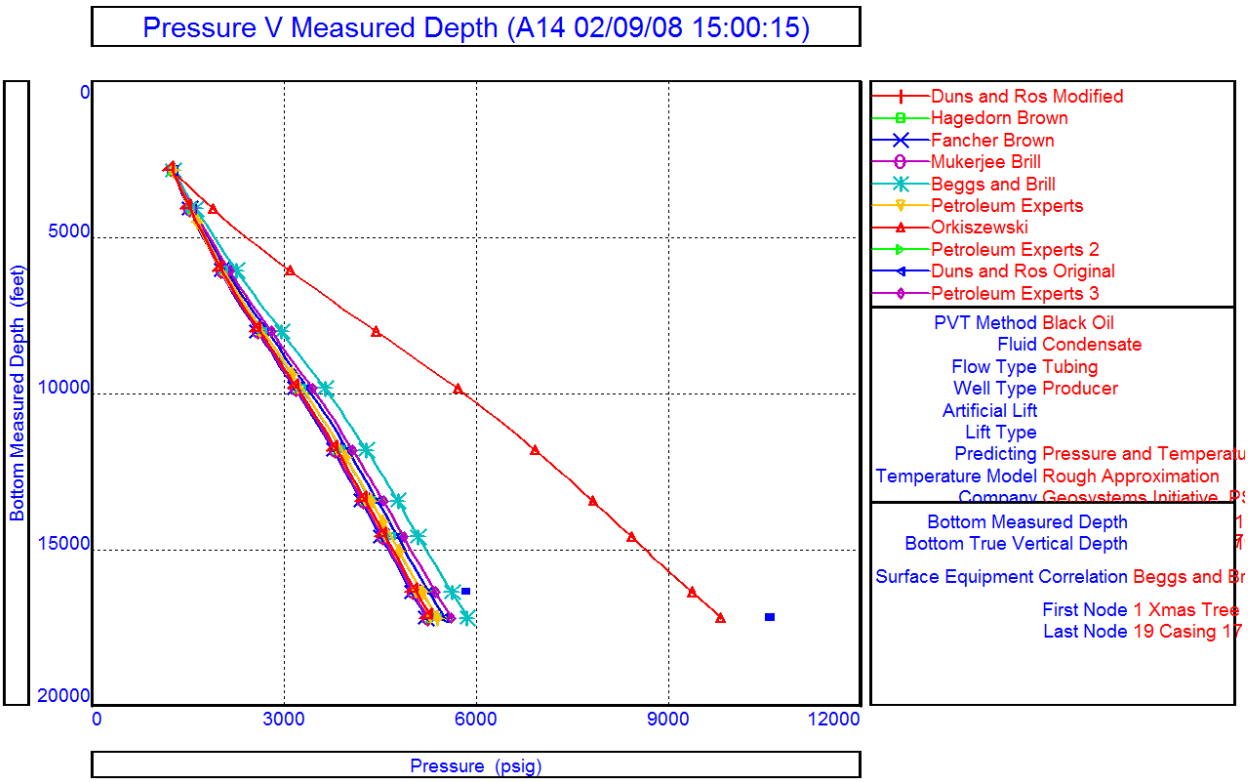

Figure 84: Well Test QC Plot, A14 Well

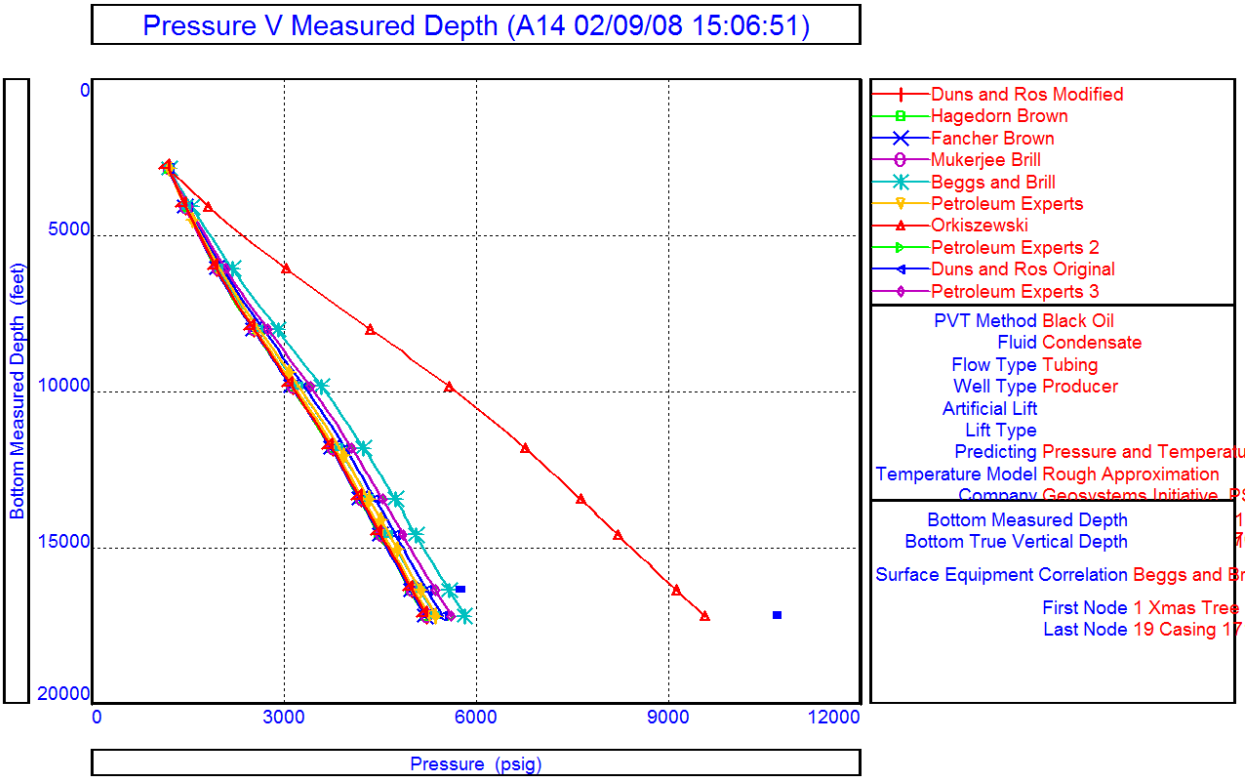

Figure 85: Well Test QC Plot, A14 Well

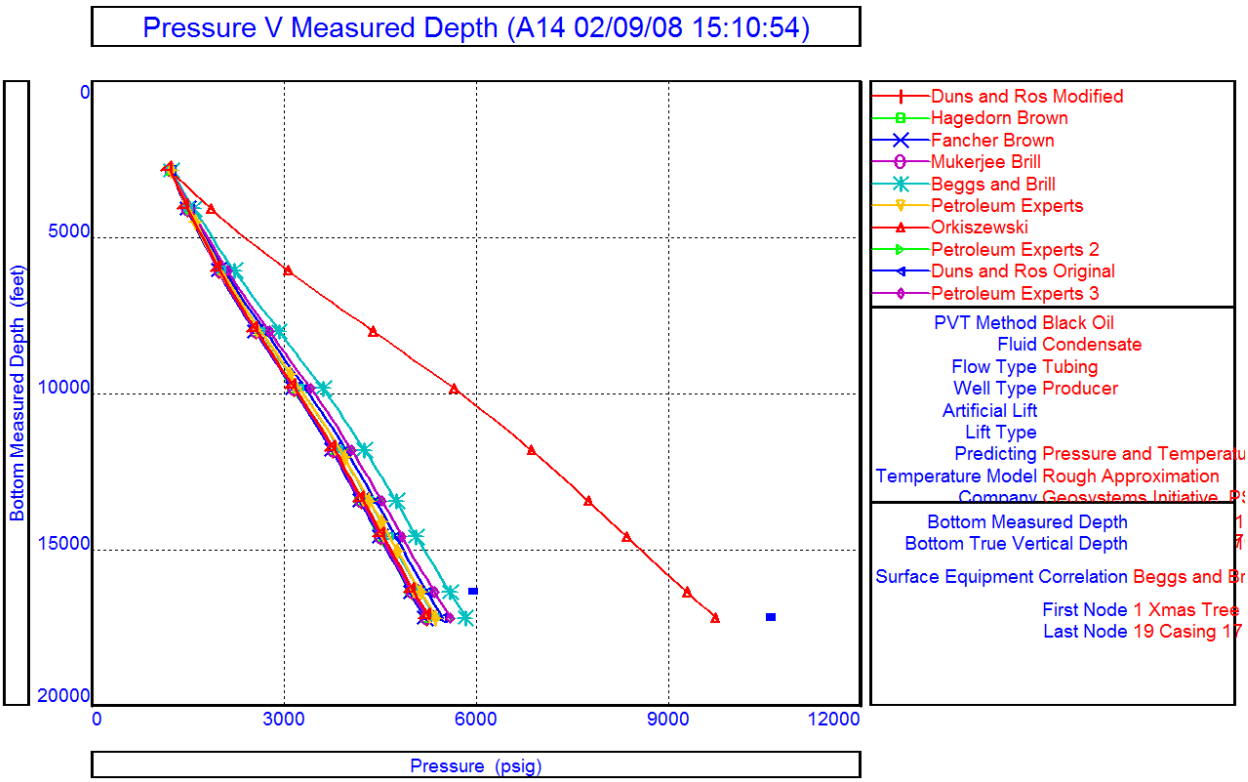

Figure 86: Well Test QC Plot, A14 Well

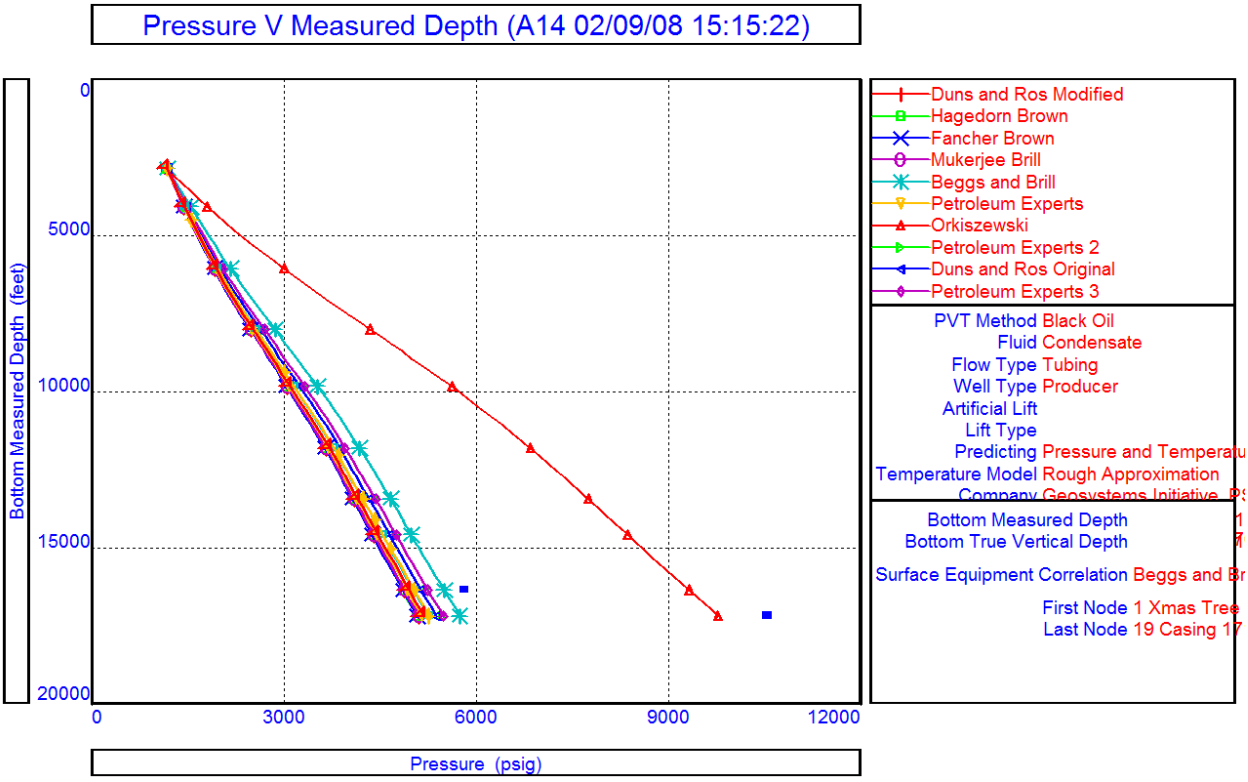

Figure 87: Well Test QC Plot, A14 Well

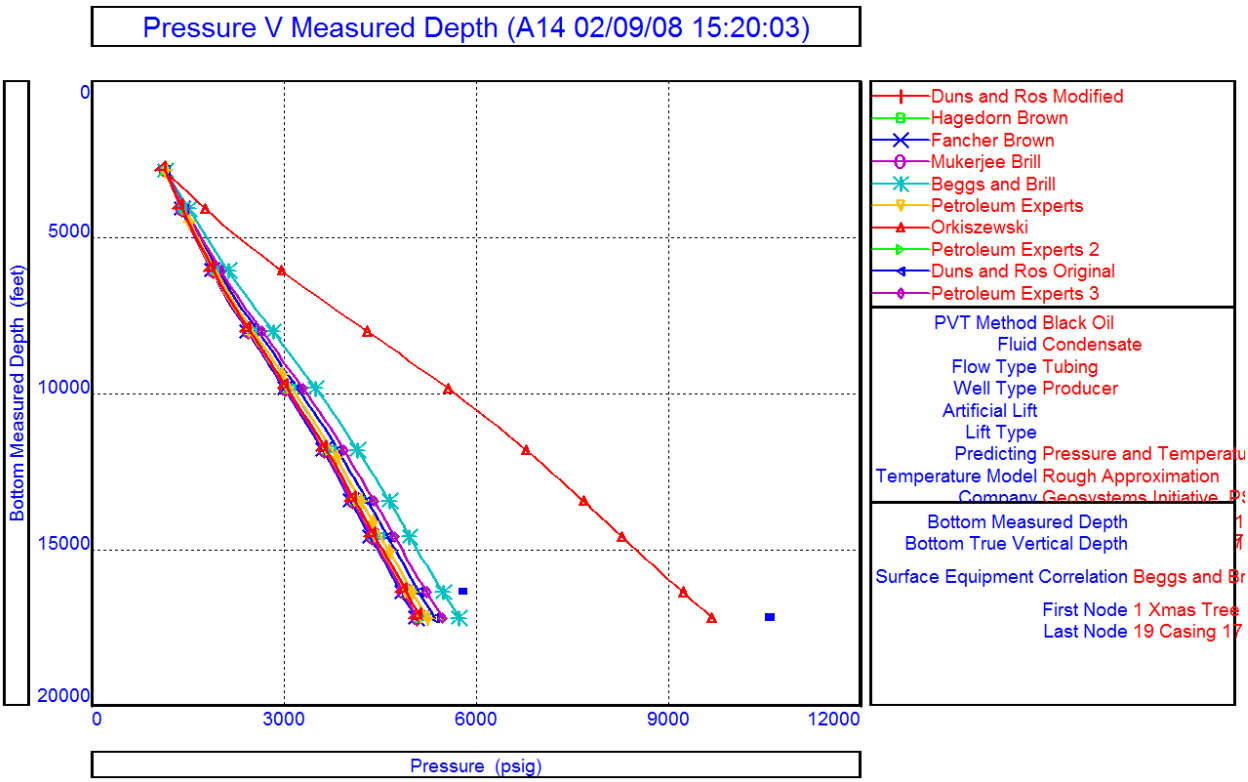

Figure 88: Well Test QC Plot, A14 Well

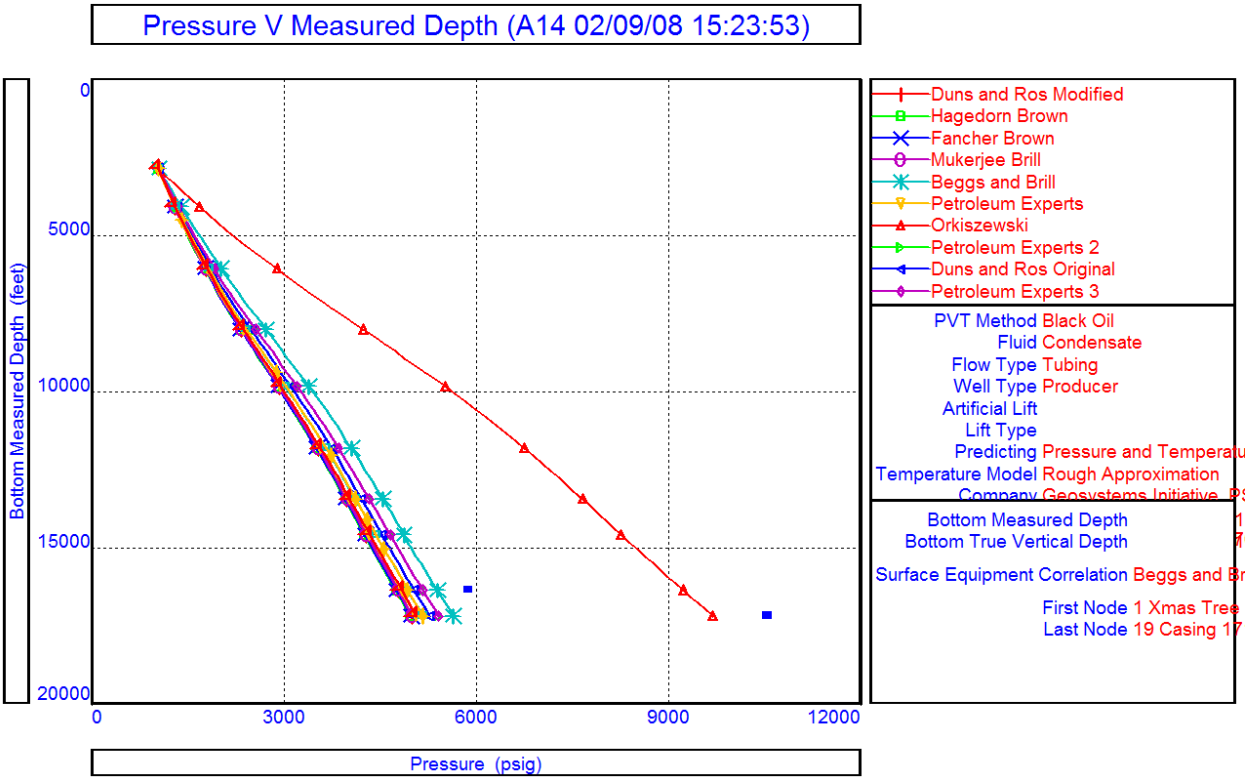

Figure 89: Well Test QC Plot, A14 Well

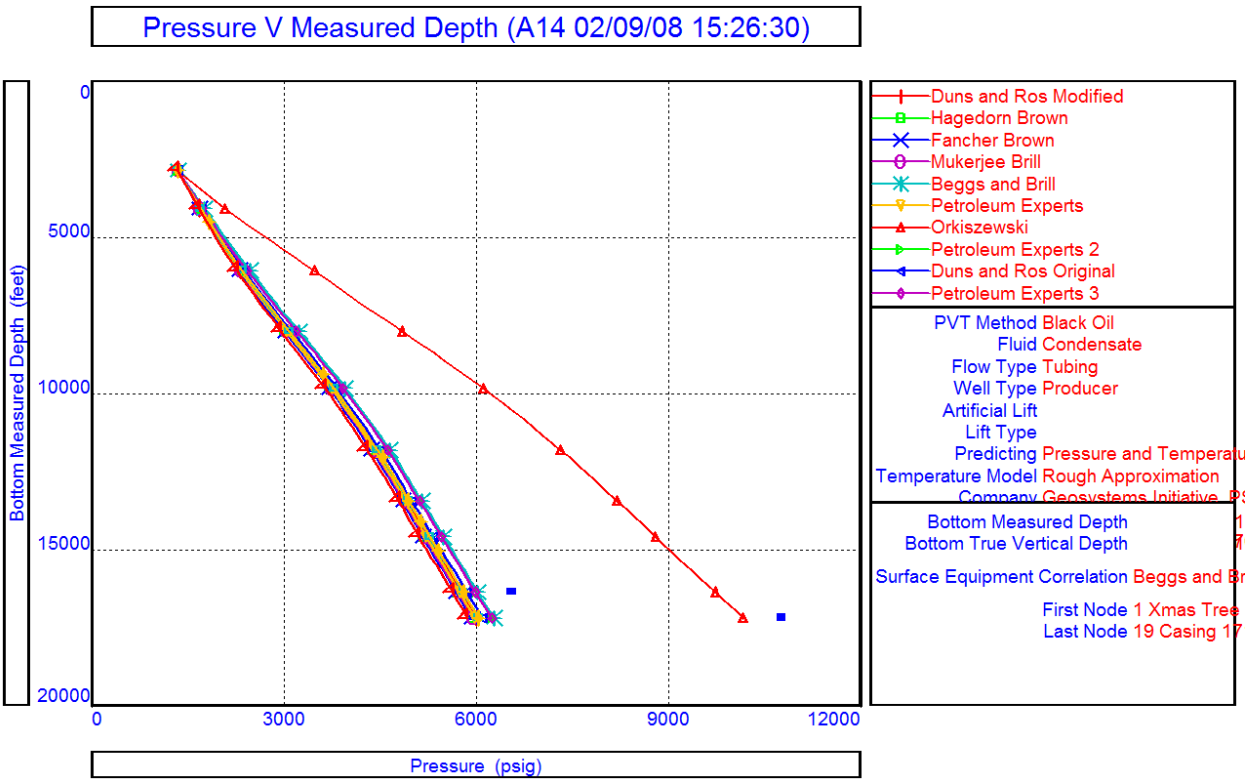

Figure 90: Well Test QC Plot, A14 Well

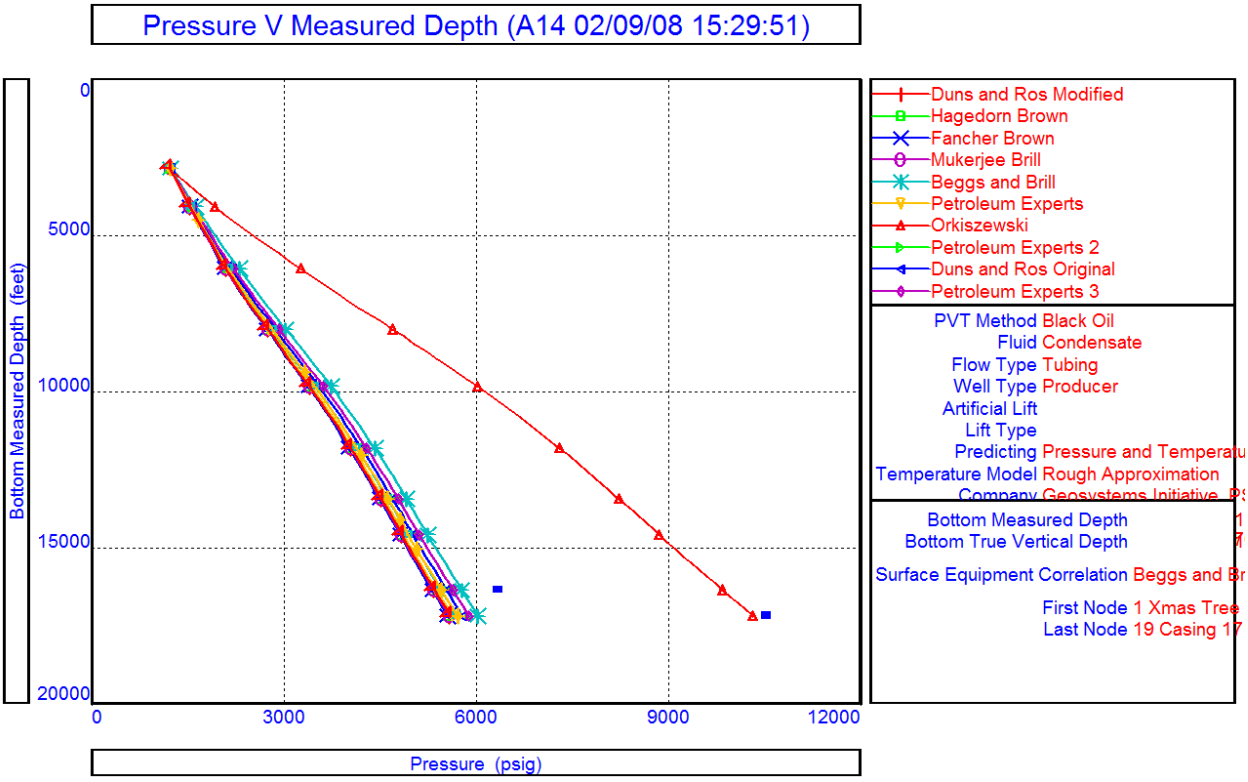

Figure 91: Well Test QC Plot, A14 Well

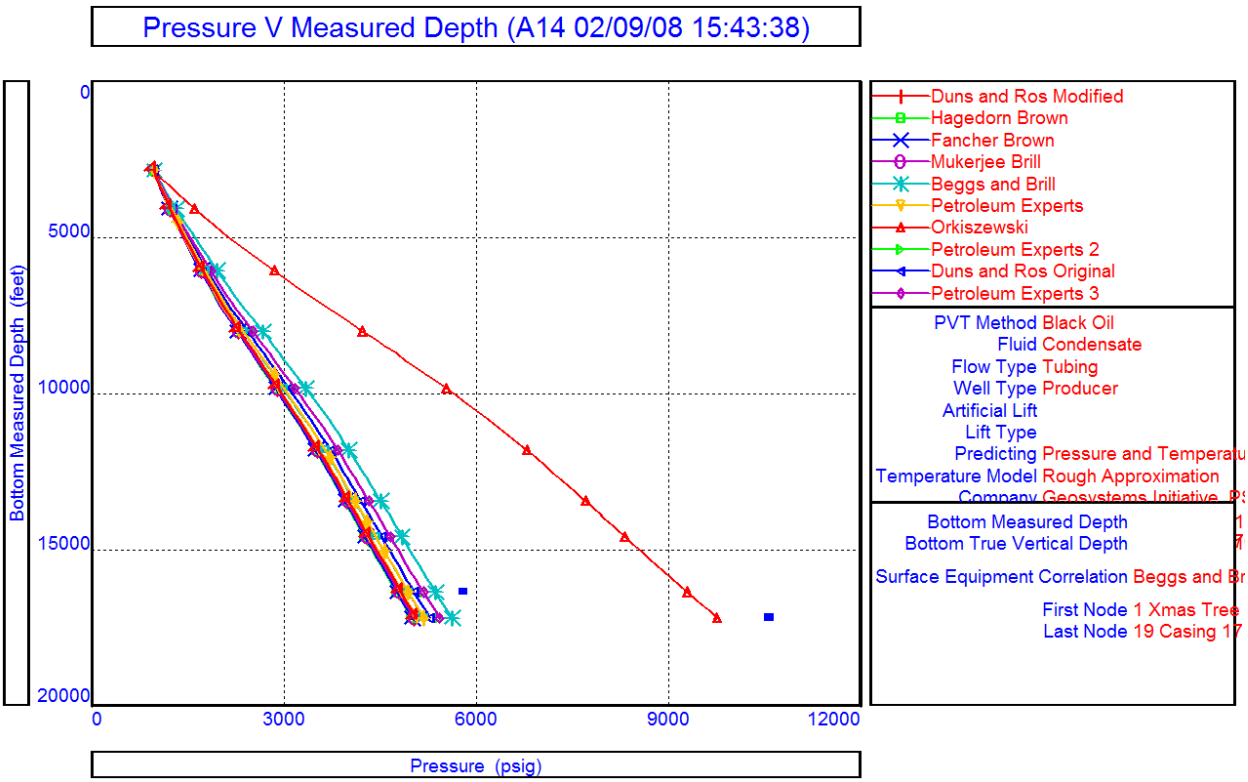

Figure 92: Well Test QC Plot, A14 Well

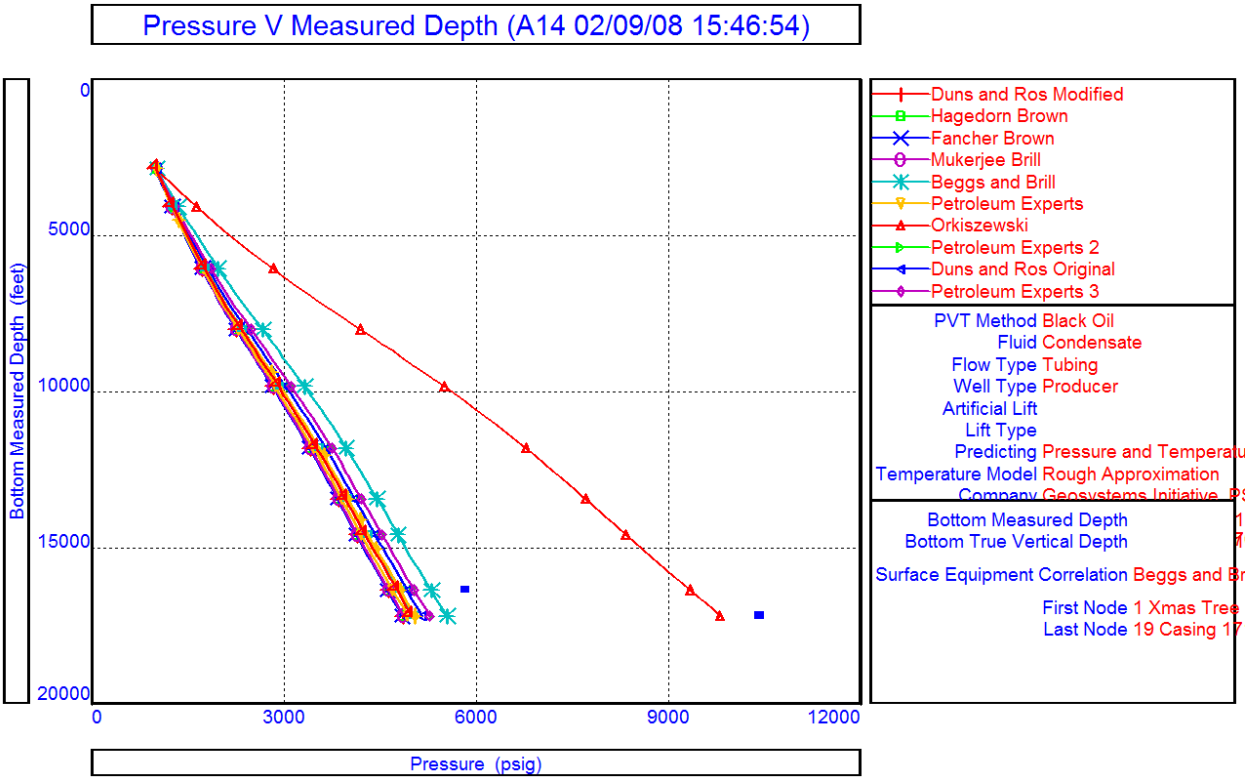

Figure 93: Well Test QC Plot, A14 Well

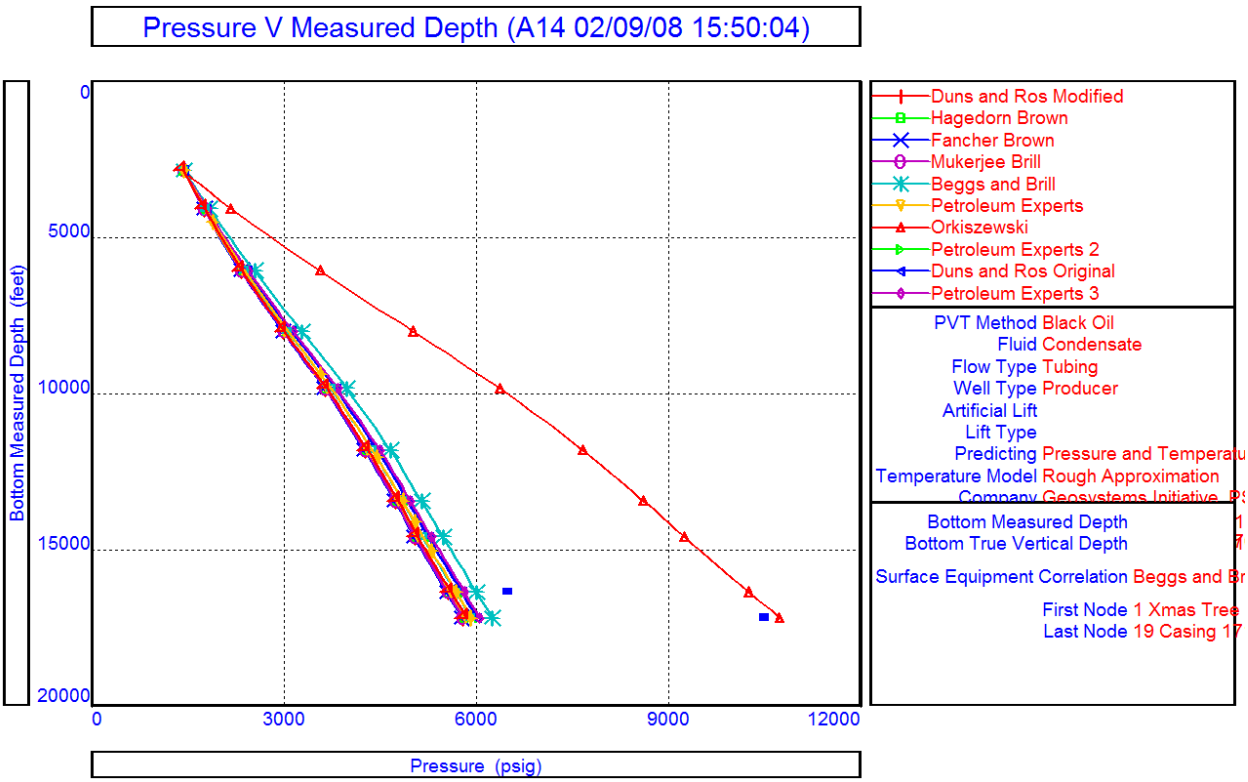

Figure 94: Well Test QC Plot, A14 Well

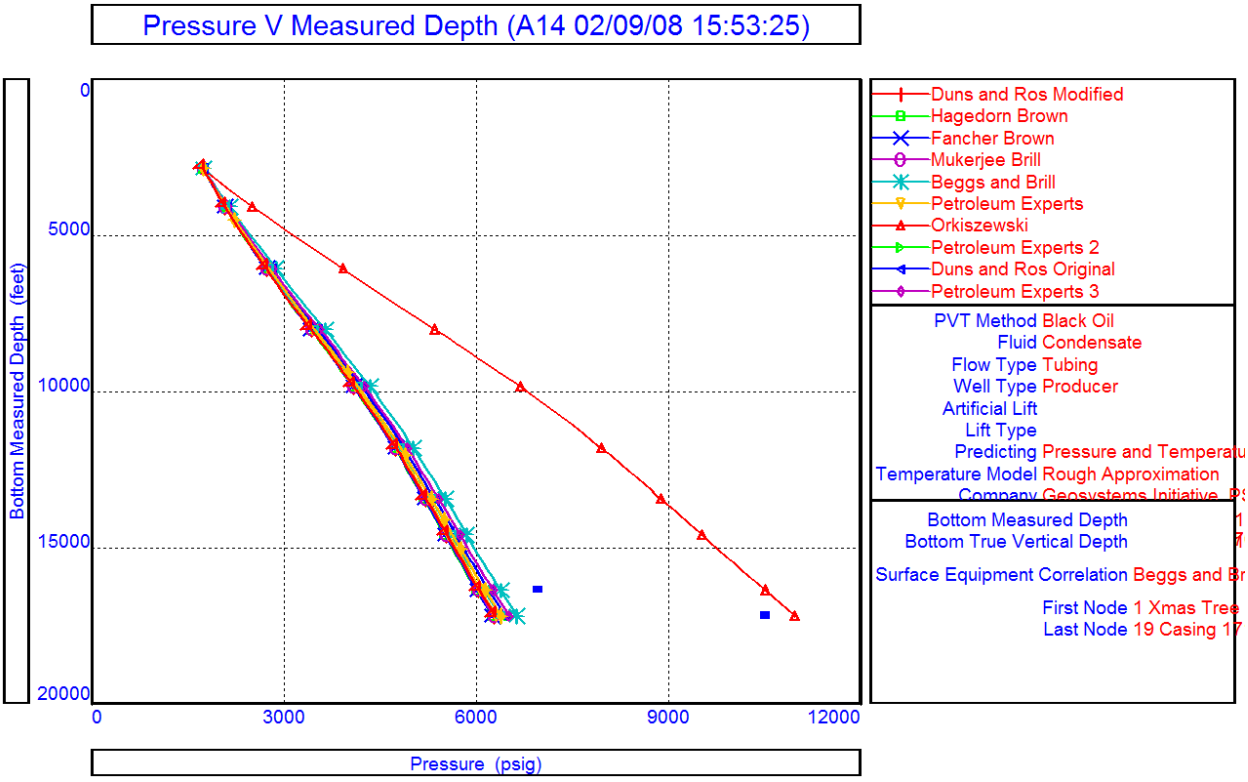

Figure 95: Well Test QC Plot, A14 Well

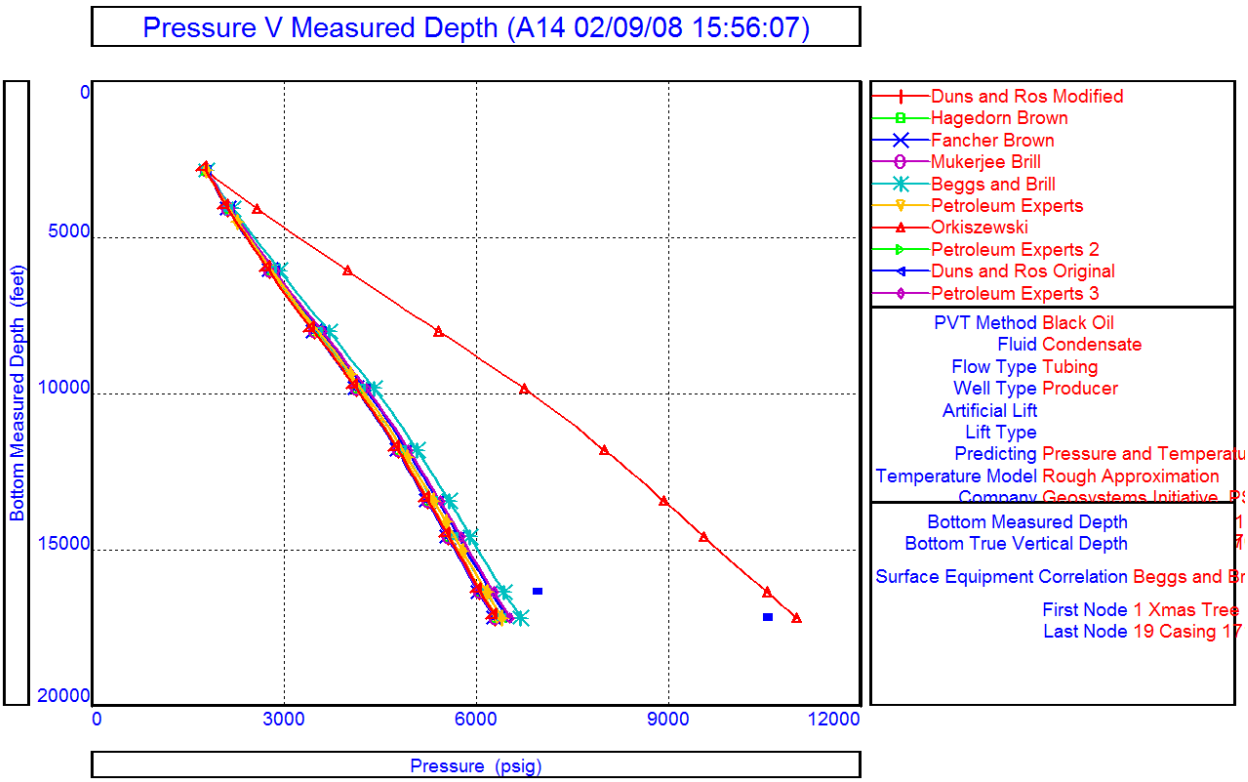

Figure 96: Well Test QC Plot, A14 Well

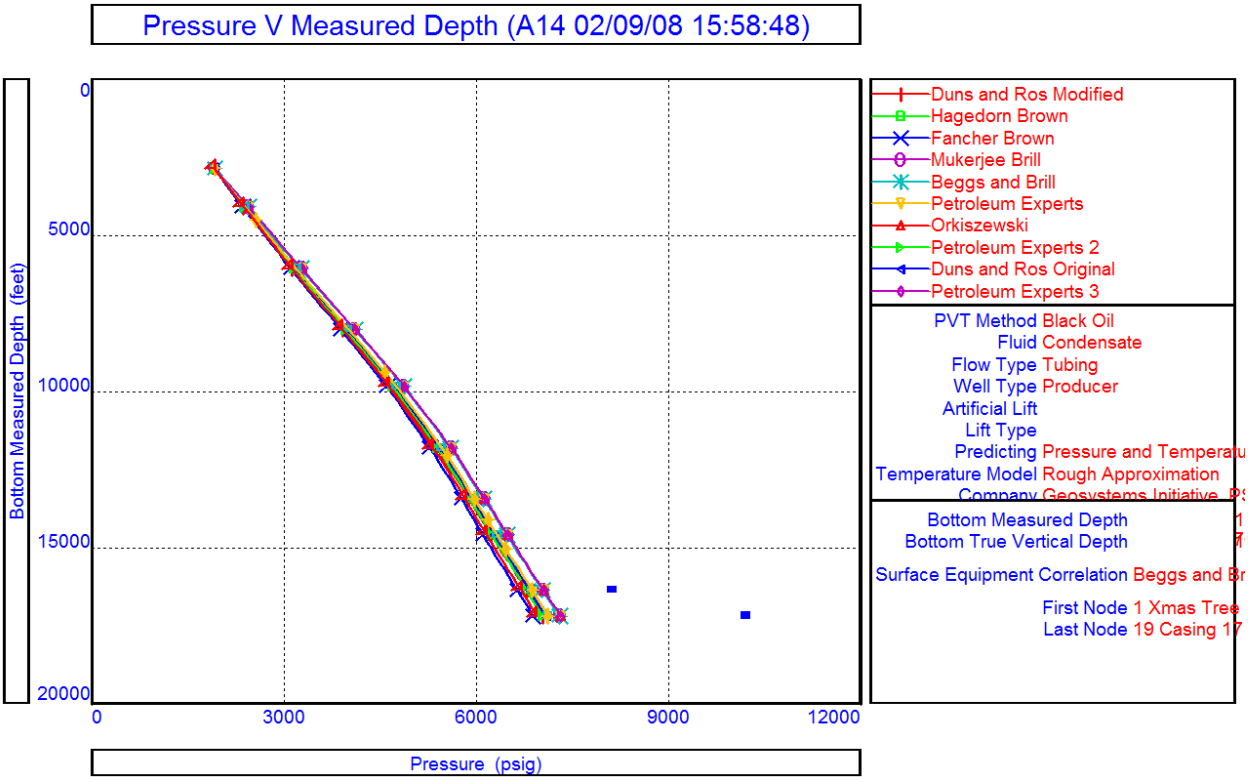

Figure 97: Well Test QC Plot, A14 Well

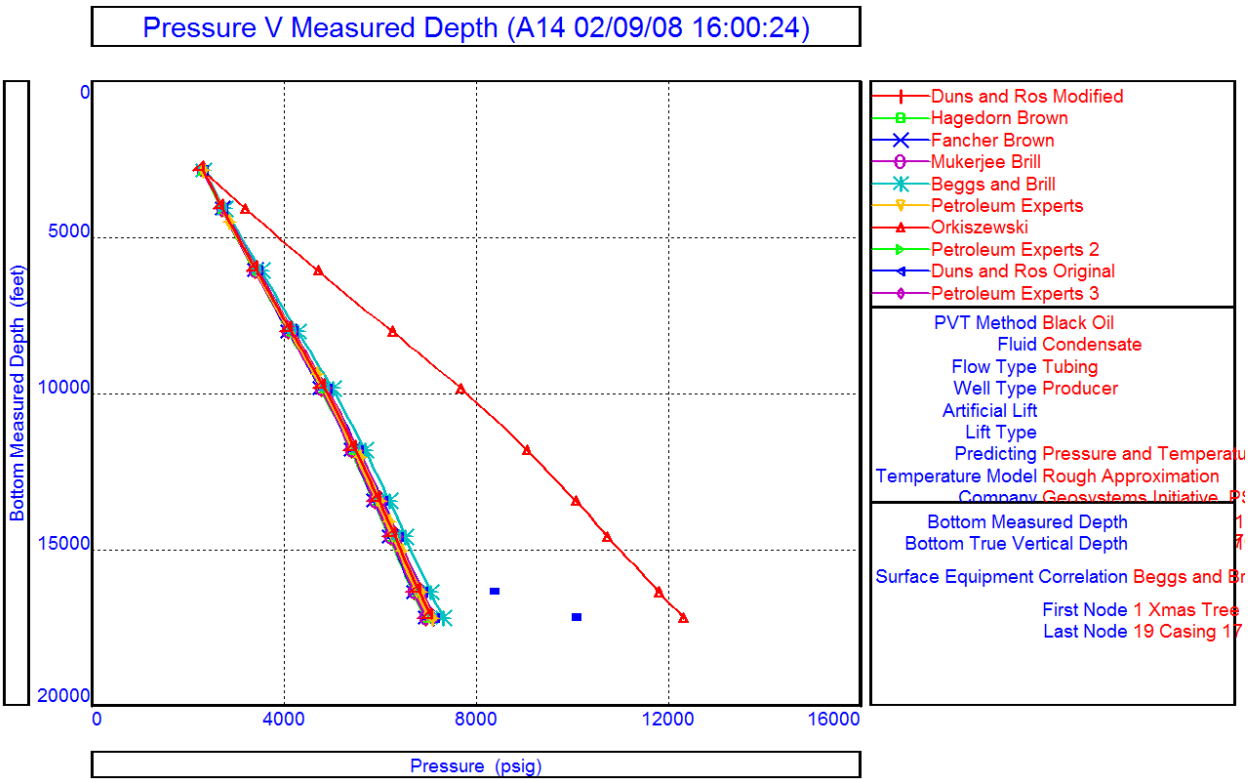

Figure 98: Well Test QC Plot, A14 Well